PEDRO MIGUEL MENDES RODRIGUES

HOW TO KEEP THE THYMUS IN SHAPE: NEW MOLECULAR INSIGHTS ON THYMIC EPITHELIAL CELL HOMEOSTASIS AND FUNCTION

Tese de Candidatura ao grau de Doutor em Ciências Biomédicas submetida ao Instituto de Ciências Biomédicas Abel Salazar da Universidade do Porto.

Orientador - Doutor Nuno Miguel de Oliveira Lages Alves
Categoria – Investigador Principal
Afiliação – Instituto de Investigação e Inovação em Saúde (i3S); Instituto de Biologia Molecular e Celular (IBMC)

Coorientador – Professor Doutor Rui Appelberg Gaio Lima
Categoria - Professor Catedrático
Afiliação - Instituto de Ciências Biomédicas Abel Salazar da Universidade do Porto (ICBAS).

This thesis is dedicated to the memory of my Grandfather Raul Rodrigues, my maternal Great-uncle Maria Antonieta and to the one who is my true inspiration in every way possible, my beloved Grandfather António Mendes.

Publications

De acordo com o disposto no Decreto-Lei nº 74/2006 de 24 de Março, esclarece-se ser da nossa responsabilidade a execução das experiências que estiveram na origem dos resultados apresentados, assim como a sua interpretação, discussão e redação. Nesta tese foram utilizados os resultados dos artigos publicados ou submetidos para publicação abaixo indicados.

Rodrigues PM, Ribeiro AR, Perrod C, Landry JJM, Araújo L, Pereira-Castro I, Benes V, Moreira A, Xavier-Ferreira H, Meireles C, Alves NL. (2017) "Thymic epithelial cells require p53 to support their long-term function in thymopoiesis in mice". Blood, 130(4):478-488.

Rodrigues PM, Peterson P, Alves NL. (2017) “Setting Up the Perimeter of Tolerance: Insights into mTEC Physiology”. Trends in Immunology, dx.doi.org/10.1016/j.it.2017.11.001

Rodrigues PM, Ribeiro AR, Serafini N, Meireles C, Di Santo JP, Alves NL. (2017) “Intrathymic deletion of IL-7 reveals a contribution of the bone marrow to thymic rebound induced by androgen blockade”. The Journal of Immunology, *Under revision*

Durante a execução dos trabalhos descritos nesta tese, o autor colaborou nos seguintes trabalhos publicados:

Ribeiro AR, **Rodrigues PM**, Meireles C, Di Santo JP, Alves NL. (2013). Thymocyte selection regulates the homeostasis of IL-7-expressing thymic cortical epithelial cells in vivo. The Journal of Immunology, 191(3):1200-9.

Ribeiro AR, Meireles C, **Rodrigues PM**, Alves NL. (2014). Intermediate expression of CCRL1 reveals novel subpopulations of medullary thymic epithelial cells that emerge in the postnatal thymus. European Journal of Immunology, 44(10):2918-24.

Meireles C, Ribeiro AR, Pinto RD, Leitão C, **Rodrigues PM**, Alves NL. (2017). Thymic crosstalk restrains the pool of cortical thymic epithelial cells with progenitor properties. European Journal of Immunology, 47(6):958-969

Table of Contents

Acknowledgments

"*O sucesso nasce do querer, da determinação e persistência em se chegar a um objetivo. Mesmo não atingindo o alvo, quem busca e vence obstáculos, no mínimo fará coisas admiráveis.*" – **José de Alencar**

Acima de todo o esforço e dedicação deixados para trás, o sucesso desta longa jornada só foi possível graças a um conjunto valioso de pessoas que, diretamente ou indiretamente, contribuíram para ultrapassar muitos dos obstáculos e tornar este doutoramento uma realidade. A admiração e reconhecimento de todo o apoio que me foi dado nunca poderá ser refletido inteiramente por palavras escritas nesta página.

Em primeiro lugar, desejo manifestar os mais sinceros agradecimentos ao meu orientador, Nuno Alves. Pela maneira incansável como me orientou, pela constante disponibilidade, pela confiança e acima de tudo, por nunca teres desistido de mim. Olhando em retrospetiva, até aos tempos em que só tínhamos um pequeno cubículo para fazer magia, toda a minha evolução e aquilo que aprendi foi em grande parte graças a ti. Não tenho palavras para agradecer pelo inestimável apoio e motivação transmitidos ao longo desta jornada, assim como por todas as criticas e discussões que não só contribuíram para o meu crescimento enquanto cientista, mas também como pessoa. És, e serás, aquilo que eu considero como um verdadeiro exemplo a seguir na ciência. Obrigado por tudo.

A todos os meus companheiros de guerra (laboratório), Rute, Gema, Pedro, Laura e Camila, pela paciência de me aturarem, pela disponibilidade para ajudarem naquilo que é necessário e acima de tudo, um obrigado por toda a boa disposição que torna tudo mais fácil de encarar. Um especial obrigado à Leonor e Chiara, por todo a ajuda, dedicação e conselhos nas mais variadas etapas e aspetos do meu trabalho. Quero também realçar o meu profundo agradecimento a dois antigos membros do grupo, Ana Rosalina e Catarina Meireles, porque caminharam a meu lado durante largos anos e tiveram um papel preponderante no sucesso dos meus projetos.

Deixo também o meu agradecimento aos serviços do IBMC/I3S, porque indiretamente, forneceram um contributo importante para a construção deste

trabalho. À Catarina Leitão pela disponibilidade e apoio prestado na citometria, assim como pela sua simpatia, amizade e conselhos. À equipa do biotério, nomeadamente Sofia Lamas e respetivas tratadoras, pela logística e manutenção dos nossos animais. Aos respetivos coordenadores das plataformas cientificas ALM, CCGen e HEMS por toda a ajuda técnica disponibilizada.

I wish to thank Dr. Thomas Boehm (Max Planck Institute of Immunobiology and Epigenetics) for kindly providing Foxn1-Cre mice, which ended up being a vital tool in this thesis. To Dr. James Di Santo and Nicolas Serafine (Institut Pasteur) for the generation of IL-7-floxed mice and indirect scientific support. Ao Professor Rui Appelberg, pela sua co-orientação.

Um grande obrigado os meus amigos por todos os momentos de descontração, pelo apoio e, acima de tudo, pela amizade ao longo destes anos. Vocês contribuíram para que tudo fosse mais fácil de encarar, mesmo nos momentos mais críticos. À Jéssica e Marina, porque apesar de muitos vezes desencontrados, ambas foram e são um porto de abrigo. Ao Miguel, porque a vida é definitivamente irónica e acabaste como um bom amigo. Ao Elísio, um especial obrigado pela amizade de tantos anos, pelas palavras e conselhos sábios, pela pessoa que és e acima de tudo, por estares sempre presente. Ao Tiago, porque mesmo estando longe continuas sempre por perto. À Andreia, porque tenho de reconhecer o teu contributo.

À Carolina, porque nem todas as palavras serão capazes de te agradecer. Apesar de teres surgido há tão pouco tempo na minha vida, se não fosse pelo teu apoio incondicional, nunca teria chegado a este momento. Tudo porque foste capaz de trazer ordem ao caos, de recolher todos os pedacinhos deixados para trás e fazer-me lembrar quem realmente sou. Deste-me todo o alento e motivação necessária para não desistir e voltar a ter gosto por aquilo que faço. Por teres sempre estado ao meu lado e pela paciência, mesmo quando te pedia para leres numerosas vezes a mesma coisa. Obrigado por seres quem és. Devo-te cada palavra desta tese.

Finalmente, como os últimos serão sempre os primeiros, agradeço aos meus pais, irmão e avó. Porque sem vocês não seria o que sou hoje. Nunca vos conseguirei agradecer por todos os sacrifícios e privações que passarem e que me permitiram chegar tão longe. É a vocês que devo tudo aquilo que sou e por muitas

vezes ausente, sei que serão sempre o meu porto de abrigo, prontos para ajudar a superar os obstáculos e partilhar todos os êxitos. Obrigado por exigirem o melhor de mim em tudo o que faço, por me amarem incondicionalmente com todos os meus defeitos e qualidades e, acima de tudo, por acreditarem sempre em mim. Vocês são o meu exemplo e é um orgulho ter-vos como família.

Dedico esta tese à memoria do meu avô António. Porque és a pessoa que eu mais admiro. Por muito que a vida te tenha sido "madrasta", sempre encaraste todas as situações com um sorriso nos lábios. És um exemplo de força de vontade, coragem e determinação. Foi um privilegio ter-te conhecido, ter aprendido contigo e de ser chamado de teu neto. Até sempre, com saudade.

Por último, ao meu avô Raul e tia Mieta, porque também nunca serão esquecidos.

Summary

The unique ability of the adaptive immune system to mount effective responses against a wide variety of environmental threats depends on the generation of a functionally diverse and self-tolerant pool of T lymphocytes. The T cell developmental program takes place within specialized cellular niches of the thymus formed by thymic epithelial cells (TECs). The thymic epithelium is classically divided into two main lineages, the cortical (c) and medullary (m) TECs, with both subpopulations having well-defined roles in coordinating distinct phases of T cell differentiation and repertoire selection. The function of the thymus decreases with age, a physiological process that is associated with structural, cellular and functional alterations in the cTEC and mTEC niches. Despite the important advances in our understanding about distinct aspects of TEC biology, the mechanisms governing the homeostasis of TECs in the adult thymus remain poorly defined.

In this thesis, by generating novel conditional loss-of-function mouse models, we studied the cellular and molecular pathways involved in the maintenance and regeneration of TEC microenvironments and their function. In **Chapter II**, we provide evidence that position p53 as a novel molecular determinant of TEC function throughout life. We report that specific loss of p53 in TECs primarily disrupts the integrity of the medullary niche, by altering RANK-driven mTEC differentiation and the transcriptional profile of mTECs. Furthermore, we show that p53 is critical to maintain regular thymopoiesis and the functional capacity of mTECs to induce self-tolerance during life. In **Chapter III**, we study the temporal and spatial requirements for Interleukin-7 (IL-7), a cytokine with chief roles in pre- and intra-thymic stages of thymopoiesis, in the regeneration of the thymus promoted by sex steroid ablation (SSA). We document that SSA enhances thymic activity in young but not aged germline IL-7 knockout mice, an outcome that correlated with a defective expansion of the hematopoietic niche in the bone marrow of the later. Moreover, conditional deletion of IL-7 in TECs show that 1) thymic renewal after SSA proceeds independently of TEC-derived IL-7 and 2) the increase in thymic function following SSA is functionally linked to the BM compartment.

Collectively, the results within this thesis provide new insights on novel molecular processes that govern the homeostasis and recovery of the TEC microenvironments

during normal and altered physiological settings. This knowledge is of fundamental importance in the design of tailor-made therapeutic strategies aimed at repairing and improving thymic functioning in different medical conditions linked to poor or misguided T cell responses.

Resumo

A capacidade única do sistema imune adaptativo de estabelecer respostas efetivas contra uma grande variedade de ameaças ambientais depende da geração de um grupo de linfócitos T funcionalmente diverso e auto-tolerante. O programa de desenvolvimento das células T ocorre em nichos celulares especializados do timo formados por células epiteliais do timo (TECs). O epitélio tímico é tipicamente dividido em duas linhagens principais, as TEC corticais (c) e medulares (m), ambas com funções bem definidas na coordenação de distintas fases da diferenciação das células T e seleção do repertório. A função do timo diminui com a idade, um processo fisiológico associado a alterações estruturais, celulares e funcionais dos nichos das cTEC e mTEC. Apesar dos importantes avanços relacionados com aspetos distintos da biologia das TEC, os mecanismos que regem a homeostasia das TEC no timo adulto permanecem mal definidos.

Nesta tese, através da geração de novos modelos de ratinho com perdas condicionais de função, estudamos as vias celulares e moleculares envolvidas na manutenção e regeneração dos microambientes das TEC, assim como na sua função. No capítulo II, fornecemos evidências que posicionam p53 como um novo determinante molecular da função das TEC ao longo da vida. Nós descrevemos que a perda especifica de p53 nas TEC altera principalmente a integridade do nicho medular, alterando a diferenciação das mTEC que dependem de RANK e o perfil transcricional das mTEC. Além disso, demonstramos que p53 é fundamental para manter a timopoiese regular e a capacidade funcional das mTEC para induzir auto-tolerância durante a vida. No capítulo III, estudamos os requisitos temporais e espaciais da interleucina-7 (IL-7), uma citoquina com um papel fundamental em estádios pré- e intra-tímicos da timopoiese, na regeneração do timo promovido pela remoção das hormonais sexuais (SSA). Nós documentamos que a SSA melhora a atividade tímica em ratinhos jovens, mas não envelhecidos, deficientes para IL-7, um efeito que se correlaciona com uma expansão defeituosa do nicho hematopoiético da medula óssea dos mesmos. Para além disso, a deleção condicional de IL-7 nas TECs mostra que 1) a regeneração do timo após a SSA ocorre independentemente de IL-7 produzida especificamente pelas TEC e 2) o aumento da função tímica após a SSA encontra-se funcionalmente à medula óssea.

Em suma, os resultados descritos nesta tese fornecem informações sobre novos processos moleculares envolvidos na homeostasia e recuperação dos microambientes das TEC durante situações fisiológicas normais ou alteradas. Este conhecimento é de extrema importância para o desenvolvimento de novas estratégias terapêuticas destinadas a reparar e melhorar o funcionamento tímico em diferentes condições médicas ligadas a respostas de células T pobres ou comprometidas.

List of Abbreviations

Aire - Autoimmune regulator;
AGM – Aorta-gonad-mesonephros;
APS-1 – Autoimmune polyglandular syndrome type 1;
BCR - B cell receptor;
BM - Bone marrow;
BMP - Bone morphogenic protein;
BMT - Bone marrow transplant;
CCL – Chemokine (C-C motif) ligand;
CCR – C-C Chemokine receptor;
CD - Cluster of differentiation;
CD40 - Cluster of differentiation 40;
CD40L - Cluster of differentiation 40 ligand;
cKO – Conditional knockout;
Cld - Claudin;
CLP – Common lymphoid progenitor;
CMJ - Cortico-medullary junction;
CNS1 – Conserved noncoding sequence 1;
cTEC - Cortical thymic epithelial cell;
CTR - Control;
CTX - Castrated;
CXCL – Chemokine (C-X-C motif) ligand;
CXCR – C-X-C Chemokine receptor;
DC - Dendritic cell;
dGuo - 2-deoxyguanosine;
Dll4 - Delta-like 4;
DN - Double negative;
DP - Double positive;
E - Embryonic day;
ECM – Extracellular matrix;
EpCAM - Epithelial cell adhesion molecule;
ETP – Early thymic progenitor;
Eya1 – Eyes absent 1 homologue;
Fezf2 – FEZ family zing finger 2;
FGF - Fibroblast growth factor;
FoxP3 - Forkhead box P3;
FoxN1 - Forkhead box N1;
FTOC - Fetal thymic organ culture;
GATA – GATA-binding protein;
Gcm2 - Glial cells missing homolog 2;
GO – Gene ontology;
GPCR - G-protein coupled receptor;
H3K4 – Histone 3 lysine 4;
HDAC3 – Histone deacetylase 3;
HSC - Hematopoietic stem cells;
Hoxa3 – Homeobox A3;
IGF - Insulin growth factor;
IL - Interleukin;
IRF – Interferon regulatory factor;
iNKT – Invariant natural killer T cell;
ISP - Immature single positive;
jTECs – Junctional thymic epithelial cells;
K - Cytokeratin;
Klf2 – Kruppel-like factor 2;
KO – Knockout;

LHRH – Luteinising hormone releasing hormone;

LPP3 – Lipid phosphate phosphatase 3;

Lti - Lymphoid tissue inducer;

LTβR - Lymphotoxin beta-receptor;

MEF – Mouse embryonic fibroblast;

MHC - Major histocompatibility complex;

mTEC - Medullary thymic epithelial cell;

MTS - Mouse thymic stroma;

NC - Neural crest;

NF-κB - Nuclear factor kappa B;

NIK - NF-κB-inducing kinase;

NK - Natural killer;

OPG - Osteoprotegerin;

pGE - Promiscuous gene expression;

Pax – Paired box gene;

PDPN – Podoplanin;

PHD – First plan homeodomain;

Plet1 – Placenta-expressed transcript-1;

PRR – Pattern recognition receptors;

pMHC - self-peptide-MHC complexes;

PP – Pharyngeal pouch;

qPCR - Quantitative polymerase chain reaction;

RA - Retinoic acid;

RAG - Recombination activating gene;

RANK - Receptor activator of nuclear factor kappa B;

RANKL - Receptor activator of nuclear factor kappa B ligand;

Rb - Retinoblastoma;

RE – Responsive element;

RelB - Reticuloendotheliosis viral oncogene related B;

RTOC - Reaggregate thymic organ culture;

Runx – Runt-related transcription factor;

S1P - Sphingosine-1-phosphate;

$S1P_1$ - Sphingosine-1-phosphate receptor 1;

SSA – Sex steroid ablation;

SCF - Stem cell factor;

SCID - Severe combined immunodeficiency;

SL-TBI – Sub-lethal total body irradiation;

SP - Single positive;

SSEA-1 – Stage-specific embryonic antigen;

STAT - Signal transducer and activator of transcription;

TCR - T cell receptor;

Th-POK – T-helper inducing POZ/Kruppel-like factor;

TECs - Thymic epithelial cells;

TECp - Thymic epithelial cell progenitor;

TNFRSF - Tumour necrosis factor receptor super family;

TOX – Thymus high mobility group box protein;

TRA - Tissue restricted antigen;

TRAF - Tumour necrosis factor receptor-associated factor;

Trp53 – Transforming related protein 53;

Treg - Regulatory T cell;

TSSP - Thymus-specific serine protease;

TSP – Thymic seeding progenitors;

UEA - *Ulex europaeus* agglutinin;

VCAM – Vascular cell adhesion molecule;

Wnt - Wingless-related MMTV integration;

WT - Wild Type;

XCL1 – Chemokine **(**X-C motif) ligand 1;

YFP - Yellow fluorescence protein;

γ_c **-** gamma chain;

List of Figures

Chapter I - Introduction

Chapter II – p53 controls thymic epithelial cell homeostasis

Chapter III – The bone marrow contributes to thymic rebound upon SSA

Chapter IV – General Discussion and Future Perspectives

Chapter V – Appendix

Chapter I

Introduction

A Brief Overview of the Immune System

During millions of years, organisms have coped with a physical and hostile environment populated by a wide variety of pathogens and toxic substances. In response to these challenges, a multiplicity of defence mechanisms centred on the discrimination between “self versus non-self” have emerged and progressively became more sophisticated amongst species in order to ensure their survival (1). This defence machinery evolved in (jawed) vertebrates to form a complex and dynamic network, called immune system, which includes a myriad of different cell types, receptors and molecular mediators prone to respond towards foreign antigens while avoiding harm the host-tissues (2).

Depending on the specificity of the immune response and the timing of activation, the immune system can be subdivided into two main compartments – innate and adaptive (3). The innate immunity, an ancient system common to all metazoan species, represents the very first line of immune protection by providing a rapid and broad inflammatory response. The innate mechanisms of defence are diverse and range from the non-specific anatomical barriers and molecular mediators (such as complement and defensins) to the selective recognition of highly conserved structural components of microbes and virus through a group of germ-line encoded pattern recognition receptors (PPRs) (4). However, since the number of PRRs became insufficient to recognize the enormous variability and molecular heterogeneity of pathogen-associated molecular structures, the development of new strategies of innate immune evasion by microorganisms became more recurrent. This event created an enormous selective pressure on the organisms, eventually contributing to the emergence of a more advanced mechanism of protection, called adaptive immunity (5)**.** The adaptive immune system is mainly centred on antigen-specific receptors that are expressed by T and B lymphocytes. An interesting feature of the adaptive immunity is the ability to form immunological memory, characterized by the formation of long-lived cells that persist in a quiescent state and rapidly respond upon re-exposure to the same antigen. In contrast with the germline-encoded PRRs, antigen-specific receptors are generated through the somatic rearrangement of different variable (V), diversity (D) and joining (J) immunoglobulin (Ig) gene segments. The random nature of this recombination process allows the

formation of a vast repertoire of different T cell receptors (TCRs) and B cell receptors (BCRs), each with unique specificities for a limitless variety of foreign antigen (6). Still, the existence of such diversity is simultaneously dangerous to the host due to the formation of specific TCRs and BCRs against self-antigens. Thus, the maintenance of an immunological self-tolerant state is ensured by the coordinated action of central and peripheral mechanisms that eliminate or regulate self-reactive lymphocytes (7, 8). Nevertheless, while fundamentally different in many aspects of their biology and function, innate and adaptive immune responses are intimately linked, relying on each other in order to build an effective defence network.

The different cell lineages that compose the immune system are originated from a highly organized process termed hematopoiesis (9). The establishment of the hematopoietic system begins early during embryogenesis with the first cells arising in the yolk sac. This event represents the most primitive wave of hematopoiesis and mainly involves the production of erythrocytes whose function is to aid tissue oxygenation during embryo development (10, 11). Nonetheless, the primitive hematopoietic wave only exists transiently and is rapidly replaced by a definitive wave of hematopoiesis characterized by the emergence of self-renewing hematopoietic stem cells (HSCs). HSCs, which provide a long-term source of all immune lineages, are first detected in the aorta-gonad-mesonephros (AGM) region of the embryo (9, 11). From this anatomical place HSCs colonize the fetal liver, where they undergo active expansion, and ultimately migrate to the bone marrow (BM) during the late phase of embryogenesis, where hematopoiesis is established throughout life (9, 11). Within the BM, distinct stromal cells populations form specialized niches (endosteal, vascular and reticular) that are responsible for HSCs maintenance and differentiation through the provision of key regulatory signals (12). Through intermediate lineage-restricted progenitors, HSCs can give rise to two main immune branches: lymphoid and myeloid. The lymphoid lineage includes T, B and natural killer (NK) cells, while the myeloid is comprised by monocyte/macrophages, granulocytes and megakaryocytes (13). Interestingly, although dendritic cells (DCs) are also of hematopoietic origin, their lineage affiliation remains unclear since they can differentiate from both lymphoid and myeloid committed progenitors (13). Remarkably, while most of the abovementioned hematopoietic cells differentiate

within the BM, the generation of a diverse and self-restricted repertoire of T lymphocytes require unique microenvironments exclusively found in the thymus.

Thymus: The Cradle of T Cell Immunity

Originally described by Galen of Pergamum (130-200 AD), the thymus has remained an enigmatic organ for centuries, surrounded by many queries regarding to its physiology and clinical relevance (14). The importance of the thymus was only documented in 1961 by Jacques Miller's studies on virus induced-leukaemia in neonatal thymectomyzed mice. His observations settled an intense dispute, ending with the recognition of the thymus as a non-redundant lymphoid organ of the immune system with a chief role in the development of T lymphocytes (15).

Evolutionary, the appearance of a prototypical thymic structure, as we know it nowadays, coincides with the introduction of the VDJ recombination system in lymphocyte development in Gnathostomata (jawed vertebrates). Since the stochastic mechanism of VDJ recombination amplifies exponentially the chance of developing self-reactivity, it is postulated that the thymus evolved as a physical separated organ with the ability to provide a sophisticated quality-control mechanism for tolerance induction (16, 17). The existence of a thymus is a common trait of all jawed vertebrates, although in jawless such as the lamprey larvae, a thymus-like structure (termed thymoid) has been identified (18). The origin of the thymus from specialized pockets of the foregut endodermal tube, termed pharyngeal pouches, is a conserved feature among different thymus-bearing vertebrates (17, 19). Still, the anatomical location and number of thymic lobes per animal can strikingly diverge between species. For instance, sharks exhibit five thymus pair, with each lobe arising from the second to six pharyngeal pouches, while many mammals only have a bilobated thymus that emanates from the third or fourth pharyngeal pouch (17). Nevertheless, irrespectively of these differences, the unique function of the thymus in supporting the development of a diverse and self-tolerant T lymphocyte population is a common characteristic across all jawed vertebrates.

In mammals, the thymus is a bilobated structure that is situated in the superior anterior mediastinum, above the heart. Each lobe is anatomically organized in two distinct compartments, an outer cortex and inner medulla, a characteristic that is

well conserved across thymus-bearing species **(Figure 1A)** (19). The ability of this organ to support T cell development, or thymopoiesis, relies on an organized three-dimensional network of thymic stromal cells that provides the essential molecular cues required for differentiation of T cell precursors, also known as thymocytes, from BM-derived hematopoietic progenitors (20). Thymic epithelial cells (TECs) are the major constituent of the thymic stroma and are categorized into cortical (cTECs) and medullary (mTECs) subtypes, according to their spatial location, morphology and functional proprieties (21). The composition and cellularity of the thymic epithelium is considerably variable over time, with TECs representing less than 1% of the total thymic cellularity during adulthood (22). Other important elements of the thymic stroma include endothelium, mesenchyme and cells with a hematopoietic origin, such as dendritic cells, macrophages and B cells **(Figure 1B)** (23). Together, they are responsible to support key events of thymopoiesis, including migration, survival, proliferation, commitment and selection of developing thymocytes.

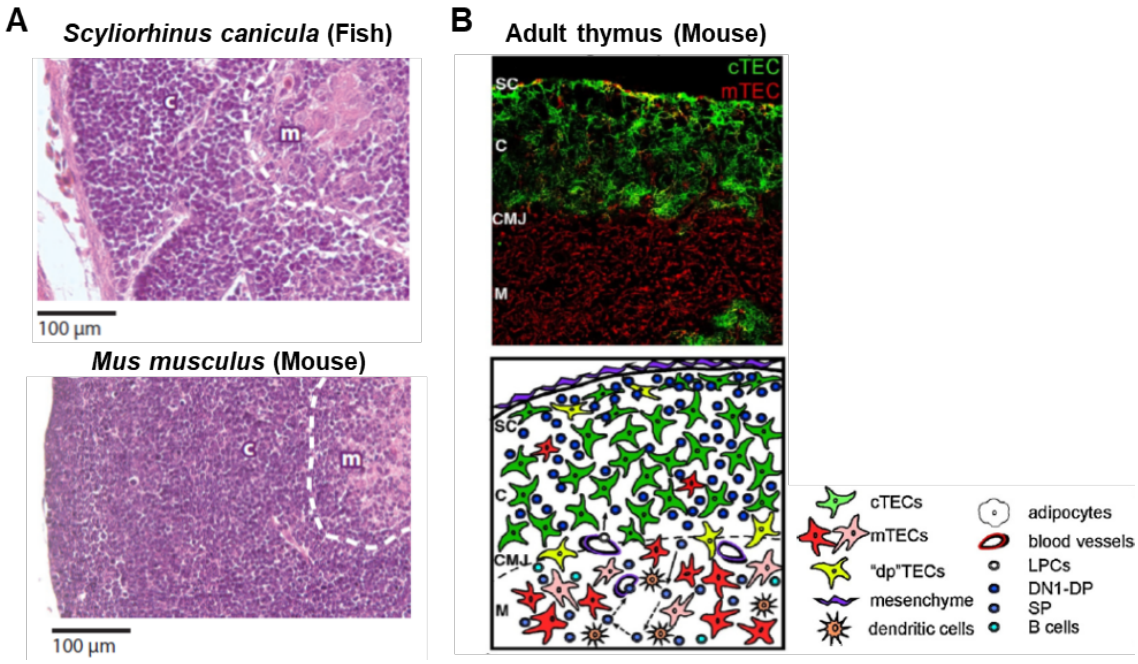

Figure 1 – Structural organization and cellular composition of the thymus. (A) Histological comparison of the thymic morphological architecture in cartilaginous fishes (Top image - *Schyliorhinus canicula*) and mouse (Bottom image - *Mus musculus*). The cortical (c) and medullary (m) compartments are identified by hematoxylin-eosin staining. **(B)** Top: Representative immunofluorescence analysis of thymic section illustrates the anatomical disposition of the different stromal subsets across the thymus (SC - subcapsular, C - cortex, M – medulla, and CMJ – cortico-medullary junction zones). Sections were stained with a cTEC marker (Ly51, green fluorescence) and mTEC marker (Keratin 5, red fluorescence). Bottom: Illustrated cartoon depict the general cellular composition of the thymic stroma in the adult thymus. Images adapted from (19, 28)

Despite the importance of the thymus in maintaining a self-tolerant and pathogen-reactive peripheral T cell compartment through the continual production of naive T lymphocytes, its function is not constant and slowly wanes with aging (24).

This phenomenon is known as thymic involution (disclosed later in this thesis) and represents one of the hallmarks of the ageing immune system in all thymic-bearing species (25). It is mainly characterized by a progressive disruption of the normal cortical and medullary thymic architecture, alongside with alterations on the cellular composition of the thymic stroma (26). As a result, the capacity of the thymus to support thymopoiesis becomes gradually compromised, leading to a reduction in the number of thymocytes and T cell output, thereby contributing for a reduced immunosurveillance. Although aged-related thymic involution does not represent a life threatening event, it can indirectly contribute for an increased susceptibility to infectious diseases, neoplastic and autoimmune disorders during elderly (27, 28).

Regulation of T Cell Development by the Thymic Stromal Microenvironments

Unlike the majority of the hematopoietic lineages, the generation of a diverse pool of self-tolerant and non-self reactive T cells occurs inside the unique niches of the thymus. Two main lineages of T cells are produced in the thymus and can distinguished based on the distinct expression of αβ or γδ TCR complexes, with the development of αβ T cells standing as the predominant pathway (20). While γδ T cell differentiation remains elusive, the differentiation of prototypical αβ $CD4^+$ and $CD8^+$ T cells is more general understood and will be detailed below. The differentiation of T lymphocytes is a highly orchestrated process that involves a series of developmental checkpoints that function to select cells bearing major histocompatibility complex (MHC)-restricted TCR while limiting the production of cells bearing non-functional or autoreactive TCRs. As consequence of such rigorous events, only 1-3% of thymocytes are able to survive and migrate into the peripheral lymphoid organs (29). As the thymus does not contain self-renewal progenitors, the long-term maintenance of thymopoiesis is assured by the recruitment of hematopoietic-derived precursors that are present in the fetal liver and BM at different phases of embryonic and postnatal life (30). Yet, thymic colonization is not a continuous event, but rather a temporally regulated phenomenon that occurs in discrete waves, depending on the availability of dedicated thymic-seeding progenitor niches (31, 32).

The precise nature of the thymic seeding progenitors (TSPs) still remains questionable. Efforts to uncover their identity have been hampered by the fact that several phenotypically distinct BM-derived progenitors possess T cell lineage potential (33). A more complex scenario emerged with the discovery that early thymic progenitor (ETPs) in the thymus possess multiple lineage potential (both myeloid and lymphoid), rather than a T cell lineage restriction, and are molecularly related to distinct BM-derived progenitors (34). The initial wave of thymic colonization occurs very early during mouse embryogenesis (embryonic day 12) (35) and is mediated by a chemotactic gradient established through the intrathymic production of three main chemokines, CCL21, CCL25 and CXCL12 (36–38). As this recruitment occurs prior to the vascularization of the thymic rudiment, TSPs home into the thymus by transversing through the surrounding mesenchymal capsule (39, 40). Nonetheless, in the post-natal thymus, once the vasculature is well established, T cell progenitors enter across blood vessels located nearby the cortico-medullary junction (CMJ) (41). At this stage, in addition to the cooperative action of chemokine signals (36), thymic colonization is also facilitated by the expression of adhesion molecules on the thymic endothelium, such as P-selectin (42, 43).

Upon arrival into the thymus, thymocyte progenitors undergo T lineage specification through a series of distinct developmental checkpoints **(Figure 2)**. At this stage, as these cells lack the expression of the CD4 and CD8 co-receptor, they are referred as double-negative (DN) thymocytes. By monitoring the expression profile of the surface markers CD44 and CD25, DN thymocytes can be further divided into four phenotypically distinct sub-stages of maturation, from DN1 to DN4. During their developmental progression, DN thymocytes are relocated outwards from the CMJ to the sub-capsular region of the cortex. Different chemokine receptors, such as CXCR4, CCR9 and CCR7, are important for the outer movement of DN thymocyte in response to respective CXCL12, CCL25 and CCL21 gradients (20, 44). Furthermore, the directional migration of DN cells across the thymic cortex is further facilitated by integrin-mediated cell-cell interactions. Adhesion molecules, such as $\alpha_4\beta$ integrins expressed by DN thymocytes and vascular cell adhesion molecule-1 (VCAM-1) expressed by cTECs have been implicated in this process (45).

The most immature population of thymocytes, known as DN1 ($CD44^+CD25^-$) cells, persists in very restricted regions of the CMJ during the first 10 days of their intrathymic residence (46). Transition into the DN2 ($CD44^+CD25^+$) stage is marked by the irreversible commitment of thymocytes towards the T cell lineage. This event involves the repression of alternative gene expression programs typical of other hematopoietic lineages and is promoted by the Notch-signalling pathway, via Dll4-Notch1 interaction (47, 48). At this stage, the recombination activating gene (RAG) enzymes -1 and -2 promote the VDJ rearrangement of the γ-, δ-, and β- TCR locus (49, 50). Moreover, progression to the DN2 stage coincides with thymocyte migration towards the outer cortex and is characterized by their active proliferation (41). The expansion and survival of these cells relies on the provision of stromal derived cytokines, in particular, stem cell factor (SCF or kit ligand) and interleukin 7 (IL-7) (30). The productive rearrangement, assembly and signalling through the γδ TCR allow the differentiation of a minor DN3 thymocyte fraction towards γδ T cell lineage (51). By the other hand, thymocytes that succeed in generating a productive in-frame *Tcrβ* rearrangement begin to assemble at its surface a pre-TCR complex, which is composed by a β-chain and an invariant pre-TCRα chain associated with CD3 signalling molecules (52). The assembling of a functional pre-TCR complex is assured by a critical checkpoint known as β-selection (53). During this process, signalling through the pre-TCR, along with Notch1 and CXCL12-derived signals (54–56), rescue DN3 ($CD44^-CD25^+$) thymocytes from apoptosis, stimulate proliferation, cease the TCRβ locus recombination (allelic exclusion) and promote cell differentiation towards the DN4 ($CD44^-CD25^-$) stage (20). Following β-selection, thymocytes initiate the rearrangement of the TCRα locus and invert their migration towards the medulla while progress through a transient state as immature CD8 single positive (ISP8) cells (20). Transition to the double positive stage is characterized by the upregulation of CD4 and CD8 co-receptors and the expression of a fully assembled αβ TCR. The $CD4^+CD8^+$ DP population encompasses the majority of developing thymocytes (~80%) and represent the unselected repertoire of T cells (29, 57).

Still in the cortex, DP thymocytes are subsequently screened for the capacity of their newly generated αβ TCR repertoire to recognize endogenous peptides in the context of self-major histocompatibility complex (MHC) molecules expressed by

cTECs (58, 59). It is considered that the specificity and binding strength of the TCR with peptide-MHC complexes (pMHC) dictates the fate of DP thymocytes. If these interactions occur within a threshold of low affinity, DP thymocytes receive signals for survival and differentiate into the single positive (SP) stage, in a process known as positive selection. This crucial checkpoint assures the selection of cells that bear potentially useful and self-MHC restricted TCR. On the other hand, high affinity interactions between TCR-pMHC lead to the apoptotic deletion of self-reactive thymocytes. Nonetheless, as most of the DP thymocytes express αβ TCR that are incapable of interact properly with self-MHC molecules, they undergo "death by neglect" through a programmed cell death process (29). Consequently, only 3-5% of developing thymocytes are able to progress beyond this developmental checkpoint at the DP stage (60).

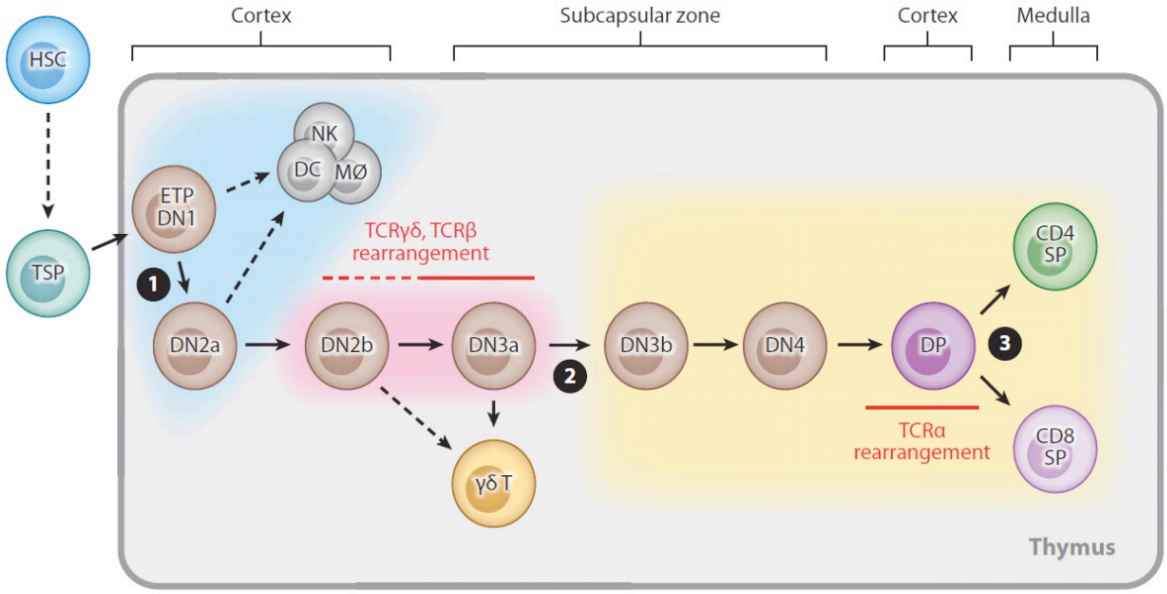

Figure 2 – Schematic overview of T cell development. Once within the thymus, thymic seeding progenitors undergo a complex differentiation pathway that encompasses cell migration and differentiation across distinct niches and checkpoints until they become functional mature SP thymocytes. Critical checkpoints of T cell development are depicted by circled numbers: 1) T cell lineage commitment through the action of the Notch signalling pathway; 2) β-selection checkpoint and 3) Positive and negative selection, where DP cells progress into either the CD4 SP or CD8 SP thymocyte lineage. Image adapted from (270)

The lineage-specific differentiation of DP thymocytes into the CD4 or CD8 SP stage is mostly determined by the specificity and restriction of the TCR to MHC molecules. DP thymocytes whose TCR recognize MHC class II (MHC-II) within the limits of moderate affinity differentiate into $CD4^+$ SP cells, while cells that express TCR recognizing MHC class I (MHC-I) commit into the $CD8^+$ SP lineage. As this decision making process is not completely understood, different models have been proposed over the years. The most recent one, known as "kinetic signalling", implies

that is the duration of the TCR-pMHC interaction rather than signal strength that dictates CD4/CD8 lineage choice (61). According to this model, TCR-signalled DP thymocytes start by terminating *Cd8* gene expression and progress through an intermediate stage characterized by a $CD4^+CD8^{low}$ phenotype (62, 63). At this point, lineage decision starts to take place depending on whether TCR signalling ceases or persists. During MHC-II restricted selection, persistent TCR signals foster $CD4^+CD8^{low}$ thymocyte differentiation towards the $CD4^+$ lineage (64). Contrariwise, the progressive reduction on CD8 cell surface levels contributes for the disruption of the MHC-I restricted TCR interaction. Ablation of TCR signalling enables intermediate thymocytes to become responsive to IL-7-derived signals, which supports "coreceptor reversal" and commitment to the CD8 differentiation lineage (64, 65). Several transcription factors have been identified as key modulators of CD4/CD8 lineage choice. Th-POK (T-helper inducing POZ/Kruppel-like factor), whose expression is upregulated in intermediate thymocytes by persistent TCR signalling, is defined as a master regulator of CD4 T cell differentiation and acts in part by repressing the expression of CD8 lineage genes (66, 67). On the other hand, RUNX3 (runt-related transcription factor 3) is critical for CD8 T cell lineage commitment. Its expression occurs following TCR signal cessation in response to IL-7 derived signals (65) and acts by promoting the silencing of the *Cd4* gene expression and block of Th-POK expression (68, 69). The regulatory negative loop involving Th-POK and RUNX3, where they reciprocally prevent each other's expression, is crucial to reinforce lineage choice (70). Additional factors, such as TOX (thymus high mobility group box protein) and GATA3 (GATA-binding protein) also appear to be important in thymocyte differentiation, particularly in CD4 lineage choice (71–73).

Following positive selection, thymocytes begin to migrate from the cortex into the medulla. This relocation event occurs as result of several changes in integrin and chemokine receptor expression profile in post-positively selected cells (44). TCR-signalled DP thymocytes start by upregulating their expression levels of CCR7 and migrate towards to the medulla in response to a chemotactic gradient established by the CCR7-ligands (CCL19/CCL21) (74, 75), mainly produced by mTECs (76, 77). Additionally, other studies have also revealed the contribution of plexinD1 and CCR4 in governing the optimal cortical-medullary transition of post-selected

thymocytes (78, 79). In the medulla, SP thymocytes are scanned for the presence of high-affinity TCR to self-antigens within their positively selected TCR repertoire. For that sole purpose, mTECs express distinct clusters of tissue-restricted antigens (TRAs) through the entire medullary region. This unique characteristic, known as promiscuous gene expression (pGE), allows the premature exposure of SP thymocytes to protein-derived antigens which are otherwise limited to specific tissues within the body (80). mTEC-dependent pGE program is partially under the control of the transcription factor autoimmune regulator (Aire) and the newly identified FEZ family zinc finger 2 (Fezf2) (81, 82). Direct presentation of mTEC-derived TRA or cross-presentation by thymic dendritic cells is responsible to shape a self-tolerant T cell repertoire (83, 84), by promoting the clonal deletion of SP thymocytes bearing potentially autoreactive TCRs. This process is named negative selection, and together with positive selection, corresponds to two critical checkpoints that fine-tune T cell repertoire. Alternatively, a fraction of self-reactive $CD4^+$ SP cells are rescued from clonal deletion and undergo differentiation into a specialized regulatory subset of T cells (85), characterized by the expression of the transcription factor Foxp3 (86). T regulatory cells (Tregs) are central to the maintenance of immune homeostasis, namely in the prevention of spontaneous autoimmunity (87). Thus, both Treg differentiation and negative selection represent two distinct, but interconnected, events in the establishment of central tolerance. Thymocytes that continue through the selection process display a medullary residency of approximately 4-5 days (88). During this period, they undergo receptor tuning and terminal maturation steps, transitioning from a semi-mature $CD69^{hi}CD24^{hi}CD62L^{low}Qa2^{low}$ to a mature $CD69^{low}CD24^{low}CD62L^{high}Qa2^{high}$ phenotype (89), before acquiring the functional competences to join the peripheral naïve T cell pool. Interestingly, the functional role of the medullary niche extends beyond negative selection and Treg generation as it was also shown to nurture the differentiation of unique non-conventional T cell lineages, including the fetal-derived $V\gamma5^+$ $\gamma\delta$ thymocytes and invariant natural killer T (iNKT) cells (90, 91).

The egress of T cells from the thymus is under the tight control of the sphingosine-1-phosphate receptor 1 ($S1P_1$), a G-protein coupled receptor (GPCR) expressed on SP thymocytes (92, 93). Increased surface expression of $S1P_1$ is only observed on mature SP cells following TCR signalling termination due to the

increased transcriptional activity of Krüppel-like factor 2 (Klf2) (94). As result, fully mature SP thymocytes are able to sense the chemotactic gradient established by the physiological ligand of $S1P_1$, the sphingosine-1-phosphate (S1P), whose concentration is higher in circulation than within most tissues (44). This bioactive sphingolipid is mainly produced by pericytes, a neurocrestal derived population positioned nearby the CMJ (95), where it functions as an egress signal and is maintained at very low levels in other thymic regions owing to the action of dendritic cell-specific S1P lyases (96) or TEC/endothelial-derived lipid phosphate phosphatase 3 (LPP3) enzyme (97). Additionally, the CCR7/CCL19 and CXCR4/CXCL12 axis have been shown to contribute for fetal thymocyte egress (98, 99), although they appear to be dispensable in the adult thymus. Hence, evidence might suggest the existence of a developmental switch between CCR7/CXCR4-dependent and S1P1-mediated emigration throughout development.

The Basics of Thymic Organogenesis

The establishment of functionally competent thymic epithelial microenvironments is a critical prerequisite for the development of a diverse and self-tolerant peripheral T cell compartment (21). Thymic organogenesis is a well-orchestrated process involving the synchronised crosstalk of cells from all three embryonic germ layers (endoderm-derived epithelium, ectoderm-derived neural crest (NC) mesenchyme, mesoderm-derived hematopoietic cells) under the influence of distinct molecular programmes (100). The murine thymus development can be temporally divided in two main phases (**Figure 3**) (101). The early organogenesis phase (from embryonic day (E) 9.5-12.5) comprises a series of morphogenetic events such as positioning, initiation and outgrowth of the thymic anlage, as well as detachment and initiation of the migration of the thymus to its final anatomical position (100). This stage is also characterized by the initial differentiation and proliferation of the thymic epithelium in a thymocyte-independent manner (102, 103). By the other hand, the late phase of thymic organogenesis (from E13-birth) essentially relies on signals derived from developing thymocytes to further support the maturation of the thymic epithelium into distinct cortical and medullary microenvironments (104, 105).

The early ontogeny of the murine thymus is intimately connected with the formation of the parathyroid gland, with both organs emerging as a shared structure from the third pharyngeal pouches (3PP) of the foregut endodermal tube around E11 of gestation (106). The patterning of specific parathyroid and thymic domains within the common primordium occurs prior to formation of the organ rudiments and is critically dependent on two lineage determinants, Glial cells missing homolog 2 (Gcm2) and Forkhead box N1 (Foxn1), respectively. The transcription factor Gcm2, a key regulator of parathyroid differentiation, is first expressed in the anterior-dorsal region of the 3PP epithelium as early as E9.5 (107, 108). By contrast, the expression of Foxn1, a chief transcription factor involved in the cell-autonomous differentiation of TECs, is only detected from E10.5 onwards at the posterior-ventral side of the pouch (107, 109). Following the establishment of two molecularly distinct organ domains, the common parathyroid-thymus primordia proliferates and detaches from the lateral surfaces of the pharynx around E11.75, in a process that is mediated by apoptotic cell death (110). At E12.5, the thymus and parathyroid gland separate from each other and begin to migrate towards their final anatomical locations at the mediastinum anterior-ventral to the heart (thymus) and adjacent to the thyroid (parathyroid) (100). Intriguingly, a small fraction of mice and humans has been shown to possess an accessory thymus that is located in the cervical region of the neck (111–113). The murine cervical thymus resembles the thoracic counterpart in many molecular and functional aspects, as it exhibits a normal cortex and medulla organization with the capability to support T cell differentiation (112, 113). Yet, organogenesis of the cervical thymus does not happen in parallel with the thoracic structure, as the onset of Foxn1 expression in the cervical anlage only occurs around E15 of gestation (114). Recent data propose two discrete developmental pathways for TECs within the cervical thymi: One possibility is that TECs arise from uncommitted endodermal cells that lag behind during the physical segregation of the parathyroid-thymus domains. Alternatively, they might develop from the transdifferentiation of parathyroid-fated cells (115).

During embryogenesis, a population of neural-crest-derived mesenchymal cells (NCCs) migrate to the third pharyngeal arch and progressively delimits the thymic epithelial anlage (116). NCCs, which contribute to the formation of the thymic mesenchymal capsule and surrounding vasculature (117, 118), also act as key

regulators of many aspects of thymus development and morphogenesis. The surrounding NCC-derived mesenchymal cells influence the proliferation and homeostasis of the thymic epithelium along embryogenesis through the provision of fibroblast growth factors (FGF) -7 and -10 (119), as well as retinoic acid (RA) and insulin-like growth factor (IGF) -1 and -2 (120, 121). Studies performing NCC-specific ablation established its functional importance in regulating the correct patterning of the third pharyngeal pouch endoderm into thymus-parathyroid domains (122), although the molecular mechanisms involved still remain unclear. Additionally, signals provided by NCCs have been implicated in the separation of the thymus from the pharynx and its subsequent migration to the thoracic cavity (123, 124). A role for NCC-derived mesenchyme in supporting the maturation of thymocyte precursors beyond the DN1 stage has all been proposed in experiments using reaggregate thymic organ cultures (RTOC) (125, 126). Although it remains unclear how mesenchymal cells influence T cell development, a possible mechanism might implicate components of the extracellular matrix (ECM) that present and concentrate essential soluble growth factors, such as cytokines (127).

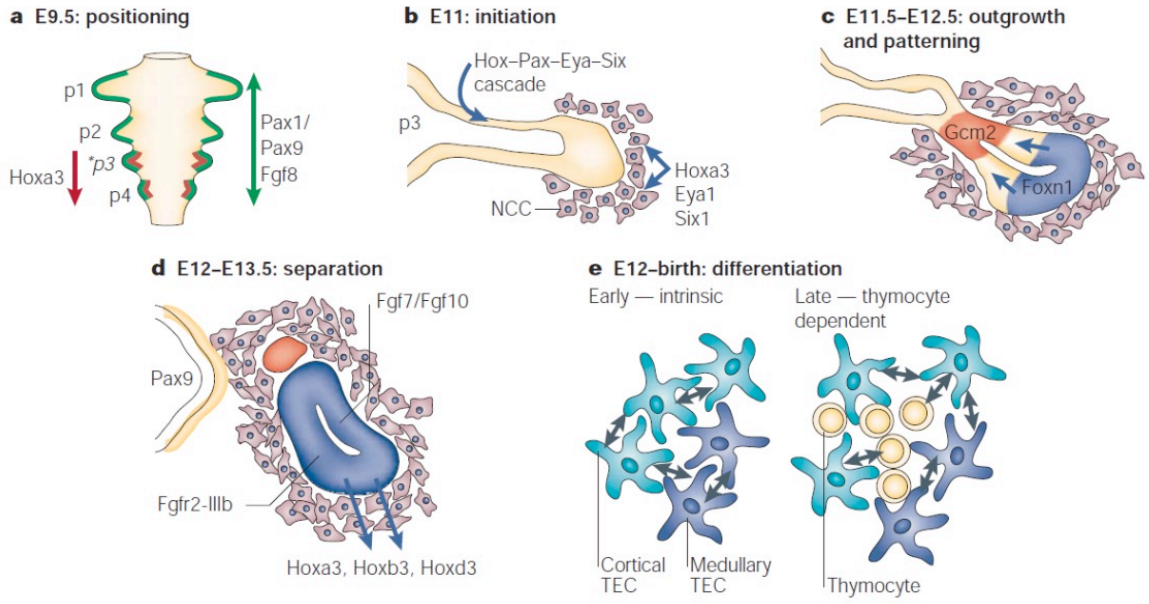

Figure 3 – General overview of thymic organogenesis. The third pharyngeal pouches emerge on the lateral surfaces of the foregut around E9.5. The establishment of a common thymus-parathyroid primordia can be detected at E11, with the patterning of two specific domains characterized by the expression of Gcm2 and Foxn1. NCCs migrate to the pharyngeal pouch and surround the common primordium where it influences the thymic anlage growth, separation from the pharynx and migration into its final anatomical location. Around E12.5, late organogenesis stage begins, with the interactions between thymocytes-TECs contributing for the further patterning of the thymic microenvironment into cortex and medulla. Image adapted from (106)

In the recent years, much progress has been made in uncovering the complex molecular network that controls the establishment and early patterning of the thymic

primordium. A number of transcription factors, including homeobox A3 (Hoxa3), eyes absent 1 homologue (Eya1), paired box gene 1 (Pax1), Pax9, sine oculis-related homeobox 1 homologue (Six1), Six4 and T-box protein 1 (Tbx1) have been associated with this regulatory network (128–134). Mutations in any of these genes lead to thymus aplasia or hypoplasia, or a complete failure of the thymic anlage to migrate towards its final anatomical location. Nonetheless, as these transcription factors are both expressed by the pharyngeal pouches and NCC-derived mesenchyme, their loss of function causes pleiotropic defects which makes challenging to attribute a direct role of these genes in thymus development (100). Hence, in order to understand their precise contribution during thymic ontogeny, experimental systems employing TEC-specific and temporal controlled gene deletions may be required.

Among the hierarchy of transcription factors involved in thymic organogenesis, Foxn1 is the most significant one as it remains the only gene described to be indispensable for TEC development (135). Foxn1 is a member of the forkhead box transcription factor and contains a winged-helix/forkhead DNA-binding domain and a transcriptional activation domain (136). Mice that lack the Foxn1 gene are referred as nude and they are athymic, since the thymic anlage is unable to differentiate in a functional TEC compartment and become colonized with lymphocyte precursors (137, 138). A small, alymphoid cystic thymic rudiment persists into adulthood which results in the lack of functional T cells and severe immunodeficiency (135). Interestingly, thymic organogenesis stills proceeds normally in nude mice until E11 with the formation of the common thymus-parathyroid primordium, suggesting that Foxn1 is not involved in the initial thymic/parathyroid fate specification (137). The transcription factor Foxn1 is found in all jawed vertebrates and is believed to appeared during evolution as result of the duplication of the Foxn4 gene (139). Although with a nearly identical protein structure, a notable feature of Foxn1 is the presence of distinct DNA binding domains when compare to its ancient paralog Foxn4 (139). Appearance of this gene might have allowed the expansion of the ancient genetic network regulating thymopoiesis, which forced the primordial thymus to become more specialized in coordinating exclusively T cell development rather than being a bipotent lymphopoietic organ supporting both T and B cell differentiation (140). In this regard, apart of being essential for the differentiation and

identity of the thymic epithelium, Foxn1 is has been shown to be a crucial transcriptional regulator of downstream targets that are important to support T cell development. Among these are genes that contribute for antigen processing and presentation, lymphocyte migration and T-cell lineage commitment (e.g. - β5t, CCL25 and Dll4) (141). At present, the mechanism that induces and maintains Foxn1 expression in TECs is far from being understood. Some evidence suggests that Bone morphogenetic protein (Bmp) and Wingless-related MMTV integration (Wnt) signals might regulate Foxn1 expression (142–144), even though the role of the Wnt family remains to be verified *in vivo*. Additionally, recent data also demonstrated that retinoblastoma (Rb) family of proteins are able to transcriptionally regulate Foxn1 expression (145). Understand the mechanisms that regulate Foxn1 is of pivotal importance, as it will permit the development of novel strategies to manipulate the thymopoietic capacity of the thymus under different physiological settings.

Thymic epithelial cells: Establishing the foundations of T cell development

In recent years, TECs have been extensively studied with the purpose of gaining a better understanding about the precursor-progeny relationship and the cellular and molecular mechanisms behind the establishment of functionally competent TEC microenvironments.

The partitioning of TECs into specialized subpopulations of cTECs and mTECs, relies on a highly dynamic differentiation process from epithelial precursors that is initiated early during fetal development and proceeds throughout post-natal life (146). In the past, there were some conflicting interpretations about the precise origin of the thymic epithelium. Several studies proposed a “dual germ layer origin” model were the cortical and medullary microenvironments result from the folding of an ectodermal layer around the endoderm (147, 148). However, the prevailing view supports that the thymic epithelium originates solely from progenitors with an exclusive endodermal origin (110). Yet, such studies did not clarify whether these two functionally distinct TEC lineages stem from a common bipotent progenitor or, alternatively, from lineage-committed progenitors. The existence of common

bipotent TEC progenitors (TECp) was first suggested by the identification of a minor TEC population co-expressing both cortical and medullary markers (149, 150). These putative TEC progenitors, identified by the co-expression of Keratin (K) 5 and 8, were located in the vicinity of the cortico-medullary junction in the adult thymus (150). Although was postulated their involvement in the maintenance of the $K5^+$ mTEC and $K8^+$ cTEC compartment, there was no direct evidence supporting the idea that such population were bipotent TECp. Years later, the existence of bipotent TECp and lineage relationship between the two main TEC subsets was finally addressed in two complementary reports that took advantage of lineage-tracing systems (151, 152). First, single yellow fluorescent protein (YFP)-labelled E12.5 TECs were shown to contribute for both cTEC and mTEC lineage when microinjected in a host thymus microenvironment. Interestingly, contribution to a single cTEC or mTEC lineage was markedly absent, indicating that most, if not all, E12 TECs might own bipotent activity (151). In the second study, using a gain-of-function strategy where a conditional mutant allele of Foxn1 was reverted to wild-type function in individual TECs of nude mice, it was shown that bipotent TECp can persist in the postnatal thymus and contribute for the generation of functional thymic niches (152). Furthermore, additional studies indicate that the size of the Foxn1-positive TEC progenitor pool is critical to determine the overall thymopoietic capacity of the thymus (153). These observations support the notion that whereas bipotent progenitors arise during thymic organogenesis independently of Foxn1, its presence is critical to initiate the core transcriptional program involved in TECp differentiation and progression into cortical and medullary TEC lineages **(Figure 4A)**.

Despite the described major advances, the robust isolation and phenotypic characterization of TEC precursors has been difficult to attain due to the paucity of cell specific markers. Initial studies suggested MTS24, a monoclonal antibody that recognize the orphan protein placenta-expressed transcript-1 (Plet-1) (154), as a putative marker to identify embryonic TEC progenitors (155, 156). $Plet1^+$ TECs were shown to possess the capacity to generate a fully functional competent and organized thymic microenvironment, compartmentalized into cortex and medulla, whereas the $Plet1^-$ subset was unable to establish such TEC niches and functional thymus. Plet1-expressing TECs are first detected as early as E12 and progressively becomes rare with age, as in the postnatal thymus its expression is limited to small

subpopulations located in the thymic medulla and cortico-medullary junction (155, 156). Nonetheless, in the subsequent years, reassessment of TEC progenitor potential using MTS24 revealed that its expression was not restricted to a progenitor population as E14 MTS24^{-} TECs also had the potential to generate a functional thymus (157). Additionally, E18 MTS24^{+} cells displayed little capacity to build a competent thymic graft when transplanted into the kidney capsule of nude mice, thereby arguing against the usage of such marker to exclusively identify TEC bipotent progenitors (157). More recently, several reports described the existence of a transitional stage where embryonic TEC progenitors might be characterized by the expression of cTEC-associated traits, including CD205, β5t and IL7^{YFP} (158–160). These observations paved the way to establish the "serial progression" model of embryonic TEC development, in which bipotent progenitors transit through a phase where they express a cTEC footprint prior to the emergence of mTECs **(Figure 4B)** (161). Supporting the notion that TEC progenitors might nestle within the thymic cortex, different studies demonstrated the ability of distinct postnatal and adult cTEC subsets to form colonies with self-renewal capacity *in vitro*, and to generate both cTEC and mTEC lineages in RTOCs (162, 163). Despite the remarkable progress in the characterization of TEC precursors, there is still a lack of consensus regarding their molecular and phenotypic characteristics in the embryonic and adult thymus. Additionally, distinct TEC precursors are all defined at the population level, as they cannot be yet recognized as single cell. Future studies involving genome-wide analysis at a single cell level would be crucial to better define the nature and specific molecular signature of TEPs in the embryonic/postnatal/adult thymus.

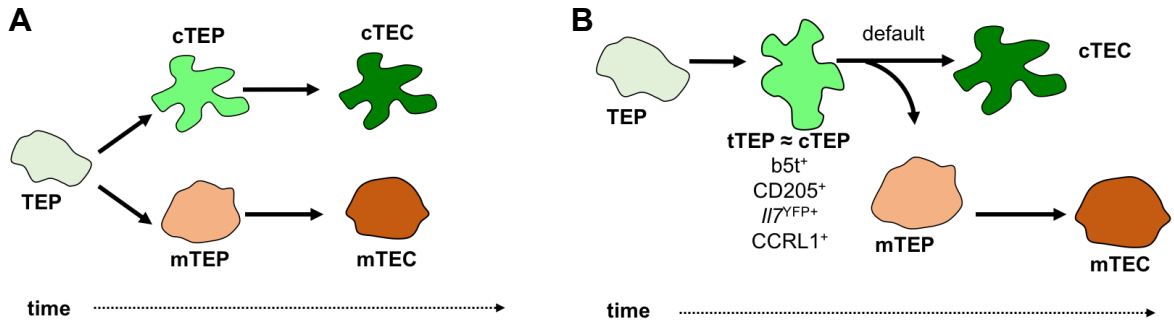

Figure 4 – Developmental models of thymic epithelial cells. (A) The functional cortical and medullary compartments of the thymus are established via lineage-committed cTEC (cTEP) and mTEC (mTEP) progenitors that share a common origin from an uncommitted bipotent TEC progenitor (TEP). In the asymmetric model, cTECs and mTECs follow independent differentiation pathways. **(B)** In the serial progression model, TEPs undergo through a transitional stage that closely resembles with cTECs, either at phenotypic and molecular level, prior to the final commitment into the cortical and medullary lineage fate.

Specialization of the thymic microenvironment – Development and function of cTECs

The development of cTECs constitutes a primitive hallmark event in the establishment of a functionally competent microenvironment, essential for attraction, lineage specification and subsequent selection of T cell precursors. Cells from the cTEC lineage can be defined by the phenotypically expression of specific surface markers such as K8 and K18, Ly-51 (also known as BP1/CD249), CD205 (also known as DEC-205) and the atypical chemokine receptor 4 (ACKR4, also known as CCRL1). Furthermore, functional molecules such as Dll4, high levels of IL-7 and β5t may be also used to aid in the identification and characterization of cTECs (164). Apart of these, the cortical epithelium also shares some classical markers with cells from the mTEC lineage, including the epithelial cell adhesion molecule (EpCAM), MHC-II and CD40. Interestingly, the expression levels of some of these markers revealed the existence of a certain heterogeneity within the cTEC compartment, with discrete subsets being defined according to the broad expression of MHC-II, CD40, Dll4 and IL-7 (22, 160, 165, 166).

In contrast to our knowledge regarding mTEC development (covered later in this thesis), the intermediate steps in cTEC differentiation downstream of bipotent progenitors and the mechanism underlying their homeostasis are still poorly comprehended. Initial studies focusing on the precursor-product relationship of the cTEC lineage revealed that TECs exhibiting a cortical phenotype (K8-positive) are already detected prior to the colonization of the thymic rudiment by lymphocyte progenitors at E11.5 (103). Interestingly, the emergence of this population is not compromised in mice with a profound arrest in early T cell development (*Rag2*$^{-/-}$*Il2rg*$^{-/-}$; CD3εTge26 and Ikaros$^{-/-}$) (103), supporting the notion that the initial stages of cTEC differentiation can proceed in a thymocyte-independent fashion. Still, during late stages of ontogeny and in the absence of thymocyte-derived signals, the cortical microenvironment displays a disturbed architecture with little organization and accumulation of TECs co-expressing K5 and K8 (103, 150). Interestingly, the presence of DN3 thymocytes in *Rag*$^{-/-}$ mice is sufficient to promote the formation of a threedimensional reticular cTEC network (104), demonstrating the existence of a DN stage-specific requirement for maturation of the cortical epithelium. However, the

lack of appropriate markers to better define the developmental maturation of the cortical niche has hindered the identification of potential cTEC-restricted progenitors. More recently, the differential expression of the CD205, CD40 and MHCII molecules permitted the identification of presumable lineage-committed cTEC progenitors and established new sequential stages of cTEC development (165). Cells with a $CD205^{+}CD40^{-}$ phenotype are proposed to represent a population of cTEC progenitors that lies in between bipotent progenitors and mature cTECs. In support of this hypothesis, intermediate cTEC progenitors are enriched in proliferating cells and express lower levels of cTEC-specific transcripts such as β5t and cathepsin L, when compared with more mature cortical cells ($CD205^{+}CD40^{+}MHC\text{-}II^{high}$) (165). Foxn1 expression but not thymocyte-derived signals were required for the initial appearance of intermediate cTEC progenitors as early as E12. Yet, the developmental maturation of cTECs, defined by the acquisition of MHC-II and CD40, did not occur in a cell-autonomous manner and was essentially dependent on the presence of DN1-3 thymocytes (165). Along with these observations, our laboratory demonstrated that the progressive acquisition of CCRL1 marked a differentiation stage in cTECs, which also relies on lymphoepithelial interactions with early DN stages, as its expression is partially blocked in *Rag2*$^{-/-}$*Il2rg*$^{-/-}$ mice (167). Still, the precise nature of signals provided by DN thymocytes to cTECs remains to be determined, and further studies to better characterize new developmental checkpoints of the cortical epithelium are warranted.

cTECs play a critical role in orchestrating multiple processes during early stages of thymopoiesis, including homing of T cell progenitors into the thymus through the production of several chemokines (CCL25 and CXCL12), T cell lineage specification via the notch ligand Dll4, and thymocyte precursor expansion via secretion of IL-7 and kit ligand (also known as stem cell factor) **(Figure 5)** (21). The ability of cTECs to support positive selection of developing thymocytes relies on their distinctive protein degradation machinery and antigen-processing capacity (168). These features ensure that the array of self-peptides presented by cTECs during selection are distinct and not redundant from those displayed by mTECs and thymic DCs. Generation of a broad repertoire of MHC-II-associated peptides have been shown to be dependent on the presence of the thymus-specific serine protease (TSSP) and the lysosomal protease cathepsin L, as deficiency in any of these proteases results

in impaired positive selection of $CD4^+$ SP cells (169, 170). Furthermore, positive selection of some MHC-II-restricted transgenic TCRs was shown to be compromised upon ablation of genes involved in macroauthophagy in the thymic epithelium (171), suggesting a role for this pathway in shaping the composition of MHC-II ligandome on cTECs **(Figure 5)**. The cytoplasmatic production of MHC-I-associated peptides is critically dependent on a specialized form of proteasome, termed the thymoproteasome. A unique characteristic of this complex is the incorporation of a cTEC-restricted proteolytic β5t subunit (encoded by the gene *Psmb11*) **(Figure 5)**, which confers an altered proteolytic activity that is distinct from other proteasomes containing other β5 subunits (172). Consequently, the β5t-containing thymoproteasome is capable of generating a unique set of low affinity peptides for MHC-I presentation. Mice lacking β5t exhibit a severe impairment in positive selection of $CD8^+$ SP cells, whereas the $CD4^+$ T cell compartment remains unaffected (172). Moreover, the few $CD8^+$ T cells that are produced in *Psmb11*$^{-/-}$ mice are functionally compromised and present an altered αβTCR repertoire (173). Interestingly, a recent study also provides evidence that thymoproteasome-dependent positive selection can impact on the antigen responsiveness of mature $CD8^+$ T cells in the periphery (174). Hence, through the expression of a unique set of intracellular proteolytic enzymes, cTECs are able to produce a distinct array of selecting self-peptides that are pivotal for the production of a functional and diverse T cell repertoire.

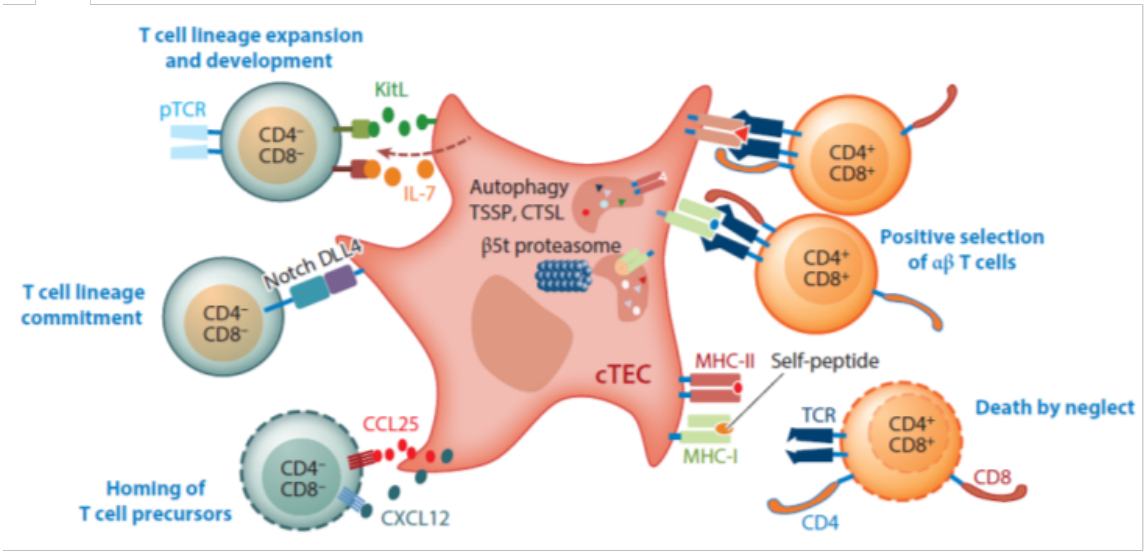

Figure 5 – Multiple functions of cTECs during T cell development. The cortical microenvironment is responsible to support distinct stages of thymopoiesis, including thymocyte progenitor attraction, lineage specification, thymocyte proliferation and positive selection of developing αβ thymocytes. Image adapted from (21)

Setting up the perimeter for tolerance induction – Cellular and functional features of mTECs

1) Associated phenotypic markers and precursor-product relations

Epithelial cells from the thymic medulla can be phenotypically identified by the surface expression of molecules such as K5 and K14 as well as by the binding of antibodies to unknown mTEC-expressing molecules, which includes ERTR5 and mouse thymic stroma 10 (MTS10). Additionally, the lectin Ulex Europeus Agglutinin 1 (UEA-1) also demonstrates selective reactivity with the vast majority of cells from the mTEC lineage. Further phenotypic identification of discrete mTEC subpopulations can be accomplished using an additional panel of molecules encompassing CD40, CD80, MHC-II, Aire, Fezf2 and Involucrin (21, 146).

Gaining a better understanding about the core network lying behind the establishment and function of the mTEC microenvironment should aid in the development of new therapeutic strategies to control autoimmune-related disorders. For that reason, the characterization of the mTEC-committed progenitors as well as the cues involved in lineage-specification and differentiation of the medullary epithelium have been under intense investigation in recent years. The first evidence of mTEC-restricted progenitors came from the observation that the development of distinct clonal islets of medullary epithelium arise from single progenitor cells (175). Subsequent studies identified a mTEC-restricted progenitor population based on the expression of the tight junction components Claudin-3 and -4 (Cld3,4), with Cld3,4^{high} cells being capable to exclusively give rise to mTECs, particularly to a mature Aire-expressing subpopulation, when mixed in RTOC and grafted into nude mice (176). Remarkably, embryonic Cld3,4^{high} TECs implanted in a mTEC-defective thymic microenvironment were capable of re-establish and sustain the generation of a functional medullary epithelium throughout life (177). A further degree of heterogeneity within the mTEC-committed progenitors was revealed with the identification of a fraction of Cld3,4^{high} TECs expressing stage-specific embryonic antigen (SSEA-1) (177), a marker commonly associated with embryonic stem cells (178). This subset was shown to be highly enriched in cells with self-renewable clonogenic capacity that also have the ability to specifically generate mature mTECs

in vivo (177). These findings render the classification of these cells as mTEC stem cells. SSEA1^{+}Cld3,4^{high} TECs are rare in the adult thymus, suggesting that the pool of unipotent mTEC-committed progenitors might become exhausted throughout life. Indeed, adult SSEA1^{+}Cld3,4^{high} TECs demonstrated a markedly reduced competence in generating mature mTEC subsets, when compared with the embryonic counterparts (177). More recently, different studies have demonstrated the existence of some heterogeneity within the pool of mTEC precursors based on additional phenotypic traits. mTEC-committed progenitors expressing the receptor activator of NF-κB (RANK), a key regulator of mTEC differentiation, were described as possible downstream progeny of SSEA1^{+}Cld3,4^{high} mTEC stem cells, although a direct lineage relationship between both subsets remains undefined. RANK^{+} mTEC progenitors are detected within the SSEA1^{-}Cld3,4^{high} subset of the E14 thymus and preferentially give rise to cells of the mTEC lineage (179). Moreover, podoplanin (PDPN)-expressing TECs located at the cortical-medullary junction (jTECs) were classified as mTEC-committed precursors due to their involvement in the generation of nearly half of the adult mTEC compartment (76). While SSEA1^{+}Cld3,4^{high} and PDPN^{+} jTECs were described to derive from embryonic and postnatal cells with a past history of β5t expression (180, 181), the exact precursors of the RANK^{+}SSEA1^{-} Cld3,4^{high} population remains unknown. Hence, further studies are required to better define the precursor-product relationship among different mTEC-committed progenitors and also their spatiotemporal contribution for the maintenance of distinct mTEC lineages along life.

The generation of a functional medullary microenvironment is essential for induction of self-tolerance. mTEC development entails several subsequent stages of maturation, with each of them being defined by the expression levels of specific molecular markers. Early analysis of the mTEC compartment in relation to MHC-II and CD80 expression levels enabled the definition of two main populations, immature/mTEC^{low} (MHC-II^{low}CD80^{low}) and mature/mTEC^{high} (MHC-II^{high}CD80^{high}) subtypes (22). A direct progenitor-progeny relationship was also demonstrated among both subsets (182–184), suggesting that the mTEC^{low} niche harbour the progenitors that contribute for the establishment of the mature medullary epithelium. Over the years, different observations revealed some further degree of heterogeneity within both mTEC sublineages. Although commonly defined as

immature, the mTEC^{low} population has been shown to contain a significant proportion of cells bearing functionally mature features. Among these are included CCL21-expressing cells (77), as well as involucrin-expressing terminally differentiated mTECs (185), a developmental stage that subsist beyond post-Aire expression (186). Likewise, distinct subpopulations within the mTEC^{high} compartment were also recognized based on the differential expression profile of Aire, Fezf2 and osteoprotegerin (OPG) (82, 187, 188).

2) Thymic crosstalk governs mTEC differentiation

The highly dynamic nature of the thymic medulla, where mTEC^{high} cells exhibit a rapid turnover time of 2-3 weeks (182, 183), is suggestive of the need for continual renewal of the mature mTEC compartment via immature precursors. Still, the differentiation of mTEC-restricted progenitors and acquisition of mature properties does not happen in a cell-autonomous manner but rather is influenced by thymocyte-derived signal, a symbiotic process named “TEC-Thymocyte crosstalk” (105, 189). Initial analysis of mice lacking signal components of both canonical and non-canonical nuclear factor kappa B (NF-κB) pathway paved the way for better comprehending the molecular mechanisms behind mTEC development. Disruption of downstream NF-κB-associated effectors molecules, such as NF-κB inducing kinase (NIK), Tumour necrosis factor receptor-associated factor 6 (TRAF6) and reticuloendotheliosis viral oncogene related B (RelB), resulted in an abnormal mTEC architecture, impaired differentiation of Aire-expressing mTECs and consequent organ-specific autoimmunity (190–192). Subsequent studies identified multiple members of the tumour necrosis factor receptor (TNFR) superfamily as the upstream key activators of NF-κB signalling during mTEC development. Among these, the lymphotoxin β receptor (LTβR), receptor activator of NF-κB (RANK) and CD40 are the best studied. The first TNFR member reported to play a pivotal role in mTEC differentiation and function was LTβR. Mice that lack LTβR have disorganized medullary architecture and a substantial overall reduction in mTEC cellularity, alongside with abnormalities in thymocyte egress and autoimmune manifestations (193). Moreover, LTβR-mediated signals in mTECs were shown to contribute for a diverse array of cellular and molecular processes. Apart of controlling the expression of Aire-independent TRAs, the LTβR pathway also

influences the thymic DC pool implicated in negative selection, the expression of chemokines (CCL19 and CCL21) by $mTEC^{low}$ cells and the terminal differentiation of post-Aire mTECs (77, 185, 194–196). In contrast to LTβR, both RANK and CD40 have been shown to play vital roles in foster the development of the Aire-expressing mTECs (184, 197, 198). In particular, RANK signalling pathway was classified as key regulator of mTEC development, advocating for the existence of a hierarchy among the different TNFR members. Contrary to the lack of CD40, RANK-deficient mice exhibit a severe phenotype characterized by a marked reduction in mTEC cellularity, particularly Aire-expressing cells, and an impaired central tolerance due to a defective promiscuous gene expression program (184, 197). Interestingly, this phenotype is further exacerbated in CD40/RANK double deficient mice supporting a cooperative role for both receptors in the optimal differentiation of the medullary epithelium (197). During the last years, several studies have investigated the intrathymic cellular sources that provide CD40 and RANK ligands (CD40L and RANKL) at distinct stages of thymus development. Different hematopoietic populations appear to express RANKL, the physiological ligand of RANK, within discrete developmental windows. Whereas in the fetal period, $CD4^+CD3^-$ lymphoid tissue inducer (LTi) cells and invariant $Vγ5^+$ thymocytes nurture mTEC emergence as the major sources of RANKL (90, 184), the expression of this ligand across the post-natal life is circumscribed to positively selected $CD4^+$ thymocytes and CD1d-restricted iNKT cells (91, 198). On the other hand, CD40L is exclusively provided by $CD4^+$ SP thymocytes (198, 199), reinforcing the notion that the CD40 pathway contributes for the establishment of a functional thymic medulla during post-natal life. Interestingly, interaction with $CD4^+$ thymocytes carrying auto-reactive TCRs was shown to be critical in fostering the optimal expansion and architectural organization of the medullary compartment (200, 201), possibly as result of an efficient delivery of RANKL and CD40L signals. Regardless of their individual contributions, the genesis of mTECs seems to rely on the sequential and coordinated interplay among the different TNFR members. A synergistic interaction between LTβR and RANK was shown to take place at early stages of fetal development, during which LTβR signals enhances RANK expression on mTEC precursors (202). In turn, RANK-mediated signalling is able to promote the rapid upregulation of CD40 levels in mTECs, prior to the acquisition of mature traits (e.g.: Aire, CD80 and TRA expression) (199). Despite the unequivocal importance of LTβR, RANK and CD40, a recent report

described a novel role of histone deacetylase 3 (HDAC3) in initiating a mTEC-specific transcriptional program, which is required for mTEC lineage specification and development (203). Interestingly, Hdac3 operates independently of the NF-κB signalling pathway, which advocates for the existence of several layers of complexity involving mTEC lineage specification and differentiation.

3) The multifarious functions of the thymic medulla

While undergoing through different phases of maturation, the medullary epithelium attains the functional competence to support the late stages of T cell development. Apart of producing multiple chemokines (e.g.: CCL21, CCL19 or XCL1) or sustaining the differentiation of specific populations of nonconventional T cell lineages, the most critical function of mTECs is to guarantee the establishment of central tolerance, both via negative selection and cell-fate diversion towards the Treg lineage **(Figure 6)** (21). Owing to their exceptional capacity to promiscuously express most of the protein-coding genes, mTECs operate as a library of ubiquitous and tissue-restricted self-antigens, continuously presenting them to screen for potential auto-reactivities within the αβ TCR repertoire of SP thymocytes (80). Although pGE is a remarkable feature of mTECs, the highest degree of this property, both in respect to number and diversity of expressed TRA, is observed within the mature medullary epithelium (204, 205). Recent data described that TRA expression in the medullary epithelium follows a mosaic pattern, with every individual mTEC progressing through different stages defined by expression of particular TRA-encoding gene clusters (206, 207). Although each TRA is expressed in only 1-3% of mTECs at a given point (208, 209), this process allows a robust coverage of the αβ TCR repertoire by ensuring maximal TRA representation at a population level. The mechanisms underlying the promiscuous expression of TRA have been partially revealed, with the transcription regulators Aire and Fezf2 emerging as the main molecular determinants of this phenomenon (81, 82). Aire, the mutated gene in the rare autoimmune polyglandular syndrome type 1 (APS-1) disorder (210, 211), is described to govern the expression of a large portion of TRAs (approximately 40%) in mature mTECs (205, 212). The mechanism of action by which Aire controls pGE is intriguing, as this regulator does not function as a classic transcription factor that bind to a promoter element and initiate transcription (213).

Instead, it was described that Aire recognizes genes that possess silenced chromatin stages (214). This process involves the selective recognition of hypomethylated histone H3 lysine 4 (H3K4), a mark associated with poorly transcribed genes, by the first plan homeodomain (PHD1) of Aire (215, 216). At the same time, this binding stabilizes Aire and initiates the recruitment of numerous transcriptional regulators involved in chromatin structure and DNA damage response, transcriptional elongation, RNA processing and nuclear export (217). This leads to the formation of a multimeric protein complex that unleashes the stalled RNA polymerase II, thereby enabling the transcription of Aire-dependent TRA genes (213, 218). Our knowledge regarding the mechanisms involved in the transcriptional regulation of this unusual factor is still incomplete. However, recent data identified a highly conversed noncoding sequence 1 (CNS1) upstream of the *Aire* coding region, containing two NF-κB responsive elements that are critical for RANK-mediated induction of Aire (219, 220). Thus, these results appreciate the direct impact of RANK signalling in Aire transcription, a role that goes beyond of its contribution for the developmental maturation of mTECs. Apart of its well-described influence in TRA induction, there are also a number of studies indicating alternative functions of Aire, namely in chemokine expression and mTEC maturation (186, 221–223). Also, expression of Aire during a perinatal age-window was reported as critical for the generation of a pool of natural-derived Tregs with unique characteristics (224, 225). More recently, the transcriptional regulator Fezf2 was reported to contribute for the selective induction of Aire-independent pGE in mTECs. Although absence of Fezf2 expression results in organ-specific autoimmunity (82), the spectrum of inflammatory lesions was different from those observed in Aire-deficient mice, suggesting that both factors work independently but synergistically in controlling TRA expression. Indeed, while some TRA genes (12.3%) are reciprocally regulated by both Aire and Fezf2, most Fezf2-dependent genes (21.1%) are still expressed in the absence of Aire (82). Fezf2 is detectable within both $mTEC^{low}$ and $mTEC^{high}$ subsets and it was described to be exclusively induced downstream of the LTβR pathway (82). In contrast with this observation, recent data established that specific deletion of LTβR in TECs failed to interfere with Fezf2 levels and TRA expression. Instead, it proposed the involvement of the RANK-signalling pathway as the major regulator of Fezf2 expression and function in tolerance induction (195). Nevertheless, as Fez2 and Aire only govern 60% of TRA genes (82), future studies are necessary to

uncover new tolerogenic transcriptional regulators of pGE in the medullary epithelium.

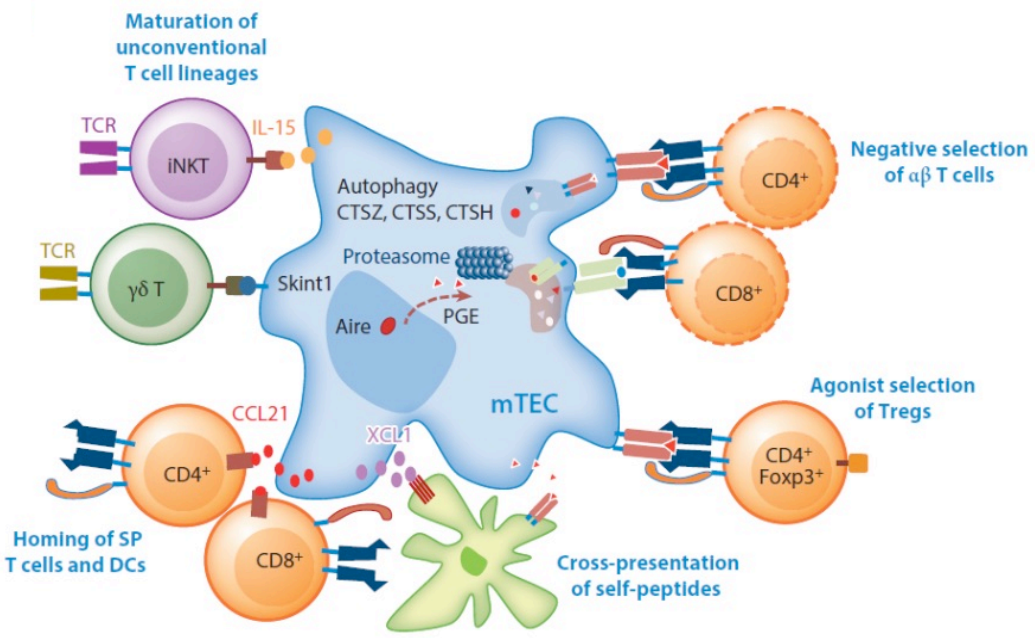

Figure 6 – Functional influence of the medullary microenvironment in T cell development. mTECs have a key role in coordinating multiple stages of late thymopoiesis. First, mTECs are the physiological source of several chemokines, including CCL21 and XCL1, which are responsible to promote the migration of positively selected SP thymocytes and DCs, respectively, into the medulla. Due to their unique ability to express a myriad of tissue-restricted self-antigens, presented in the context of both MHC-I and MHC-II to SP thymocytes, mTECs controls the clonal deletion of self-reactive T cell clones and the differentiation of Tregs. Both of these processes are further supported by DCs through the cross-presentation of mTEC-derived self-peptides. In addition, mTECs also foster the differentiation of different non-conventional T cell lineages, which includes γδ T cells and iNKT cells. Image adapted from (21)

Thymic degeneration and regeneration

One of the hallmarks of the ageing vertebrate immune system is the progressive deterioration of the thymic function, an evolutionary conserved physiological process termed “Thymic involution” (25). Aged-related involution of the thymus occurs much earlier than other acknowledged features of aging, although with different onsets across species. For instance, whereas atrophy of the murine thymus was shown to commence around the time of sexual maturity (22, 226), aged-related involution in human thymus is already detected from the first year of life (227). Nevertheless, in both mice and human, the major features of thymic atrophy include perturbations in the stromal epithelial microenvironment, characterized by a dramatic reduction in total TEC cellularity, loss of the normal cortex and medulla compartmentalization, appearance of areas devoid of epithelium and the expansion of adipose tissue and fibroblasts in perivascular spaces **(Figure 7)** (22, 27, 228–232). Albeit the aged thymus still presents some residual capacity to support T cell development (233), its

regression is intimately linked with abnormalities, both at a quantitative and qualitative level, in the peripheral T cell compartment. These changes comprise a noticeable reduction in the frequency of functional naïve T cells with a skewing towards an increased memory T cell pool, a constriction of the TCR repertoire and impaired immune responses to new antigens **(Figure 7)** (24). Under normal circumstances, thymic involution is of minimal consequences to a healthy individual, but the diminished competence of the immune system during elderly has been implicated with an augmented incidence of diseases, such as autoimmunity, cancer or opportunistic infections (27, 28).

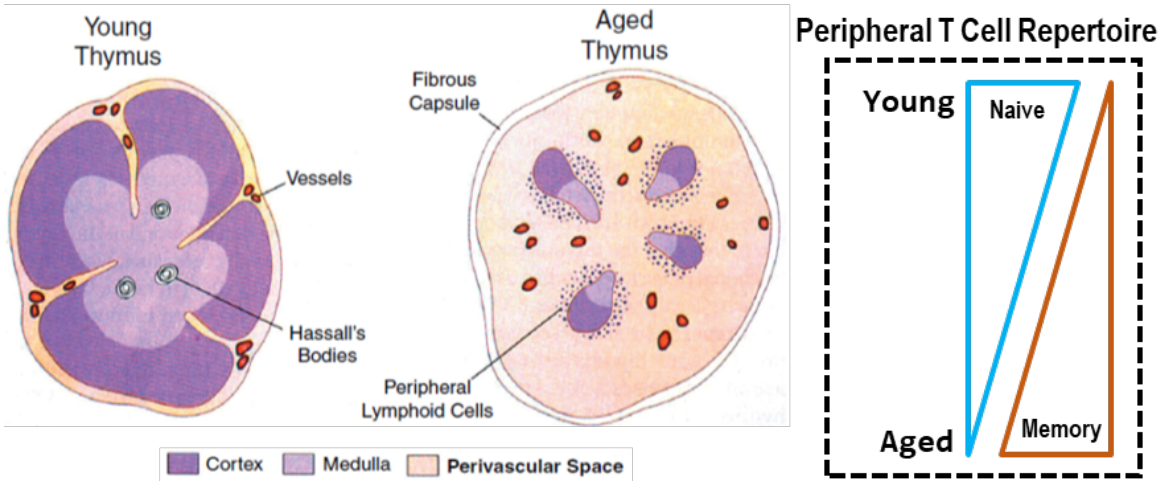

Figure 7 – Physiological consequences of age-related thymic involution. The process of thymic degeneration is characterized by the progressive disruption of the normal cortical and medullary microenvironments, together with alterations in the cellular composition of the thymic stroma and the gradual appearance of areas devoid of epithelium. As a result, the capacity of the thymus to support T cell development decays with time, leading to a reduced T cell output and consequence changes in the peripheral T cell compartment. Image adapted from (26).

Despite being recognized as a natural biological cause for more than one century (234), the precise mechanism(s) responsible for the atrophy of the thymus remains poorly understood. The significant impact of aging on the HSC compartment led to the notion that a primary cause of thymic involution would be related with a reduced intrinsic capacity of the aged T cell progenitors to home the thymus (24). Yet, different studies provided evidence that transferring young HSCs or ETPs into old mice did not reverse thymic involution (235, 236). Furthermore, the functional capacity of aged ETP to settle the thymus was shown not to be considerably different from their young counterparts (229). Although aged-dependent alterations in the BM might contribute to exacerbate the degeneration of the thymus over time (237), there is no clear indication that positions downstream changes in the HSC niche as the primary cause of thymic atrophy. Over the years, several studies revealed multiple layers of complexity regarding the cellular and molecular

mediators of thymic involution. Nevertheless, thymic atrophy is currently recognized to unfold due to intrinsic and extrinsic age-dependent alterations of the thymic stroma, in particular in TECs (28). During the course of involution, TECs were shown to downregulate expression of several genes that are crucial in controlling the epithelial niche activity and maintenance (238). Specifically, the expression of the key regulator Foxn1 was observed to diminish with age, concomitantly with the progressive expansion of Foxn1-negative cells within both cortical and medullary thymic epithelium (114, 239, 240). Interestingly, evidence suggests that cortex-specific downregulation of Foxn1 may be the main driver of thymic involution as result of an impaired expression of genes involved in cTEC-dependent T cell differentiation (240). Moreover, attenuation of Foxn1 levels in the perinatal thymus leads to a premature atrophy (241), whereas inducible upregulation of Foxn1 in a fully involuted thymus was able to revert organ aged-associated defects, as shown by the improvement of thymic architecture, thymopoietic capacity and TEC molecular profile close to those of the young thymus (242). Hence, these observations suggest that both the onset and progression of thymic involution may be linked to a decline in Foxn1 expression, although the existence of other factors cannot be formally excluded.

The intrathymic microenvironment is characterized by a complex network of paracrine, autocrine and endocrine signals involving a number of soluble mediators (243), which may act as secondary agents in exacerbating the age-related decline of the thymus. For example, many thymic cytokines and hormones are differentially expressed with age. Different studies revealed a pro-inflammatory signature in the microenvironment of aged thymus, which result of an increased expression of cytokines *Il1a*, *Il1b*, *Il6*, *Il12b*, *Il18*, and *Tnf* (238, 244). Some of these cytokines were shown to have suppressive effect on the thymic function. In line with this, IL-1 and IL-6 administration to mice resulted in thymic involution (244, 245). On the other hand, mice lacking the Nlrp3 inflammasome were protected against age-related thymic deterioration, due to the inability to produce active IL-1 (246). Among the different hormonal factors proposed to stimulate thymic involution are the sex steroids (247). The rapid declined in thymic function during puberty has been associated with a raise in sex hormone levels, which are known to exert profound inhibitory effects on immune functions (248, 249). This concept is consistent with

observations that both thymocytes and TECs express sex steroid receptor and that the exogenous administration of sexual hormones caused a collapse in thymic function (250–255). More recently, genome-wide transcriptome analysis revealed that androgen signalling in TECs represses the expression of several genes involved in their maintenance and function, including Foxn1 (256). Furthermore, evidence demonstrates that androgen-mediated thymic atrophy is mainly caused by a direct influence on TECs, despite the expression of the androgen receptor by thymocytes (252). The clear influence of sex steroids in the homeostasis of the thymus led to the consideration that intervening in this pathway could represent a mean of reversing thymic atrophy. Indeed, blockade sex steroid production, either surgically or via luteinising hormone releasing hormone (LHRH) analogues, stimulates thymic rejuvenation in old mice (257–259). These alterations include the rebuilding of the TEC microenvironment, both at phenotypic, numerical and functional level, and a boost in the thymopoietic capacity of the aged thymus to the levels observed in their young counterpart (22, 257, 258, 260). Interestingly, studies revealed similar beneficial effects of sex steroid ablation (SSA) in the BM, such as reverting deficits in the hematopoietic and stromal niche. These changes comprise an expansion in HSCs, CLPs and B cells as well as an elevated production of stromal-derived factors (261, 262). Also, SSA has a beneficial effect in accelerating thymic recovery in clinical setting related with bone marrow transplantation and cytoablative therapies (263–267). Whereas the influence of SSA for thymic regrowth has been described from more than one century ago (268), the exact molecular mechanism underlying these regenerative effects still remains elusive, even though some recent studies suggested the participation of IL-7, CCL25 and Dll4 (260, 266, 269). Understand these mechanisms would be of importance, as transient ablation of sex steroids could represent an attractive immune regenerative strategy in diverse clinical contexts.

Despite the substantial advances in our understanding about many aspects of TEC biology, we still lack knowledge regarding the mechanisms that govern the homeostasis of the thymic epithelium throughout life. In the next chapters of this thesis, I will summarize the findings of our work that together provide insights on novel molecular processes that regulate the maintenance and function of the TEC niche during normal and altered physiological settings.

Aims

In this thesis, we aimed at investigating the cellular and molecular basis that governs the maintenance, function and regeneration of TEC compartments. In **Chapter II**, we investigated the contribution of the transcription factor p53 to the homeostasis of the thymic epithelium. In **Chapter III**, we studied the temporal and spatial requirements for Interleukin-7 (IL-7) in the regeneration of the thymus promoted by sex steroid ablation (SSA). To address these questions, we generated novel conditional loss-of-function mouse models, which were characterized by taking advantage of multicolour flow cytometry analysis, thymic organotypic cultures, next-generation sequencing technology and *in vitro and in vivo* functional assays.

Uncovering the rules that determine the establishment and function of distinct TEC microenvironments remains as one of the most important challenges in the field of thymus research. Ultimately, knowledge in this area will contribute to a better comprehension about the mechanisms that govern T cell generation and tolerance induction.

References

1. Boehm, T. 2012. Evolution of vertebrate immunity. *Curr. Biol.* 22: R722–R732.

2. Eberl, G. 2016. Immunity by equilibrium. *Nat. Rev. Immunol.* 16: 524–532.

3. Parkin, J., and B. Cohen. 2001. An overview of the immune system. *Lancet* 357: 1777–89.

4. Medzhitov, R., and C. A. Janeway Jr. 1997. Innate immunity: impact on the adaptive immune response. *Curr. Opin. Immunol.* 9: 4–9.

5. Buchmann, K. 2014. Evolution of innate immunity: Clues from invertebrates via fish to mammals. *Front. Immunol.* 5: 1–8.

6. Schatz, D. G., and Y. Ji. 2011. Recombination centres and the orchestration of V(D)J recombination. *Nat. Rev. Immunol.* 11: 251–63.

7. Bluestone, J. A. 2011. Mechanisms of tolerance. *Immunol. Rev.* 241: 5–19.

8. Basten, A., and P. A. Silveira. 2010. B-cell tolerance: Mechanisms and implications. *Curr. Opin. Immunol.* 22: 566–574.

9. Orkin, S. H., and L. I. Zon. 2008. Hematopoiesis: An Evolving Paradigm for Stem Cell Biology. *Cell* 132: 631–644.

10. Silver, L., and J. Palis. 1997. Initiation of murine embryonic erythropoiesis: a spatial analysis. *Blood* 89: 1154–64.

11. Jagannathan-Bogdan, M., and L. I. Zon. 2013. Hematopoiesis. *Development* 140: 2463–2467.

12. Anthony, B. A., and D. C. Link. 2014. Regulation of hematopoietic stem cells by bone marrow stromal cells. *Trends Immunol.* 35: 32–37.

13. Kondo, M. 2010. Lymphoid and myeloid lineage commitment in multipotent hematopoietic progenitors. *Immunol. Rev.* 238: 37–46.

14. Rezzani, R., F. Bonomini, and L. F. Rodella. 2008. Histochemical and molecular overview of the thymus as site for T-cells development. *Prog. Histochem. Cytochem.* 43: 73–120.

15. Miller, J. F. 1961. Immunological function of the thymus. *Lancet* 2: 748–749.

16. Boehm, T., and C. C. Bleul. 2007. The evolutionary history of lymphoid organs. *Nat. Immunol.* 8: 131–135.

17. Rodewald, H.-R. 2008. Thymus organogenesis. *Annu. Rev. Immunol.* 26: 355–88.

18. Boehm, T. 2011. Design principles of adaptive immune systems. *Nat. Rev. Immunol.* 11: 307–317.

19. Boehm, T., and J. B. Swann. 2014. Origin and evolution of adaptive immunity. *Annu. Rev. Anim. Biosci.* 2: 259–83.

20. Ciofani, M., and J. C. Zúñiga-Pflücker. 2007. The thymus as an inductive site for T

lymphopoiesis. *Annu. Rev. Cell Dev. Biol.* 23: 463–93.

21. Abramson, J., and G. Anderson. 2016. Thymic Epithelial Cells. *Annu. Rev. Immunol.* 34: 85–118.

22. Gray, D. H. D., N. Seach, T. Ueno, M. K. Milton, A. Liston, A. M. Lew, C. C. Goodnow, and R. L. Boyd. 2006. Developmental kinetics, turnover, and stimulatory capacity of thymic epithelial cells. *Blood* 108: 3777–85.

23. Boyd, R. L., C. L. Tucek, D. I. Godfrey, D. J. Izon, T. J. Wilson, N. J. Davidson, A. G. D. Bean, H. M. Ladyman, M. A. Ritter, and P. Hugo. 1993. The thvmic microenvironment. *Immunol. Today* 14: 445–459.

24. Linton, P. J., and K. Dorshkind. 2004. Age-related changes in lymphocyte development and function. *Nat. Immunol.* 5: 133–9.

25. Shanley, D. P., D. Aw, N. R. Manley, and D. B. Palmer. 2009. An evolutionary perspective on the mechanisms of immunosenescence. *Trends Immunol.* 30: 374–81.

26. Ventevogel, M. S., and G. D. Sempowski. 2013. Thymic rejuvenation and aging. *Curr. Opin. Immunol.* 25: 516–522.

27. Taub, D. D., and D. L. Longo. 2005. Insights into thymic aging and regeneration. *Immunol. Rev.* 205: 72–93.

28. Chinn, I. K., C. C. Blackburn, N. R. Manley, and G. D. Sempowski. 2012. Changes in primary lymphoid organs with aging. *Semin. Immunol.* 24: 309–320.

29. Takahama, Y. 2006. Journey through the thymus: stromal guides for T-cell development and selection. *Nat. Rev. Immunol.* 6: 127–35.

30. Petrie, H. T., and J. C. Zúñiga-Pflücker. 2007. Zoned out: functional mapping of stromal signaling microenvironments in the thymus. *Annu. Rev. Immunol.* 25: 649–679.

31. Foss, D. L., E. Donskoy, and I. Goldschneider. 2001. The importation of hematogenous precursors by the thymus is a gated phenomenon in normal adult mice. *J. Exp. Med.* 193: 365–74.

32. Ziętara, N., M. Łyszkiewicz, J. Puchałka, K. Witzlau, A. Reinhardt, R. Förster, O. Pabst, I. Prinz, and A. Krueger. 2015. Multicongenic fate mapping quantification of dynamics of thymus colonization. *J. Exp. Med.* 212: 1589–1601.

33. Bhandoola, A., H. von Boehmer, H. T. Petrie, and J. C. Zúñiga-Pflücker. 2007. Commitment and Developmental Potential of Extrathymic and Intrathymic T Cell Precursors: Plenty to Choose from. *Immunity* 26: 678–689.

34. Luc, S., T. C. Luis, H. Boukarabila, I. C. Macaulay, N. Buza-Vidas, T. Bouriez-Jones, M. Lutteropp, P. S. Woll, S. J. Loughran, A. J. Mead, A. Hultquist, J. Brown, T. Mizukami, S. Matsuoka, H. Ferry, K. Anderson, S. Duarte, D. Atkinson, S. Soneji, A. Domanski, A. Farley, A. Sanjuan-Pla, C. Carella, R. Patient, M. de Bruijn, T. Enver, C. Nerlov, C. Blackburn, I. Godin, and S. E. W. Jacobsen. 2012. The earliest thymic T cell progenitors sustain B cell and myeloid lineage potential. *Nat. Immunol.* 13: 412–9.

35. Suniara, R. K., E. J. Jenkinson, and J. J. T. Owen. 1999. Studies on the phenotype of migrant thymic stem cells. *Eur. J. Immunol.* 29: 75–80.

36. Calderón, L., and T. Boehm. 2011. Three chemokine receptors cooperatively regulate homing of hematopoietic progenitors to the embryonic mouse thymus. *Proc. Natl. Acad. Sci. U. S. A.* 108: 7517–7522.

37. Liu, C., T. Ueno, S. Kuse, F. Saito, T. Nitta, L. Piali, H. Nakano, T. Kakiuchi, M. Lipp, G. A. Hollander, and Y. Takahama. 2004. Role of CCL21 in recruitment of T precursor cells to fetal thymus. *Blood* 105: 31–39.

38. Liu, C., F. Saito, Z. Liu, Y. Lei, S. Uehara, P. Love, M. Lipp, S. Kondo, N. Manley, and Y. Takahama. 2006. Coordination between CCR7- and CCR9-mediated chemokine signals in prevascular fetal thymus colonization. *Blood* 108: 2531–2539.

39. Douarin, N. M., and F. V. Jotereau. 1975. Tracing of cells of the avian thymus through embryonic life in interspecific chimeras. *J. Exp. Med.* 142: 17–40.

40. Itoi, M., H. Kawamoto, Y. Katsura, and T. Amagai. 2001. Two distinct steps of immigration of hematopoietic progenitors into the early thymus anlage. *Int. Immunol.* 13: 1203–11.

41. Lind, E. F., S. E. Prockop, H. E. Porritt, and H. T. Petrie. 2001. Mapping precursor movement through the postnatal thymus reveals specific microenvironments supporting defined stages of early lymphoid development. *J. Exp. Med.* 194: 127–134.

42. Rossi, F. M. V., S. Y. Corbel, J. S. Merzaban, D. A. Carlow, K. Gossens, J. Duenas, L. So, L. Yi, and H. J. Ziltener. 2005. Recruitment of adult thymic progenitors is regulated by P-selectin and its ligand PSGL-1. *Nat. Immunol.* 6: 626–634.

43. Gossens, K., S. Naus, S. Y. Corbel, S. Lin, F. M. V. Rossi, J. Kast, and H. J. Ziltener. 2009. Thymic progenitor homing and lymphocyte homeostasis are linked via S1P-controlled expression of thymic P-selectin/CCL25. *J. Exp. Med.* 206: 761–78.

44. Love, P. E., and A. Bhandoola. 2011. Signal integration and crosstalk during thymocyte migration and emigration. *Nat. Rev. Immunol.* 11: 469–77.

45. Petrie, H. T. 2003. Cell migration and the control of post-natal T-cell lymphopoiesis in the thymus. *Nat. Rev. Immunol.* 3: 859–66.

46. Porritt, H. E., K. Gordon, and H. T. Petrie. 2003. Kinetics of steady-state differentiation and mapping of intrathymic-signaling environments by stem cell transplantation in nonirradiated mice. *J. Exp. Med.* 198: 957–962.

47. Koch, U., E. Fiorini, R. Benedito, V. Besseyrias, K. Schuster-Gossler, M. Pierres, N. R. Manley, A. Duarte, H. R. Macdonald, and F. Radtke. 2008. Delta-like 4 is the essential, nonredundant ligand for Notch1 during thymic T cell lineage commitment. *J. Exp. Med.* 205: 2515–23.

48. Hozumi, K., C. Mailhos, N. Negishi, K. Hirano, T. Yahata, K. Ando, S. Zuklys, G. A. Holländer, D. T. Shima, and S. Habu. 2008. Delta-like 4 is indispensable in thymic environment specific for T cell development. *J. Exp. Med.* 205: 2507–13.

49. Capone, M., J. Richard D. Hockett, and A. Zlotnik. 1998. Kinetics of T cell receptor beta, gamma, and delta rearrangements during adult thymic development: T cell receptor rearrangements are present in CD44(+)CD25(+) Pro-T thymocytes. *Proc. Natl. Acad. Sci. U. S. A.* 95: 12522–12527.

50. Livák, F., M. Tourigny, D. G. Schatz, and H. T. Petrie. 1999. Characterization of TCR Gene Rearrangements during Adult Murine T Cell Development. *J. Immunol.* 162: 2575–2580.

51. Ciofani, M., and J. C. Zúñiga-Pflücker. 2010. Determining γδ versus αβ T cell development. *Nat. Rev. Immunol.* 10: 657–663.

52. von Boehmer, H. 2005. Opinion: Unique features of the pre-T-cell receptor α-chain: not just a surrogate. *Nat. Rev. Immunol.* 5: 571–577.

53. Michie, A. M., and J. C. Zúñiga-Pflücker. 2002. Regulation of thymocyte differentiation: pre-TCR signals and β-selection. *Semin. Immunol.* 14: 311–323.

54. Maillard, I., L. Tu, A. Sambandam, Y. Yashiro-Ohtani, J. Millholland, K. Keeshan, O. Shestova, L. Xu, A. Bhandoola, and W. S. Pear. 2006. The requirement for Notch signaling at the β-selection checkpoint in vivo is absolute and independent of the pre–T cell receptor. *J. Exp. Med.* 203: 2239–2245.

55. Trampont, P. C., A.-C. Tosello-Trampont, Y. Shen, A. K. Duley, A. E. Sutherland, T. P. Bender, D. R. Littman, and K. S. Ravichandran. 2010. CXCR4 acts as a costimulator during thymic beta-selection. *Nat. Immunol.* 11: 162–170.

56. Janas, M. L., G. Varano, K. Gudmundsson, M. Noda, T. Nagasawa, and M. Turner. 2010. Thymic development beyond beta-selection requires phosphatidylinositol 3-kinase activation by CXCR4. *J. Exp. Med.* 207: 247–261.

57. Hayday, A. C., and D. J. Pennington. 2007. Key factors in the organized chaos of early T cell development. *Nat. Immunol.* 8: 137–44.

58. Klein, L., B. Kyewski, P. M. Allen, and K. A. Hogquist. 2014. Positive and negative selection of the T cell repertoire: what thymocytes see (and don't see). *Nat. Rev. Immunol.* 14: 377–91.

59. Klein, L., M. Hinterberger, G. Wirnsberger, and B. Kyewski. 2009. Antigen presentation in the thymus for positive selection and central tolerance induction. *Nat. Rev. Immunol.* 9: 833–44.

60. Egerton, M., R. Scollay, and K. Shortman. 1990. Kinetics of mature T-cell development in the thymus. *Proc. Natl. Acad. Sci. U. S. A.* 87: 2579–2582.

61. Singer, A., S. Adoro, and J.-H. Park. 2008. Lineage fate and intense debate: myths, models and mechanisms of CD4- versus CD8-lineage choice. *Nat. Rev. Immunol.* 8: 788–801.

62. Lundberg, K., W. Heath, F. Kntgen, F. R. Carbone, and K. Shortman. 1995. Intermediate Steps in Positive Selection: Differentiation of CD4+8int TCRint Thymocytes into CD4-CD8+ TCRhi Thymocytes. *J. Exp. Med.* 181: 1643–1651.

63. Suzuki, H., J. A. Punt, L. G. Granger, and A. Singer. 1995. Asymmetric signaling requirements for thymocyte commitment to the CD4+ versus CD8+ T cell lineages: A new perspective on thymic commitment and selection. *Immunity* 2: 413–425.

64. Brugnera, E., A. Bhandoola, R. Cibotti, Q. Yu, T. I. Guinter, Y. Yamashita, S. O. Sharrow, and A. Singer. 2000. Coreceptor reversal in the thymus: signaled CD4+8+

thymocytes initially terminate CD8 transcription even when differentiating into CD8+ T cells. *Immunity* 13: 59–71.

65. Park, J.-H., S. Adoro, T. Guinter, B. Erman, A. S. Alag, M. Catalfamo, M. Y. Kimura, Y. Cui, P. J. Lucas, R. E. Gress, M. Kubo, L. Hennighausen, L. Feigenbaum, and A. Singer. 2010. Signaling by intrathymic cytokines, not T cell antigen receptors, specifies CD8 lineage choice and promotes the differentiation of cytotoxic-lineage T cells. *Nat. Immunol.* 11: 257–64.

66. He, X., X. He, V. P. Dave, Y. Zhang, X. Hua, E. Nicolas, W. Xu, B. A. Roe, and D. J. Kappes. 2005. The zinc finger transcription factor Th-POK regulates CD4 versus CD8 T-cell lineage commitment. *Nature* 433: 826–33.

67. Egawa, T., and D. R. Littman. 2008. ThPOK acts late in specification of the helper T cell lineage and suppresses Runx-mediated commitment to the cytotoxic T cell lineage. *Nat. Immunol.* 9: 1131–9.

68. Sato, T., S. Ohno, T. Hayashi, C. Sato, K. Kohu, M. Satake, and S. Habu. 2005. Dual functions of runx proteins for reactivating CD8 and silencing CD4 at the commitment process into CD8 thymocytes. *Immunity* 22: 317–328.

69. Setoguchi, R., M. Tachibana, Y. Naoe, S. Muroi, K. Akiyama, C. Tezuka, T. Okuda, and I. Taniuchi. 2008. Repression of the transcription factor Th-POK by Runx complexes in cytotoxic T cell development. *Science.* 319: 822–825.

70. Carpenter, A. C., and R. Bosselut. 2010. Decision checkpoints in the thymus. *Nat. Immunol.* 11: 666–73.

71. Pai, S. Y., M. L. Truitt, C. N. Ting, J. M. Leiden, L. H. Glimcher, and I.-C. Ho. 2003. Critical Roles for Transcription Factor GATA-3 in Thymocyte Development. *Immunity* 19: 863–875.

72. Wang, L., K. F. Wildt, J. Zhu, X. Zhang, L. Feigenbaum, L. Tessarollo, W. E. Paul, B. J. Fowlkes, and R. Bosselut. 2008. Distinct functions for the transcription factors GATA-3 and ThPOK during intrathymic differentiation of CD4+ T cells. *Nat. Immunol.* 9: 1122–1130.

73. Aliahmad, P., and J. Kaye. 2008. Development of all CD4 T lineages requires nuclear factor TOX. *J. Exp. Med.* 205: 245–256.

74. Nitta, T., S. Nitta, Y. Lei, M. Lipp, and Y. Takahama. 2009. CCR7-mediated migration of developing thymocytes to the medulla is essential for negative selection to tissue-restricted antigens. *Proc. Natl. Acad. Sci. U. S. A.* 106: 17129–33.

75. Ueno, T., F. Saito, D. H. D. Gray, S. Kuse, K. Hieshima, H. Nakano, T. Kakiuchi, M. Lipp, R. L. Boyd, and Y. Takahama. 2004. CCR7 signals are essential for cortex-medulla migration of developing thymocytes. *J. Exp. Med.* 200: 493–505.

76. Onder, L., V. Nindl, E. Scandella, Q. Chai, H. W. Cheng, S. Caviezel-Firner, M. Novkovic, D. Bomze, R. Maier, F. Mair, B. Ledermann, B. Becher, A. Waisman, and B. Ludewig. 2015. Alternative NF-κB signaling regulates mTEC differentiation from podoplanin-expressing presursors in the cortico-medullary junction. *Eur. J. Immunol.* 45: 2218–2231.

77. Lkhagvasuren, E., M. Sakata, I. Ohigashi, and Y. Takahama. 2013. Lymphotoxin beta receptor regulates the development of CCL21-expressing subset of postnatal medullary

thymic epithelial cells. *J. Immunol.* 190: 5110–5117.

78. Choi, Y. I., J. S. Duke-Cohan, W. B. Ahmed, M. A. Handley, F. Mann, J. A. Epstein, L. K. Clayton, and E. L. Reinherz. 2008. PlexinD1 Glycoprotein Controls Migration of Positively Selected Thymocytes into the Medulla. *Immunity* 29: 888–898.

79. Hu, Z., J. N. Lancaster, C. Sasiponganan, and L. I. R. Ehrlich. 2015. CCR4 promotes medullary entry and thymocyte-dendritic cell interactions required for central tolerance. *J. Exp. Med.* 212: 1947–1965.

80. Derbinski, J., A. Schulte, B. Kyewski, and L. Klein. 2001. Promiscuous gene expression in medullary thymic epithelial cells mirrors the peripheral self. *Nat. Immunol.* 2: 1032–9.

81. Anderson, M. S., E. S. Venanzi, L. Klein, Z. Chen, S. P. Berzins, S. J. Turley, H. von Boehmer, R. Bronson, A. Dierich, C. Benoist, and D. Mathis. 2002. Projection of an immunological self shadow within the thymus by the aire protein. *Science.* 298: 1395–401.

82. Takaba, H., Y. Morishita, Y. Tomofuji, L. Danks, T. Nitta, N. Komatsu, T. Kodama, and H. Takayanagi. 2015. Fezf2 Orchestrates a Thymic Program of Self-Antigen Expression for Immune Tolerance. *Cell* 163: 975–987.

83. Perry, J. S. A., C.-W. J. Lio, A. L. Kau, K. Nutsch, Z. Yang, J. I. Gordon, K. M. Murphy, and C.-S. Hsieh. 2014. Distinct contributions of Aire and antigen-presenting-cell subsets to the generation of self-tolerance in the thymus. *Immunity* 41: 414–426.

84. Klein, L., M. Hinterberger, J. von Rohrscheidt, and M. Aichinger. 2011. Autonomous versus dendritic cell-dependent contributions of medullary thymic epithelial cells to central tolerance. *Trends Immunol.* 32: 188–193.

85. Josefowicz, S. Z., L.-F. Lu, and A. Y. Rudensky. 2012. Regulatory T cells: mechanisms of differentiation and function. *Annu. Rev. Immunol.* 30: 531–564.

86. Fontenot, J. D., M. A. Gavin, and A. Y. Rudensky. 2003. Foxp3 programs the development and function of CD4+CD25+ regulatory T cells. *Nat. Immunol.* 4: 330–6.

87. Misako, I., T. Takahashi, N. Sakaguchi, Y. Kuniyasu, J. Shimizu, F. Otsuka, and S. Sakaguchi. 1999. Thymus and Autoimmunity: Production of CD25+CD4+ Naturally Anergic and Suppressive T cells as a Key Function of the Thymus in Maintaining Immunological Self-Tolerance. *J. Immunol.* 162: 5317–5326.

88. McCaughtry, T. M., M. S. Wilken, and K. A. Hogquist. 2007. Thymic emigration revisited. *J. Exp. Med.* 204: 2513–2520.

89. Hogquist, K. A., Y. Xing, F.-C. Hsu, and V. S. Shapiro. 2015. T Cell Adolescence: Maturation Events Beyond Positive Selection. *J. Immunol.* 195: 1351–1357.

90. Roberts, N. A., A. J. White, W. E. Jenkinson, G. Turchinovich, K. Nakamura, D. R. Withers, F. M. McConnell, G. E. Desanti, C. Benezech, S. M. Parnell, A. F. Cunningham, M. Paolino, J. M. Penninger, A. K. Simon, T. Nitta, I. Ohigashi, Y. Takahama, J. H. Caamano, A. C. Hayday, P. J. L. Lane, E. J. Jenkinson, and G. Anderson. 2012. Rank signaling links the development of invariant γδ T cell progenitors and Aire(+) medullary epithelium. *Immunity* 36: 427–37.

91. White, A. J., W. E. Jenkinson, J. E. Cowan, S. M. Parnell, A. Bacon, N. D. Jones, E. J.

Jenkinson, and G. Anderson. 2014. An Essential Role for Medullary Thymic Epithelial Cells during the Intrathymic Development of Invariant NKT Cells. *J. Immunol.* 192: 2659–2666.

92. Matloubian, M., C. G. Lo, G. Cinamon, M. J. Lesneski, Y. Xu, V. Brinkmann, M. L. Allende, R. L. Proia, and J. G. Cyster. 2004. Lymphocyte egress from thymus and peripheral lymphoid organs is dependent on S1P receptor 1. *Nature* 427: 355–60.

93. Allende, M. L., J. L. Dreier, S. Mandala, and R. L. Proia. 2004. Expression of the Sphingosine 1-Phosphate Receptor, S1P1, on T-cells Controls Thymic Emigration. *J. Biol. Chem.* 279: 15396–15401.

94. Carlson, C. M., B. T. Endrizzi, J. Wu, X. Ding, M. A. Weinreich, E. R. Walsh, M. A. Wani, J. B. Lingrel, K. A. Hogquist, and S. C. Jameson. 2006. Kruppel-like factor 2 regulates thymocyte and T-cell migration. *Nature* 442: 299–302.

95. Zachariah, M. A., and J. G. Cyster. 2010. Neural crest-derived pericytes promote egress of mature thymocytes at the corticomedullary junction. *Science.* 328: 1129–1135.

96. Zamora-Pineda, J., A. Kumar, J. H. Suh, M. Zhang, and J. D. Saba. 2016. Dendritic cell sphingosine-1-phosphate lyase regulates thymic egress. *J. Exp. Med.* 213: 2773–2791.

97. Bréart, B., W. D. Ramos-Perez, A. Mendoza, A. K. Salous, M. Gobert, Y. Huang, R. H. Adams, J. J. Lafaille, D. Escalante-Alcalde, A. J. Morris, and S. R. Schwab. 2011. Lipid phosphate phosphatase 3 enables efficient thymic egress. *J. Exp. Med.* 208: 1267–1278.

98. Ueno, T., K. Hara, M. S. Willis, M. A. Malin, U. E. Höpken, D. H. D. Gray, K. Matsushima, M. Lipp, T. A. Springer, R. L. Boyd, O. Yoshie, and Y. Takahama. 2002. Role for CCR7 ligands in the emigration of newly generated T lymphocytes from the neonatal thymus. *Immunity* 16: 205–18.

99. Vianello, F., P. Kraft, Y. T. Mok, W. K. Hart, N. White, and M. C. Poznansky. 2005. A CXCR4-dependent chemorepellent signal contributes to the emigration of mature single-positive CD4 cells from the fetal thymus. *J. Immunol.* 175: 5115–5125.

100. Gordon, J., and N. R. Manley. 2011. Mechanisms of thymus organogenesis and morphogenesis. *Development* 138: 3865–78.

101. Manley, N. R. 2000. Thymus organogenesis and molecular mechanisms of thymic epithelial cell differentiation. *Semin. Immunol.* 12: 421–8.

102. Jenkinson, W. E., S. W. Rossi, E. J. Jenkinson, and G. Anderson. 2005. Development of functional thymic epithelial cells occurs independently of lymphostromal interactions. *Mech. Dev.* 122: 1294–9.

103. Klug, D. B., C. Carter, I. B. Gimenez-Conti, and E. R. Richie. 2002. Cutting edge: thymocyte-independent and thymocyte-dependent phases of epithelial patterning in the fetal thymus. *J. Immunol.* 169: 2842–5.

104. van Ewijk, W., G. Holländer, C. Terhorst, and B. Wang. 2000. Stepwise development of thymic microenvironments in vivo is regulated by thymocyte subsets. *Development* 127: 1583–91.

105. van Ewijk, W., E. W. Shores, and A. Singer. 1994. Crosstalk in the mouse thymus. *Immunol. Today* 15: 214–7.

106. Blackburn, C. C., and N. R. Manley. 2004. Developing a new paradigm for thymus organogenesis. *Nat. Rev. Immunol.* 4: 278–89.

107. Gordon, J., A. R. Bennett, C. C. Blackburn, and N. R. Manley. 2001. Gcm2 and Foxn1 mark early parathyroid- and thymus-specific domains in the developing third pharyngeal pouch. *Mech. Dev.* 103: 141–3.

108. Liu, Z., S. Yu, and N. R. Manley. 2007. Gcm2 is required for the differentiation and survival of parathyroid precursor cells in the parathyroid/thymus primordia. *Dev. Biol.* 305: 333–346.

109. Blackburn, C. C., C. L. Augustine, R. Li, R. P. Harvey, M. A. Malin, R. L. Boyd, J. F. A. P. Miller, and G. Morahan. 1996. The nu gene acts cell-autonomously and is required for differentiation of thymic epithelial progenitors. *Proc. Natl. Acad. Sci. U. S. A.* 93: 5742–6.

110. Gordon, J., V. A. Wilson, N. F. Blair, J. Sheridan, A. Farley, L. Wilson, N. R. Manley, and C. C. Blackburn. 2004. Functional evidence for a single endodermal origin for the thymic epithelium. *Nat. Immunol.* 5: 546–53.

111. Tovi, F., and A. J. Mares. 1976. The Aberrant Cervical Thymus: Embryology , Pathology , and Clinical Implications. *Am. J. Surg.* 136: 631–637.

112. Dooley, J., M. Erickson, G. O. Gillard, and A. G. Farr. 2006. Cervical thymus in the mouse. *J. Immunol.* 176: 6484–6490.

113. Terszowski, G., S. M. Muller, C. C. Bleul, C. Blum, R. Schirmbeck, J. Reimann, L. Du Pasquier, T. Amagai, T. Boehm, and H.-R. Rodewald. 2006. Evidence for a Functional Second Thymus in Mice. *Science.* 312: 284–287.

114. Corbeaux, T., I. Hess, J. B. Swann, B. Kanzler, A. Haas-Assenbaum, and T. Boehm. 2010. Thymopoiesis in mice depends on a Foxn1-positive thymic epithelial cell lineage. *Proc. Natl. Acad. Sci. U. S. A.* 107: 16613–8.

115. Li, J., Z. Liu, S. Xiao, and N. R. Manley. 2013. Transdifferentiation of parathyroid cells into cervical thymi promotes atypical T-cell development. *Nat. Commun.* 4: 1–8.

116. Yamazaki, H., E. Sakata, T. Yamane, A. Yanagisawa, K. Abe, K. I. Yamamura, S. I. Hayashi, and T. Kunisada. 2005. Presence and distribution of neural crest-derived cells in the murine developing thymus and their potential for differentiation. *Int. Immunol.* 17: 549–558.

117. Muller, S. M., C. C. Stolt, G. Terszowski, C. Blum, T. Amagai, N. Kessaris, P. Iannarelli, W. D. Richardson, M. Wegner, and H.-R. Rodewald. 2008. Neural Crest Origin of Perivascular Mesenchyme in the Adult Thymus. *J. Immunol.* 180: 5344–5351.

118. Foster, K., J. Sheridan, H. Veiga-Fernandes, K. Roderick, V. Pachnis, R. Adams, C. Blackburn, D. Kioussis, and M. Coles. 2008. Contribution of neural crest-derived cells in the embryonic and adult thymus. *J. Immunol.* 180: 3183–9.

119. Revest, J.-M., R. K. Suniara, K. Kerr, J. J. T. Owen, and C. Dickson. 2001. Development of the thymus requires signaling through the fibroblast growth factor receptor R2-IIIb. *J. Immunol.* 167: 1954–1961.

120. Sitnik, K. M., K. Kotarsky, A. J. White, W. E. Jenkinson, G. Anderson, and W. W.

Agace. 2012. Mesenchymal cells regulate retinoic acid receptor-dependent cortical thymic epithelial cell homeostasis. *J. Immunol.* 188: 4801–9.

121. Jenkinson, W. E., S. W. Rossi, S. M. Parnell, E. J. Jenkinson, and G. Anderson. 2007. PDGFRalpha-expressing mesenchyme regulates thymus growth and the availability of intrathymic niches. *Blood* 109: 954–60.

122. Griffith, A. V., K. Cardenas, C. Carter, J. Gordon, A. Iberg, K. Engleka, J. A. Epstein, N. R. Manley, and E. R. Richie. 2009. Increased thymus- and decreased parathyroid-fated organ domains in Splotch mutant embryos. *Dev. Biol.* 327: 216–227.

123. Chojnowski, J. L., K. Masuda, H. A. Trau, K. Thomas, M. Capecchi, and N. R. Manley. 2014. Multiple roles for HOXA3 in regulating thymus and parathyroid differentiation and morphogenesis in mouse. *Development* 141: 3697–3708.

124. Foster, K. E., J. Gordon, K. Cardenas, H. Veiga-fernandes, T. Makinen, E. Grigorieva, and M. C. Coles. 2010. EphB – ephrin-B2 interactions are required for thymus migration during organogenesis. *Proc. Natl. Acad. Sci. U. S. A.* 107: 13414–13419.

125. Anderson, G., E. J. Jenkinson, N. C. Moore, and J. J. T. Owen. 1993. MHC class II-positive epithelium and mesenchyme cells are both required for T-cell development in the thymus. *Nature* 362: 70–73.

126. Anderson, G., K. L. Anderson, E. Z. Tchilian, J. J. T. Owen, and E. J. Jenkinson. 1997. Fibroblast dependency during early thymocyte development maps to the CD25+ CD44+ stage and involves interactions with fibroblast matrix molecules. *Eur. J. Immunol.* 27: 1200–6.

127. Banwell, C. M., K. M. Partington, E. J. Jenkinson, and G. Anderson. 2000. Studies on the role of IL-7 presentation by mesenchymal fibroblasts during early thymocyte development. *Eur. J. Immunol.* 30: 2125–2129.

128. Xu, P.-X., W. Zheng, C. Laclef, P. Maire, R. L. Maas, H. Peters, and X. Xu. 2002. Eya1 is required for the morphogenesis of mammalian thymus, parathyroid and thyroid. *Development* 129: 3033–44.

129. Manley, N. R., and M. R. Capecchi. 1995. The role of Hoxa-3 in mouse thymus and thyroid development. *Development* 121: 1989–2003.

130. Su, D.-M., S. Ellis, A. Napier, K. Lee, and N. R. Manley. 2001. Hoxa3 and pax1 regulate epithelial cell death and proliferation during thymus and parathyroid organogenesis. *Dev. Biol.* 236: 316–29.

131. Wallin, J., H. Eibel, A. Neubüser, J. Wilting, H. Koseki, and R. Balling. 1996. Pax1 is expressed during development of the thymus epithelium and is required for normal T-cell maturation. *Development* 122: 23–30.

132. Hetzer-Egger, C., M. Schorpp, A. Haas-Assenbaum, R. Balling, H. Peters, and T. Boehm. 2002. Thymopoiesis requires Pax9 function in thymic epithelial cells. *Eur. J. Immunol.* 32: 1175–1181.

133. Zou, D., D. Silvius, J. Davenport, R. Grifone, P. Maire, and P.-X. Xu. 2006. Patterning of the third pharyngeal pouch into thymus/parathyroid by Six and Eya1. *Dev. Biol.* 293: 499–512.

134. Jerome, L. A., and V. E. Papaioannou. 2001. DiGeorge syndrome phenotype in mice mutant for the T-box gene, Tbx1. *Nat. Genet.* 27: 286–91.

135. Romano, R., L. Palamaro, A. Fusco, G. Giardino, V. Gallo, L. Del Vecchio, and C. Pignata. 2013. FOXN1: A master regulator gene of thymic epithelial development program. *Front. Immunol.* 4: 1–13.

136. Schüddekopf, K., M. Schorpp, and T. Boehm. 1996. The whn transcription factor encoded by the nude locus contains an evolutionarily conserved and functionally indispensable activation domain. *Proc. Natl. Acad. Sci. U. S. A.* 93: 9661–4.

137. Nehls, M., B. Kyewski, M. Messerle, R. Waldschutz, K. Schuddekopf, A. J. H. Smith, and T. Boehm. 1996. Two genetically separable steps in the differentiation of thymic epithelium. *Science.* 272: 886–889.

138. Bleul, C. C., and T. Boehm. 2000. Chemokines define distinct microenvironments in the developing thymus. *Eur. J. Immunol.* 30: 3371–3379.

139. Bajoghli, B., N. Aghaallaei, I. Hess, I. Rode, N. Netuschil, B. H. Tay, B. Venkatesh, J. K. Yu, S. L. Kaltenbach, N. D. Holland, D. Diekhoff, C. Happe, M. Schorpp, and T. Boehm. 2009. Evolution of Genetic Networks Underlying the Emergence of Thymopoiesis in Vertebrates. *Cell* 138: 186–197.

140. Swann, J. B., A. Weyn, D. Nagakubo, C. C. Bleul, A. Toyoda, C. Happe, N. Netuschil, I. Hess, A. Haas-Assenbaum, Y. Taniguchi, M. Schorpp, and T. Boehm. 2014. Conversion of the thymus into a bipotent lymphoid organ by replacement of FOXN1 with its paralog, FOXN4. *Cell Rep.* 8: 1184–1197.

141. Žuklys, S., A. Handel, S. Zhanybekova, F. Govani, M. Keller, S. Maio, C. E. Mayer, H. Y. Teh, K. Hafen, G. Gallone, T. Barthlott, C. P. Ponting, and G. A. Holländer. 2016. Foxn1 regulates key target genes essential for T cell development in postnatal thymic epithelial cells. *Nat. Immunol.* 17: 1206–1215.

142. Tsai, P. T., R. A. Lee, and H. Wu. 2003. BMP4 acts upstream of FGF in modulating thymic stroma and regulating thymopoiesis. *Blood* 102: 3947–53.

143. Balciunaite, G., M. P. Keller, E. Balciunaite, L. Piali, S. Zuklys, Y. D. Mathieu, J. Gill, R. Boyd, D. J. Sussman, and G. A. Holländer. 2002. Wnt glycoproteins regulate the expression of FoxN1, the gene defective in nude mice. *Nat. Immunol.* 3: 1102–8.

144. Soza-Ried, C., C. C. Bleul, M. Schorpp, and T. Boehm. 2008. Maintenance of thymic epithelial phenotype requires extrinsic signals in mouse and zebrafish. *J. Immunol.* 181: 5272–5277.

145. Garfin, P. M., D. Min, J. L. Bryson, T. Serwold, B. Edris, C. C. Blackburn, E. R. Richie, K. I. Weinberg, N. R. Manley, J. Sage, and P. Viatour. 2013. Inactivation of the RB family prevents thymus involution and promotes thymic function by direct control of Foxn1 expression. *J. Exp. Med.* 210: 1087–1097.

146. Alves, N. L., N. D. Huntington, H.-R. Rodewald, and J. P. Di Santo. 2009. Thymic epithelial cells: the multi-tasking framework of the T cell “cradle”. *Trends Immunol.* 30: 468–74.

147. Cordier, A. C., and J. F. Heremans. 1975. Nude Mouse Embryo: Ectodermal Nature of

the Primordial Thymic Defect. *Scand. J. Immunol.* 4: 193–196.

148. Cordier, A. C., and S. M. Haumont. 1980. Development of thymus, parathyroids, and ultimo-branchial bodies in NMRI and nude mice. *Am. J. Anat.* 157: 227–263.

149. Röpke, C., P. Van Soest, P. Paul Platenburg, and W. Van Ewijk. 1995. A Common Stem Cell for Murine Cortical and Medullary Thymic Epithelial Cells? *Dev. Immunol.* 4: 149–156.

150. Klug, D. B., C. Carter, E. Crouch, D. Roop, C. J. Conti, and E. R. Richie. 1998. Interdependence of cortical thymic epithelial cell differentiation and T-lineage commitment. *Proc. Natl. Acad. Sci. U. S. A.* 95: 11822–7.

151. Rossi, S. W., W. E. Jenkinson, G. Anderson, and E. J. Jenkinson. 2006. Clonal analysis reveals a common progenitor for thymic cortical and medullary epithelium. *Nature* 441: 988–91.

152. Bleul, C. C., T. Corbeaux, A. Reuter, P. Fisch, J. S. Mönting, and T. Boehm. 2006. Formation of a functional thymus initiated by a postnatal epithelial progenitor cell. *Nature* 441: 992–6.

153. Jenkinson, W. E., A. Bacon, A. J. White, G. Anderson, and E. J. Jenkinson. 2008. An epithelial progenitor pool regulates thymus growth. *J. Immunol.* 181: 6101–8.

154. Depreter, M. G. L., N. F. Blair, T. L. Gaskell, C. S. Nowell, K. Davern, A. Pagliocca, F. H. Stenhouse, A. M. Farley, A. Fraser, J. Vrana, K. Robertson, G. Morahan, S. R. Tomlinson, and C. C. Blackburn. 2008. Identification of Plet-1 as a specific marker of early thymic epithelial progenitor cells. *Proc. Natl. Acad. Sci. U. S. A.* 105: 961–966.

155. Gill, J., M. Malin, G. A. Holländer, and R. Boyd. 2002. Generation of a complete thymic microenvironment by MTS24(+) thymic epithelial cells. *Nat. Immunol.* 3: 635–42.

156. Bennett, A. R., A. Farley, N. F. Blair, J. Gordon, L. Sharp, and C. C. Blackburn. 2002. Identification and characterization of thymic epithelial progenitor cells. *Immunity* 16: 803–14.

157. Rossi, S. W., A. P. Chidgey, S. M. Parnell, W. E. Jenkinson, H. S. Scott, R. L. Boyd, E. J. Jenkinson, and G. Anderson. 2007. Redefining epithelial progenitor potential in the developing thymus. *Eur. J. Immunol.* 37: 2411–8.

158. Baik, S., E. J. Jenkinson, P. J. L. Lane, G. Anderson, and W. E. Jenkinson. 2013. Generation of both cortical and Aire+ medullary thymic epithelial compartments from CD205+ progenitors. *Eur. J. Immunol.* 43: 589–594.

159. Ohigashi, I., S. Zuklys, M. Sakata, C. E. Mayer, S. Zhanybekova, S. Murata, K. Tanaka, G. A. Hollander, and Y. Takahama. 2013. Aire-expressing thymic medullary epithelial cells originate from 5t-expressing progenitor cells. *Proc. Natl. Acad. Sci. U. S. A.* 110: 9885–9890.

160. Ribeiro, A. R., P. M. Rodrigues, C. Meireles, J. P. Di Santo, and N. L. Alves. 2013. Thymocyte selection regulates the homeostasis of IL-7-expressing thymic cortical epithelial cells in vivo. *J. Immunol.* 191: 1200–9.

161. Alves, N. L., Y. Takahama, I. Ohigashi, A. R. Ribeiro, S. Baik, G. Anderson, and W. E. Jenkinson. 2014. Serial progression of cortical and medullary thymic epithelial

microenvironments. *Eur. J. Immunol.* 44: 16–22.

162. Wong, K., N. L. Lister, M. Barsanti, J. M. C. Lim, M. V. Hammett, D. M. Khong, C. Siatskas, D. H. D. Gray, R. L. Boyd, and A. P. Chidgey. 2014. Multilineage potential and self-renewal define an epithelial progenitor cell population in the adult thymus. *Cell Rep.* 8: 1198–1209.

163. Meireles, C., A. R. Ribeiro, R. D. Pinto, C. Leitão, P. M. Rodrigues, and N. L. Alves. 2017. Thymic crosstalk restrains the pool of cortical thymic epithelial cells with progenitor properties. *Eur. J. Immunol.* 47: 958–969.

164. Ohigashi, I., M. Kozai, and Y. Takahama. 2016. Development and developmental potential of cortical thymic epithelial cells. *Immunol. Rev.* 271: 10–22.

165. Shakib, S., G. E. Desanti, W. E. Jenkinson, S. M. Parnell, E. J. Jenkinson, and G. Anderson. 2009. Checkpoints in the development of thymic cortical epithelial cells. *J. Immunol.* 182: 130–7.

166. Fiorini, E., I. Ferrero, E. Merck, S. Favre, M. Pierres, S. A. Luther, and H. R. MacDonald. 2009. Cutting Edge: Thymic Crosstalk Regulates Delta-Like 4 Expression on Cortical Epithelial Cells. *J. Immunol.* 181: 8199–8203.

167. Ribeiro, A. R., C. Meireles, P. M. Rodrigues, and N. L. Alves. 2014. Intermediate expression of CCRL1 reveals novel subpopulations of medullary thymic epithelial cells that emerge in the postnatal thymus. *Eur. J. Immunol.* 44: 2918–2924.

168. Takada, K., K. Kondo, and Y. Takahama. 2017. Generation of Peptides That Promote Positive Selection in the Thymus. *J. Immunol.* 198: 2215–2222.

169. Gommeaux, J., C. Grégoire, P. Nguessan, M. Richelme, M. Malissen, S. Guerder, B. Malissen, and A. Carrier. 2009. Thymus-specific serine protease regulates positive selection of a subset of CD4+ thymocytes. *Eur. J. Immunol.* 39: 956–64.

170. Nakagawa, T., W. Roth, P. Wong, A. Nelson, A. Farr, J. Deussing, J. A. Villadangos, H. Ploegh, C. Peters, and A. Y. Rudensky. 1998. Cathepsin L: Critical Role in Ii Degradation and CD4 T Cell Selection in the Thymus. *Science.* 280: 450–453.

171. Nedjic, J., M. Aichinger, J. Emmerich, N. Mizushima, and L. Klein. 2008. Autophagy in thymic epithelium shapes the T-cell repertoire and is essential for tolerance. *Nature* 455: 396–400.

172. Murata, S., K. Sasaki, T. Kishimoto, S. Niwa, H. Hayashi, Y. Takahama, and K. Tanaka. 2007. Regulation of CD8+ T Cell Development by Thymus-Specific Proteasomes. *Science.* 316: 1349–1353.

173. Nitta, T., S. Murata, K. Sasaki, H. Fujii, A. M. Ripen, N. Ishimaru, S. Koyasu, K. Tanaka, and Y. Takahama. 2010. Thymoproteasome Shapes Immunocompetent Repertoire of CD8+ T Cells. *Immunity* 32: 29–40.

174. Takada, K., F. Van Laethem, Y. Xing, K. Akane, H. Suzuki, S. Murata, K. Tanaka, S. C. Jameson, A. Singer, and Y. Takahama. 2015. TCR affinity for thymoproteasome-dependent positively selecting peptides conditions antigen responsiveness in CD8+ T cells. *Nat. Immunol.* 16: 1069–1076.

175. Rodewald, H.-R., S. Paul, C. Haller, H. Bluethmann, and C. Blum. 2001. Thymus medulla consisting of epithelial islets each derived from a single progenitor. *Nature* 414: 763–8.

176. Hamazaki, Y., H. Fujita, T. Kobayashi, Y. Choi, H. S. Scott, M. Matsumoto, and N. Minato. 2007. Medullary thymic epithelial cells expressing Aire represent a unique lineage derived from cells expressing claudin. *Nat. Immunol.* 8: 304–11.

177. Sekai, M., Y. Hamazaki, and N. Minato. 2014. Medullary thymic epithelial stem cells maintain a functional thymus to ensure lifelong central T cell tolerance. *Immunity* 41: 753–761.

178. Andrews, P. W. 2002. From teratocarcinomas to embryonic stem cells. *Philos. Trans. R. Soc. B Biol. Sci.* 357: 405–417.

179. Baik, S., M. Sekai, Y. Hamazaki, W. E. Jenkinson, and G. Anderson. 2016. Relb acts downstream of medullary thymic epithelial stem cells and is essential for the emergence of RANK+ medullary epithelial progenitors. *Eur. J. Immunol.* 46: 857–862.

180. Ohigashi, I., S. Zuklys, M. Sakata, C. E. Mayer, Y. Hamazaki, N. Minato, G. A. Hollander, and Y. Takahama. 2015. Adult Thymic Medullary Epithelium Is Maintained and Regenerated by Lineage-Restricted Cells Rather Than Bipotent Progenitors. *Cell Rep.* 13: 1432–1443.

181. Mayer, C. E., S. Žuklys, S. Zhanybekova, I. Ohigashi, H. Y. Teh, S. N. Sansom, N. Shikama-Dorn, K. Hafen, I. C. Macaulay, M. E. Deadman, C. P. Ponting, Y. Takahama, and G. A. Holländer. 2016. Dynamic spatio-temporal contribution of single β5t+ cortical epithelial precursors to the thymus medulla. *Eur. J. Immunol.* 46: 846–856.

182. Gray, D., J. Abramson, C. Benoist, and D. Mathis. 2007. Proliferative arrest and rapid turnover of thymic epithelial cells expressing Aire. *J. Exp. Med.* 204: 2521–2528.

183. Gäbler, J., J. Arnold, and B. Kyewski. 2007. Promiscuous gene expression and the developmental dynamics of medullary thymic epithelial cells. *Eur. J. Immunol.* 37: 3363–3372.

184. Rossi, S. W., M.-Y. Kim, A. Leibbrandt, S. M. Parnell, W. E. Jenkinson, S. H. Glanville, F. M. McConnell, H. S. Scott, J. M. Penninger, E. J. Jenkinson, P. J. L. Lane, and G. Anderson. 2007. RANK signals from CD4(+)3(-) inducer cells regulate development of Aire-expressing epithelial cells in the thymic medulla. *J. Exp. Med.* 204: 1267–72.

185. White, A. J., K. Nakamura, W. E. Jenkinson, M. Saini, C. Sinclair, B. Seddon, P. Narendran, K. Pfeffer, T. Nitta, Y. Takahama, J. H. Caamano, P. J. L. Lane, E. J. Jenkinson, and G. Anderson. 2010. Lymphotoxin Signals from Positively Selected Thymocytes Regulate the Terminal Differentiation of Medullary Thymic Epithelial Cells. *J. Immunol.* 185: 4769–4776.

186. Nishikawa, Y., H. Nishijima, M. Matsumoto, J. Morimoto, F. Hirota, S. Takahashi, H. Luche, H. J. Fehling, Y. Mouri, and M. Matsumoto. 2014. Temporal Lineage Tracing of Aire-Expressing Cells Reveals a Requirement for Aire in Their Maturation Program. *J. Immunol.* 192: 2585–2592.

187. Hubert, F.-X., S. A. Kinkel, K. E. Webster, P. Cannon, P. E. Crewther, A. I. Proeitto, L.

Wu, W. R. Heath, and H. S. Scott. 2008. A specific anti-Aire antibody reveals aire expression is restricted to medullary thymic epithelial cells and not expressed in periphery. *J. Immunol.* 180: 3824–3832.

188. McCarthy, N. I., J. E. Cowan, K. Nakamura, A. Bacon, S. Baik, A. J. White, S. M. Parnell, E. J. Jenkinson, W. E. Jenkinson, and G. Anderson. 2015. Osteoprotegerin-Mediated Homeostasis of Rank $^{+}$ Thymic Epithelial Cells Does Not Limit Foxp3 $^{+}$ Regulatory T Cell Development. *J. Immunol.* 195: 2675–2682.

189. Ritter, M. A., and R. L. Boyd. 1993. Development in the thymus: it takes two to tango. *Immunol. Today* 14: 462–469.

190. Kajiura, F., S. Sun, T. Nomura, K. Izumi, T. Ueno, Y. Bando, N. Kuroda, H. Han, Y. Li, A. Matsushima, Y. Takahama, S. Sakaguchi, T. Mitani, and M. Matsumoto. 2004. NF-kappa B-inducing kinase establishes self-tolerance in a thymic stroma-dependent manner. *J. Immunol.* 172: 2067–75.

191. Akiyama, T., S. Maeda, S. Yamane, K. Ogino, M. Kasai, F. Kajiura, M. Matsumoto, and J. Inoue. 2005. Dependence of self-tolerance on TRAF6-directed development of thymic stroma. *Science.* 308: 248–51.

192. Burkly, L., C. Hession, L. Ogata, C. Rellly, L. A. Marconi, D. Olson, R. Tizard, R. Cate, and D. Lo. 1995. Expression of relB is required for the development of thymic medulla and dendritic cells. *Nature* 373: 531–536.

193. Boehm, T., S. Scheu, K. Pfeffer, and C. C. Bleul. 2003. Thymic medullary epithelial cell differentiation, thymocyte emigration, and the control of autoimmunity require lympho-epithelial cross talk via LTbetaR. *J. Exp. Med.* 198: 757–69.

194. Seach, N., T. Ueno, A. L. Fletcher, M. Mattesich, C. R. Engwerda, H. S. Scott, C. F. Ware, A. P. Chidgey, D. H. D. Gray, and R. L. Boyd. 2008. The Lymphotoxin Pathway Regulates Aire-Independent Expression of Ectopic Genes and Chemokines in Thymic Stromal Cells. *J. Immunol.* 180: 5384–5392.

195. Cosway, E. J., B. Lucas, K. D. James, S. M. Parnell, M. Carvalho-Gaspar, A. J. White, A. V. Tumanov, W. E. Jenkinson, and G. Anderson. 2017. Redefining thymus medulla specialization for central tolerance. *J. Exp. Med.* 1–13.

196. Zhu, M., R. K. Chin, A. V. Tumanov, X. Liu, and Y. Fu. 2007. Lymphotoxin β Receptor is Required for the Selection of Autoreactive T Cells in Thymic Medulla. *J. Immunol.* 179: 8069–8075.

197. Akiyama, T., Y. Shimo, H. Yanai, J. Qin, D. Ohshima, Y. Maruyama, Y. Asaumi, J. Kitazawa, H. Takayanagi, J. M. Penninger, M. Matsumoto, T. Nitta, Y. Takahama, and J. Inoue. 2008. The tumor necrosis factor family receptors RANK and CD40 cooperatively establish the thymic medullary microenvironment and self-tolerance. *Immunity* 29: 423–37.

198. Hikosaka, Y., T. Nitta, I. Ohigashi, K. Yano, N. Ishimaru, Y. Hayashi, M. Matsumoto, K. Matsuo, J. M. Penninger, H. Takayanagi, Y. Yokota, H. Yamada, Y. Yoshikai, J.-I. Inoue, T. Akiyama, and Y. Takahama. 2008. The cytokine RANKL produced by positively selected thymocytes fosters medullary thymic epithelial cells that express autoimmune regulator. *Immunity* 29: 438–50.

199. Desanti, G. E., J. E. Cowan, S. Baik, S. M. Parnell, A. J. White, J. M. Penninger, P. J. L. Lane, E. J. Jenkinson, W. E. Jenkinson, and G. Anderson. 2012. Developmentally regulated availability of RANKL and CD40 ligand reveals distinct mechanisms of fetal and adult cross-talk in the thymus medulla. *J. Immunol.* 189: 5519–26.

200. Irla, M., S. Hugues, J. Gill, T. Nitta, Y. Hikosaka, I. R. Williams, F.-X. Hubert, H. S. Scott, Y. Takahama, G. A. Holländer, and W. Reith. 2008. Autoantigen-specific interactions with CD4+ thymocytes control mature medullary thymic epithelial cell cellularity. *Immunity* 29: 451–63.

201. Irla, M., L. Guerri, J. Guenot, A. Sergé, O. Lantz, A. Liston, B. A. Imhof, E. Palmer, and W. Reith. 2012. Antigen recognition by autoreactive $CD4^+$ thymocytes drives homeostasis of the thymic medulla. *PLoS One* 7: e52591.

202. Mouri, Y., M. Yano, M. Shinzawa, Y. Shimo, F. Hirota, Y. Nishikawa, T. Nii, H. Kiyonari, T. Abe, H. Uehara, K. Izumi, K. Tamada, L. Chen, J. M. Penninger, J. Inoue, T. Akiyama, and M. Matsumoto. 2011. Lymphotoxin signal promotes thymic organogenesis by eliciting RANK expression in the embryonic thymic stroma. *J. Immunol.* 186: 5047–57.

203. Goldfarb, Y., N. Kadouri, B. Levi, A. Sela, Y. Herzig, R. N. Cohen, A. N. Hollenberg, and J. Abramson. 2016. HDAC3 Is a Master Regulator of mTEC Development. *Cell Rep.* 15: 651–665.

204. Derbinski, J., J. Gäbler, B. Brors, S. Tierling, S. Jonnakuty, M. Hergenhahn, L. Peltonen, J. Walter, and B. Kyewski. 2005. Promiscuous gene expression in thymic epithelial cells is regulated at multiple levels. *J. Exp. Med.* 202: 33–45.

205. Sansom, S. N., N. Shikama-Dorn, S. Zhanybekova, G. Nusspaumer, I. C. Macaulay, M. E. Deadman, A. Heger, C. P. Ponting, and G. A. Hollander. 2014. Population and single-cell genomics reveal the Aire dependency, relief from Polycomb silencing, and distribution of self-antigen expression in thymic epithelia. *Genome Res.* 24: 1918–1931.

206. Pinto, S., C. Michel, H. Schmidt-Glenewinkel, N. Harder, K. Rohr, S. Wild, B. Brors, and B. Kyewski. 2013. Overlapping gene coexpression patterns in human medullary thymic epithelial cells generate self-antigen diversity. *Proc. Natl. Acad. Sci. U. S. A.* 110: E3497–E3505.

207. Brennecke, P., A. Reyes, S. Pinto, K. Rattay, M. Nguyen, R. Küchler, W. Huber, B. Kyewski, and L. M. Steinmetz. 2015. Single-cell transcriptome analysis reveals coordinated ectopic gene-expression patterns in medullary thymic epithelial cells. *Nat. Immunol.* 16: 933–941.

208. Cloosen, S., J. Arnold, M. Thio, G. M. J. Bos, B. Kyewski, and W. T. V. Germeraad. 2007. Expression of tumor-associated differentiation antigens, MUC1 glycoforms and CEA, in human thymic epithelial cells: Implications for self-tolerance and tumor therapy. *Cancer Res.* 67: 3919–3926.

209. Derbinski, J., S. Pinto, S. Rosch, K. Hexel, and B. Kyewski. 2008. Promiscuous gene expression patterns in single medullary thymic epithelial cells argue for a stochastic mechanism. *Proc. Natl. Acad. Sci. U. S. A.* 105: 657–662.

210. Finnish-German APECED Consortium. 1997. An autoimmune disease, APECED,

caused by mutations in a novel gene featuring two PHD-type zinc-finger domains. *Nat. Genet.* 17: 399–403.

211. Nagamine, K., P. Peterson, H. S. Scott, J. Kudoh, S. Minoshima, M. Heino, K. J. E. Krohn, M. D. Lalioti, P. E. Mullis, S. E. Antonarakis, K. Kawasaki, S. Asakawa, F. Ito, and N. Shimizu. 1997. Positional cloning of the APECED gene. *Nat. Genet.* 17: 393–398.

212. St-Pierre, C., A. Trofimov, S. Brochu, S. Lemieux, and C. Perreault. 2015. Differential Features of AIRE-Induced and AIRE-Independent Promiscuous Gene Expression in Thymic Epithelial Cells. *J. Immunol.* 195: 498–506.

213. Anderson, M. S., and M. A. Su. 2016. AIRE expands: new roles in immune tolerance and beyond. *Nat. Rev. Immunol.* 16: 247–258.

214. Org, T., A. Rebane, K. Kisand, M. Laan, U. Haljasorg, R. Andreson, and P. Peterson. 2009. AIRE activated tissue specific genes have histone modifications associated with inactive chromatin. *Hum. Mol. Genet.* 18: 4699–4710.

215. Koh, A. S., A. J. Kuo, S. Y. Park, P. Cheung, J. Abramson, D. Bua, D. Carney, S. E. Shoelson, O. Gozani, R. E. Kingston, C. Benoist, and D. Mathis. 2008. Aire employs a histone-binding module to mediate immunological tolerance, linking chromatin regulation with organ-specific autoimmunity. *Proc. Natl. Acad. Sci. U. S. A.* 105: 15878–15883.

216. Org, T., F. Chignola, C. Hetényi, M. Gaetani, A. Rebane, I. Liiv, U. Maran, L. Mollica, M. J. Bottomley, G. Musco, and P. Peterson. 2008. The autoimmune regulator PHD finger binds to non-methylated histone H3K4 to activate gene expression. *EMBO Rep.* 9: 370–376.

217. Abramson, J., M. Giraud, C. Benoist, and D. Mathis. 2010. Aire's Partners in the Molecular Control of Immunological Tolerance. *Cell* 140: 123–135.

218. Giraud, M., H. Yoshida, J. Abramson, P. B. Rahl, R. A. Young, D. Mathis, and C. Benoist. 2012. Aire unleashes stalled RNA polymerase to induce ectopic gene expression in thymic epithelial cells. *Proc. Natl. Acad. Sci. U. S. A.* 109: 535–540.

219. Haljasorg, U., R. Bichele, M. Saare, M. Guha, J. Maslovskaja, K. Kõnd, A. Remm, M. Pihlap, L. Tomson, K. Kisand, M. Laan, and P. Peterson. 2015. A highly conserved NF-kB-responsive enhancer is critical for thymic expression of Aire in mice. *Eur. J. Immunol.* 45: 3246–3256.

220. LaFlam, T. N., G. Seumois, C. N. Miller, W. Lwin, K. J. Fasano, M. Waterfield, I. Proekt, P. Vijayanand, and M. S. Anderson. 2015. Identification of a novel cis-regulatory element essential for immune tolerance. *J. Exp. Med.* 212: 1993–2002.

221. Lei, Y., A. M. Ripen, N. Ishimaru, I. Ohigashi, T. Nagasawa, L. T. Jeker, M. R. Bösl, G. A. Holländer, Y. Hayashi, R. de Waal Malefyt, T. Nitta, and Y. Takahama. 2011. Aire-dependent production of XCL1 mediates medullary accumulation of thymic dendritic cells and contributes to regulatory T cell development. *J. Exp. Med.* 208: 383–394.

222. Yano, M., N. Kuroda, H. Han, M. Meguro-Horike, Y. Nishikawa, H. Kiyonari, K. Maemura, Y. Yanagawa, K. Obata, S. Takahashi, T. Ikawa, R. Satoh, H. Kawamoto, Y. Mouri, and M. Matsumoto. 2008. Aire controls the differentiation program of thymic epithelial cells in the medulla for the establishment of self-tolerance. *J. Exp. Med.* 205: 2827–2838.

223. Gillard, G. O., J. Dooley, M. Erickson, L. Peltonen, and A. G. Farr. 2007. Aire-Dependent Alterations in Medullary Thymic Epithelium Indicate a Role for Aire in Thymic Epithelial Differentiation. *J. Immunol.* 178: 3007–3015.

224. Guerau-de-Arellano, M., M. Martinic, C. Benoist, and D. Mathis. 2009. Neonatal tolerance revisited: a perinatal window for Aire control of autoimmunity. *J. Exp. Med.* 206: 1245–1252.

225. Yang, S., N. Fujikado, D. Kolodin, C. Benoist, and D. Mathis. 2015. Regulatory T cells generated early in life play a distinct role in maintaining self-tolerance. *Science.* 348: 589–594.

226. Sempowski, G. D., M. E. Gooding, H. X. Liao, P. T. Le, and B. F. Haynes. 2002. T cell receptor excision circle assessment of thymopoiesis in aging mice. *Mol. Immunol.* 38: 841–848.

227. Steinmann, G. G., B. Klaus, and H. -K. Muller-Hermelink. 1985. The Involution of the Ageing Human Thymic Epithelium is Independent of Puberty: A Morphometric Study. *Scand. J. Immunol.* 22: 563–575.

228. Takeoka, Y., S.-Y. Chen, H. Yago, R. L. Boyd, S. Suehiro, L. D. Shultz, A. A. Ansari, and M. E. Gershwin. 1996. The Murine Thymic Microenvironment: Changes with Age. *Int. Arch. Allergy Immunol.* 111: 5–12.

229. Gui, J., X. Zhu, J. Dohkan, L. Cheng, P. F. Barnes, and D.-M. Su. 2007. The aged thymus shows normal recruitment of lymphohematopoietic progenitors but has defects in thymic epithelial cells. *Int. Immunol.* 19: 1201–1211.

230. Aw, D., A. B. Silva, M. Maddick, T. von Zglinicki, and D. B. Palmer. 2008. Architectural changes in the thymus of aging mice. *Aging Cell* 7: 158–67.

231. Aw, D., F. Taylor-Brown, K. Cooper, and D. B. Palmer. 2009. Phenotypical and morphological changes in the thymic microenvironment from ageing mice. *Biogerontology* 10: 311–322.

232. Yang, H., Y.-H. Youm, Y. Sun, J.-S. Rim, C. J. Galbán, B. Vandanmagsar, and V. D. Dixit. 2009. Axin expression in thymic stromal cells contributes to an age-related increase in thymic adiposity and is associated with reduced thymopoiesis independently of ghrelin signaling. *J. Leukoc. Biol.* 85: 928–38.

233. Hale, J. S., T. E. Boursalian, G. L. Turk, and P. J. Fink. 2006. Thymic output in aged mice. *Proc. Natl. Acad. Sci. U. S. A.* 103: 8447–52.

234. Hoskins, E. R. 1918. Is there a thymic hormone? *Endocrinology* 2: 241–257.

235. Mackall, C. L., J. A. Punt, P. Morgan, A. G. Farr, and R. E. Gress. 1998. Thymic function in young/old chimeras: Substantial thymic T cell regenerative capacity despite irreversible age-associated thymic involution. *Eur. J. Immunol.* 28: 1886–1893.

236. Zhu, X., J. Gui, J. Dohkan, L. Cheng, P. F. Barnes, and D.-M. Su. 2007. Lymphohematopoietic progenitors do not have a synchronized defect with age-related thymic involution. *Aging Cell* 6: 663–672.

237. Dudakov, J. A., D. M. P. Khong, R. L. Boyd, and A. P. Chidgey. 2010. Feeding the fire:

the role of defective bone marrow function in exacerbating thymic involution. *Trends Immunol.* 31: 191–8.

238. Ki, S., D. Park, H. J. Selden, J. Seita, H. Chung, J. Kim, V. R. Iyer, and L. I. R. Ehrlich. 2014. Global transcriptional profiling reveals distinct functions of thymic stromal subsets and age-related changes during thymic involution. *Cell Rep.* 9: 402–415.

239. Rode, I., V. C. Martins, G. Küblbeck, N. Maltry, C. Tessmer, and H.-R. Rodewald. 2015. Foxn1 Protein Expression in the Developing, Aging, and Regenerating Thymus. *J. Immunol.* 195: 5678–5687.

240. O'Neill, K. E., N. Bredenkamp, C. Tischner, H. J. Vaidya, F. H. Stenhouse, C. D. Peddie, C. S. Nowell, T. Gaskell, and C. C. Blackburn. 2016. Foxn1 is dynamically regulated in thymic epithelial cells during embryogenesis and at the onset of thymic involution. *PLoS One* 11: 1–14.

241. Chen, L., S. Xiao, and N. R. Manley. 2009. Foxn1 is required to maintain the postnatal thymic microenvironment in a dosage-sensitive manner. *Blood* 113: 567–574.

242. Bredenkamp, N., C. S. Nowell, and C. C. Blackburn. 2014. Regeneration of the aged thymus by a single transcription factor. *Development* 141: 1627–1637.

243. Hadden, J. W. 1998. Thymic endocrinology. *Ann. N. Y. Acad. Sci.* 840: 352–358.

244. Sempowski, G. D., L. P. Hale, J. S. Sundy, J. M. Massey, R. A. Koup, D. C. Douek, D. D. Patel, and B. F. Haynes. 2000. Leukemia inhibitory factor, oncostatin M, IL-6, and stem cell factor mRNA expression in human thymus increases with age and is associated with thymic atrophy. *J. Immunol.* 164: 2180–2187.

245. Morrissey, P. J., K. Charrier, A. Alpert, and L. Bressler. 1988. In vivo administration of IL-1 induces thymic hypoplasia and increased levels of serum corticosterone. *J. Immunol.* 141: 1456–1463.

246. Youm, Y. H., T.-D. Kanneganti, B. Vandanmagsar, X. Zhu, A. Ravussin, A. Adijiang, J. S. Owen, M. J. Thomas, J. Francis, J. S. Parks, and V. D. Dixit. 2012. The NLRP3 Inflammasome Promotes Age-Related Thymic Demise and Immunosenescence. *Cell Rep.* 1: 56–68.

247. Hince, M., S. Sakkal, K. Vlahos, J. Dudakov, R. Boyd, and A. Chidgey. 2008. The role of sex steroids and gonadectomy in the control of thymic involution. *Cell. Immunol.* 252: 122–38.

248. Velardi, E., J. A. Dudakov, and M. R. M. van den Brink. 2015. Sex steroid ablation: an immunoregenerative strategy for immunocompromised patients. *Bone Marrow Transplant.* 50 Suppl 2: S77-81.

249. Grossman, C. J. 1985. Interactions between the gonadal steroids and the immune system. *Science.* 227: 257–261.

250. Hyojin, L., H. Kim, Y. Chung, J. Kim, and H. Yang. 2013. Thymocyte Differentiation is Regulated by a Change in Estradiol Levels during the Estrous Cycle in Mouse. *Dev. Reprod.* 17: 441–449.

251. Viselli, S. M., N. J. Olsen, K. Shults, G. Steizer, and W. J. Kovacs. 1995.

Immunochemical and flow cytometric analysis of androgen receptor expression in thymocytes. *Mol. Cell. Endocrinol.* 109: 19–26.

252. Olsen, N. J., G. Olson, S. M. Viselli, X. Gu, and W. J. Kovacs. 2001. Androgen receptors in thymic epithelium modulate thymus size and thymocyte development. *Endocrinology* 142: 1278–83.

253. Staples, J. E., T. A. Gasiewicz, N. C. Fiore, D. B. Lubahn, K. S. Korach, and A. E. Silverstone. 1999. Estrogen receptor alpha is necessary in thymic development and estradiol-induced thymic alterations. *J. Immunol.* 163: 4168–74.

254. Barr, I. G., B. A. K. Khalid, P. Pearce, B.-H. Toh, P. F. Bartlett, R. G. Scollay, and J. W. Funder. 1982. Dihydrotestosterone and estradiol deplete corticosensitive thymocytes lacking in receptors for these hormones. *J. Immunol.* 128: 2825–2828.

255. Rijhsinghani, A. G., K. Thompson, S. K. Bhatia, and T. J. Waldschmidt. 1996. Estrogen Blocks Early T Cell Development in the Thymus. *Am. J. Reprod. Immunol.* 36: 269–277.

256. Dumont-Lagacé, M., C. St-Pierre, and C. Perreault. 2015. Sex hormones have pervasive effects on thymic epithelial cells. *Sci. Rep.* 5: 12895.

257. Heng, T. S. P., G. L. Goldberg, D. H. D. Gray, J. S. Sutherland, A. P. Chidgey, and R. L. Boyd. 2005. Effects of Castration on Thymocyte Development in Two Different Models of Thymic Involution. *J. Immunol.* 5: 2982–2993.

258. Sutherland, J. S., G. L. Goldberg, M. V. Hammett, A. P. Uldrich, S. P. Berzins, T. S. Heng, B. R. Blazar, J. L. Millar, M. A. Malin, A. P. Chidgey, and R. L. Boyd. 2005. Activation of Thymic Regeneration in Mice and Humans following Androgen Blockade. *J. Immunol.* 4: 2741–2753.

259. Greenstein, B. D., F. T. A. Fitzpatrick, M. D. Kendall, and M. J. Wheeler. 1987. Regeneration of the thymus in old male rats treated with a stable analogue of LHRH. *J. Endocrinol.* 112: 345–350.

260. Williams, K. M., P. J. Lucas, C. V. Bare, J. Wang, Y.-W. Chu, E. Tayler, V. Kapoor, and R. E. Gress. 2008. CCL25 increases thymopoiesis after androgen withdrawal. *Blood* 112: 3255–63.

261. Dudakov, J. A., G. L. Goldberg, J. J. Reiseger, A. P. Chidgey, and R. L. Boyd. 2009. Withdrawal of sex steroids reverses age- and chemotherapy-related defects in bone marrow lymphopoiesis. *J. Immunol.* 182: 6247–6260.

262. Khong, D. M., J. A. Dudakov, M. V. Hammett, M. I. Jurblum, S. M. L. Khong, G. L. Goldberg, T. Ueno, L. Spyroglou, L. F. Young, M. R. M. van Den Brink, R. L. Boyd, and A. P. Chidgey. 2015. Enhanced hematopoietic stem cell function mediates immune regeneration following sex steroid blockade. *Stem Cell Reports* 4: 445–458.

263. Dudakov, J. A., G. L. Goldberg, J. J. Reiseger, K. Vlahos, A. P. Chidgey, and R. L. Boyd. 2009. Sex steroid ablation enhances hematopoietic recovery following cytotoxic antineoplastic therapy in aged mice. *J. Immunol.* 183: 7084–94.

264. Goldberg, G. L., J. A. Dudakov, J. J. Reiseger, N. Seach, T. Ueno, K. Vlahos, M. V. Hammett, L. F. Young, T. S. P. Heng, R. L. Boyd, and A. P. Chidgey. 2010. Sex steroid ablation enhances immune reconstitution following cytotoxic antineoplastic therapy in young

mice. *J. Immunol.* 184: 6014–24.

265. Goldberg, G. L., C. G. King, R. A. Nejat, D. Y. Suh, O. M. Smith, J. C. Bretz, R. M. Samstein, J. A. Dudakov, A. P. Chidgey, S. Chen-Kiang, R. L. Boyd, and M. R. M. van den Brink. 2009. Luteinizing hormone-releasing hormone enhances T cell recovery following allogeneic bone marrow transplantation. *J. Immunol.* 182: 5846–54.

266. Goldberg, G. L., O. Alpdogan, S. J. Muriglan, M. V. Hammett, M. K. Milton, J. M. Eng, V. M. Hubbard, A. Kochman, L. M. Willis, A. S. Greenberg, K. H. Tjoe, J. S. Sutherland, A. Chidgey, M. R. M. van den Brink, and R. L. Boyd. 2007. Enhanced immune reconstitution by sex steroid ablation following allogeneic hemopoietic stem cell transplantation. *J. Immunol.* 178: 7473–84.

267. Goldberg, G. L., J. S. Sutherland, M. V. Hammet, M. K. Milton, T. S. P. Heng, A. P. Chidgey, and R. L. Boyd. 2005. Sex steroid ablation enhances lymphoid recovery following autologous hematopoietic stem cell transplantation. *Transplantation* 80: 1604–1613.

268. Henderson, J. 1904. On the relationship of the thymus to the sexual organs. I. The influence of castration on the thymus. *J. Physiol.* 31: 222–229.

269. Velardi, E., J. J. Tsai, A. M. Holland, T. Wertheimer, V. W. C. Yu, J. L. Zakrzewski, A. Z. Tuckett, N. V. Singer, M. L. West, O. M. Smith, L. F. Young, F. M. Kreines, E. R. Levy, R. L. Boyd, D. T. Scadden, J. A. Dudakov, and M. R. M. van den Brink. 2014. Sex steroid blockade enhances thymopoiesis by modulating Notch signaling. *J. Exp. Med.* 211: 2341–2349.

270. Koch, U., and F. Radtke. 2011. Mechanisms of T Cell Development and Transformation. *Annu. Rev. Cell Dev. Biol.* 27: 539–62.

Chapter II

Thymic epitelial cells require p53 to support their long-term function in thymopoiesis in mice

Pedro M. Rodrigues[1,2,3], Ana R. Ribeiro[1,2,3], Chiara Perrod[1,2], Jonathan J.M. Landry[4], Leonor Araújo[1,2], Isabel Pereira-Castro[1,5], Vladimir Benes[4], Alexandra Moreira[1,5,6], Helena Xavier-Ferreira[1,2], Catarina Meireles[1,2] and Nuno L. Alves[1,2].

[1] Instituto de Investigação e Inovação em Saúde, Universidade do Porto, Portugal.
[2] Thymus Development and Function Laboratory, Instituto de Biologia Molecular e Celular, Porto, Portugal.
[3] Doctoral Program in Biomedical Sciences, Instituto de Ciências Biomédicas Abel Salazar, Universidade do Porto, Porto, Portugal.
[4] Genomics Core Facility, European Molecular Biology Laboratory, Heidelberg, Germany.
[5] Gene Regulation Laboratory, Instituto de Biologia Molecular e Celular, Porto, Portugal.
[6] Instituto de Ciências Biomédicas Abel Salazar, Universidade do Porto, Portugal.

Blood 2017 130:478-488

Abstract

Thymic epithelial cells (TECs) provide crucial microenvironments for T-cell development and tolerance induction. As the regular function of the thymus declines with age, it is of fundamental and clinical relevance to decipher new determinants that control TEC homeostasis *in vivo.* Beyond its recognized tumour suppressive function, p53 controls several immunoregulatory pathways. To study the cell-autonomous role of p53 in thymic epithelium functioning, we developed and analysed mice with conditional inactivation of *Trp53* in TECs (p53cKO). We report that loss of p53 primarily disrupts the integrity of medullary TEC (mTEC) niche, a defect that spreads to the adult cortical TEC (cTEC) compartment. Mechanistically, we found that p53 controls specific and broad programs of mTEC differentiation. Apart from restraining the expression and responsiveness of RANK, which is central for mTEC differentiation, deficiency of p53 in TECs altered multiple functional modules of the mTEC transcriptome, including tissue-restricted antigen expression. As a result, p53cKO mice presented premature defects in mTEC-dependent regulatory T cell differentiation and thymocyte maturation, which progressed to a failure in regular and regenerative thymopoiesis and peripheral T-cell homeostasis in the adulthood. Lastly, peripheral signs of altered immunological tolerance unfold in mutant mice and in immunodeficient mice that received p53cKO-derived thymocytes. Our findings position p53 as a novel molecular determinant of thymic epithelium function throughout life.

Introduction

Within the thymus, thymic epithelial cells (TECs) orchestrate the development of functionally diverse and self-tolerant T cells (1). Importantly, impaired TEC functions arise with aging, cytoablative regimens and infection, which compromise T-cell responses to pathogens and vaccination in the elderly and patients undergoing bone marrow transplantations (BMT) or chemotherapy. Equally, failures in TEC-mediated tolerance induction lead to autoimmunity (2). Hence, the identification of novel regulators of TEC homeostasis is crucial to comprehend the foundations of immunity and to intervene medically in disorders linked to a dysfunctional thymus.

Cortical (c) and medullary (m) TECs define two functionally distinct microenvironments, which differentiate from bipotent TEC progenitors (1). While cTECs drive T-cell lineage specification and positive selection, mTECs promote the maturation of positively selected thymocytes, regulatory T cell differentiation and elimination of autoreactive T cells (1). Important to mTEC function is their ability to express tissue-restricted antigens (TRA) (2), which depends in part on Auto-immune regulator (Aire) and Fezf2 (3, 4). Past studies elucidated the role of members of TNF receptor superfamily (TNFRSF) receptor activator of NF-κB (RANK), lymphotoxin β receptor (LtβR) and CD40 in the maturation of mTECs (1). Still, the molecular determinants that control the function of these key inducers of mTECs remain unknown. Other uncertainties concern the signalling pathways that maintain the multilayered function of TECs *in vivo*.

The tumour suppressor protein p53 is a recognized regulator of cell-cycle arrest and apoptosis. Yet, recent studies have revealed alternative roles for p53 in immunoregulation and autoimmunity (5). Relatively to the thymic epithelium, the observations that the p53 homologue p63 controls the turnover of TEC progenitors (6) imply a possible functional relationship within the p53 family. The analysis of the role of p53 in TEC physiology has been precluded due to its broad expression pattern and the complex phenotype of germline p53-null mice, which ultimately develop thymic lymphomas (7). Despite such limitations, several studies link p53 to TEC homeostasis. While germline deletion in wild-type p53-induced phosphatase 1 (Wip1), a p53-target gene, impairs the maturation of mTECs and thymic regeneration (8), the systemic administration of p53 inhibitors moderately improves TEC recovery and thymopoiesis following BMT (9). As genetically engineered mouse models and pharmacological studies often hide lineage-specific functions of broadly acting genes, the cell-autonomous relevance of p53 in the dynamic differentiation of TECs *in vivo* remains unexplored. Our findings underscore the requirement for p53 in TECs to support their role in T-cell development and selection.

Results

Inactivation of *Trp53* in TECs reduces the mTEC compartment.

To investigate the function of p53 in the thymic epithelium, we conditionally deleted the p53 gene (*Trp53*) in TECs by crossing mice with loxP-flanked alleles of *Trp53* (*Trp53*$^{fl/fl}$) (10) to mice expressing Cre recombinase under the control of the *Foxn1* promoter (*Foxn1*^{Cre}), which directs the expression of Cre recombinase to virtually all TECs during embryonic and postnatal life (11). *Foxn1*^{Cre}:*Trp53*$^{fl/fl}$ (p53cKO) mice were born without obvious abnormalities and did not develop spontaneous tumours in the thymus or skin, which also contains Foxn1^{+} keratinocytes (11). Cre-mediated deletion of *Trp53*^{fl} allele was detected in TECs but neither in thymocytes from p53cKO mice nor in TECs from *Trp53*$^{fl/fl}$ littermate controls (Ctr) (**Figure 1A** and **supplemental Figure 1A-B**). Although not statistically different, *Trp53* levels were moderately increased in mTECs compared to cTECs from control thymus (**Figure 1B**), indicating that p53 is expressed under physiological conditions. The same transcript was nearly absent in cTECs and mTECs from p53cKO mice (**Figure 1B**), but remained similarly expressed in thymocytes from Ctr and p53cKO mice (**supplemental Figure 1C).**

We started by comparing the thymic epithelium composition in control and p53cKO mice throughout life. Although with altered proportions relative to controls, cTEC numbers were normal during fetal, postnatal and pre-puberty periods, becoming moderately diminished in 10-week-old p53cKO mice (**Figure 1C-D**). In contrast, while seemingly similar to control mice at E16.5, the frequency and numbers of mTECs were continually reduced in mutant mice from the postnatal period onwards (**Figure 1C-D**). Concordantly, the global medullary compartment and the number of UEA^{+} mTECs were reduced in adult p53cKO thymus, without affecting the compartmentalization into cortex and medulla (**supplemental Figure 1D**). We assessed possible Cre-mediated cellular toxicity, and found no major changes in thymic and cTEC/mTEC cellularities of *Foxn1*^{Cre}:*Trp53*$^{+/+}$ mice compared with *Trp53*$^{+/+}$ mice (**supplemental Figure 1E**). Age-matched *Trp53*$^{fl/fl}$ littermates were used as controls in subsequent experiments.

The impact of *Trp53* deletion in mTECs led us to examine their differentiation program. First, we subdivided mTECs into CD80^{lo}, which include immature cells and

a minor subset of post-Aire terminally differentiated cells in the adult thymus, and mature CD80^{hi}, which contains Aire-expressing cells (1, 12). The development of

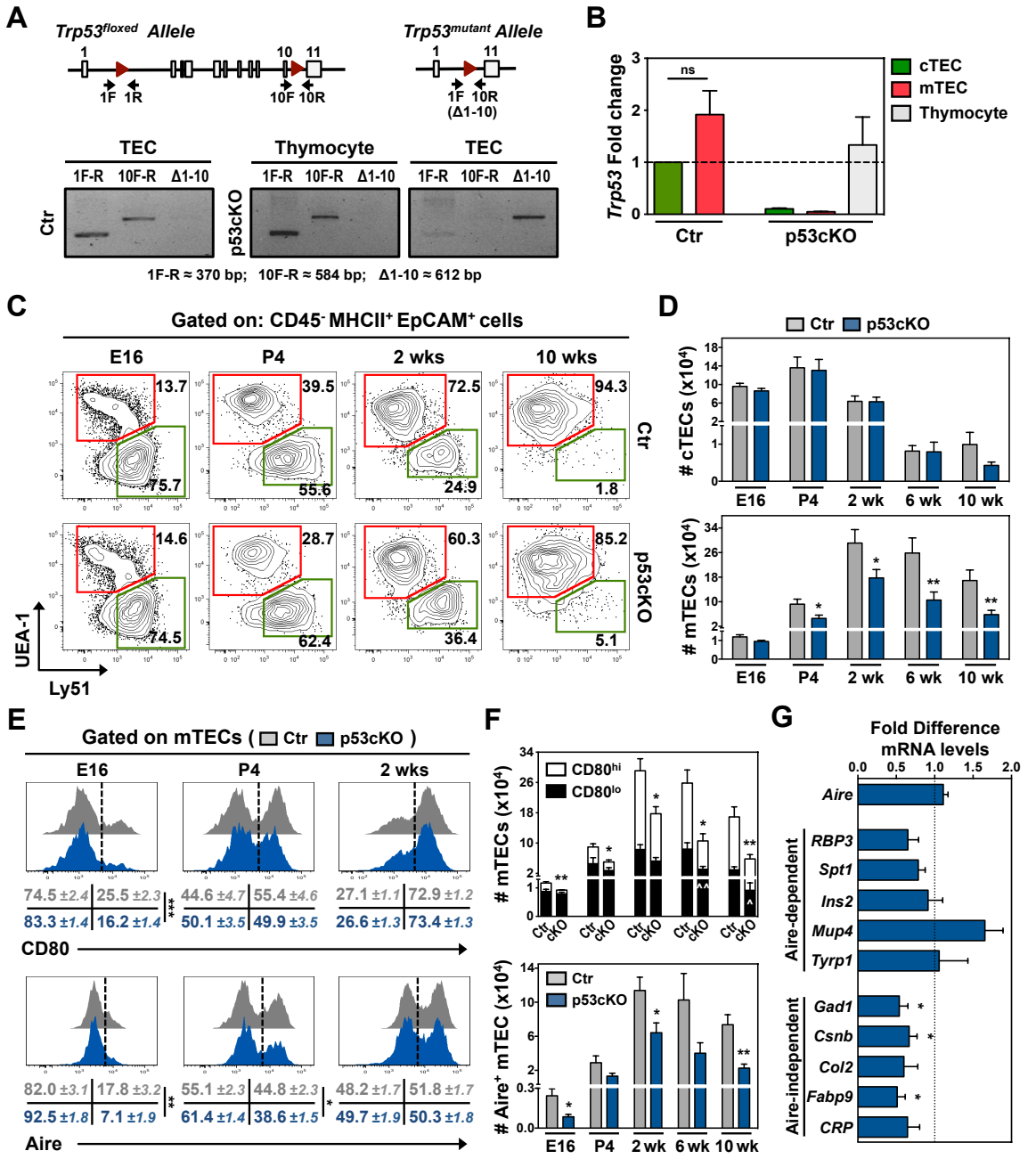

Figure 1 - Ablation of *Trp53* in TECs diminishes the size of the mTEC niche. (A) Diagram of the genomic floxed and targeted *Trp53* alleles (top). *LoxP* sequences flank exons 2-10 (arrowheads). Examination of Foxn1:Cre-driven deletion of *Trp53* floxed allele by genomic PCR analysis (bottom) in FACS sorted TECs (CD45$^-$EpCAM$^+$MHCII$^+$) from control (Ctr) mice and thymocytes (CD45$^+$) and TECs from p53cKO mice at 2-week of age, using the depicted primers (1F, 1R, 10F and 10R). **(B)** qRT-PCR analysis of *Trp53* expression in FACS sorted cTECs (UEA$^-$Ly51$^+$), mTECs (UEA$^+$Ly51$^-$) and thymocytes from 2-week-old Ctr and p53cKO mice. Products detected by amplification of cDNA sequence spanning exons 5 and 6. Values were normalized to *18s* ribosomal RNA. Values from Ctr cTECs were set as 1 and the fold change in *Trp53* was calculated relatively to the other subsets (mean ± SEM, representative of four independent experiments). (**C** and **D)** The composition of TECs was analyzed at the indicated time points. **(C)** Flow cytometry analysis of cTECs and mTECs. Dot plots show representative Ly51/UEA staining in TECs. **(D)** Average cellularity of cTECs (Top) and mTECs (Bottom). Graphs represent data from 2-4 independent experiments per time point (n = 5-17 per group). (**E)** Expression of CD80 and Aire in mTECs of Ctr and p53cKO mice at the indicated time points. Numbers represent the average percentages (± SEM) of the gated mTEC subsets. (**F)** Average cellularity of the mTEC subsets depicted in (**E**). Symbols (^) and (*) compare immature and mature mTECs, respectively. Results in **E-F** are shown as mean ± SEM of 5-17 mice/group from 3-4 independent experiments. (**G)** Expression of Aire-dependent and Aire-independent TRAs measured by qRT-PCR in FACS sorted mTECs from 2-week-old Ctr and p53cKO mice. Values were normalized to *18s* ribosomal RNA, and those in Ctr mTECs were set as 1. Graphs represent data from 3 independent experiments (mean ± SEM). */^ $P < 0.05$; **/^^ $P < 0.01$; ***$P < 0.001$.

CD80^{hi} and Aire^{+} mTECs was delayed in the embryonic p53cKO thymus, but normalized to the proportions of the control thymus during pre-puberty (**Figure 1E**). Despite the restoration of complete mTEC differentiation, the number of CD80^{hi} and Aire^{+} mTECs was diminished in p53cKO thymus throughout life, while the CD80^{lo} subset became affected only in adult mice (**Figure 1F**). Second, analysis of mTEC turnover revealed an increase in the rate of p53cKO mTECs in active cycling (S/G2/M) (**supplemental Figure 1F**). Moreover, we monitored the extent of DNA double-strand breaks (13) and apoptosis, and respectively found that the percentages of phosphorylated γ-H2AX and annexin V^{+} were slightly increased in p53cKO mTECs, particularly within CD80^{lo} cells (**supplemental Figure 1G-H**). These findings suggest that increased apoptosis rather than defective proliferation might contribute to the reduced number of mTECs in p53cKO mice. Lastly, analysis of the expression of a panel of TRAs showed that Aire-independent genes were downregulated in p53cKO mTECs, whereas Aire-dependent genes presented a variable pattern in both mTEC subtypes (**Figure 1G**). Our data suggest that p53 is superfluous for cTEC/mTEC specification, but instead controls mTEC homeostasis.

p53 regulates RANK expression in TECs.

The similarity between the mTEC-phenotype of p53cKO mice and that of mice with defects in RANK, CD40 and LTβR (14) led us to evaluate whether p53 fine-tunes the expression of these TNFRSF members. Additionally, we analysed the expression of osteprotegerin (OPG), a decoy receptor of RANK ligand (14). While the levels of *Tnfrsf5* (CD40) *Tnfrsf3* (LTβR) and *Tnfrsf11b* (OPG) were normal, the expression of *Tnfrsf11a* (RANK) was reduced in p53cKO mTECs (**Figure 2A**). To examine the functional relationship between p53 and RANK, we used well-defined *in vitro* models of mTEC differentiation, in which E15.5 dGuo-FTOCs were depleted of hematopoietic cells and then stimulated through RANK (15). Strikingly, the frequency and numbers of mature CD80^{+} and Aire^{+} mTECs in RANK-stimulated p53cKO dGuo-FTOCs were reduced relatively to controls (**Figure 2B**). Contrarily, CD40-mediated mTEC maturation and CD40 expression on p53cKO mTECs were unaffected (**supplemental Figure 2A-B**). Hence, loss of p53 appeared to specifically dampen *in vitro* mTEC differentiation induced by RANK.

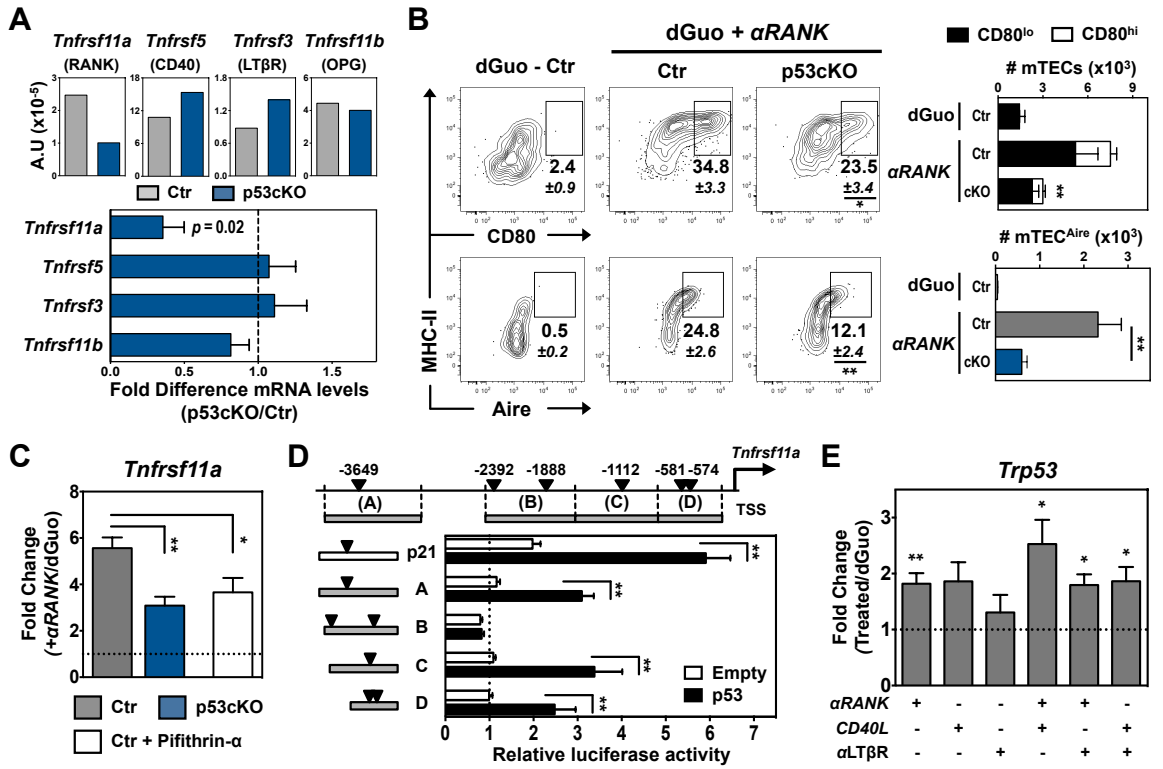

Figure 2 - **Ablation of *Trp53* in TECs limits the expression and responsiveness of RANK.** (**A**) The expression of *Tnfrsf11a*, *Tnfrsf5*, *Tnfrsf3* and *Tnfrsf11b* was assessed by qRT-PCR in FACS sorted mTECs (UEA$^+$Ly51$^-$) from 2-week-old control (Ctr) and p53cKO mice. Values were normalized to *18s* ribosomal RNA. Graphs represent data from 4 independent experiments (top). Fold difference in the relative mRNA levels between Ctr (dashed line) and p53cKO mTECs (bottom). A.U. (arbitrary units). (**B**) E15.5 dGuo-treated FTOCs from Ctr and p53cKO mice were cultured for 4 days with anti-RANK (αRANK). Expression of CD80 and Aire was analyzed in mTECs (UEA$^+$Ly51$^-$) by flow cytometry. Numbers indicate the mean percentage of gated cells. Graphs show the cellularity of mTEC subsets/thymic lobe. Top graph, symbol (* and **) compares mature mTECs from Ctr versus p53cKO mice. Results are presented as mean ± SEM of 10-12 thymic lobes/group from 5 independent experiments. (**C**) The expression of *Tnfrsf11a* was analyzed by qRT-PCR in FACS sorted TECs from Ctr and p53cKO E15.5 dGuo-treated FTOC stimulated over 24 hours with αRANK or αRANK plus Pifithrin-α. Values were normalized as in (**A**), and those in TECs from non-stimulated dGuo-treated FTOC were set to 1. Graphs represent data from 3-6 independent experiments (mean ± SEM). (**D**) The region upstream the *Tnfrsf11a* (RANK) transcription start site (TSS) contains putative p53 RE (triangles), identified based on the p53 RE matrix logo (RRRC-A/T-A/T-GYYY motifs, in which R is a purine and Y is a pyrimidine) (MatInspector and/or rVista software tolls). DNA fragments (A-D) from the *Tnfrsf11a* (RANK) and *Cdkn1a* (p21) loci were cloned into the pGL3-Promoter reporter plasmid. p53 KO MEFs were transiently transfected with the indicated luciferase plasmids along with a p53 overexpressing (p53) or an empty (Empty) constructs. Luciferase reporter activity was normalized to the relative pGL3-promoter signal. Represented is the average of 3 independent experiments (± SEM). (**E**) The expression of *Trp53* was analyzed by qRT-PCR in FACS sorted TECs from Ctr and p53cKO E15.5 dGuo-treated FTOC stimulated over 24 hours with anti-RANK, recombinant CD40L and anti-LTβR at different combinations. Values were normalized as in (**A**), and those in TECs from non-stimulated dGuo-treated FTOC were set to 1. Data is representative of 4 independent experiments (mean ± SEM) * $P < 0.05$; ** $P < 0.01$; ***$P < 0.001$.

Given that RANK activation induces its own expression (16), we evaluated whether p53 positively controls this self-amplification loop. Concordantly, RANK-mediated stimulation augmented the expression of *Tnfrsf11a* in TECs from control dGuo-FTOC. Noticeably, this increase was attenuated in TECs from both RANK-activated p53cKO dGuo-FTOC and RANK-activated control dGuo-FTOC co-treated with the p53 inhibitor pifithrin-α (**Figure 2C**), indicating that p53 controls the expression of *Tnfrsf11a*. *In silico* analysis identified six putative p53 response elements (RE) (17) within the 4kb region upstream of the transcription start site (TSS) of *Tnfrsf11a* **(Figure 2D**). We cloned 1kb genomic DNA fragments containing

these potential p53 RE (named A-D) into a luciferase reporter plasmid and assessed their p53-mediated transactivation in p53-deficient MEFs, which were co-transfected with a p53-expressing vector. As positive control we used a *Cdkn1a* (p21)-derived fragment containing a bona-fide p53 RE (17). Notably, p53 increased luciferase expression driven by *Tnfrsf11a*-derived fragments A, C and D, but not B **(Figure 2D**). These results imply that p53 has the potential to control the activity of *Tnfrsf11a* promoter. To study whether p53 was reciprocally induced under mTEC differentiating conditions, control dGuo-FTOCs were activated with RANK, CD40 and LTβR agonists. Contrarily to LTβR stimulation, individual RANK- and CD40-engagement induced *Trp53* expression in TECs, an effect that was further augmented by combined activation (**Figure 2E**). These results indicate that both RANK and CD40 signalling induce p53, which in turn promotes RANK expression and RANK-driven mTEC differentiation.

p53 specifically regulates a broad network of the mTEC transcriptome.

Given that p53 governs multiple transcriptional programs in distinct cells (18–20), we examined its genome-wide influence in TECs. To do so, we performed RNA sequencing (RNA-Seq) analysis and compared the transcriptome of cTECs and mTECs isolated from 2-week-old control and p53cKO mice. We selected this age to permit the maturation of mTEC, the emergence of p53cKO phenotype and the sufficient abundance of cTEC/mTEC subsets for analysis. The number of genes expressed in the control and p53cKO mTECs was higher than in their cTEC counterparts, resulting in the expected cTEC/mTEC segregation (**Figure 3A** and **supplemental Figure 3A-B**). *Trp53* levels were increased in control mTECs and markedly reduced in p53cKO-derived TEC subsets. The expression of cTEC- and mTEC-associated genes separated the two lineages independently of their genotype (**supplemental Figure 3 C-D**), validating the accuracy of sorted samples. Strikingly, while randomly associated within cTEC subsets, the biological replicates of control and p53cKO mTECs defined two distinct clusters (**Figure 3A**). Accordingly, the number of differentially expressed genes between p53cKO and control mTECs was substantially larger than in cTECs (**Figure 3B** and **supplemental Tables 1-2**). The identification of 1418 upregulated and 1945 downregulated genes in p53cKO mTECs implies that p53 negatively and positively

regulates gene expression in mTECs (**Figure 3C**). Concordant with previous observations, *Tnfrsf11a* expression was reduced in p53cKO mTECs analysed by RNA-seq and qRT-PCR (**supplemental Figure 3E**). Yet, RANK was not identified among the list of differentially expressed genes most possibly due to the stringent statistical analysis of RNA-seq, differences in gene normalization and intrathymic sample variation.

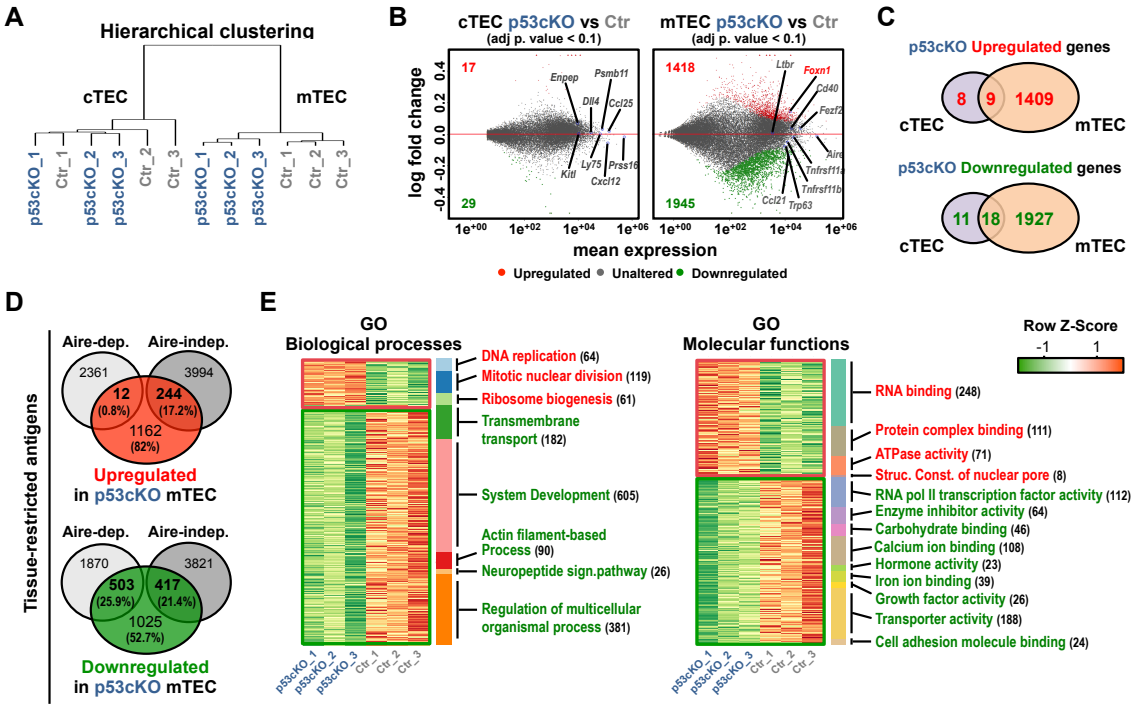

Figure 3 - Impact of p53 in the transcriptome of cTECs and mTECs. RNA-seq analysis of FACS sorted cTECs and mTECs purified from 2-week-old control (Ctr) and p53cKO mice, including three biological replicates per subset. (A) Hierarchical clustering of all samples by gene expression correlation distance for the top 1000 most diverse genes. (B) Comparison of the transcriptome of cTECs from p53cKO *vs* Ctr mice (left) and mTECs from p53cKO *vs* Ctr mice (right). Minus-average plots showed the log2fold change (y-axis) versus the mean expression (x-axis) of total genes obtained by comparison. Genes with a log2fold change that present a p-adj value < 0,1 were called as differentially expressed (DE). Upregulated and downregulated DE genes in p53cKO samples are respectively highlighted in red and green, together with their numbers. Unaltered genes are depicted in gray. (C) Venn diagrams represent the number of upregulated (top) or downregulated (bottom) DE genes in cTECs (violet) and mTECs (orange) of p53cKO vs Ctr mice. (D) Venn diagrams show the number and proportion of upregulated (red) and downregulated genes (green) of p53cKO mTECs within Aire-dependent (Aire-dep.) or -independent (Aire-indep.) TRA genes, as defined in (21). (E) Heat map of enriched biological processes (left) and molecular functions (right) in upregulated (red) or downregulated (green) DE genes of p53cKO mTECs. Represented are activated (red) or inhibited (green) categories with a marginal posterior probability estimate > 0.65. In parentheses are indicated the number of DE genes/GO category.

Using a publicly available annotated list of TRA genes (21), we next cross-examined their representation within differentially expressed genes of p53cKO mTECs. Notably, nearly half of the downregulated genes in p53cKO mTECs comprised purported TRAs, with a similar incidence of Aire-dependent and Aire-independent targets (**Figure 3D**). The proportion of TRAs within upregulated genes of p53cKO mTECs was lower, including mostly Aire-independent targets (**Figure 3D**). These data suggest that p53 regulates promiscuous gene expression in

mTECs. Additionally, GO enrichment analysis in differentially expressed genes did not reveal any particular term in cTECs, but was associated to diverse functional categories in p53cKO mTECs. Specifically, upregulated genes indicated an increase in DNA replication, mitosis, ribosome biogenesis, RNA- and protein complex-binding, ATPase activity and constituents of nuclear pore. Conversely, downregulated genes suggested an attenuation in transmembrane transport, actin filament-based process, neuropeptide signalling pathway, carbohydrate- and ion-binding and RNAPII transcription factor-, enzyme inhibitor-, hormone- and growth factor activity (**Figure 3E** and **supplemental Tables 3-6**). Concordantly to the mTEC-restricted phenotype of p53cKO mice, these results suggest that p53 controls a multifaceted transcriptional program in mTECs.

Adult p53cKO mice display an impaired regular and regenerative thymopoiesis.

We then analysed how the described changes in TEC microenvironments impacted in the thymic activity of p53cKO mice. The frequency and abundance of major thymocyte subsets, including early thymic precursors (ETP), double-negative (DN) subsets, double-positive (DP) and single positive (SP) CD4 and CD8 cells, were comparable in control and mutant mice during fetal and pre-puberty life (**Figure 4A-C**). Notably, a global deficit in thymopoiesis appeared in 10-week-old p53cKO mice **(Figure 4A**), without altering the global T-cell differentiation program. Namely, the progression through DN1-DN4 stages and the rate of positive selection, as measured by the frequency of $CD3^{+}CD69^{+}$ thymocytes, were largely similar between the control and p53cKO thymus (**Figure 4B**). However, we found a reduction in the proportion of DN1s and ETPs in p53cKO thymus (**Figure 4B**). Correspondingly, the numbers of all major thymic subsets steadily declined in p53cKO mice, being this trend apparent in 6-week-old mice (**Figure 4C**). These perturbations extended to the peripheral T-cell compartment of adult p53cKO mice, with a reduction in splenic CD4 and CD8 T cell counts (**Figure 4D**). The dysfunctional nature of the adult mutant thymus led us to further analyse their regenerative capacity following ionizing radiation. Although numerically different at baseline, mTECs were markedly depleted in both groups five days after sublethal

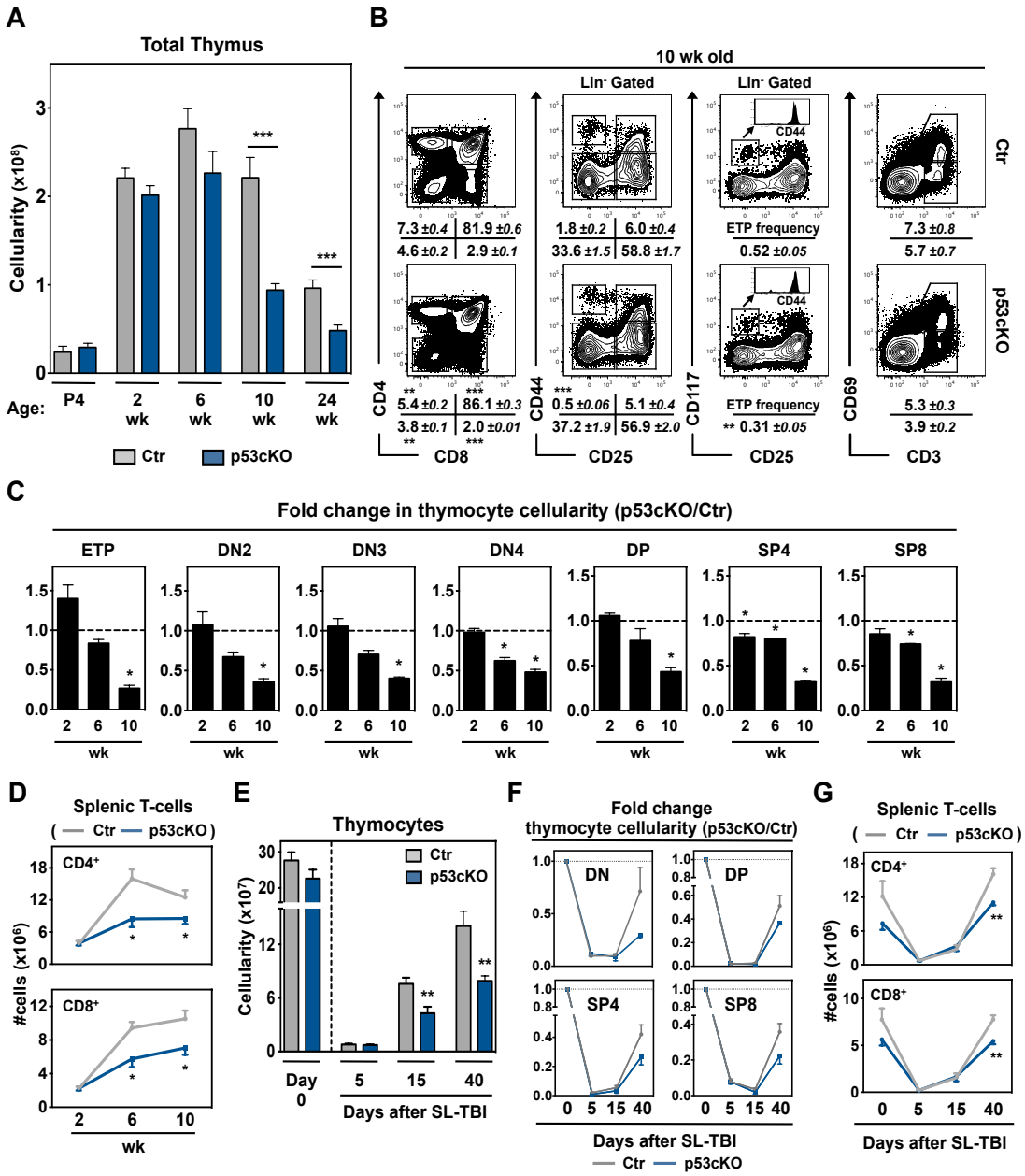

Figure 4 - Altered thymopoiesis in p53cKO mice. (A) Thymic cellularity of control (Ctr) and p53cKO mice at various ages. (B) Flow cytometry analysis of T cell development in 10-week-old Ctr and p53cKO thymus: (left) CD4/CD8 expression on total thymocytes; (middle-left) CD44/CD25 expression on DN thymocytes (gated on Lin$^-$ cells); (middle-right) CD177/CD25 expression on DN thymocytes (gated on Lin$^-$ cells). ETPs are defined as Lin$^-$ CD177$^+$CD44$^+$CD25$^-$; (right) CD69/CD3 expression on total thymocytes. Numbers indicate the frequencies of the different subsets (mean ± SEM). (C) Fold change in the number of the indicated thymocyte subsets. For each time point, the values of Ctr mice were set as 1 (dashed line) and compared relatively to p53cKO mice. Graphs represent data from 2-3 experiments/time point (n=6-8 mice per group; mean ± SEM). (D) Absolute number of splenic CD4$^+$ and CD8$^+$ T cells in Ctr and p53cKO mice at different time points. (E) Thymocyte cellularity of sub-lethally irradiated 6-week-old Ctr and p53cKO mice at the indicated time points post-treatment. (F) Fold change in the cellularity of the thymocyte subsets following sublethal total-body irradiation (SL-TBI). For each time point, the values of non-irradiated Ctr or p53cKO mice were set as 1 (dashed line) and respectively to the ones obtained for SL-TBI Ctr and p53cKO thymus at each time point (G) Numbers of splenic CD4$^+$ and CD8$^+$ T cells in Ctr and p53cKO mice after SL-TBI. * $P < 0.05$; ** $P < 0.01$; *** $P < 0.001$.

total-body irradiation (**supplemental Figure 4A).** This reduction was attenuated in p53cKO mTECs **supplemental Figure 4A)**, suggesting that ablation of p53 conferred a slight protection to radiation-induced apoptosis. While the recovery of cTECs was similar in both groups, the restoration of mTEC cellularity, including

$CD80^+$ and $Aire^+$ subsets, was markedly impaired in p53cKO mice (**supplemental Figure 4A-C).** Additionally, the recovery of thymopoiesis was also significantly compromised in p53cKO mice (**Figure 4E),** affecting *de novo* generation of all major thymic subsets (**Figure 4F**) and the reconstitution of the peripheral T cells (**Figure 4G**). Our findings indicate that adult p53cKO mice fail to maintain normal and regenerative thymopoiesis.

mTEC-dependent thymopoiesis is compromised in p53cKO mice.

As the loss of mTECs preceded the deterioration of thymopoiesis during adulthood, we examined whether the stages of T-cell development functionally linked to mTECs (1) were prematurely affected in p53cKO thymus. To survey cortical and medullary clonal deletion, we respectively assessed the frequency of DP and SP4 thymocytes that co-expressed PD-1 and Helios (22), and found no major differences between control and p53cKO thymus (**Figure 5A**). Moreover, we crossed p53cKO mice with Marilyn-$Rag2^{-/-}$ TCR transgenic mice, in which thymocytes express I-A^b-restricted HY-specific TCR (15). Thymocyte development in the p53cKO background reproduced that observed in controls, with a similar number of positively and negatively selected thymocytes in female and male mice, respectively (**Figure 5B**). In line with the absence of SP4 accumulation at steady state (**Figure 4B**), these results indicated that negative selection seemed intact in p53cKO mice. Strikingly, analysis of regulatory T cell differentiation and post-selection SP maturation showed a respective decrease in the proportions and numbers of $CD25^+Foxp3^+$ regulatory T cells and mature $CD24^{lo}CD62L^{hi}$ SP4 thymocytes in mutant thymus (**Figure 5 C-D**). These findings implicate a requirement for p53 in TECs to maintain continual mTEC-dependent thymopoiesis.

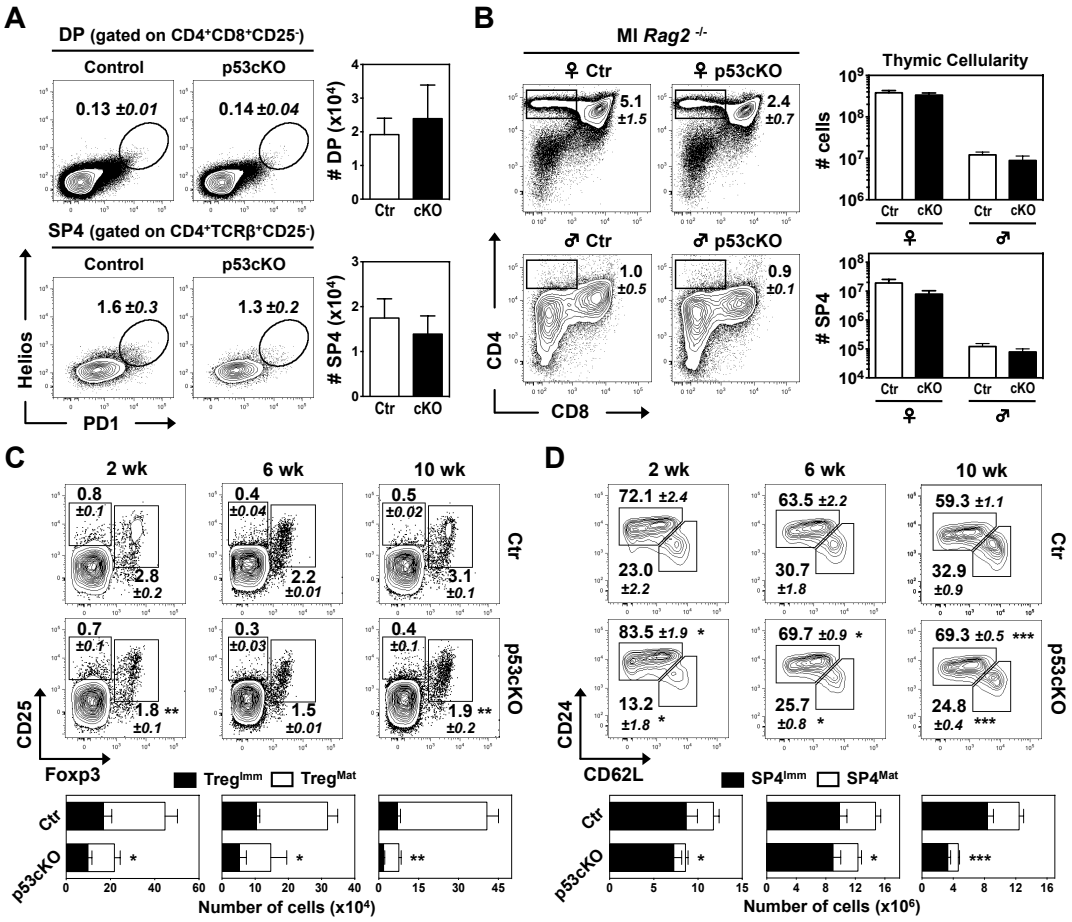

Figure 5 - Loss of p53 in TECs reduces specific mTEC-mediated functions. (**A**) DP (TCRβ$^+$CD4$^+$CD8$^+$CD25$^-$) and SP4 (TCRβ$^+$CD4$^+$CD8$^-$CD25$^-$) thymocytes isolated from 8-week-old Control (Ctr) and p53cKO mice were analyzed for the expression of Helios and PD1. Numbers indicate the mean percentage of gated cells. Graphs show the total number of Helios$^+$PD1$^+$ thymocytes within the DP and SP4 stage and represent data from 2 independent experiments (n=4-5 mice per group; mean ± SEM). (**B**) Flow cytometry analysis of thymic selection in 8-week-old female (♀) and male (♂) Ctr and p53cKO Marilyn-*Rag2*$^{-/-}$ thymus (MI). Numbers indicate the frequencies of SP4 thymocytes (mean± SEM). Thymic cellularity (top) and the number of SP4 thymocytes (bottom) are depicted on the graphs. Data represents the average of 3 independent experiments (n=5-6 mice per group; mean ± SEM). (**C-D**) SP4 thymocytes (CD8$^-$CD4$^+$TCRb$^+$) were analyzed for the expression of CD25 and Foxp3 **(C)** and CD24 and CD62L **(D)** at the indicated time points. Numbers indicate the average percentage of gated cells (± SEM). Graphs represent: (**C**) the number of immature (CD25$^+$Foxp3$^-$) and mature (CD25$^+$Foxp3$^+$) regulatory T cells (Tregs) (left); (**D**) the number of immature (CD24^{hi}CD62L^{low}) and mature (CD24^{low}CD62L^{hi}) SP4 thymocytes (right). Symbol (*) compares mature Treg and mature SP4 cells between Ctr versus p53cKO mice. In (**C-D**) graphs represent data from 3 independent experiments (n= 4-13 mice per group). Results are presented as mean ± SEM. * $P < 0.05$; ** $P < 0.01$; *** $P < 0.001$.

Signs of disturbed peripheral tolerance unfold in p53cKO mice.

The alterations in mTECs led us to seek for signs of peripheral autoimmune manifestations in mutant mice. We did not detect the presence of autoantibodies against multiple organs (stomach, testis, liver, salivary and lacrimal glands) in the serum of aged p53cKO mice compared to controls (data not shown). Yet, larger and more prevalent lymphocytic infiltrations were found in the salivary and lacrimal glands of aged p53cKO mice (**Figure 6A-B, supplemental Figure 5A**). Despite the reduction in the numbers of thymic regulatory T cells, their frequency in the spleen of adult p53cKO mice was normal (**supplemental Figure 5B).** However, as total

peripheral CD4 T cell counts were reduced (**Figure 4D**), both conventional and regulatory T cells were diminished in mutant mice (**supplemental Figure 5B)**. Moreover, p53cKO-derived peripheral regulatory T cells suppressed polyclonal T cell activation *in vitro* (**supplemental Figure 5C)**, showing a broad intact function and potentially explaining the mild autoimmune manifestations. These findings suggest that the perturbed mTEC niche of p53cKO mice might predispose to defects in tolerance.

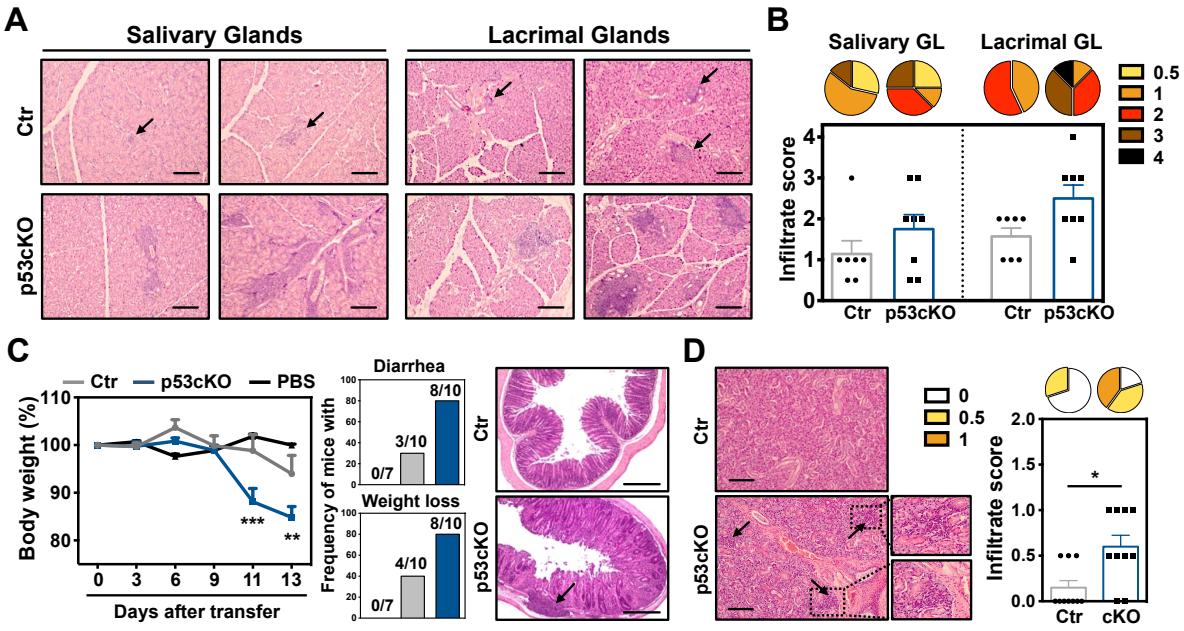

Figure 6 - TEC-specific deletion of p53 impacts on the establishment of peripheral T cell tolerance. (**A**) Representative analysis (HE staining) of the salivary and lacrimal glands obtained from 6-7-month-old Ctr and p53cKO mice. (**B**) Histological scores of inflammatory infiltrates. Pie graphs show the frequency of inflammatory lesions according to their severity. (**C**) Thymocytes from 10-week-old Ctr (gray line) and p53cKO (blue line) mice were intravenously transferred into *Rag2*$^{-/-}$ mice. As control, *Rag2*$^{-/-}$ mice were treated with PBS (black line). Left graph: change in the body weight of *Rag2*$^{-/-}$ recipients after thymocyte transfer; Middle graphs: incidence of diarrhea and weight loss, with the indicated number of recipient mice that develop symptoms. Right: images show the histological analysis (HE staining) of the colon of the *Rag2*$^{-/-}$ recipients 14 days after transfer. (**D**) Histological analysis and inflammatory score of the salivary glands. Pie graphs represent the frequency of inflammatory lesions according to their severity. Arrows in (**A, C and D**) outline lymphocytic infiltrates. Bars: 100 µm. Results are presented as mean ± SEM. *P < 0.05; ** P < 0.01; *** P < 0.001.

The development of autoimmunity coupled to defects in mTECs is normally contained in the C56BL/6 background, but is potentiated by lymphopenia, as observed in the case of Aire and XCL1 deficiencies (23, 24). To examine the functional link between scarce mTEC niches and disturbed T-cell tolerance in p53cKO mice, we adoptively transferred thymocytes derived from control and mutant adult thymus into *Rag2*$^{-/-}$ mice, and monitored recipient mice for clinical signs of disease. Recipient mice that received p53cKO-derived thymocytes exhibited accelerated weight loss, developed diarrhea and presented lymphocytic infiltration and tissue damage in the colon (**Figure 6C**). The presence of T cells in the spleen

of both groups indicated an effective cell transfer (**supplemental Figure 5D**). Similarly to the analysis at steady state, small lymphocyte infiltrates were also more frequent in the salivary glands of the same group (**Figure 6D**). Our results indicate that the p53 mutant thymus renders developing T cells more susceptible to failure in establishing peripheral self-tolerance in aged and lymphopenia settings.

Discussion

Our study positions p53 as a prime determinant of mTEC integrity *in vivo,* mapping a functional link between p53 and RANK in mTECs. This was manifested by a reduced RANK-driven mTEC induction in p53cKO thymus *in vitro*, an observation that curiously mirrored the delayed appearance of embryonic p53cKO mature mTECs *in vivo.* We found that mTECs express higher levels of p53 than cTECs and p53 was reciprocally induced following RANK and CD40 stimulation. These results are consistent with previous studies coupling p53 induction to the NFκB pathway (25), which is in turn engaged by mTEC-inducing TNFRSF signalling (14). Yet, the reduction in mTECs of p53cKO mice was not as severe as that reported in RANK-deficient mice (14). The differentiation of mTECs depends on the coordinated action of RANK, CD40 and LTβR signalling (1). It is conceivable that compensatory signals via CD40 and LTbR contribute to the mTEC maturation program of p53cKO mice. Hence, p53 seems to fine-tune, rather than determine, RANK signalling in mTECs, cooperating in a functional feed-forward loop to sustain the medullary epithelial compartment.

Our results suggest that p53 functions as a molecular hub in mTECs, regulating a wide transcriptional program that extends beyond balancing RANK expression. Typically, p53 is maintained at low levels under steady-state conditions, being activated in response to various stress signals (17). Nonetheless, p53 has also basal transcriptional functions in unstressed cells (19). Apart from RANK and CD40, it is possible that additional extrinsic and intrinsic cues generated within the thymus trigger a p53-driven response in mTECs. Although the mechanisms that induce p53 in mTECs remain elusive, our observations argue that its activity is not dormant. Genome-wide chromatin-binding approaches revealed extensive and distinct cell-specific p53-driven transcription programs (18–20), indicating that p53-mediated gene expression is context-dependent. We found that p53 controls a broad set of

genes linked to core processes in mTEC biology, which are not related to other well-known mechanisms controlling mTEC maintenance. The increased apoptosis susceptibility of p53-deficient mTECs might be a corollary of these broad alterations, possibly explaining the reduced mTEC compartment of p53cKO mice. Yet, the presumed asynchrony of apoptosis at a population level and the rapid clearance of dying cells may confound measurements of cell death *in vivo.* Moreover, it remains to be determined whether differentially expressed genes are directly regulated by p53 or indirectly influenced through the perturbation of downstream genes of the p53-induced pathway. Further studies should elucidate the individual contribution of these gene products or processes to the maintenance of mTEC homeostasis and their homo- and heterotypic cellular interactions within the thymus. It is also important to consider that the hyperactive transcriptional state of mTECs might facilitate the accessibility of p53 to its target genes. The large prevalence of TRAs among the differentially expressed genes of p53cKO mTECs suggests that p53 influences promiscuous gene expression. Still, the expression of Aire (21) and Fezf2 (4) was normal in p53cKO mTECs. Since mTECs express clusters of TRAs at a single-cell level (3, 26), the reduction in TRAs might alternatively reflect an underrepresentation of certain mTEC subsets in mutant thymus.

The disruption in the mTEC niche appeared to spread to the cTEC compartment in the adult p53cKO mice, evolving to a global failure in regular and regenerative thymopoiesis. The deficit in thymic activity extended to a decrease in splenic T cells, reinforcing the notion that peripheral T-cell homeostasis in mice also depends on regular thymic output (27). Thus, the sustainability of the mTEC niche seems to be a deterministic factor in regulating thymic function. How the changes in mTECs are reflected in the cortex is intriguing. The phenotype and transcriptional profile of cTECs, as well as the early T-cell development and positive selection, were apparently normal in p53cKO mice. Yet, we cannot formally exclude that p53 directly regulates cTEC homeostasis later in life. Alternatively, changes in mTECs might perturb the cortico-medullary junction and cortex, thereby limiting the number of BM-derived thymic progenitors and the magnitude of pre-medullary stages of T cell differentiation. Accordingly, the numbers of ETPs, DN and DP thymocytes were diminished in aged p53cKO mice, providing a possible explanation for thymic hypoplasia. These findings could implicate the existence of a complex functional and

structural interplay between TEC and non-epithelial cell subsets (e.g. endothelia and mesenchyme) in balancing thymopoiesis.

The contracted mTEC compartment of p53cKO mice was physiologically linked to abnormalities in mTEC-dependent regulatory T cell differentiation and SP maturation, providing a possible molecular explanation for the signs of deregulated immunological tolerance in mutant mice. Albeit negative selection seemed normal at a polyclonal level, we cannot exclude the possibility that rare auto-reactive thymocytes escape from the p53cKO thymus. In line with previous studies (28), we reason that the underrepresentation of regulatory T cells and mature SP4 represents a footprint of a decrease in the availability of mTEC niches. Concordantly, mild signs of autoimmune manifestations unfolded in aged p53cKO mice and in immunodeficient mice receiving p53cKO-derived thymocytes. Although we did not provide a direct link between the disturbed tolerance and the deficiency in regulatory T cell numbers and/or their specificities and/or the specificities of conventional T cells, our findings suggest that the insufficient mTEC niche of p53cKO mice predisposes to defects in immune tolerance under lymphopenia. Also, the signs of abnormal immunological tolerance in p53cKO mice were less strong compared to other mTEC-deficient conditions (14). We reason that the remaining mTEC niche of mutant thymus together with the genetic background and extra-thymic compensatory mechanisms, allow the establishment of peripheral tolerance during the first weeks of age, a period that is sufficient to prevent the development of autoimmunity (29). Future studies should identify the distinct contribution of altered thymic and peripheral T-cell subsets to the disturbed tolerance induction of mutant mice.

Beyond positioning p53 as a novel guardian of thymus function, our findings are also of clinical relevance and reinforce the notion of a modulatory role for p53 in immune homeostasis and autoimmunity (5). Moreover, the use of p53 inhibitors, such as Pifithrin-α, has been approved in clinical trials to attenuate the side effects of chemotherapy (9). Given the described adverse impact of disrupting p53 in TECs and in T-cells (5), the therapeutic use of p53 inhibitors must be implemented with care in order to safeguard the balance between immune reconstitution and tolerance induction.

Methods

Mice and Procedures. Homozygous $p53^{fl/fl}$ mice purchased from The Jackson Laboratory (10) and bred to *Foxn1*^{Cre} mice obtained from Dr. Thomas Boehm (11). *Foxn1*^{Cre}:*Trp53*$^{fl/fl}$ mice were also backcrossed with Marylin-*Rag2*$^{-/-}$ mice. All mice were in a C57BL/6 background and housed under specific pathogen-free conditions. For fetal studies, the day of the vaginal plug detection was designated as embryonic day (E) 0.5. To study thymic recovery, mice received sublethal total-body irradiation (450 rads) with a Cs^{137} radiation source (Gammacell 1000, Nordion). For transfer experiments, 2.5×10^7 thymocytes isolated either from control or p53cKO mice were intravenously transferred into *Rag2*$^{-/-}$ mice. All animal experiments were performed in accordance with European guidelines for animals used for scientific purposes (Directive 2010/63/EU).

PCR genotyping. PCR analysis to detect the excision of exons 2-8 of the Trp53 gene was done as described (10). Briefly, primers spanning the *loxP* sites in intron 1 (F: 5′-cacaaaaacaggttaaacccag-3′ and R: 5′-agcacataggaggcagagac-3′) and intron 10 (F: 5′-aaggggtatgagggacaagg-3′ and R: 5′-gaagacagaaaaggggaggg-3′) were used to detect intact $p53^{fl}$ allele. The excision was accessed using the primers 1 F and 10 R.

TEC and hematopoietic cell isolation. Thymic stromal cells were isolated by enzymatic digestion and TECs were further enriched using a MACS-based $CD45^+$ cell depletion kit (Miltenyi Biotec). Hematopoietic cells from thymus and spleen were prepared as previously described (15).

Flow cytometry. Cells were pre-treated with FC block (anti-CD16/CD32 antibodies TruStain fcX; Biologend). Cell suspensions were stained as described (15) with FITC-conjugated anti-CD8α (53-6.7) and anti-CD44 (IM7); PE-conjugated anti-CD4 (GK1.5), anti-CD62L (MEL-14), anti-TCRβ (H57-597), anti-CD40 (3/23), anti-CD80 (16-10A1) and anti-Ly51 (6C3); PerCP-Cy5.5-conjugated anti-CD45.2 (104); PerCP-eFluor710 anti-CD4 (GK1.5); PE-Cy7-conjugated anti-CD25 (PC.61.5) and anti-CD69 (H1.2F3); APC/eFluor660-conjugated anti-CD8 (53-6.7), anti-CD3 (17A2), anti-CD80 (16-10A1) and anti-EpCAM (G8.8); anti-CD279 (29F.1A12); APC-

eFluor780-conjugated anti-I-A/I-E (M5/114-15-2) and anti-cKit (2B8); eFluor450-conjugated anti-EpCAM (G8.8) and anti-CD24 (M1/69) (eBioscience). The binding of biotinylated *Ulex europaeus* agglutinin-1 (UEA-1) (Vector Laboratories, Burlingame, CA, USA) or anti-Ly51 (6C3) was revealed by PE-Cy7-conjugated streptavidin (eBioscience). For intracellular staining, cells were prepared according to the supplier's protocol (Foxp3 staining kit, eBioscience) and stained with FITC-conjugated anti-Helios (22F6), anti-Ki67 (SolA15) (eBioscience), anti-γ-H2AX pS139 (REA502) (MACS Miltenyi Biotec), APC/eFluor660-conjugated anti-Foxp3 (FJK-165) and anti-Aire (5H12) antibodies (eBioscience). For thymic progenitor population analysis APC/eFluor660-conjugated antibodies against CD4 (GK1.5), CD8 (53-6.7), CD11b (M1/70), CD11c (N418), CD19 (eBio1D3), Gr1 (RB6-8CS), Ter119 (TER-119), CD3 (17A2), NK1.1 (PK136) and γδTCR (eBioGL3) (eBioscience) were used as lineage markers. For detection of apoptosis, FITC-conjugated Annexin V apoptosis detection kit was used in accordance to the supplier's protocol (Biolegend). Flow cytometry was performed on a FACSCanto II and LSRFortessa, with data analysed on FlowJo software (BD). Cell sorting was performed using the FACSAria I (BD Biosciences), with purities >96%.

Histology, Histopathology and Immunofluorescence. Paraffin-embedded tissue sections from thymus, lacrimal and salivary glands and colon were stained with haematoxylin and eosin. Images were acquired either on a light microscope (Olympus CX31 with DP-25 camera) or IN Cell Analyzer 2000 (GE Healthcare). Area analysis was performed using Fiji software. Histopathology was scored in a blinded and randomized fashion by three independent observers for the presence of lymphocytic infiltrates, using the following criteria: 0 - no infiltrate; 0.5 – mild trace of infiltrates; 1 – minor infiltrates; 2 – moderate infiltrates; 3 – severe infiltrates; 4 – tissue destruction. For immunofluorescence analysis, thymic lobes were prepared as described (15). Briefly, fixed thymi sections were stained with biotinylated UEA-1 and streptavidin Alexa 555 as secondary Abs (Invitrogen). Images were obtained on a Leica TCS SP5 II confocal microscope (Leica Microsystems, Germany) and analysed with Fiji Software.

Gene expression. mRNA (RNAeasy MicroKit, Qiagen) isolation and cDNA synthesis (Superscript First-Strand Synthesis System, Invitrogen) were done as

described (15). Real-time PCR (iCycler iQ5) was performed using TaqMan Universal PCR Master Mix and probes for *18s*, *Il7*, *Psmb11, Dll4*, *Aire*, *Ccl19, Ccl21, Foxn1, Trp63, Tnfrsf11a, Tnfrsf11b, Tnfrsf5, Tnfrsf3, Trp53, Rbp3, Spt1, Ins2, Mup4, Tyrp1, Crp, Fabp9, Col2, Csnb* and *Gad1*. Triplicated samples were analyzed and the delta-delta Ct method was used to calculate relative levels of targets mRNA compared with *18s*.

Fetal Thymic Organ Culture. FTOCs were established with E15.5 embryos, as described (15). 2-deoxyguanosine (dGuo)-treated FTOC were culture either alone or with 5μg/ml of recombinant CD40L (CD40L), 1μg/ml anti-RANK agonist antibody (αRANK) (R&D Systems), 10μg/ml of anti-LTβR (AC.H6, kindly provided by Dr. Jeff Browning, Boston University) and/or 50μg/ml Pifithrin-α (Sigma-Aldrich) for either 1 or 4 days and TECs analyzed by flow cytometry.

Luciferase assay. MatInspector and/or rVista software tolls were used for searching of potential p53-binding sites of the consensus p53-binding site (RRRC-A/T-A/T-GYYY motifs, in which R is a purine and Y is a pyrimidine) upstream of the *Tnfrsf11a* transcription start site. MEFs were isolated from E14.5 p53 KO embryos according to standard procedures. Promoter fragments of *Tnfrsf11a* or *Cdkn1a* were PCR-amplified (Thermo Scientific) from genomic DNA of wild-type (WT) mice and cloned into the pGL3-Promoter (Promega) plasmid. MEFs were transfected with target firefly plasmid along with an expression vector encoding p53, kindly provided by Dr. Manuel Serrano (Spain), or the correspondent empty vector. Renilla luciferase plasmid (Promega) were cotransfected in all conditions for transfection efficiency control. Transfection was performed with JetPrime (Polyplus transfection) according to manufacturer's protocol. Luciferease activity was measured 36 hors later using Dual-Luciferase Reporter Assay System (Promega) and Luciferase activity was normalized for Renilla luciferase activity.

RNA-seq analysis of TEC subsets. Total RNA was extracted from three biological replicates of cTECs and mTECs, each containing 100.000 pooled FACS-sorted cells per subset from four to six 2-week-old p53cKO and control littermates. Library preparation and high-throughput sequencing were performed at Gene Core facility (EMBL, Germany). Twelve sequencing libraries (three for cTEC Ctr, three

cTEC p53cKO, three for mTEC Ctr and three for mTEC p53cKO) were prepared using NEB Next RNA ultra protocol (#E7530 NEB). Obtained libraries were quantified fluorimetrically, pooled in equimolar amounts in two lanes (cTEC samples in one lane and mTEC samples in other lane) and sequenced on the Illumina NextSeq sequencer (NextSeqHi-75) by a mode enabling determination of uni-directional 75 bases and indices, following manufacturer's instructions (Illumina). 372 and 424 millions of reads were produced for cTEC and mTEC lanes. Sequencing reads were submitted to ENA (http://www.ebi.ac.uk/ena) and are accessible under the accession number PRJEB15124. RNA-seq reads were mapped to the mouse genome (mm10) using STAR (version 2.4.2a) with mm10 GTF annotation. An average of 63 (51-71), 61.3 (58-63), 71.5 (65-76) and 69.8 (67-71) million reads were mapped per control cTEC, p53cKO cTEC, control mTEC and p53cKO mTEC samples, respectively. The number of reads per gene was counted using HTSeq-count (30). DESeq2 package was used to normalize and compare the different groups of cells (31). We selected differentially expressed genes based on the p-adjusted p-value lower than 0.1. Reads per kb of exon model per million mapped reads (RPKM) values were computed from normalized read counts. We identify enriched GO terms (biological processes and molecular functions) in the differentially expressed genes using model-based gene set analysis (MGSA) (32). The analysis was performed with 20 independent runs of the Markov chain of 1.10^9 steps each. For each parameter, we used a regularly spaced grid with 11 points. The search intervals for the parameters p, alpha, and beta were set to [0.001, 0.1], [0, 0.2], and [0.5, 0.9] respectively for the search on biological process terms, and [0.001, 0.1], [0, 0.15], and [0.5, 0.9] for the search on molecular function terms. Functional categories with a marginal posterior probability estimate higher than 0.65 were retained for further analysis. The hierarchical clustering, represented as a dendrogram, of TEC populations were performed using the hclust function in R on euclidean distances between the variance of the rlog-transformed read counts for each genes across samples

***In vitro* regulatory T cell Suppression Assays.** For *in vitro* suppression assay, $5x10^4$ control conventional T cells ($CD4^+CD25^-$) were labelled with 1 µM CFSE after cell sorting and cultured in duplicates for 3 days in round bottom 96-well plates together with different ratios of either control or p53cKO-derived regulatory T cells

($CD4^+CD25^+$) and in the presence of 1 ug/ml anti-CD3 (Clone: 145-2C11; BD Pharmingen) and γ-irradiated spleenocytes (200 rads; $1x10^5$/well). Suppressive ability of regulatory T cells was assessed based on the CFSE dilution of conventional T cells. The precursor frequency of dividing cells (percentage of cells in the initial population that undergone one or more divisions after culture) was calculated as follows: $[\sum_{n\geq1}(P_n/2^n)]/[\sum_{n\geq0}(P_n/2^n)]$, where n is the division number that cells have gone through and P_n is the number of cells in division n (33).

Statistical Analysis. Analysis was performed using Prism 6.0g software (GraphPad Software). The two-tailed Mann-Whitney test was used for statistical differences between groups. For multiple comparisons, a two-way ANOVA was used. $p < 0.05$ was considered significant.

Acknowledgements

We thank Dr. Thomas Boehm (Max Planck Institute of Immunology and Epigenetics) for Foxn1-Cre mice, Drs. Rui Appelberg (I3S) and Nuno Rodrigues dos Santos (I3S) for critical reading the manuscript, Drs. Matthias Futschik and José Pedro Pinto (University of Algarve) for critical discussions and Drs. Sofia Lamas, Rui Fernandes, Catarina Leitão and the caretakers from the animal facility for technical assistance. This study was supported by FEDER funds through the Operational Competitiveness Programme – COMPETE and by National Funds through Fundação para a Ciência e a Tecnologia (FCT) under the project PTDC/SAU-IMU/117057/2010 and a starting grant from the European Research Council (ERC) under the project 637843. The Investigator program, PhD and Post-doctoral fellowships from FCT support N.L.A., P.M.R., A.R.R., I.P.C. and C.M..

References

1. Anderson, G., and Y. Takahama. 2012. Thymic epithelial cells: working class heroes for T cell development and repertoire selection. *Trends Immunol.* 33: 256–63.

2. Kyewski, B., and L. Klein. 2006. A central role for central tolerance. *Annu. Rev. Immunol.* 24: 571–606.

3. Meredith, M., D. Zemmour, D. Mathis, and C. Benoist. 2015. Aire controls gene expression in the thymic epithelium with ordered stochasticity. *Nat. Immunol.* 16: 942–949.

4. Takaba, H., Y. Morishita, Y. Tomofuji, L. Danks, T. Nitta, N. Komatsu, T. Kodama, and H. Takayanagi. 2015. Fezf2 Orchestrates a Thymic Program of Self-Antigen Expression for Immune Tolerance. *Cell* 163: 975–987.

5. Munoz-Fontela, C., A. Mandinova, S. A. Aaronson, and S. W. Lee. 2016. Emerging roles of p53 and other tumour-suppressor genes in immune regulation. *Nat. Rev. Immunol.* 16: 741–750.

6. Senoo, M., F. Pinto, C. P. Crum, and F. McKeon. 2007. p63 Is essential for the proliferative potential of stem cells in stratified epithelia. *Cell* 129: 523–36.

7. Murray-Zmijewski, F., E. A. Slee, and X. Lu. 2008. A complex barcode underlies the heterogeneous response of p53 to stress. *Nat. Rev. Mol. Cell Biol.* 9: 702–712.

8. Sun, L., H. Li, H. Luo, L. Zhang, X. Hu, T. Yang, C. Sun, H. Chen, L. Zhang, and Y. Zhao. 2013. Phosphatase Wip1 is essential for the maturation and homeostasis of medullary thymic epithelial cells in mice. *J. Immunol.* 191: 3210–20.

9. Kelly, R. M., E. M. Goren, P. A. Taylor, S. N. Mueller, H. E. Stefanski, M. J. Osborn, H. S. Scott, E. A. Komarova, A. V Gudkov, G. A. Holländer, and B. R. Blazar. 2010. Short-term inhibition of p53 combined with keratinocyte growth factor improves thymic epithelial cell recovery and enhances T-cell reconstitution after murine bone marrow transplantation. *Blood* 115: 1088–97.

10. Marino, S., M. Vooijs, H. Van Der Gulden, J. Jonkers, and A. Berns. 2000. Induction of medulloblastomas in p53-null mutant mice by somatic inactivation of Rb in the external granular layer cells of the cerebellum. *Genes Dev.* 14: 994–1004.

11. Soza-Ried, C., C. C. Bleul, M. Schorpp, and T. Boehm. 2008. Maintenance of thymic epithelial phenotype requires extrinsic signals in mouse and zebrafish. *J. Immunol.* 181: 5272–5277.

12. Gray, D. H. D., N. Seach, T. Ueno, M. K. Milton, A. Liston, A. M. Lew, C. C. Goodnow, and R. L. Boyd. 2006. Developmental kinetics, turnover, and stimulatory capacity of thymic epithelial cells. *Blood* 108: 3777–85.

13. Abramson, J., M. Giraud, C. Benoist, and D. Mathis. 2010. Aire's Partners in the Molecular Control of Immunological Tolerance. *Cell* 140: 123–135.

14. Irla, M., G. Hollander, and W. Reith. 2010. Control of central self-tolerance induction by autoreactive CD4+ thymocytes. *Trends Immunol.* 31: 71–9.

15. Ribeiro, A. R., P. M. Rodrigues, C. Meireles, J. P. Di Santo, and N. L. Alves. 2013.

Thymocyte selection regulates the homeostasis of IL-7-expressing thymic cortical epithelial cells in vivo. *J. Immunol.* 191: 1200–9.

16. Mouri, Y., M. Yano, M. Shinzawa, Y. Shimo, F. Hirota, Y. Nishikawa, T. Nii, H. Kiyonari, T. Abe, H. Uehara, K. Izumi, K. Tamada, L. Chen, J. M. Penninger, J. Inoue, T. Akiyama, and M. Matsumoto. 2011. Lymphotoxin signal promotes thymic organogenesis by eliciting RANK expression in the embryonic thymic stroma. *J. Immunol.* 186: 5047–57.

17. Vousden, K. H., and C. Prives. 2009. Blinded by the Light: The Growing Complexity of p53. *Cell* 137: 413–31.

18. Li, M., Y. He, W. Dubois, X. Wu, J. Shi, and J. Huang. 2012. Distinct Regulatory Mechanisms and Functions for p53-Activated and p53-Repressed DNA Damage Response Genes in Embryonic Stem Cells. *Mol. Cell* 46: 30–42.

19. Kenzelmann Broz, D., S. S. Mello, K. T. Bieging, D. Jiang, R. L. Dusek, C. A. Brady, A. Sidow, and L. D. Attardi. 2013. Global genomic profiling reveals an extensive p53-regulated autophagy program contributing to key p53 responses. *Genes Dev.* 27: 1016–1031.

20. Liu, Y., S. E. Elf, Y. Miyata, G. Sashida, Y. Liu, G. Huang, S. Di Giandomenico, J. M. Lee, A. Deblasio, S. Menendez, J. Antipin, B. Reva, A. Koff, and S. D. Nimer. 2009. p53 Regulates Hematopoietic Stem Cell Quiescence. *Cell Stem Cell* 4: 37–48.

21. Sansom, S. N., N. Shikama-Dorn, S. Zhanybekova, G. Nusspaumer, I. C. Macaulay, M. E. Deadman, A. Heger, C. P. Ponting, and G. A. Hollander. 2014. Population and single-cell genomics reveal the Aire dependency, relief from Polycomb silencing, and distribution of self-antigen expression in thymic epithelia. *Genome Res.* 24: 1918–1931.

22. Daley, S. R., D. Y. Hu, and C. C. Goodnow. 2013. Helios marks strongly autoreactive CD4+ T cells in two major waves of thymic deletion distinguished by induction of PD-1 or NF-κB. *J. Exp. Med.* 210: 269–285.

23. Anderson, M. S., E. S. Venanzi, L. Klein, Z. Chen, S. P. Berzins, S. J. Turley, H. von Boehmer, R. Bronson, A. Dierich, C. Benoist, and D. Mathis. 2002. Projection of an immunological self shadow within the thymus by the aire protein. *Science (80-.).* 298: 1395–401.

24. Lei, Y., A. M. Ripen, N. Ishimaru, I. Ohigashi, T. Nagasawa, L. T. Jeker, M. R. Bösl, G. A. Holländer, Y. Hayashi, R. de Waal Malefyt, T. Nitta, and Y. Takahama. 2011. Aire-dependent production of XCL1 mediates medullary accumulation of thymic dendritic cells and contributes to regulatory T cell development. *J. Exp. Med.* 208: 383–394.

25. Perkins, N. D. 2007. Integrating cell-signalling pathways with NF-κB and IKK function. *Nat. Rev. Mol. Cell Biol.* 8: 49–62.

26. Brennecke, P., A. Reyes, S. Pinto, K. Rattay, M. Nguyen, R. Küchler, W. Huber, B. Kyewski, and L. M. Steinmetz. 2015. Single-cell transcriptome analysis reveals coordinated ectopic gene-expression patterns in medullary thymic epithelial cells. *Nat. Immunol.* 16: 933–941.

27. Almeida, A. R. M., J. A. M. Borghans, and A. A. Freitas. 2001. T cell homeostasis: thymus regeneration and peripheral T cell restoration in mice with a reduced fraction of competent precursors. *J. Exp. Med.* 194: 591–9.

28. Cowan, J. E., S. M. Parnell, K. Nakamura, J. H. Caamano, P. J. L. Lane, E. J. Jenkinson, W. E. Jenkinson, and G. Anderson. 2013. The thymic medulla is required for Foxp3+ regulatory but not conventional CD4+ thymocyte development. *J. Exp. Med.* 210: 675–81.

29. Guerau-de-Arellano, M., M. Martinic, C. Benoist, and D. Mathis. 2009. Neonatal tolerance revisited: a perinatal window for Aire control of autoimmunity. *J. Exp. Med.* 206: 1245–1252.

30. Anders, S., P. T. Pyl, and W. Huber. 2015. HTSeq-A Python framework to work with high-throughput sequencing data. *Bioinformatics* 31: 166–169.

31. Love, M. I., W. Huber, and S. Anders. 2014. Moderated estimation of fold change and dispersion for RNA-seq data with DESeq2. *Genome Biol.* 15: 550.

32. Bauer, S., J. Gagneur, and P. N. Robinson. 2010. Going Bayesian: Model-based gene set analysis of genome-scale data. *Nucleic Acids Res.* 38: 3523–3532.

33. Alves, N. L., B. Hooibrink, F. A. Arosa, and R. A. W. Van Lier. 2003. IL-15 induces antigen-independent expansion and differentiation of human naive CD8+ T cells in vitro. *Blood* 102: 2541–2546.

Supplementary Information

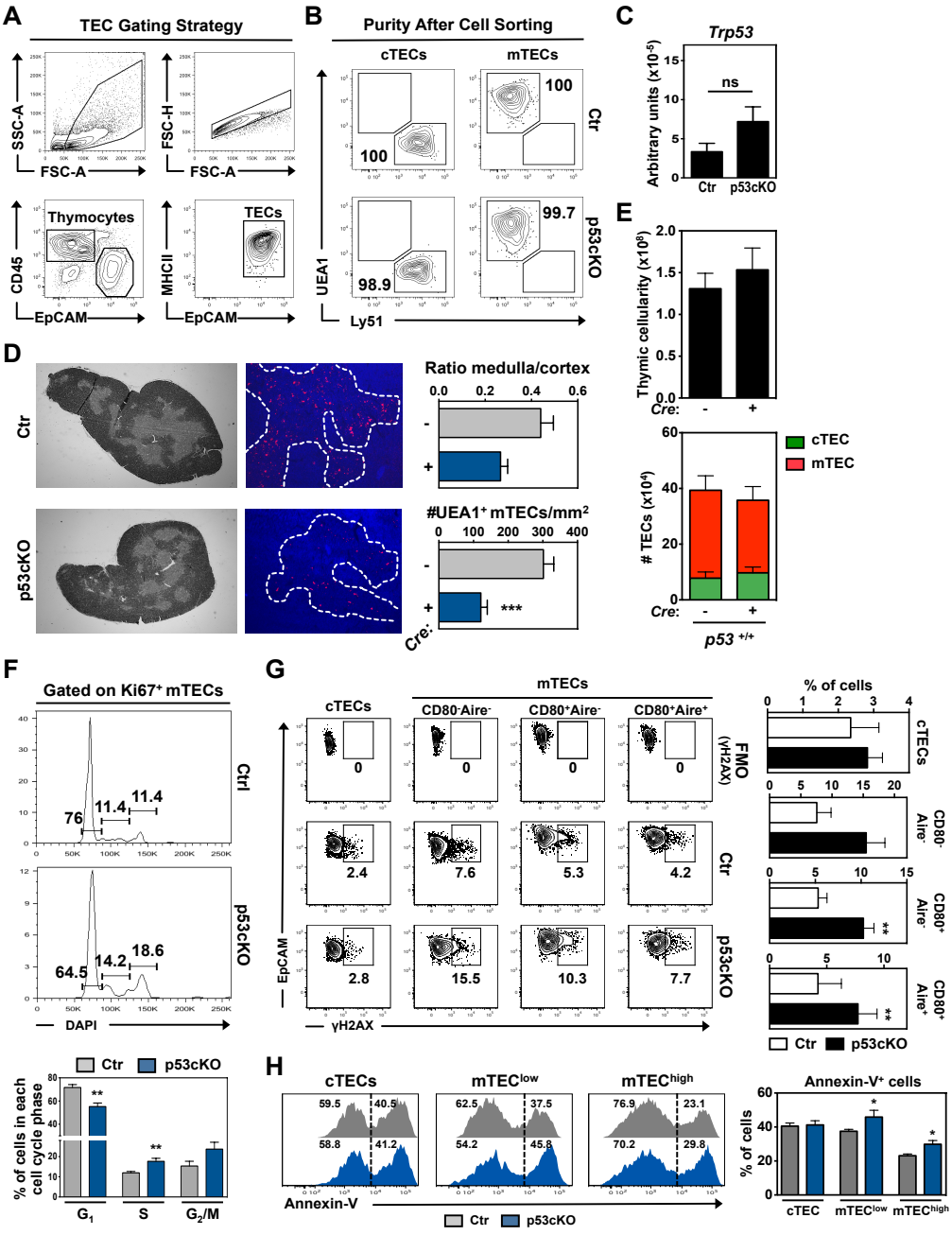

Supplemental Figure 1 - Histological, molecular and proliferative analysis of p53cKO TECs. (A) Flow cytometry analysis and gating strategy used to identify thymocytes (CD45$^+$) and TECs (CD45$^-$EpCAM$^+$MHCII$^+$). **(B)** Representative flow cytometry post-sort analysis of cTECs (Ly51$^+$UEA1$^-$) and mTECs (Ly51$^-$UEA1$^+$) from 2-weeks-old control (Ctr) and p53cKO mice. Numbers indicate the percentage of purified cells within each gate. **(C)** qRT-PCR analysis of *Trp53* expression in thymocytes from 2-week-old Ctr and p53cKO mice. Products detected by amplification of cDNA sequence spanning exons 5 and 6. Values were normalized to *18s* ribosomal RNA (mean ± SEM of three independent experiments). **(D)** Thymic sections from 10-weeks-old Ctr and p53cKO mice stained for hematoxylin and eosin (HE) (left) or UEA1 (red) and DAPI (blue) (right). Graphs represent the ratio of medullary to cortical areas based on HE staining (2-3 sections per thymus of Ctr (2) and p53cKO (2) mice) and the number of UEA1$^+$ cells per unit area (n=14-15 sections from 4 thymi). Bars: 100 µm. **(E)** Number of thymocytes (top) and cTEC/mTEC subsets (bottom) in 2-weeks-old *Trp53*$^{+/+}$ and *Foxn1*^{Cre}-*Trp53*$^{+/+}$ mice (n=7-8 mice per group from 3 independent experiments). **(F)** Cell cycle analysis with Ki67/DAPI staining was performed on mTECs from 2-weeks-old Ctr and p53cKO mice. Representative histogram of DAPI staining in Ki67$^+$ mTECs (top). Graph shows the average percentages of cells in the different phases of the cell cycle (bottom). Data is representative of 2 independent experiments (n=6 mice per group). **(G)** Flow cytometry analysis of phosphorylated γ-H2AX levels in 10 days-old Ctr and p53cKO TECs. Bar graphs display the results (mean ± SEM) of 3 independent experiments (n = 6 mice per condition). (H) Apoptosis of TECs was measured with Annexin V in 10 days-old mice. Bar graphs display the results (mean ± SEM) of 3 independent experiments (n = 6 mice per condition). * $P < 0.05$; ** $P < 0.01$; *** $P < 0.001$.

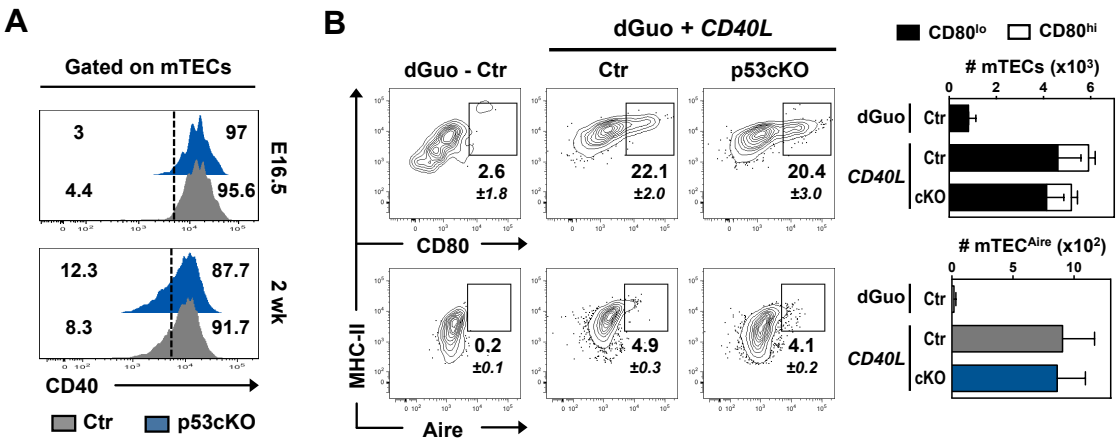

Supplemental Figure 2 - The expression and responsiveness of CD40 in mTECs are not affected by p53 inactivation. (A) Representative flow cytometry profiles of CD40 expression on mTECs (UEA^+Ly51^-) from E16 and 2-week-old control (Ctr) and p53cKO mice. Numbers indicate the percentage of gated cells. Results are representative of at least 3 independent experiments with 3-5 mice per group. **(B)** E15.5 dGuo-treated FTOCs from control and p53cKO mice were cultured for 4 days in the presence of recombinant CD40L, and mTECs (UEA^+Ly51^-) were analyzed for CD80 and Aire expression. Numbers indicate the mean percentage of gated cells. Bar graphs display the cellularity of mTEC subpopulations per thymic lobe. Results are presented as mean ± SEM of 10-12 thymic lobes per group.

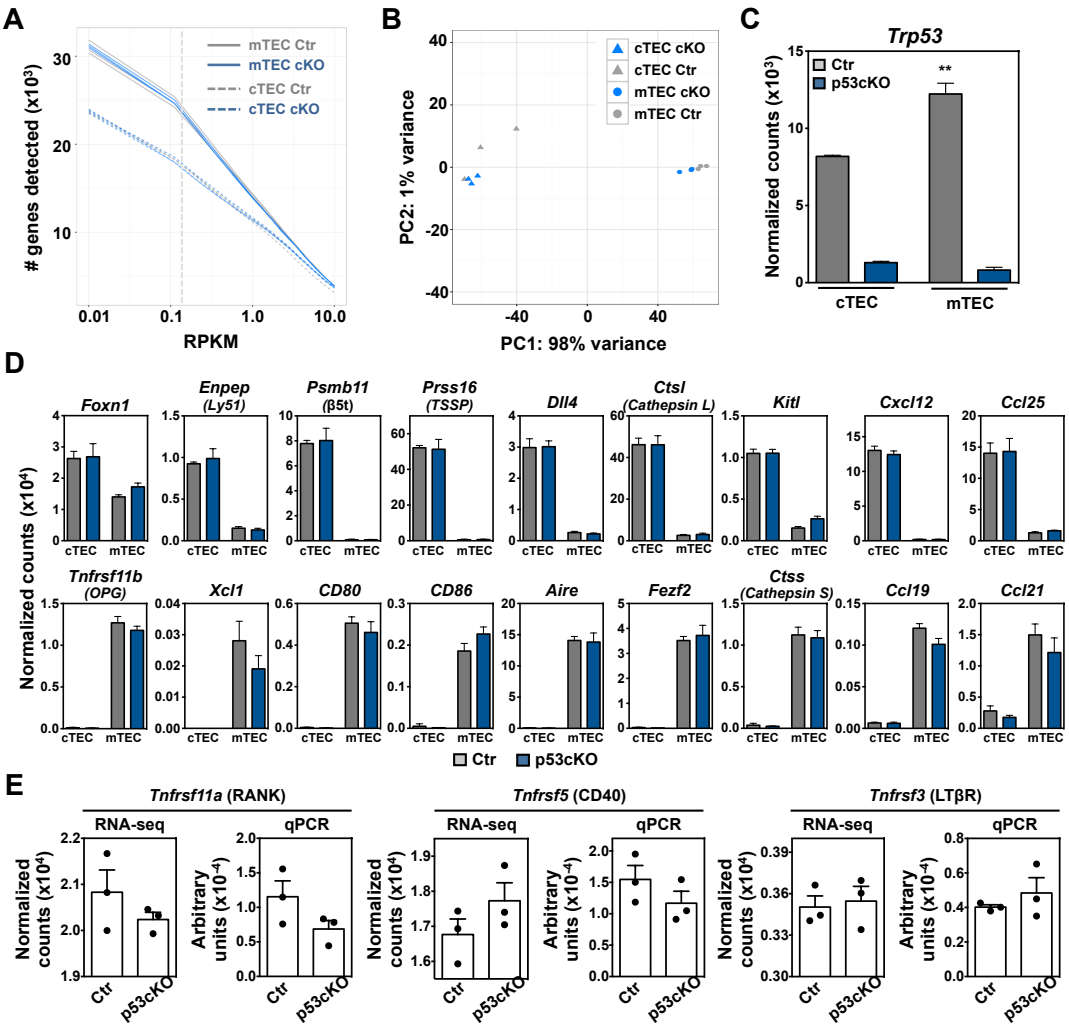

Supplemental Figure 3 - Bioinformatic analysis of the transcriptome of TEC subsets from control and p53cKO mice. (A) Number of Ensembl listed genes detected in cTEC/mTEC subsets from control (Ctr) and p53cKO mice at different RPKM thresholds. The average number of genes detected in WT and p53cKO mTECs was *23.490*, whereas in cTECs counterparts was *17.480*. Vertical dashed line depicts the RPKM threshold (0.15) at which genes can be consistently detected in TEC subsets. **(B)** Principal component analysis (PCA) for the transcriptome of cTECs and mTECs from Ctr and p53cKO mice. The dominant PC1 distinguishes cTEC and mTEC samples irrespectively of their genotype. While Ctr and p53cKO cTEC samples have overlapped positions along the horizontal axis, Ctr and p53cKO mTEC samples show a clearer segregation. **(C)** *Trp53* expression in the indicated Ctr and p53cKO TEC subsets; Symbol (*) compares the normalized counts of *Trp53* in mTECs vs cTECs from Ctr mice. ** $P < 0.01$; Unpaired t-test with Welch's correction **(D)** Expression of cTEC- (top) or mTEC-associated genes in Ctr and p53cKO TEC subsets (bottom). **(E)** The expression of *Tnfrsf11a*, *Tnfrsf5* and *Tnfrsf3* was validated by qRT-PCR on the sequenced mTEC samples from Ctr and p53cKO mice and compared with the values (normalized counts) obtained by RNA-seq. Error bars represent mean ± SEM.

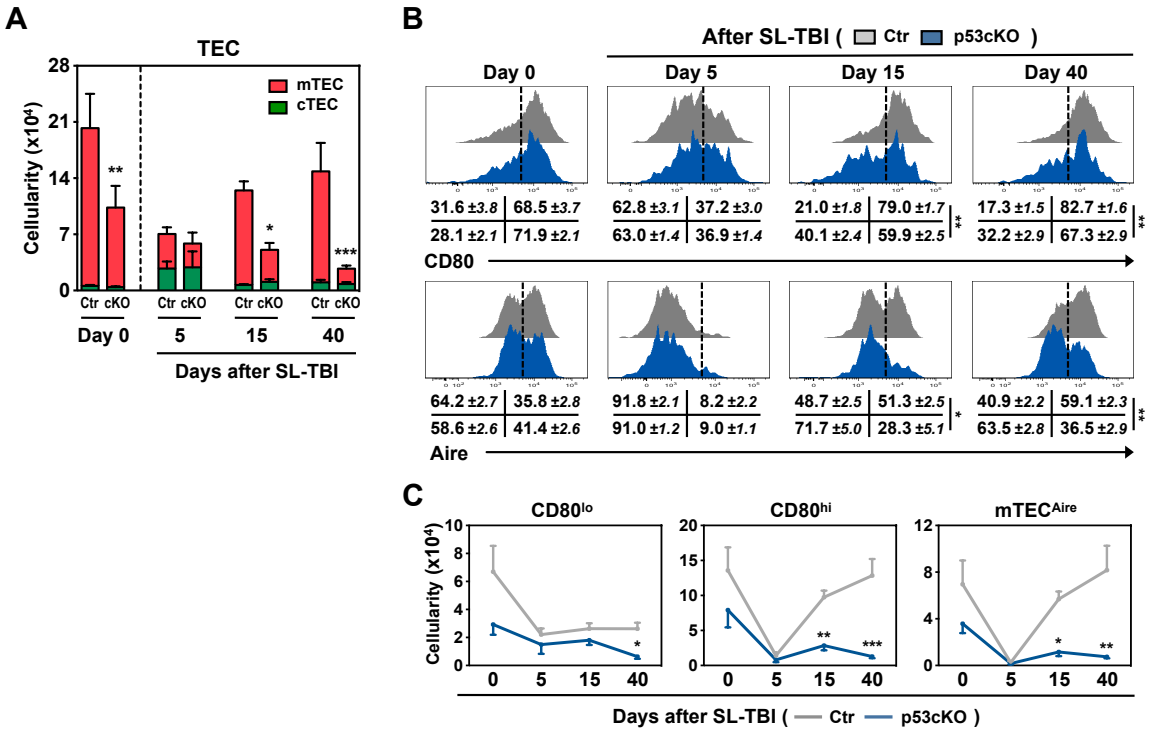

Supplemental Figure 4 – The regeneration of the mTEC microenvironment is compromised in p53cKO mice following radiation. 6-week-old control (Ctr) and p53cKO mice were sub-lethally irradiated and TECs were analyzed at the indicated time points following treatment. **(A)** Cellularity of TEC subsets. Symbol (*) compares mTECs from Ctr versus p53cKO mice. The fold reduction on mTEC cellularity (day 0/ day5) shortly after SL-TBI is depicted as numbers above the bar. **(B)** mTECs (UEA^+Ly51^-) from Ctr and p53cKO mice were analysed for CD80 and Aire expression. Numbers indicate the average percentages (mean ± SEM) of indicated mTEC subsets. **(C)** Absolute numbers of mTEC subsets depicted in B. **(A-C)** Graphs represent data from 3 experiments/time point (n=6-8 mice per group). Error bars represent mean ± SEM. * $P < 0.05$; ** $P < 0.01$; *** $P < 0.001$.

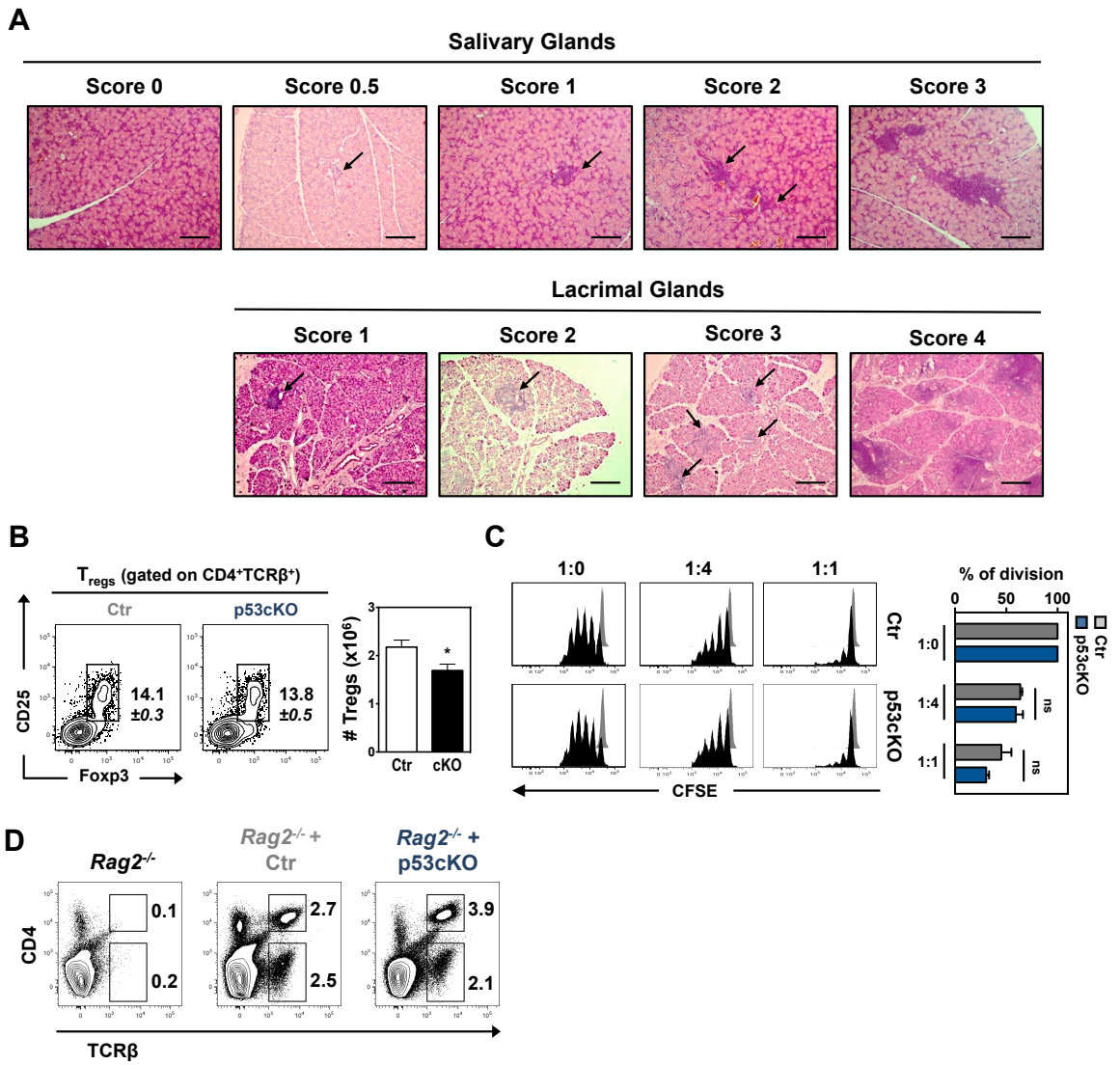

Supplemental Figure 5 – (A) Scoring system used to assess leucocyte infiltration. Representative hematoxylin and eosin stained sections of salivary and lacrimal glands from control (Ctr) and p53cKO mice are represented. Bars: 100 µm. **(B)** Total splenic CD4 T cells ($CD4^+TCRb^+$) from Ctr and p53cKO were analyzed for the expression of CD25 and Foxp3. Numbers indicate the percentage of gated cells. Graphs represent the number of regulatory T cells ($CD25^+Foxp3^+$) (Tregs); **(C)** *In vitro* assay measuring the suppressive capacity of Ctr and p53cKO-derived regulatory T cells co-cultured with CFSE-labeled Ctr CD4+CD25- T cells (conventional). On day 3 after stimulation, CFSE dilution was assessed by flow cytometry. Graph represents the precursor frequency of dividing conventional T cells. The % of dividing cells in 1:0 were set as 100 and the suppression of division was calculated relatively to the other conditions. Results are presented as mean ± SEM of 3 independent experiments. **(D)** T cell splenic reconstitution of the *Rag2*$^{-/-}$ mice 14 days upon thymocyte transfer. FACS plots represent data from 2-3 independent experiments (n=5-13 mice per group).

Chapter III

Intrathymic deletion of IL-7 reveals a contribution of the bone marrow to thymic rebound induced by androgen blockade

Pedro M. Rodrigues[*,†,‡], Ana R. Ribeiro[*,†], Nicolas Serafine[§,#], Catarina Meireles[*,†], James P. Di Santo[§,#] and Nuno L. Alves[*,†].

[*] Instituto de Investigação e Inovação em Saúde, Universidade do Porto, Portugal.
[†] Thymus Development and Function Laboratory, Instituto de Biologia Molecular e Celular, Porto, Portugal.
[‡] Doctoral Program in Biomedical Sciences, Instituto de Ciências Biomédicas Abel Salazar, Universidade do Porto, Porto, Portugal.
[§] Innate Immunity Unit, Institut Pasteur, 75724 Paris, France.
[#] Inserm U1223, 75015 Paris, France.

Under revision in The Journal of Immunology

Abstract

Despite the well-documented effect of castration in thymic regeneration, the singular contribution of the bone marrow (BM) versus the thymus to this process remains unclear. The chief role of Interleukin-7 (IL-7) in pre- and intra-thymic stages of T lymphopoiesis led us to investigate the impact of disrupting this cytokine during thymic rebound induced by androgen blockade. We found that castration promoted thymopoiesis in young and aged WT mice. In contrast, only young germline IL-7 deficient (*Il7*$^{-/-}$) mice consistently augmented thymopoiesis after castration. The increase in T cell production was accompanied by the expansion of the sparse medullary thymic epithelial cell (mTEC) and the peripheral T cell compartment in young *Il7*$^{-/-}$ mice. In contrast to young *Il7*$^{-/-}$ and WT mice, the poor thymic response of aged *Il7*$^{-/-}$ mice after castration was associated with a defect in the expansion of BM hematopoietic progenitors. These findings suggest that BM-derived T cell precursors contribute to thymic rebound driven by androgen blockade. To assess the role of IL-7 within the thymus, we generated mice with conditional deletion of IL-7 (*Il7*cKO) in thymic epithelial cells. As expected, *Il7*cKO mice presented a profound defect in T cell development while maintaining an intact BM hematopoietic compartment across life. Unlike *Il7*$^{-/-}$ mice, castration promoted the expansion of BM precursors and enhanced thymic activity in *Il7*cKO mice independently of age. Our findings suggest that the mobilization of BM precursors acts as a prime catalyst of castration-driven thymopoiesis.

Introduction

The thymus is a crucial organ in adaptive immune responses as the generative site of functionally diverse and self-tolerant T cells. Importantly, the activity of the thymus decreases with age, leading to a reduced and more restricted pool of newly generated T cells. While of marginal consequence in healthy individuals, thymic involution may predispose to infections, autoimmunity, and possibly cancer, in the elderly or patients undergoing allogeneic hematopoietic stem cell transplantation (HSCT) (1). Within the thymus, thymic epithelial cells (TECs) provide chief inductive microenvironments for T cell development and selection (2). As the number of TECs and thymocytes decline throughout life (3), it is thought that thymic involution stems

in part from deficits that affect both populations. Still, upstream alterations in the bone marrow (BM) influence the number of thymic seeding precursors, and this can also affect thymic function (4).

Androgens are well-recognized regulators of thymopoiesis. This notion is supported by the observations that sex steroid ablation (SSA) augments thymic cellularity, restores TEC architecture and enhances T cell output in distinct conditions of thymic hypoplasia (5–8). Hence, manipulation of sex steroids levels represents an attractive therapy to correct thymic degeneration during aging or upon HSCT. Several reports indicate that SSA has direct effects in the thymic stromal cells. In particular, castration augments the proliferation and number of TECs (3, 9) and enhances the expression of Notch ligand Dll4 and CCL25 (10, 11), suggesting an improvement in TEC functioning. On the other hand, other studies revealed an equal beneficial impact of androgen blockade in the bone marrow (BM), such as reverting deficits in the numbers of lymphoid progenitors and B cells induced by radiation and aging (12–14) and regenerating the BM stromal microenvironment of aged mice (15). Therefore, thymic rebound driven by castration might also depend on upstream effects at the level of the BM. However, the lack of experimental models to uncouple the activity of these two key hematopoietic niches (BM and thymus) maintains this possibility unanswered.

Interleukin 7 (IL-7) is a critical growth factor in thymopoiesis (16). The deficiency in IL-7 markedly inhibits T cell development, resulting in a severe combined immunodeficiency (SCID) both in humans, mice and jawed fish (17, 18). These results indicate a high functional conservation of the IL-7 signalling pathway in thymopoiesis. Within the thymus, IL-7 is predominantly produced by TECs (19, 20), wherein it regulates several aspects of T cell development, including survival and proliferation of early T cell precursors, αβ/γδ lineage commitment and CD4/CD8 lineage determination during positive selection (21, 22). Previous studies suggest that intrathymic IL-7 expression is not altered following castration (7, 9). Still, surgical castration of aged mice with germline deletion of IL-7 (*Il7*$^{-/-}$) suggests a requirement for this cytokine in thymic rebound induced by androgen blockade (13). One possibility is that intrathymic IL-7 drives castration-driven augment in thymopoiesis. However, the role of IL-7 in pre-thymic stages of T cell development may confound the interpretation of results obtained with mice with germline deletion

of *Il7* (23). In particular, the number of common lymphoid progenitors and B cell precursors are profoundly reduced in the BM of *Il7*$^{-/-}$ mice, a defect that is further enhanced with age (16, 24). As such, the defective thymic rebound of *Il7*$^{-/-}$ mice following castration might result from the deterioration in the number of BM-derived thymic seeding progenitors.

Using distinct loss-of-function genetic approaches, we examined the temporal and spatial requirements for IL-7 in thymic rebound induced by surgical castration. We found that castration enhances thymopoiesis in young but not aged germline *Il7*$^{-/-}$ mice. The loss of thymic response induced by androgen blockade correlated with a defective expansion of hematopoietic progenitors in the BM of aged *Il7*$^{-/-}$mice. Conversely, conditional deletion of IL-7 in TECs normalized the castration-driven BM and thymic reactivation across life. Our results indicate that the increase in thymopoiesis upon androgen blockade is functionally linked to the BM compartment.

Results

Androgen blockade augments thymopoiesis in both young and aged mice.

We began by evaluating the impact of androgen blockade in the activity of the thymus of young and aged WT mice (**Figure 1A**) (3). We found that castration of young (4-week-old) mice induced an increase in thymic cellularity 2 weeks post-surgery, which was of the same extent as the one observed in their aged counterparts (≥ 8 months) (**Figure 1A**) (6, 29). Androgen blockade did not alter the T-cell developmental program. Instead, it led to an expansion of all main thymocyte subsets (ETPs, DN2-DN4, DP, SP4 and SP8 cells) in both young and aged mice (**Supplemental Figure 1A and B**). Still, the cellularity of the thymus of mice castrated during puberty dropped 10 weeks post-surgery (**Figure 1A**), suggesting that age-related thymic involution is uncoupled of the effect of sex steroids (30). Using previously described IL-7 reporter mice (19, 31), we next examined the influence of castration on the expression of thymic IL-7. In these mice, IL-7^{YFP} (Yellow Fluorescent Protein) cells identify a subtype of cTECs that expresses high levels of *Il7*. While abundant during embryonic and early postnatal life, IL-7^{YFP} cells represent a minor subset in both young and aged thymus (19, 31) (**Figure 1B**,

control IL-7 reporter mice (Ctr); non-reporter aged-matched mice are shown in **Supplemental Figure 1C**). We found that the frequency and number of IL-7^{YFP} cells remained unaltered 2 weeks post-castration in young and aged mice (**Figure 1B, upper panel, and C**). These findings suggested that thymic rebound driven by castration seemed to proceed independently of changes in the intrathymic expression of IL-7. Further analysis of the composition of TEC subsets showed that the number of total cTECs (Ly51^{+}) remained unaltered 2 weeks following castration (**Figure 1B, middle panel, and C**). Complementary analysis using CCRL1^{GFP} (Green Fluorescent Protein) reporter mice, in which high levels of GFP expression identifies cTECs (26), corroborated this observation (**Supplemental Figure 1D**). In contrast, the frequency and numbers of mature CD80^{+} mTECs, including Aire^{+} cells, augmented in both young and aged thymus 2 weeks after castration (**Figure 1B, middle and lower panels, and C**).

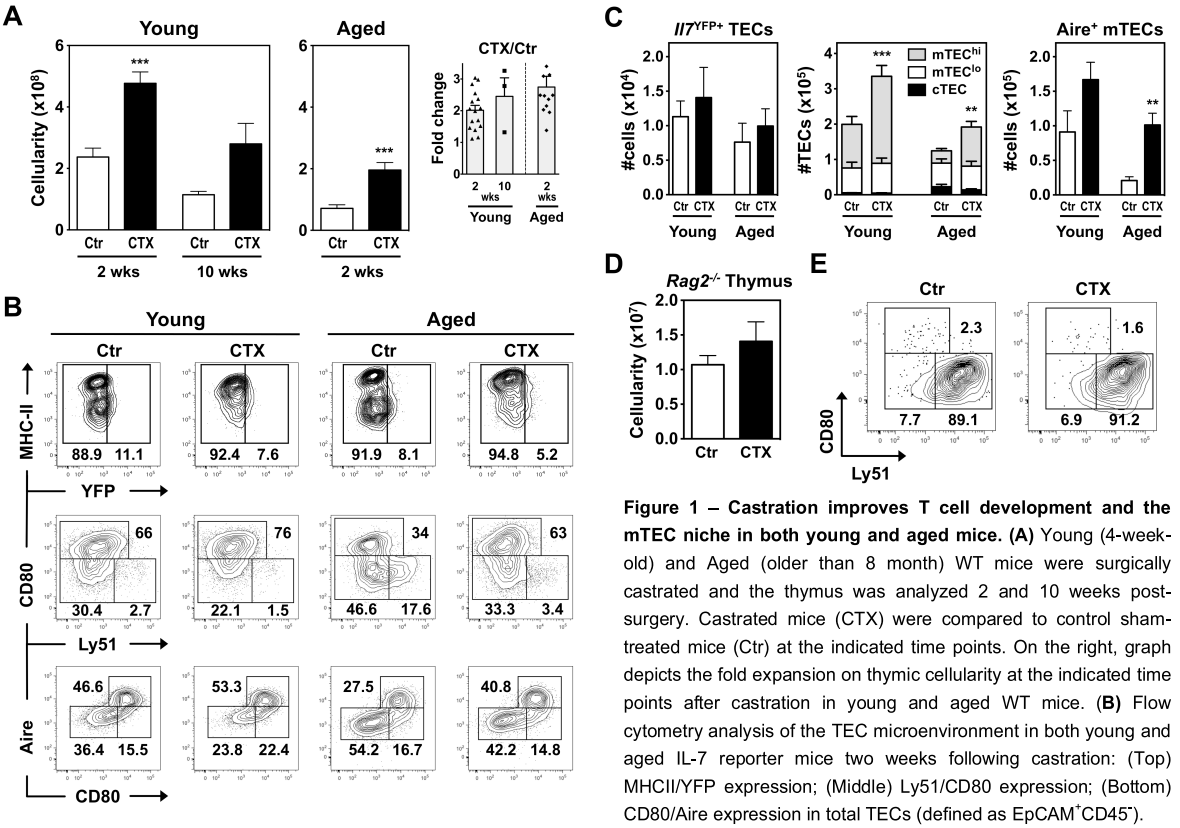

Figure 1 – Castration improves T cell development and the mTEC niche in both young and aged mice. (A) Young (4-week-old) and Aged (older than 8 month) WT mice were surgically castrated and the thymus was analyzed 2 and 10 weeks post-surgery. Castrated mice (CTX) were compared to control sham-treated mice (Ctr) at the indicated time points. On the right, graph depicts the fold expansion on thymic cellularity at the indicated time points after castration in young and aged WT mice. (**B)** Flow cytometry analysis of the TEC microenvironment in both young and aged IL-7 reporter mice two weeks following castration: (Top) MHCII/YFP expression; (Middle) Ly51/CD80 expression; (Bottom) CD80/Aire expression in total TECs (defined as EpCAM^{+}CD45^{-}). Numbers indicate the percentage of gated cells. **(C)** Cellularity of the different TEC subsets depicted in (**B)** Results in **A-C** are shown as mean ± SEM of 3-17 mice/group from 2-3 independent experiments. **(D-E)** Young (4-week-old) *Rag2*$^{-/-}$ mice were castrated and the thymus was analyzed 2 weeks post-surgery. **(D)** Thymocyte cellularity and **(E)** Expression of Ly51 and CD80 in TECs of control (Ctr) and castrated (CTX) *Rag2*$^{-/-}$ mice. Numbers indicate the percentage of gated cells. Results are presented as mean ± SEM. * $P < 0.05$; ** $P < 0.01$; *** $P < 0.001$.

To determine whether the enlarged mTEC compartment resulted from direct effects of androgen depletion on TECs, we performed similar experiments in *Rag2*$^{-/-}$

mice, which present sparse mTEC areas due to the absence of thymocyte-derived signals (32). Although castration induced a small increase in thymic cellularity of *Rag2*$^{-/-}$ mice, mTECs remained underdeveloped under this condition (**Figure 1D and E**). These findings indicate that the augmented mTEC compartment following castration represents a footprint of an increased TEC-thymocyte crosstalk. Furthermore, our results suggest that enhanced thymopoiesis driven by castration can be stimulated prior to the onset of age-associated thymic involution.

Androgen blockade promotes thymic renewal in young IL-7-deficient mice.

Next, we examined the temporal requirement of IL-7 during castration-induced thymic rebound. To do so, we castrated young and aged germline IL-7-deficient (*Il7*$^{-/-}$) mice, which displayed a profound thymic atrophy(16), and analyzed them 2 and 10 weeks post-surgery. Similar to previous findings (13), most of aged *Il7*$^{-/-}$ mice did not augment thymopoiesis 2 weeks upon castration (**Figure 2A and Supplemental Figure 2A**). Contrarily, we found an expansion in the thymic cellularity of all

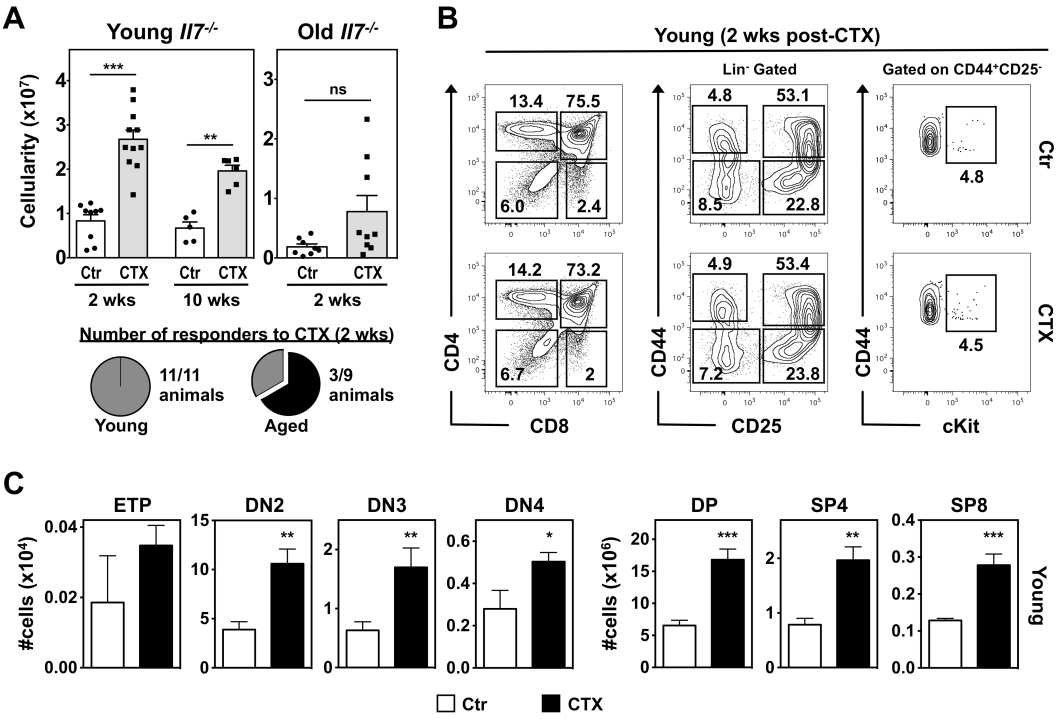

Figure 2 – Castration boosts thymopoiesis in young *Il7*$^{-/-}$ mice. (A) Young (4-week-old) and Aged (older than 8 month) *Il7*$^{-/-}$ mice were castrated and the thymus was analyzed at the indicated time-points after surgery. Castrated mice (CTX) were compared to control sham-treated mice (Ctr). On the bottom, pie graphs depict the number of mice in which thymic rebound was detected 2 weeks after castration (Nr. of responders to castration) **(B)** Analysis of T cell development in young control and castrated *Il7*$^{-/-}$ mice 2 weeks after surgery: (left) CD4/CD8 expression on total thymocytes; (middle) CD44/CD25 expression on DN thymocytes (gated on Lin$^-$ cells); (right) cKit/CD44 expression on DN1 thymocytes. ETPs are defined as Lin$^-$ cKit$^+$CD44$^+$CD25$^-$; Numbers indicate the frequencies of the different thymocyte subsets. (**C**) Number of the indicated thymocyte subsets in young control (Ctr) and castrated (CTX) *Il7*$^{-/-}$ mice 2 weeks post-surgery. Results are presented as mean ± SEM. * $P < 0.05$; ** $P < 0.01$; *** $P < 0.001$.

castrated young *Il7*$^{-/-}$ mice (**Figure 2A**). Still, androgen blockade did not restore thymic cellularity in *Il7*$^{-/-}$ mice to the level of WT mice and failed to correct the lymphopoietic defects that result from the lack IL-7 signalling, such as the developmental arrest at DN2-DN3 stage and the augmented SP4/SP8 ratio (22) (**Figure 2B, compare to Supplemental Figure 1A**). Instead, castration induced a global increase in the number of ETPs, immature and mature thymocytes subsets in *Il7*$^{-/-}$ mice (**Figure 2C**). The increase in thymocyte cellularity of *Il7*$^{-/-}$ mice castrated during puberty was maintained 10 weeks post-surgery (**Figure 2A**), indicating a durable benefit of castration in thymopoiesis. Yet, akin to WT mice, castrated *Il7*$^{-/-}$ mice displayed an age-dependent thymic involution (**Figure 2A**). Additionally, we analyzed the impact of androgen blockade in the TEC microenvironment and peripheral T cell composition of young *Il7*$^{-/-}$ mice. At steady state, the differentiation and number of mature mTECs, including Aire^{+} subset, were profoundly reduced in *Il7*$^{-/-}$ thymus, presumably due to the lack of thymocyte-derived signals (**Figure 3A**).

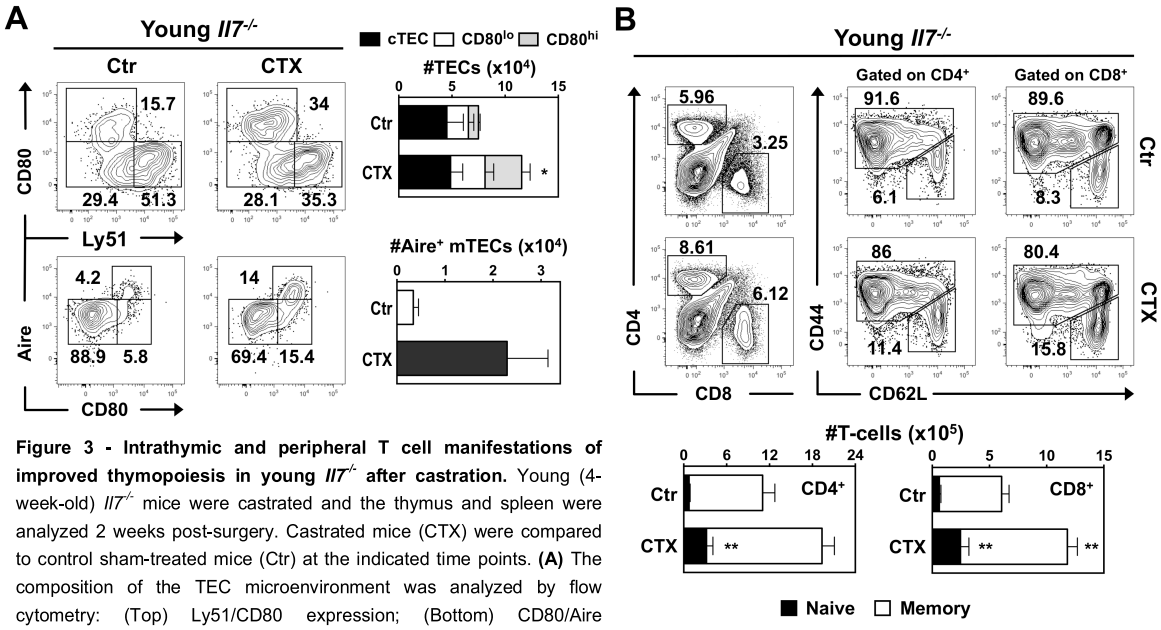

Figure 3 - Intrathymic and peripheral T cell manifestations of improved thymopoiesis in young *Il7*$^{-/-}$ after castration. Young (4-week-old) *Il7*$^{-/-}$ mice were castrated and the thymus and spleen were analyzed 2 weeks post-surgery. Castrated mice (CTX) were compared to control sham-treated mice (Ctr) at the indicated time points. **(A)** The composition of the TEC microenvironment was analyzed by flow cytometry: (Top) Ly51/CD80 expression; (Bottom) CD80/Aire expression on total TECs (defined as EpCAM^{+}CD45^{-}). Numbers indicate the percentage of gated cells. On the right, graphs represent the cellularity of the different TEC subsets. **(B)** Flow cytometry analysis of the splenic T cell compartment. (Left panel) Representative CD4/CD8 staining in total spleenocytes; (Middle/right panels). Dot plots depict the CD62L/CD44 staining on gated CD4^{+} and CD8^{+} splenic T cells. Numbers indicate the frequencies of the different subsets. On the bottom, graphs show the number of naive (CD62L^{+}CD44^{-}) and memory (CD62L^{-}CD44^{+}) splenic T cells in control and castrated *Il7*$^{-/-}$ mice. Results are presented as mean ± SEM. * $P < 0.05$; ** $P < 0.01$; *** $P < 0.001$.

Strikingly, castration increased the frequency and cellularity of mature mTECs (CD80^{+} and Aire^{+} mTECs) in *Il7*$^{-/-}$ thymi (**Figure 3A**). Similarly to WT mice, the numbers of immature mTECs and cTECs remained unaltered 2 weeks post-castration (**Figure 3A**). Analysis of the lymphopenic T cell pool of *Il7*$^{-/-}$ mice (33)

showed that castration enhanced the frequency and number of peripheral CD4 and CD8 T cells, with a particular increase in the naïve T cell subset (**Figure 3B**). None of these alterations were found in castrated aged *Il7*$^{-/-}$ mice (**Supplemental Figure 2A and B**), which lacked a consistent thymic response. Thus, the described intrathymic and peripheral improvements in castrated young *Il7*$^{-/-}$ mice seemed to derive directly from enhanced thymopoiesis.

Androgen blockade fails to expand BM hematopoietic precursors in aged IL-7-deficient mice.

The observation that young, but not aged, *Il7*$^{-/-}$ thymi rebound after castration suggested the existence of a temporal window in which this process could be stimulated independently of IL-7. Given that thymopoiesis requires a continual input of BM-derived progenitors (34) and castration promotes the expansion of common lymphoid progenitors (CLPs) and B cells in the BM (12), we examined whether the loss of castration-induced thymic rebound in aged *Il7*$^{-/-}$ mice was functionally linked to a defective BM response. We determined the influence of castration in the number of HSCs and CLPs, which were defined as previously described (35) (**Supplemental Figure 3A**). In agreement with previous reports [14], the numbers of LSK, CLPs and B cells increased in both young and aged WT mice 2 weeks after castration (**Figure 4A and B**). As expected, CLPs and B cell cellularities were markedly reduced in the BM of *Il7*$^{-/-}$ mice, being the numbers of CLPs further diminished with aged (**Figure 4B**) (24). Similarly to the thymus, the response of BM hematopoietic progenitors in *Il7*$^{-/-}$ mice was age-dependent. Particularly, we found a specific expansion of LSK and CLPs in castrated young *Il7*$^{-/-}$ mice (**Figure 4B**). Still, castration did not correct B lymphopoiesis in *Il7*$^{-/-}$ mice, indicating that androgen blockade did not bypass the requirement of IL-7 for B cell development in the adult BM (**Figure 4B**). These findings indicate the existence of a temporal-restricted window in which BM hematopoietic progenitors of *Il7*$^{-/-}$ mice respond to castration. Interestingly, the augmented numbers of LSK in castrated young *Il7*$^{-/-}$ mice correlated with the increased thymic cellularity at the individual mouse level, similar to young and aged WT counterparts. Albeit CLPs numbers expanded moderately in young *Il7*$^{-/-}$ mice after castration (**Figure 4B**), the correlation between their expansion and the increased thymic cellularity was not statistically significant

(**Figure 4C**). These results suggest that the engagement of BM progenitors may be a requisite for castration-driven thymic rebound.

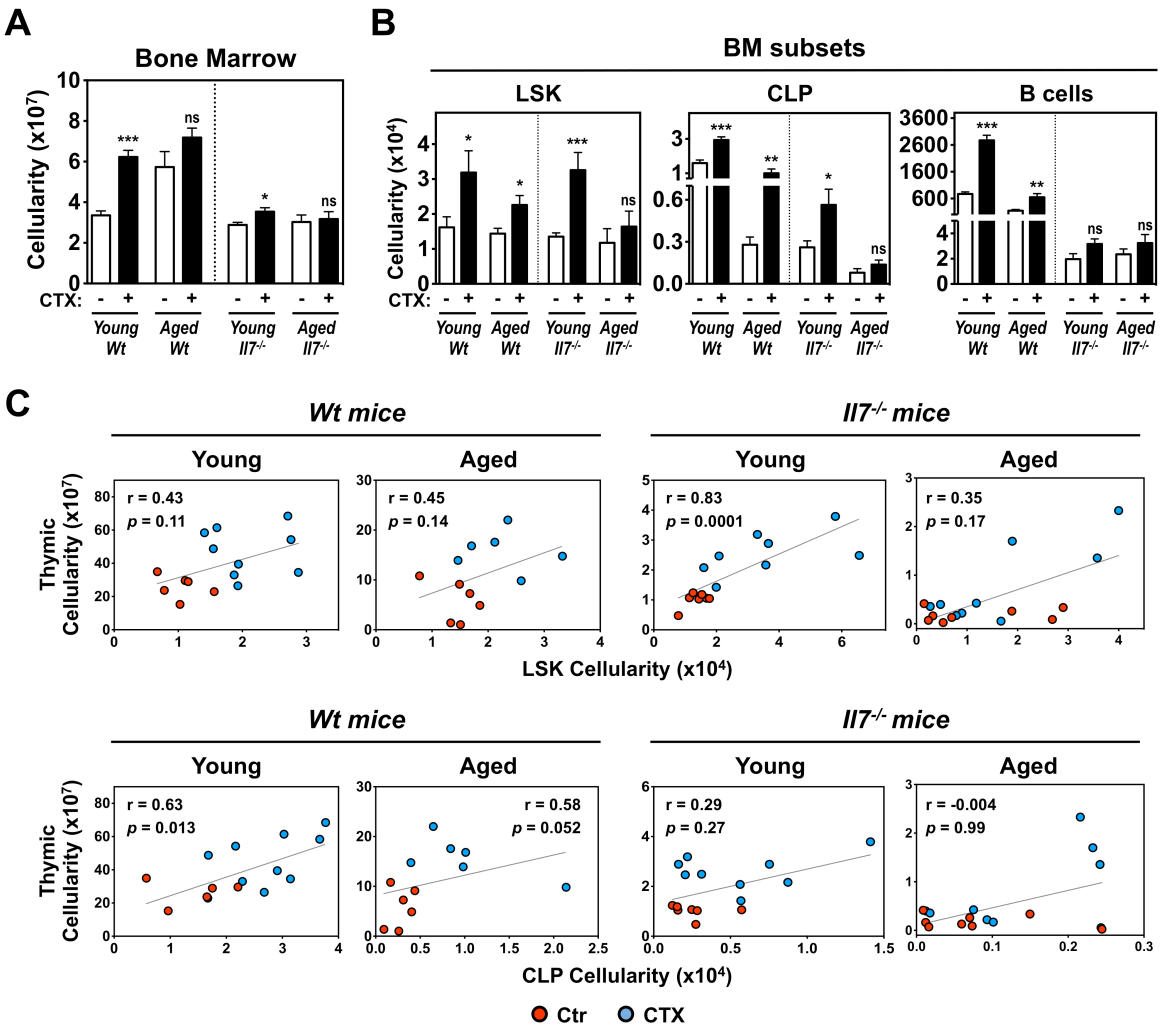

Figure 4 – The absence of thymic rebound in castrated aged *Il7*$^{-/-}$ mice correlates with a defective expansion of BM hematopoietic precursors. Young/aged wild type (WT) and *Il7*$^{-/-}$ mice were castrated and the BM composition was analyzed 2 weeks after surgery. Castrated mice (CTX) were compared to control sham-treated mice (Ctr) at the indicated time points. **(A)** Total BM cellularity. **(B)** Number of LSK (Lin^{-} CD127^{-}cKit^{+}Sca-1^{+}), CLP (Lin^{-}CD127^{+}cKit^{int}Sca-1^{int}) and B cells (CD19^{+}) in control (Ctr) and castrated (CTX) mice. **(C)** Spearman correlation between the thymic cellularity and the number of LSK and CLPs in the BM of control (Ctr) and castrated (CTX) groups. Results are presented as mean ± SEM. * $P < 0.05$; ** $P < 0.01$; *** $P < 0.001$.

Androgen blockade induces thymic rebound in aged mice with conditional deletion of IL-7 in the thymus.

We reasoned that the loss of castration-driven thymic rebound in aged *Il7*$^{-/-}$ mice could be linked to a defective expansion of BM hematopoietic precursors. However, the use of mice with a germline deficiency in *Il7* fails to uncouple the spatial requirements of this cytokine in the BM and thymus. To study whether thymic IL-7 was a chief mediator of thymic renewal after castration, we generated and analyzed mice with conditional inactivation of *Il7* in TECs. We developed mice with loxP-

flanked alleles of *Il7* (*Il7*$^{fl/fl}$) and crossed them to mice expressing the Cre-recombinase under the transcriptional control of the *Foxn1* promoter (*Foxn1*^{Cre}) (27), referred hereafter as *Il7*cKO (**Supplemental Figure 4A**). Young and old *Il7*cKO mice revealed a normal hematopoietic composition in the BM relatively to their aged-matched littermate controls (*Il7*$^{fl/fl}$), containing similar numbers of total cells, LSK, CLPs and B cell subsets (**Figure 5A, *Il7*$^{fl/fl}$ *vs* *Il7*cKO**). In contrast, and consistently with a previous report (20), thymic cellularity was markedly decreased in young and aged *Il7*cKO mice, resulting in a reduction in the numbers of DN, DP, SP4 and SP8 subsets (**Figure 5B and C; Supplemental Figure 4B *Il7*$^{fl/fl}$ *vs* *Il7*cKO**). Similar to germline *Il7*$^{-/-}$ mice, *Il7*cKO mice displayed thymic developmental defects linked to the lack of IL-7 signalling, including the partial block in DN2-DN3 transition and altered SP4/SP8 ratio (**Figure 5C; Supplemental Figure 4B *Il7*$^{fl/fl}$ *vs* *Il7*cKO**). These results reinforce the notion that TECs are the physiological source of IL-7 within the thymus. Hence, we used *Il7*cKO mice as a model system to interrogate whether the maintenance of the BM homeostasis overcame the requirement for intrathymic IL-7 in castration-driven thymopoiesis. As expected, the numbers of LSK, CLPs and B cells expanded in both young and aged *Il7*cKO mice 2 weeks post-castration (**Figure 5A, Ctr *Il7*cKO *vs* CTX *Il7*cKO**). Notably, castration induced the rebound of the thymus in young *Il7*cKO and restored this effect in their aged counterparts (**Figure 5B; Ctr *Il7*cKO *vs* CTX *Il7*cKO**). Androgen blockade promoted the expansion of all major thymic subsets in both age groups of *Il7*cKO mice, but failed to correct the developmental blocks linked to the absence of IL-7, similar to young *Il7*$^{-/-}$ mice (**Figure 5C, Supplemental Figure 4B; Ctr *Il7*cKO *vs* CTX *Il7*cKO**). The correlation between the augmented numbers of LSK and CLPs in the BM and the increased in thymic cellularity was normalized in both young and aged *Il7*cKO castrated mice (**Supplemental Figure 4C**). We further analyzed whether the enhanced thymopoiesis after castration was manifested in the peripheral T cell pool of *Il7*cKO mice. Under steady state conditions, *Il7*cKO mice presented a peripheral T cell lymphopenia relatively to wild-type controls, with a reduction in the percentage and number of naïve CD4 and CD8 T cells (**Figure 5D, *Il7*$^{fl/fl}$ *vs* *Il7*cKO**). Strikingly, castration improved the peripheral T cell compartment of *Il7*cKO mice, with an increase in the frequency and number of naïve and total CD4 and CD8 T cells (**Figure 5D, Ctr *Il7*cKO *vs* CTX *Il7*cKO**). These results indicated that the maintenance of functional BM hematopoietic progenitors along life

bypasses the requirements for TEC-derived IL-7 during thymic rebound induced by androgen blockade. Together, our data provide evidence that the capacity of castration to stimulate thymic rebound also depends on the engagement of BM-derived hematopoietic precursors.

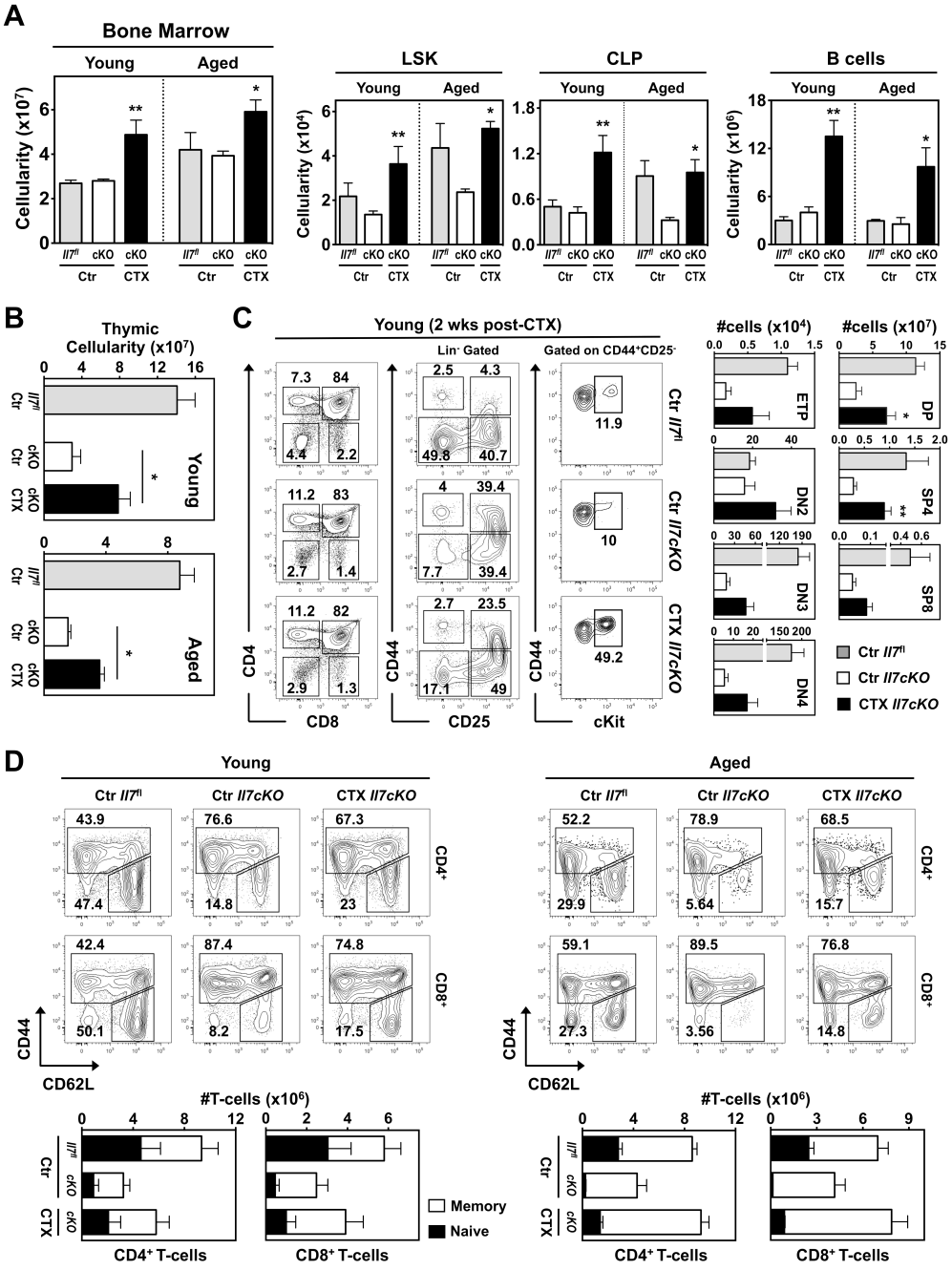

Figure 5 – Thymic rebound upon castration does not depend on thymic-derived IL-7. Young/aged control IL7-floxed (*Il7*$^{fl/fl}$) and IL7-conditional KO (*Il7cKO*) mice were castrated and analyzed 2 weeks post-surgery. Castrated mice (CTX) were compared to control sham-treated mice (Ctr) at the indicated time points. **(A)** Number of the total bone marrow cells, LSK (Lin$^-$CD127$^-$cKit$^+$Sca-1$^+$), CLP (Lin$^-$CD127$^+$cKit^{int}Sca-1^{int}) and B cells (CD19$^+$) in the indicated young and aged mice. **(B)** Thymic cellularity in the indicated young and aged mice. **(C)** Analysis of T cell development: (left) CD4/CD8 expression on total thymocytes; (middle) CD44/CD25 expression on DN thymocytes (gated on Lin$^-$ cells); (right) cKit/CD44 expression on DN1 thymocytes. ETPs are defined as Lin$^-$ cKit$^+$CD44$^+$CD25$^-$; Numbers indicate the frequencies of the different thymocyte subsets. On the right, graphs represent the number of the different thymocyte subsets. **(D)** Flow cytometry analysis of the naïve and memory splenic T cell compartment in control (Ctr) and castrated (CTX) young and aged mice. Dot plots depict the CD62L/CD44 staining on gated CD4$^+$ and CD8$^+$ splenic T cells. Numbers indicate the frequencies of the different subsets. On the bottom, graphs show the absolute number of naive (CD62L$^+$CD44$^-$) and memory (CD62L$^-$CD44$^+$) splenic T cells in control (Ctr) and castrated (CTX) mice. Results are presented as mean ± SEM. * $P < 0.05$; ** $P < 0.01$; *** $P < 0.001$.

Discussion

Although it is well known that castration augments thymopoiesis under circumstances of thymic atrophy (6, 7), the mechanism underlying this regenerative process remains poorly understood. Our study provides evidence that the engagement of BM-derived precursors is a prime regulator of thymic renewal induced by castration. In mice, thymic activity reaches its maximum during puberty (3). Our initial observations that castration boosts thymopoiesis in young mice indicate that the function of the thymus can be enhanced independently of its atrophic status. Age-related thymic involution is accompanied by a loss in TEC cellularity (36), being these perturbations more pronounced in mature mTECs, including in Aire^{+} cells. Given their important role in tolerance induction (32), the drop in Aire^{+} cells with age might contribute to the predisposition to autoimmunity in the elderly (37). Our results showed that castration specifically expands mTECs in cohorts of animals that showed enhanced thymopoiesis, namely in young and aged immunocompetent mice and young *Il7*$^{-/-}$ mice. In contrast, the growth of the mTEC niche was not detected in thymi that failed to rebound after castration, as in the case of *Rag2*$^{-/-}$ or aged *Il7*$^{-/-}$ mice. These findings suggest that androgen blockade expands mTECs in a non-autonomous manner. In this regard, the establishment of the mTEC microenvironment involves the participation of TNFRSF RANK, LTβR and CD40 that are expressed in mTECs and their precursors (32). Given that castration augmented thymocyte cellularity, we infer that the growth of mTECs results from the increase in the bioavailability of TNFRSF ligands provided by distinct thymocyte subsets. Our results also suggest that the reduced mTEC compartment of aged or immunodeficient mice can be regenerated, providing that it is properly stimulated. Although the cellularity of cTECs was not affected after castration, one cannot exclude that androgen blockade does not influence their functionality. It has been reported that castration increases the expression of thymopoietic factors in cTECs, which promote the attraction, commitment and selection of thymocytes (38). These results implicate the existence of a complex intrathymic impact of androgen depletion in thymopoiesis.

TECs are the intrathymic physiological source of IL-7 (16, 20). Although thymic IL-7 levels drop after testosterone administration (10), our observations indicate that castration does not reciprocally augment its expression in TECs. Given that IL-7

reporter mice identify a particular subset of cTECs expressing high levels of IL-7 (28), we cannot exclude that androgen blockade regulates IL-7 expression in other thymic subsets expressing lower levels of this cytokine, such as non-IL-7 reporting cTECs and mTECs (39). In addition, oestrogen deficiency augments thymopoiesis in female mice through an increase in the levels of thymic IL-7 (40). These findings point to the existence of a sexual dimorphism concerning the action of sex steroids in regulation of IL-7 that needs to be further investigated. Intriguingly, we found that castration promotes thymic rebound in young (but not aged) germline *Il7*$^{-/-}$ mice, indicating the existence of a temporal window in which this regenerative process can be elicited independently of IL-7. The boost in thymopoiesis was intrathymically accompanied by an augment in mTEC cellularity and a moderate increase in naïve T cell counts. Still, castration neither restored thymic cellularity to normal levels nor corrected the specific defects that result from the absence of IL-7 signalling. In line with a previous study, most of the thymus of aged germline *Il7*$^{-/-}$ mice did not respond after castration (13). One hypothesis could be that cumulative intrathymic defects arising from the lack of IL-7 lead to this unresponsive state. Yet, the fact that the thymus of aged *Il7*cKO mice rebounded after castration argues against this possibility, and suggests that TEC-derived IL-7 is dispensable for this process.

Previous findings show that androgen blockade influence the BM compartment, reverting age-related defects in the numbers of LSK, CLP and B cells (12). Thus, upstream effects in the BM niche might also contribute to the enhanced thymopoiesis upon castration, through the provision of an increased number of thymic seeding progenitors. Concordantly, we found a striking correlation between the expansion of hematopoietic progenitors (LSK) in the BM and the thymic rebound after castration in young/aged WT and *Il7*cKO mice as well as in young *Il7*$^{-/-}$ counterparts. Additionally, the castration-induced increase in the number of ETPs in these groups suggests an enhanced thymic colonization by BM-derived progenitors. Given that the number of DP and SP cells is proportional to the number of DN cells in the thymus (41, 42), the provision of a higher number of thymic seeding progenitors might contribute to an increase in the overall number of subsequent DN, DP, and SP subsets. Contrarily, castration failed to expand the hematopoietic progenitors in the BM of aged *Il7*$^{-/-}$ mice, which directly correlated to their poor thymic response. Despite the profound thymic hypoplasia, *Il7*cKO mice displayed a

normal BM hematopoietic composition, which restored the association between BM and thymus responses after castration. Our results do not exclude that castration might also directly influence the thymic microenvironment of *Il7*cKO or *Il7*$^{-/-}$ mice, for example enhancing the expression of thymopoietic factors Notch ligand Dll4 and CCL25 (10, 11). Still, upstream defects in the BM of aged *Il7*$^{-/-}$ mice might also actively contribute to a failure in thymic rebound, potentially explaining the discrepancy in castration-driven thymopoiesis between young and aged groups. Whether androgen blockade directly stimulates BM progenitors and/or acts indirectly on supportive BM stromal cells remains to be further investigated. HSCs and CLPs reside within the BM microenvironment, which secrete factors that promote their maintenance and differentiation (4). *Il7* transcripts are found in multiple cell types within the BM, including osteoblasts, endothelial and mesenchymal progenitor cells (43)**.** Despite evidence showing that *Il7* transcripts are moderately increased in the BM after castration (15), it remains unclear what is/are the physiological source(s) of this cytokine within the BM microenvironment. Moreover, while IL-7 contributes to the maintenance of CLPs, LSKs do not express IL-7 receptor (44) and there is no evidence that IL-7 directly regulates their homeostasis. Thus, how androgen blockade drives the response of LSK and CLPs in the absence of IL-7 remains an open question. Previous results showed that castration promotes changes in the BM stromal niche (15). One possibility is that androgen blockade induces compensatory microenvironmental signals that act on HSCs and CLPs. Albeit the nature of these alternative stimulatory signals remains to be identified, our findings suggest that this compensatory mechanism ceases in aged *Il7*$^{-/-}$ mice. It is possible that IL-7 might directly influence the function of BM stromal cells. This scenario is in our view unlikely, as IL-7 receptor has been primarily found in hematopoietic cells and there is no experimental evidence that stromal cells respond to IL-7 (18). Alternatively, the severe and continual B lymphopenia provoked by the absence of IL-7 might alter the regular lympho-stromal interactions in aged *Il7*$^{-/-}$ mice, indirectly deteriorating the functional capacity of the BM stromal niches to produce the stimulatory signal(s), which in turn drive the engagement of hematopoietic progenitors after castration. Further in-depth studies are required to comprehend the molecular cues that promote androgen blockade-mediated response of LSK/CLPs in the BM.

Taken together, our results indicate that the mobilization of BM precursors acts

as a prime catalyst of castration-driven thymopoiesis, providing a functional link between the response in the BM and thymus. These findings are also of clinical relevance as paediatric patients with defective IL-7-mediated signalling lack T lymphocytes but have a normal number of B lymphocytes. These patients are diagnosed during infancy and undergo corrective HSCT, which takes place following the identification of MHC-compatible BM donors (45). As such, our findings show the potential usage of androgen blockade as a readily therapeutic approach to boost thymic function in male paediatric patients with congenital immunodeficiencies, not only post but also pre-HSCT.

Methods

Mice. *Il7*$^{-/-}$, *Rag2*$^{-/-}$, CCRL1 and IL-7 reporter mice [B6.Cg-Tg (Il7-EYFP)5Pas] have been described previously (16, 19, 25, 26) and are all maintained on a C57Bl/6 background. IL7 floxed mice (*Il7*$^{fl/fl}$) were developed by a gene-targeting strategy that utilized the Flp-*FRT* and Cre-*loxP* recombinase systems. Briefly, embryonic stem (ES) cell clones containing a targeted Il7 allele (Il7$^{tm1a(EUCOMM)Wtsi}$) were obtained from the European Conditional Mouse Mutagenesis Program (EUCOMM)/International Knockout Mouse Consortium (IKMC). In the targeted allele, the loxP-flanked neomycin phosphotransferase (NeoR) gene was inserted upstream the exon 3 and a third loxP site was also placed downstream the exon 4. ES cell clones were injected into C57Bl/6 blastocysts to generate mice bearing the EUCOMM IL7 allele. The *Neo*R cassette was deleted *in vivo* by Flp-mediated excision using Act-*flippase* (FLP) mice to create Il7 floxed mice, which were then crossed with Foxn1-Cre mice (27). Mice were housed under specific pathogen-free conditions and studies were conducted in accordance with the European guidelines for animal experimentation.

Surgical castration. Mice were anesthetized by inhalation of a gaseous mixture of 3% isofluorane and oxygen, using an anaesthetic machine and maintained via a nose cone. Mice were pre-treated with an intraperitoneal injection of the analgesic buprenorphine at a dose of 0.05 mg/kg of body weight. A small incision was made in the scrotum to expose the testis, which were subsequently clamped and removed. The wound was closed with absorbable sutures. For surgical control, mice were

subjected to the entire surgical procedure, except removal of the testis (sham/control castration).

Isolation of hematopoietic cells and flow cytometry analysis. Single cell suspensions from thymus and spleen were obtained by mechanical disruption of the respective tissues. Bone marrow cell suspensions were prepared by flushing femurs with cold FACS buffer (PBS supplemented with 2% heat-inactivated FCS) with a 26-gauge needle. For the spleen and bone marrow, red blood cells were lysed using erythrocyte lysis solution (155 mM ammonium chloride; and 10 mM potassium bicarbonate). Three to ten million cells were stained in FACS buffer with a mixture of directly labelled specific antibodies: FITC-conjugated anti-Sca1 (D7) and anti-CD44 (IM7); PE-conjugated anti-CD4 (GK1.5), anti-CD62L (MEL-14), anti-CD19 (eBio-1D3), anti-CD127 (A7R34); PerCP-Cy5.5-conjugated anti-CD45.2 (104); PerCP-eFluor710 anti-CD4 (GK1.5); PE-Cy7-conjugated anti-CD25 (PC.61.5); APC/eFluor660-conjugated anti-CD8 (53-6.7); APC-eFluor780-conjugated anti-cKit (2B8); eFluor450-conjugated anti-CD24 (M1/69) (eBioscience). For thymic and bone marrow progenitor population analysis APC/eFluor660-conjugated antibodies against CD4 (GK1.5), CD8 (53-6.7), CD11b (M1/70), CD11c (N418), CD19 (eBio1D3), Gr1 (RB6-8CS), Ter119 (TER-119), CD3 (17A2), NK1.1 (PK136) and γδTCR (eBioGL3) (eBioscience) were used as lineage markers. Analysis was performed using FACS Canto II and a LSR Fortessa (BD Bioscience) and FlowJo software.

Isolation and flow cytometry analysis of TECs. TECs were isolated as described (28). Before staining, cells were pre-treated with FC block (anti-CD16/CD32 antibodies TruStain fcX; Biologend). Cell suspensions were stained with PE-conjugated anti-CD80 (16-10A1) and anti-Ly51 (6C3); PerCP-Cy5.5-conjugated anti-CD45.2 (104); APC/eFluor660-conjugated anti-CD80 (16-10A1) and anti-EpCAM (G8.8); APC-eFluor780-conjugated anti-I-A/I-E (M5/114-15-2); eFluor450-conjugated anti-EpCAM (G8.8) (eBioscience). The binding of biotinylated anti-Ly51 (6C3) was revealed by PE-Cy7-conjugated streptavidin (eBioscience). For intracellular staining, cells were prepared according to the supplier's protocol (Foxp3 staining kit, eBioscience) and stained with APC/eFluor660-conjugated anti-Aire (5H12) antibodies (eBioscience). Analysis was performed using FACS Canto II and a LSR Fortessa (BD Bioscience) and FlowJo software.

Statistical Analysis. Statistical analysis of the results was performed using the GraphPad Prism Software. The two-tailed Mann-Whitney test was used for analysis between groups. For multiple comparisons, a two-way ANOVA was used. A 95% confidence interval was applied in the calculations and samples with p values under 0.05 were considered significant (marked with *). For correlations, the spearman nonparametric correlation test was used.

Acknowledgements

We thank Dr. Thomas Boehm (Max Planck Institute of Immunology and Epigenetics) for Foxn1-Cre and CCRL1-GFP mice, Dr. Francina Langa Vives (Institut Pasteur) for technical assistance in the generation of *Il7*$^{fl/fl}$ mice, and Dr. S. Lamas and the caretakers from the animal facility for technical assistance. We thank Dr. Rui Appelberg (I3S) for critical reading of the manuscript.

Footnotes

This study was supported by the European Research Council (ERC) under the European Union's Horizon 2020 research and innovation program (grant agreement No 637843-TEC_Pro) starting grant attributed to N.L.A., by FEDER (Fundo Europeu de Desenvolvimento Regional) funds through the Operational Competitiveness Programme–COMPETE, and by National Funds through Fundação para a Ciência e Tecnologia (FCT) under the project FCOMP-01-0124-FEDER-021075 (PTDC/SAU-IMU/117057/2010), by NORTE-01-0145- FEDER-000012–Structured program on bioengineered therapies for infectious diseases and tissue regeneration, supported by Norte Portugal Regional Operational Programme (NORTE 2020), under the PORTUGAL 2020 Partnership Agreement, through the European Regional Development Fund (FEDER); by FEDER funds through the COMPETE 2020–Operational Programme for Competitiveness and Internationalisation (POCI), Portugal 2020, and by Portuguese funds through FCT/Ministério da Ciência, Tecnologia e Inovação in the framework of the project Institute for Research and Innovation in Health Sciences (POCI-01-0145- FEDER-007274). This study was also supported by the European Research Council (ERC) under the European

Union's Horizon 2020 research and innovation program (grant agreement No 695467-ILC_REACTIVITY) advanced grant attributed to J.P.D.. N.L.A., P.M.R., A.R.R., and C.M. received funding from the Investigator Program and doctoral fellowships from FCT. J.P.D. and N.S. received funding from the Institut Pasteur and Inserm.

References

1. Holländer, G. A., W. Krenger, and B. R. Blazar. 2010. Emerging strategies to boost thymic function. *Curr. Opin. Pharmacol.* 10: 443–453.

2. Takahama, Y. 2006. Journey through the thymus: stromal guides for T-cell development and selection. *Nat. Rev. Immunol.* 6: 127–135.

3. Gray, D. H. D., N. Seach, T. Ueno, M. K. Milton, A. Liston, A. M. Lew, C. C. Goodnow, and R. L. Boyd. 2006. Developmental kinetics, turnover, and stimulatory capacity of thymic epithelial cells. *Blood* 108: 3777–3785.

4. Dudakov, J. A., D. M. P. Khong, R. L. Boyd, and A. P. Chidgey. 2010. Feeding the fire: the role of defective bone marrow function in exacerbating thymic involution. *Trends Immunol.* 31: 191–198.

5. Goldberg, G. L., J. S. Sutherland, M. V. Hammet, M. K. Milton, T. S. P. Heng, A. P. Chidgey, and R. L. Boyd. 2005. Sex Steroid Ablation Enhances Lymphoid Recovery Following Autologous Hematopoietic Stem Cell Transplantation. *Transplantation* 80: 1604–1613.

6. Heng, T. S. P., G. L. Goldberg, D. H. D. Gray, J. S. Sutherland, A. P. Chidgey, and R. L. Boyd. 2005. Effects of Castration on Thymocyte Development in Two Different Models of Thymic Involution. *J. Immunol.* 5: 2982–2993.

7. Sutherland, J. S., G. L. Goldberg, M. V Hammett, A. P. Uldrich, S. P. Berzins, T. S. Heng, B. R. Blazar, J. L. Millar, M. A. Malin, A. P. Chidgey, and R. L. Boyd. 2005. Activation of Thymic Regeneration in Mice and Humans following Androgen Blockade. *J. Immunol.* 4: 2741–2753.

8. Kelly, R. M., S. L. Highfill, A. Panoskaltsis-Mortari, P. A. Taylor, R. L. Boyd, G. A. Holländer, and B. R. Blazar. 2008. Keratinocyte growth factor and androgen blockade work in concert to protect against conditioning regimen-induced thymic epithelial damage and enhance T-cell reconstitution after murine bone marrow transplantation. *Blood* 111: 5734–5744.

9. Goldberg, G. L., J. A. Dudakov, J. J. Reiseger, N. Seach, T. Ueno, K. Vlahos, M. V Hammett, L. F. Young, T. S. P. Heng, R. L. Boyd, and A. P. Chidgey. 2010. Sex steroid ablation enhances immune reconstitution following cytotoxic antineoplastic therapy in young mice. *J. Immunol.* 184: 6014–6024.

10. Velardi, E., J. J. Tsai, A. M. Holland, T. Wertheimer, V. W. C. Yu, J. L. Zakrzewski, A. Z. Tuckett, N. V. Singer, M. L. West, O. M. Smith, L. F. Young, F. M. Kreines, E. R. Levy, R. L.

Boyd, D. T. Scadden, J. A. Dudakov, and M. R. M. van den Brink. 2014. Sex steroid blockade enhances thymopoiesis by modulating Notch signaling. *J. Exp. Med.* 211: 2341–2349.

11. Williams, K. M., P. J. Lucas, C. V Bare, J. Wang, Y.-W. Chu, E. Tayler, V. Kapoor, and R. E. Gress. 2008. CCL25 increases thymopoiesis after androgen withdrawal. *Blood* 112: 3255–3263.

12. Dudakov, J. A., G. L. Goldberg, J. J. Reiseger, A. P. Chidgey, and R. L. Boyd. 2009. Withdrawal of sex steroids reverses age- and chemotherapy-related defects in bone marrow lymphopoiesis. *J. Immunol.* 182: 6247–6260.

13. Goldberg, G. L., O. Alpdogan, S. J. Muriglan, M. V Hammett, M. K. Milton, J. M. Eng, V. M. Hubbard, A. Kochman, L. M. Willis, A. S. Greenberg, K. H. Tjoe, J. S. Sutherland, A. Chidgey, M. R. M. van den Brink, and R. L. Boyd. 2007. Enhanced immune reconstitution by sex steroid ablation following allogeneic hemopoietic stem cell transplantation. *J. Immunol.* 178: 7473–7484.

14. Dudakov, J. A., G. L. Goldberg, J. J. Reiseger, K. Vlahos, A. P. Chidgey, and R. L. Boyd. 2009. Sex steroid ablation enhances hematopoietic recovery following cytotoxic antineoplastic therapy in aged mice. *J. Immunol.* 183: 7084–7094.

15. Khong, D. M., J. A. Dudakov, M. V. Hammett, M. I. Jurblum, S. M. L. Khong, G. L. Goldberg, T. Ueno, L. Spyroglou, L. F. Young, M. R. M. Van Den Brink, R. L. Boyd, and A. P. Chidgey. 2015. Enhanced hematopoietic stem cell function mediates immune regeneration following sex steroid blockade. *Stem Cell Reports* 4: 445–458.

16. von Freeden-Jeffry, U., P. Vieira, L. A. Lucian, T. McNeil, S. E. G. Burdach, and R. Murray. 1995. Lymphopenia in interleukin (IL)-7 gene-deleted mice identifies IL-7 as a nonredundant cytokine. *J. Exp. Med.* 181: 1519–1526.

17. Poliani, P. L., F. Facchetti, M. Ravanini, A. R. Gennery, A. Villa, C. M. Roifman, and L. D. Notarangelo. 2009. Early defects in human T-cell development severely affect distribution and maturation of thymic stromal cells: Possible implications for the pathophysiology of Omenn syndrome. *Blood* 114: 105–108.

18. Iwanami, N., F. Mateos, I. Hess, N. Riffel, C. Soza-Ried, M. Schorpp, and T. Boehm. 2011. Genetic evidence for an evolutionarily conserved role of IL-7 signaling in T cell development of zebrafish. *J. Immunol.* 186: 7060–7066.

19. Alves, N. L., O. Richard-Le Goff, N. D. Huntington, A. P. Sousa, V. S. G. Ribeiro, A. Bordack, F. L. Vives, L. Peduto, A. Chidgey, A. Cumano, R. Boyd, G. Eberl, and J. P. Di Santo. 2009. Characterization of the thymic IL-7 niche in vivo. *Proc. Natl. Acad. Sci. U. S. A.* 106: 1512–1517.

20. Shitara, S., T. Hara, B. Liang, K. Wagatsuma, S. Zuklys, G. a Holländer, H. Nakase, T. Chiba, S. Tani-ichi, and K. Ikuta. 2013. IL-7 produced by thymic epithelial cells plays a major role in the development of thymocytes and TCRγδ+ intraepithelial lymphocytes. *J. Immunol.* 190: 6173–6179.

21. Ye, S. K., Y. Agata, H. C. Lee, H. Kurooka, T. Kitamura, A. Shimizu, T. Honjo, and K. Ikuta. 2001. The IL-7 receptor controls the accessibility of the TCRγ locus by Stat5 and

histone acetylation. *Immunity* 15: 813–823.

22. Park, J.-H., S. Adoro, T. Guinter, B. Erman, A. S. Alag, M. Catalfamo, M. Y. Kimura, Y. Cui, P. J. Lucas, R. E. Gress, M. Kubo, L. Hennighausen, L. Feigenbaum, and A. Singer. 2010. Signaling by intrathymic cytokines, not T cell antigen receptors, specifies CD8 lineage choice and promotes the differentiation of cytotoxic-lineage T cells. *Nat. Immunol.* 11: 257–264.

23. Fry, T. J., and C. L. Mackall. 2005. The Many Faces of IL-7: From Lymphopoiesis to Peripheral T Cell Maintenance. *J. Immunol.* 174: 6571–6576.

24. Dias, S., H. Silva, A. Cumano, and P. Vieira. 2005. Interleukin-7 is necessary to maintain the B cell potential in common lymphoid progenitors. *J. Exp. Med.* 201: 971–979.

25. Shinkai, Y., G. Rathbun, K.-P. Lam, E. M. Oltz, V. Stewart, M. Mendelsohn, J. Charron, M. Datta, F. Young, A. M. Stall, and F. W. Alt. 1992. RAG-2-deficient mice lack mature lymphocytes owing to inability to initiate V(D)J rearrangement. *Cell* 68: 855–867.

26. Rode, I., and T. Boehm. 2012. Regenerative capacity of adult cortical thymic epithelial cells. *Proc. Natl. Acad. Sci. U. S. A.* 109: 3463–3468.

27. Soza-Ried, C., C. C. Bleul, M. Schorpp, and T. Boehm. 2008. Maintenance of Thymic Epithelial Phenotype Requires Extrinsic Signals in Mouse and Zebrafish. *J. Immunol.* 5272–5277.

28. Ribeiro, A. R., P. M. Rodrigues, C. Meireles, J. P. Di Santo, and N. L. Alves. 2013. Thymocyte selection regulates the homeostasis of IL-7-expressing thymic cortical epithelial cells in vivo. *J. Immunol.* 191: 1200–1209.

29. Griffith, A. V, M. Fallahi, T. Venables, and H. T. Petrie. 2012. Persistent degenerative changes in thymic organ function revealed by an inducible model of organ regrowth. *Aging Cell* 11: 169–177.

30. Lai, K.-P., J.-J. Lai, P. Chang, S. Altuwaijri, J.-W. Hsu, K.-H. Chuang, C.-R. Shyr, S. Yeh, and C. Chang. 2013. Targeting Thymic Epithelia AR Enhances T-Cell Reconstitution and Bone Marrow Transplant Grafting Efficacy. *Mol. Endocrinol.* 27: 25–37.

31. Alves, N. L., N. D. Huntington, J.-J. Mention, O. Richard-Le Goff, and J. P. Di Santo. 2010. Cutting Edge: a thymocyte-thymic epithelial cell cross-talk dynamically regulates intrathymic IL-7 expression in vivo. *J. Immunol.* 184: 5949–5953.

32. Anderson, G., and Y. Takahama. 2012. Thymic epithelial cells: working class heroes for T cell development and repertoire selection. *Trends Immunol.* 33: 256–263.

33. Schluns, K. S., W. C. Kieper, S. C. Jameson, and L. Lefrançois. 2000. Interleukin-7 mediates the homeostasis of naïve and memory CD8 T cells in vivo. *Nat. Immunol.* 1: 426–432.

34. Chidgey, A., J. Dudakov, N. Seach, and R. Boyd. 2007. Impact of niche aging on thymic regeneration and immune reconstitution. *Semin. Immunol.* 19: 331–340.

35. Carvalho, T. L., T. Mota-Santos, A. Cumano, J. Demengeot, and P. Vieira. 2001. Arrested B Lymphopoiesis and Persistence of Activated B Cells in Adult Interleukin 7 $^{-/-}$ Mice. *J. Exp. Med.* 194: 1141–1150.

36. Heng, T. S. P., A. P. Chidgey, and R. L. Boyd. 2010. Getting back at nature: understanding thymic development and overcoming its atrophy. *Curr. Opin. Pharmacol.* 10: 425–433.

37. Prelog, M. 2006. Aging of the immune system: a risk factor for autoimmunity? *Autoimmun. Rev.* 5: 136–139.

38. Dumont-Lagacé, M., C. St-Pierre, and C. Perreault. 2015. Sex hormones have pervasive effects on thymic epithelial cells. *Sci. Rep.* 5: 12895.

39. Hara, T., S. Shitara, K. Imai, H. Miyachi, S. Kitano, H. Yao, S. Tani-ichi, and K. Ikuta. 2012. Identification of IL-7-producing cells in primary and secondary lymphoid organs using IL-7-GFP knock-in mice. *J. Immunol.* 189: 1577–1584.

40. Ryan, M. R., R. Shepherd, J. K. Leavey, Y. Gao, F. Grassi, F. J. Schnell, W.-P. Qian, G. J. Kersh, M. N. Weitzmann, and R. Pacifici. 2005. An IL-7-dependent rebound in thymic T cell output contributes to the bone loss induced by estrogen deficiency. *Proc. Natl. Acad. Sci. U. S. A.* 102: 16735–16740.

41. Almeida, A. R. M., J. A. M. Borghans, and A. A. Freitas. 2001. T cell homeostasis: thymus regeneration and peripheral T cell restoration in mice with a reduced fraction of competent precursors. *J. Exp. Med.* 194: 591–599.

42. Prockop, S. E., and H. T. Petrie. 2004. Regulation of Thymus Size by Competition for Stromal Niches among Early T Cell Progenitors. *J. Immunol.* 173: 1604–1611.

43. Cordeiro Gomes, A., T. Hara, V. Y. Lim, D. Herndler-Brandstetter, E. Nevius, T. Sugiyama, S. Tani-ichi, S. Schlenner, E. Richie, H. R. Rodewald, R. A. Flavell, T. Nagasawa, K. Ikuta, and J. P. Pereira. 2016. Hematopoietic Stem Cell Niches Produce Lineage-Instructive Signals to Control Multipotent Progenitor Differentiation. *Immunity* 45: 1219–1231.

44. Mazzucchelli, R., and S. K. Durum. 2007. Interleukin-7 receptor expression: intelligent design. *Nat. Rev. Immunol.* 7: 144–154.

45. Puel, A., and W. J. Leonard. 2000. Mutations in the gene for the IL-7 receptor result in T-B+NK+ severe combined immunodeficiency disease. *Curr. Opin. Immunol.* 12: 468–473.

Supplementary Information

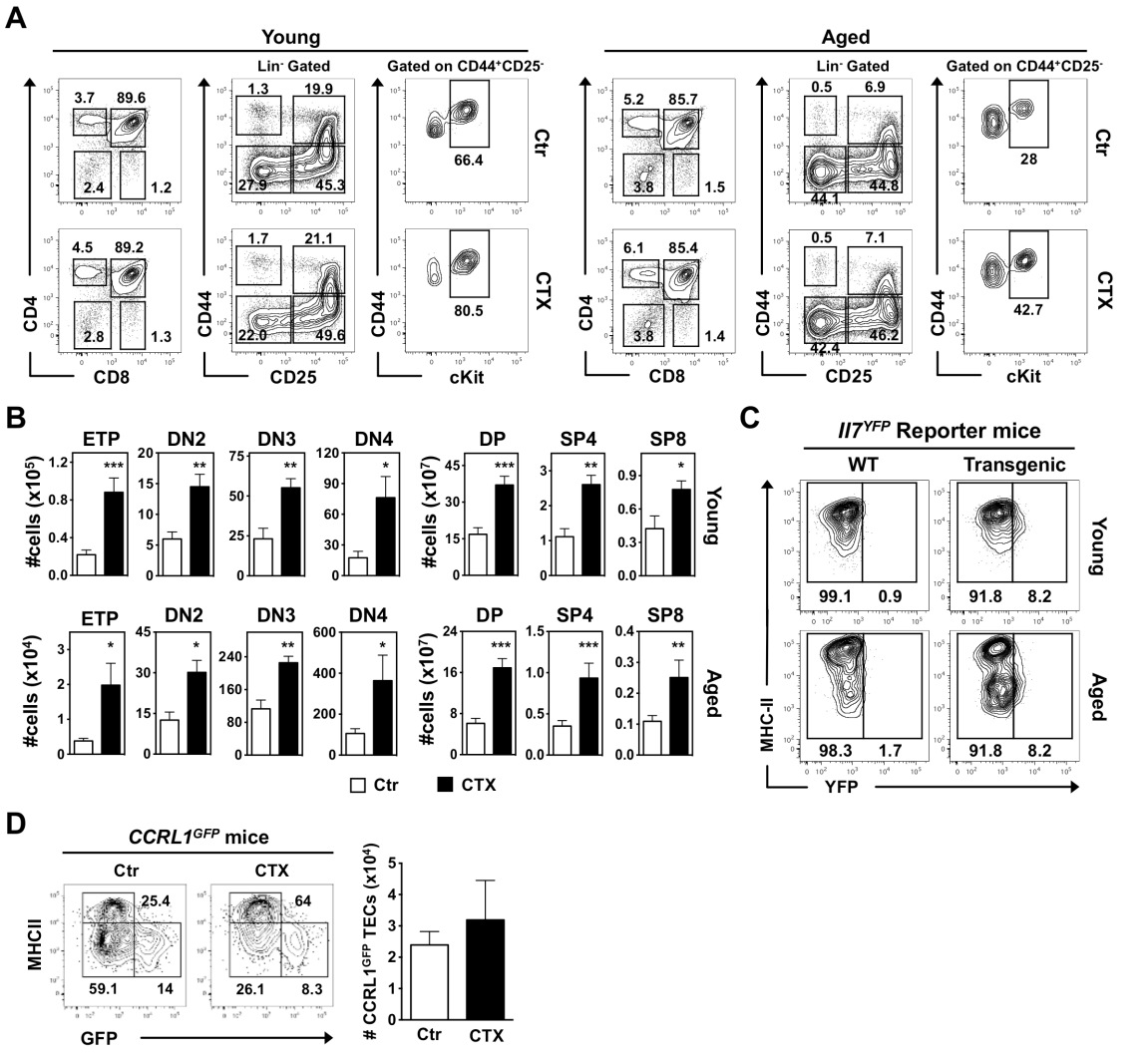

Figure S1 – Effects of castration in T cell development of both young and aged mice (A) Young (4 weeks-old) and aged (older than 8 month) mice were castrated and the T-cell developmental program was analysed 2 weeks post-surgery. Castrated (CTX) and control Sham-treated (Ctr) mice were analysed at the indicated time points: (left graphs) CD4/CD8 expression on total thymocytes; (middle graphs) CD44/CD25 expression on DN thymocytes (gated on Lin^- cells); (right graphs) cKit/CD44 expression on DN1 thymocytes. ETPs are defined as Lin^- $cKit^+CD44^+CD25^-$; Numbers indicate the frequencies of the different thymocyte subsets. **(B)** Absolute number of the different thymocyte subsets depicted in **(A)**. **(C)** Flow cytometric analysis compares the expression of YFP on total TECs (defined as $EpCAM^+CD45^-$) of young/aged wild-type (WT) and transgenic IL-7 reporter mice. Numbers indicate the percentage of gated cells. **(D)** Flow cytometry analysis of the TEC microenvironment in young CCRL1-GFP mice 2 weeks after castration. Graphs show the expression of GFP and MHCII on total TECs (defined as $EpCAM^+CD45^-$). Numbers indicate the percentage of gated cells. Results are presented as mean ± SEM. * $P < 0.05$; ** $P < 0.01$; *** $P < 0.001$.

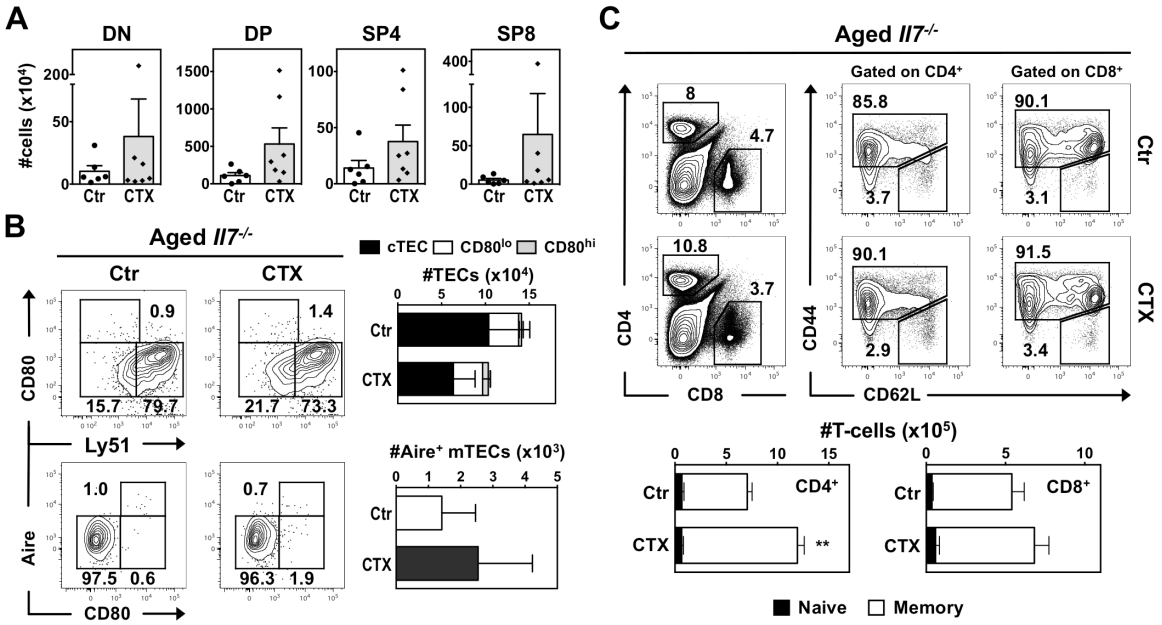

Figure S2 - Intrathymic and peripheral manifestations of improved thymopoiesis are abrogated in aged IL-7KO mice after castration. Aged (more than 6 month-old) *Il7*$^{-/-}$ mice were castrated and the T-cell developmental program was analysed 2 weeks post-surgery. Castrated (CTX) and control Sham-treated (Ctr) mice were analysed at the indicated time point. **(A)** Absolute number of the different thymocyte subsets. **(B)** The composition of the TEC microenvironment was analysed by flow cytometry: (Top) Ly51/CD80 expression; (Bottom) CD80/Aire expression on total TECs (defined as EpCAM^{+}CD45^{-}). Numbers indicate the percentage of gated cells. On the right, graphs represent the overall cellularity of the different TEC subsets. **(C)** Flow cytometric analysis of the splenic T cell compartment. (Left panel) Representative CD4/CD8 staining in total spleenocytes; (Middle/right panels). Dot plots depict the CD62L/CD44 staining on gated CD4^{+} and CD8^{+} splenic T cells. Numbers indicate the frequencies of the different subsets. On the bottom, graphs show the absolute number of naive (CD62L^{+}CD44^{-}) and memory (CD62L^{-}CD44^{+}) splenic T cells in control and castrated *Il7*$^{-/-}$ mice. Results are presented as mean ± SEM. ** $P < 0.01$

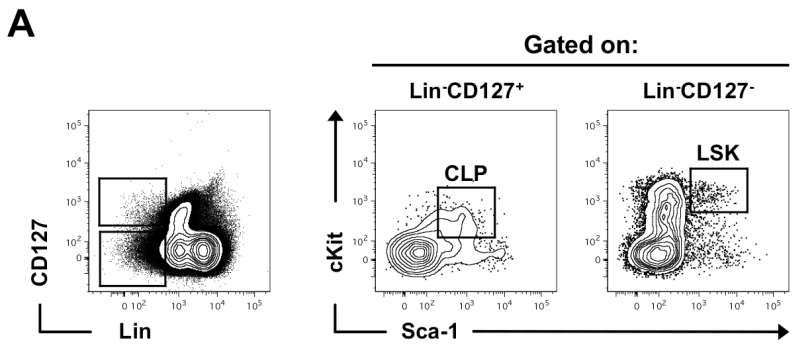

Figure S3 – (A) Flow cytometry analysis and gating strategy used to identify common lymphoid progenitors ($Lin^{-}CD127^{+}$) and LSK cells ($Lin^{-}CD127^{-}$).

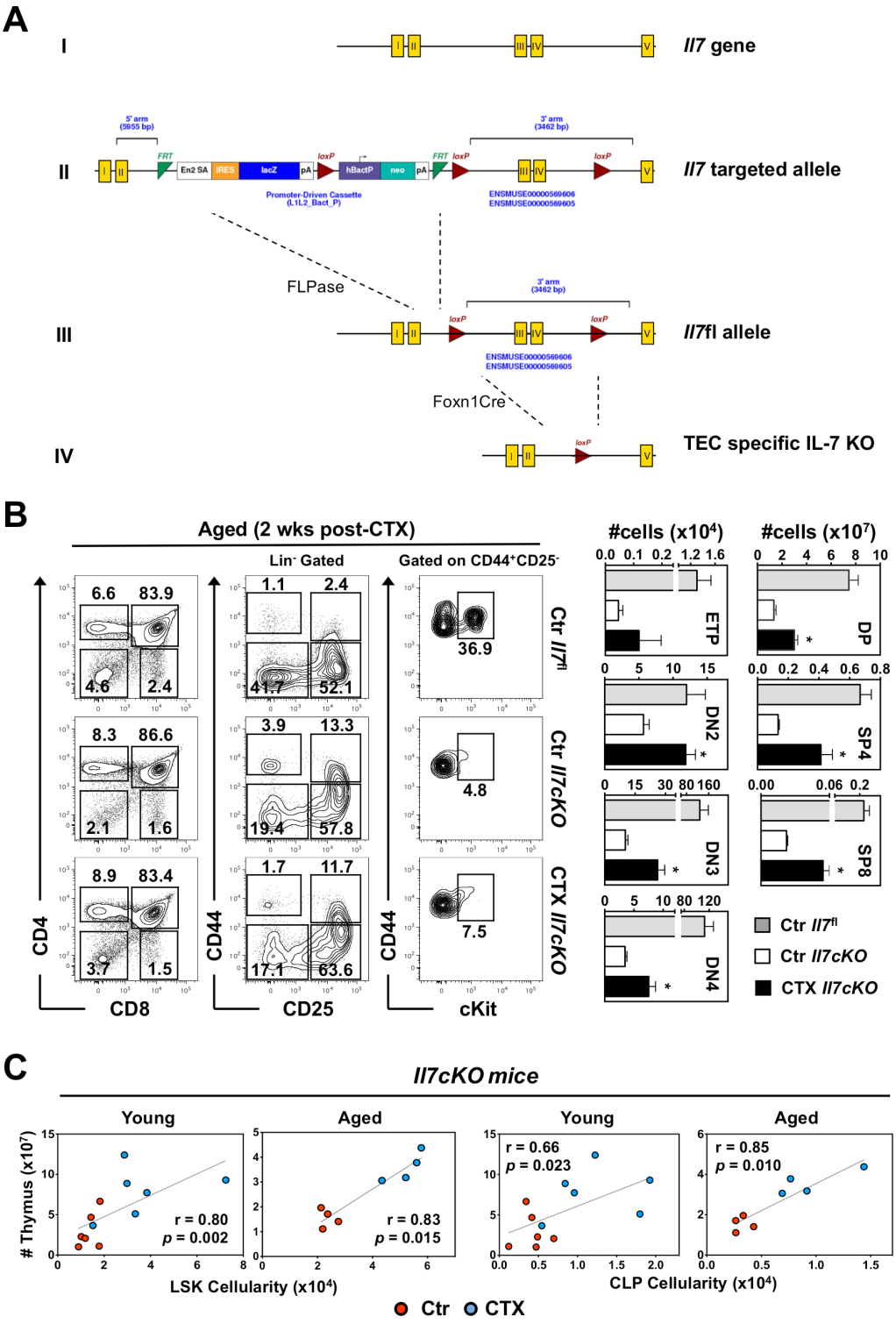

Figure S4 – Generation of IL-7 conditional knockout mice. (A) *I* - Schematic representation of the *Il7* gene. Yellow boxes indicate exons. Targeting strategy for the IL-7-floxed allele. *II* - *Il7* targeted allele with the neomycin cassette (neo, light green rectangle), FRT (green triangles) and loxP (maroon triangles) sequences. The neomycin cassette has been removed by crossing mice bearing the *Il7* targeted allele ($Il7^{tm1a(EUCOMM)Wtsi}$) with FLPase mice to generate (*III*) *Il7*floxed mice (*Il7*fl). *IV* - IL-7 conditional knockout mice in TECs was generated by crossing *Il7*floxed mice with Foxn1Cre animals. **(B)** Aged control IL7-floxed (*Il7*fl/fl) and IL7-conditional KO (*Il7*cKO) mice were castrated and analyzed 2 weeks after surgery. Castrated (CTX) and control Sham-treated (Ctr) mice were analysed at the indicated time points. Analysis of T cell development: (left) CD4/CD8 expression on total thymocytes; (middle) CD44/CD25 expression on DN thymocytes (gated on Lin^- cells); (right) cKit/CD44 expression on DN1 thymocytes. ETPs are defined as Lin^- $cKit^+CD44^+CD25^-$; Numbers indicate the frequencies of the different thymocyte subsets. On the right, graphs represent the number of the different thymocyte subsets. **(C)** Spearman correlation between the thymic cellularity and the absolute number of LSK and CLPs in the bone marrow of control (Ctr) and castrated (CTX) young/aged Il7cKO mice. Results are presented as mean ± SEM. * P < 0.05;

Chapter IV

General Discussion and Future Perspectives

Within the thymus, specialized subtypes of thymic epithelial cells provide unique microenvironments that support the development and selection of functionally diverse and self-tolerant T lymphocytes (1). The establishment of the cortical and medullary epithelial niches is a highly dynamic process that is initiated during the fetal period and maintained throughout life by the continuous replenishment of mature TECs (2). Yet, the number of differentiated TECs begins to slowly decay during adulthood as consequence of aged-related thymic involution (3). Furthermore, TECs also undergo age-independent punctual aggressions as result of cellular stress or stromal damage caused by infections, hormonal alterations, or cytoablative regimens such as chemotherapy or irradiation (4). Whereas these abovementioned changes might qualitatively differ from the ones occurring as a consequence of aging, the perturbations on the thymic microenvironment in both circumstances potentially reduce the production of newly generated T cells and/or contribute to the escape of autoreactive T cells during negative selection. Thus, understanding the molecular mechanisms harnessing the homeostasis of TECs has come to the foreground of the research field in the past few years. This knowledge will have important implications in comprehending how the current thymic rejuvenatory strategies operate (e.g.: sex steroid ablation) as well as in aiding the development of new approaches to re-establish thymic function in the context of acquired and/or congenital immunodeficiencies and autoimmune syndromes. In my thesis, we provide information concerning the maintenance (**Chapter II**) and regeneration (**Chapter III**) of TECs that helps to improve our current knowledge on how thymic function is regulated under different physiological conditions.

Adding another piece to the puzzle: uncovering a novel regulator of the mTEC "engine"

The transcription factor p53, initially described in 1979 (5–7), is classified as one of the key sentinels of the genome integrity due to its ability to prevent oncogenic transformation in cells with DNA damage or other cellular insults (8). Yet, beyond its undisputable importance as a tumour suppressor, an increasing number of recent studies have highlighted alternative roles for p53 as a regulator of metabolism, immunity, and among other aspects of cellular differentiation and development (9–

11). Our interest in p53 stemmed from previous studies conducted in our laboratory, aimed at understanding the mechanisms that control the dynamic of IL-7-expressing TECs under circumstances of stress-induced thymic atrophy. Taking advantage of an IL-7 reporter mice, in which yellow fluorescent protein (YFP) identifies a subtype of cTECs that expresses high levels of IL-7 (12, 13), we found that thymic damage induced by γ-irradiation, but not by glucocorticoids, led to the re-emergence of IL-7^{YFP} TECs in adult mice (unpublished data). As γ-irradiation is a bona-fide DNA damage-inducing stimulus that engages the p53-mediated pathway (14), we decided to investigate whether this transcription factor could potentially be involved in the reestablishment of the IL-7-expressing cortical epithelium following injury. This premise led to the generation of a mouse model with a conditional deletion of p53 in TECs (p53cKO mice). While the re-induction of IL-7^{YFP} TECs was p53-independent (unpublished data), a closer analysis of cTEC/mTEC composition of p53cKO mice paved the way for the findings described in **Chapter II** of this thesis, herein we identified p53 as a novel regulator of mTEC homeostasis.

The role of p53 in the thymus has been widely studied in the context of T cell development, where this transcription factor plays a crucial role in controlling thymocyte transition from the DN into DP stage and preventing malignant transformation (15–17). On the other hand, whereas p53 mutations have been reported in thymic epithelial tumours (18, 19), little is known about its potential role in the thymic stroma, particularly in the control of TEC physiology. The generation of p53cKO mice allowed us to demonstrate that p53 is fundamental to preserve thymic function and immune tolerance during life, through the regulation of the integrity of the mTEC niche. Interestingly, consistent with the specific impact of p53 inactivation on the medullary compartment, our analysis revealed that mTECs express higher levels of *Trp53* transcripts than cTECs. These observations raised the question on whether the differential induction of p53 in TECs might be linked with distinct levels of cellular stress that both epithelial subtypes have to cope with. The outcome of p53-mediated responses depends on many variables, which includes the nature of the stress signal and the microenvironment in which the cell lives in (20). For instance, sustained levels of stress result in a robust induction of p53, leading to the activation of apoptotic cell death pathways and elimination of the irreparable damaged cells. Contrariwise, under non-stressed conditions, healthy cells can

transiently induce low levels of p53 activity, which elicits protective responses that support cell survival and development. Our results suggest that p53 induction on mTECs seems to occur via RANK- and CD40-activation of the NF-kB signalling pathway. Yet, we cannot exclude the potential influence of other mediators and/or stress signals in governing p53 levels in TECs. Previous reports demonstrated that the transcriptional regulation of Aire-dependent TRAs involves the induction of DNA double-stranded breaks through the coordinated action of topoisomerases-1 and -2 (21, 22). Furthermore, while the detection of the Aire protein has been confined to a fraction of mature mTECs, a recent study suggested that Aire expression is an inherent property of the majority of mTECs across their differentiation program (23). Hence, though p53 was not previously identified as a putative Aire-associated protein (21, 24), one can postulate that cellular stress resultant from Aire-mediated DNA double-stranded breaks during TRA expression might also indirectly account for p53 induction in mTECs. In the future, it would be interesting to study whether and/or to what degree Aire might influence p53 activity on mTECs, by analysing p53cKO mice in an *Aire*$^{-/-}$ background.

p53 belongs to a family of transcription factors that includes two other related homologues, p63 and p73 (25–27). Regardless their remarkable sequence similarity and conservation of the functional domains, current information suggests that the members of the p53 family control a network of overlapping as well as divergent cellular processes (28). In relation to the thymic epithelium, while little is known about a possible role for p73, a number of studies have emphasized the importance of p63 in controlling the proliferative potential of TEC progenitors (29). Remarkably, our findings suggest a division of labour between p63 and p53 in the establishment of the thymic microenvironment. We demonstrated that TEC-intrinsic deficiency in p53 causes a specific reduction in the size of the mTEC niche, probably as result of an impaired expression and responsiveness of RANK in mTECs. Yet, our observations do not utterly exclude a possible participation of p53 in the maintenance of TEC progenitors, particularly at the level of lineage-restricted mTEC precursors. In this regard, we found that p53cKO mice exhibit a progressive disruption of the immature mTEC compartment later life. Although the reason behind the reduction in immature cells remains unclear, one can speculate that such alterations might occur as consequent perturbations in the survival and/or

differentiation of mTEC-committed progenitors. In recent years, several studies revealed the existence of a heterogeneous pool of mTEC progenitor cells with unique phenotypic characteristics (2). Noticeably, some of the aforementioned subpopulations of mTEC progenitors have been identified on the basis of their RANK expression. Nonetheless, apart of being used as a surrogate marker (30), RANK-mediated activation of the NFκB pathway in progenitor cells was also shown to be critical for their stepwise differentiation into mature Aire^{+} mTECs (31). As the results depicted on this thesis establish a novel functional association between p53 and RANK, future studies are necessary to investigate if the absence of p53 impacts the maintenance of RANK-expressing mTEC progenitors. Additionally, another interesting question that remains open concerns the effect of p53 on the expression of RANK across distinct stages of mTEC development. Previous studies revealed that RANK-derived signals elicit the upregulation of its own receptor on mTECs (31, 32). Using a FTOC system, we gathered evidence that supports the involvement of p53 in an auto-amplification mechanism that regulates RANK expression, as p53 inactivation on TECs impaired RANK upregulation following *in vitro* stimulation with agonist anti-RANK antibody. Nevertheless, given that our experiments were performed on the bulk population of TECs, one cannot exclude that p53 might also contribute to sustain the basal expression of RANK in mTECs. Therefore, detailed co-expression analysis of RANK and p53 within distinct medullary subpopulations would be of valuable information to better comprehend the potential existence of a stage-specific action of p53 during mTEC differentiation (**Figure 1A**).

Consistent with observations that p53 governs wide transcriptional programs in different cell types (33–35), our genome wide study revealed that a broad set of genes linked to core biological processes, such as *Foxn1, CD86, Il15 and Irf7* (among many others), were compromised in p53cKO mTECs. Therefore, the function of p53 in mTEC homeostasis appears to extend beyond influencing RANK expression. Gene ontology (GO) analysis predicted the dysregulation of diverse pathways in p53-deficient mTECs that differ from the well-known mechanisms that control their maintenance. As knowledge about the molecular determinants of mTEC homeostasis is still limited, we speculate that the genome wide data produced in this thesis may provide an interesting framework to further identify new putative regulators of the medullary epithelial niche. In the last years, several different

studies uncovered how post-translational modifications differentially affect the transcriptional function of p53. In particular, the tight balance among acetylation, methylation and phosphorylation is crucial to control the cellular outcome of p53 activity, as it may have discriminatory impacts on some target genes comparatively to others (20, 36). For instance, on the one hand, acetylation of the lysine 317 residue in the linker region of the p53 protein was shown to decrease its ability to activate proapoptotic target genes following DNA damage without, however, influencing *p21* transcription and cell-cycle arrest (37). On the other hand, recent data also revealed that acetylation of the lysine 320 of p53 is crucial for neurite outgrowth and axonal regeneration in mice by specifically governing the expression of two p53 transcriptional target, Coronin 1b and Rab13 (38). Interestingly, whereas acetylation functions as a dominant mechanism for activation, lysine methylation appears to restrains p53 transcriptional activity either by preventing p53 binding to coactivators or inhibiting other posttranslational modifications to take place on the same lysine residues (36). Our current research did not examine the status of the p53 protein on mTECs or the potential outcomes of post-translational p53 modifications on the transcriptome of TECs. Actually, such studies would be as challenging as interesting in light of our findings that p53 regulates the regenerative capacity of the thymic microenvironment upon ionizing radiation. One can imagine that γ-irradiation-derived stress on TECs prompts specific post-translational modifications on p53, which in turn, would shift the transcriptional network of these cells towards the activation of survival and regenerative pathways. In this regard, comparison of the transcriptional profile of p53-deficient mTECs among distinct physiological conditions would provide valuable information about hypothetical p53-mediated pathways involved in TEC recovery following radiation-induced damage. Uncovering the underlying mechanisms involved in TEC regeneration is one of the current goals of researchers in the thymus field, as it will provide new means to design strategies for therapeutical intervention in order to treat, repair or revert the deterioration of the immune system in different pathophysiological conditions.

Interestingly, during the bioinformatic analysis of the sequencing data, we further noticed that the majority of the functional categories disclosed by the GO enrichment analysis in p53cKO mTECs incorporated purported TRAs. Taking in consideration the unique capacity of mTECs to virtually express all the protein-coding genes of the

body (39), one can assume that the presence of TRA within these pathways occurs as result of the promiscuous gene expression program. However, it cannot be ruled out that some TRAs may possess a pertinent biological activity in mTECs. As an example is RANK, which plays a pivotal role in mTEC differentiation and has been recently classified as a TRA (40). Given that some TRAs are only expressed by a minor fraction of mTECs (1-3%) at a certain point (41, 42), one can envision that a putative TRA that is functional relevant in mTEC biology should be more broadly expressed across the entire medullary epithelium. Future studies are warranted to decipher the possible influence of genes classified as TRAs in the maintenance of the mTEC niche.

It is well documented the importance of RANK, CD40 and LTβR in fostering the maturation of the medullary epithelium (43). Nevertheless, emerging studies have been disclosing the novel role of numerous transcription factors in selectively regulating the maintenance and function of mTECs. Among these are members of the interferon regulatory factors (IRF) and signal transducer and activator of transcription (STAT) protein family (**Figure 1A**). The IRF group of proteins, which includes nine members in mammals, plays a critical function in the regulation of many aspects of innate and adaptive immune responses (44). Two recent reports described the participation of IRF4 and IRF7 in controlling distinct aspects of mTEC physiology (45, 46). Haljasorg *et al.* generated TEC-specific IRF4 knockout (IRF4cKO) mice and found that disruption of *Irf4* leads to an increase in the frequency of mature mTECs and alters the expression of important chemokine and costimulatory molecules in these cells (45). Regardless of these alterations, the size of the medullary niche remained unaffected in IRF4cKO mice. These data raise the possibility that IRF4 controls a new checkpoint of mTEC differentiation. Interestingly, akin to p53cKO mice (47), inactivation of IRF4 provokes a reduction in thymic regulatory T cell numbers and peripheral manifestations of autoimmunity (45). In another study, Otero *et al.* demonstrated that loss of IRF7 has a detrimental impact on the medullary niche, characterized by a severe reduction in the overall number of mTECs and diminished levels of *Aire* transcripts (46). A more in-depth analysis revealed that IRF7 controls the production of IFN-β, which in turn promotes mTEC development (46). Contrarily to the study using IRF4cKO mice, it remains undetermined the physiological consequences of TEC-specific IRF7 loss in terms of

T cell development and tolerance induction. Curiously, while we demonstrated that p53 is induced by RANK and CD40 stimulation (47), both reports suggest the involvement of RANK-derived signals in regulating the expression of IRF4 and IRF7 (45, 46). Yet, it remains to be further investigated whether these pathways can be activated by additional signals. Thus, p53-, IRF4- and IRF7-driven pathways seem to branch downstream of TNFRSF-induced activation of the NF-κB signalling pathway and coordinate multiple aspects of mTEC homeostasis (**Figure 1B).**

More recently, two complementary studies demonstrated that alternative signalling pathways also participate in the maintenance of the medullary microenvironments in the adult thymus. Satoh *et al.* and Lomada *et al.* have shown that conditional inactivation of *Stat3* in TECs prevents the expansion of thymic medullary areas during postnatal life (48, 49). Despite exhibiting a reduction in the mTEC compartment similar to that in p53cKO mice, the number of thymic regulatory T cells is unaltered in mice with STAT3-deficient TECs, indicating that STAT3 and p53 might control complementary programs in mTECs. STAT3 is activated by various cytokines and growth factors *in vivo*. Satoh *et al.* provide further evidence that STAT3 signalling in TECs might be induced by the epithelial growth factor receptor (EGFR), although the intrathymic physiological source of its ligand remains unclear (48). Cosway *et al.* have recently shown that targeted deletion of LTβR in TECs disturbs the architecture of mTECs without an overt effect on their functionality (50). Unlike the profound defects caused by the lack of RelB-signalling (51), conditional deficiency of LTβR does not affect thymic regulatory T cells and induces a milder phenotype reminiscent of STAT3 deficiency. These new studies highlight that the establishment, maintenance, and architecture of the thymus medulla are determined by the integration of multiple signals, although it remains unclear whether proper mTEC structure is required for its functionality. Further studies should aim to unravel the genetic program driven by the recently identified transcription factors in mTECs and their possible relationship in maintaining a functional mTEC compartment (**Figure 1B**).

Intriguingly, the specific role of these transcription factors in mTEC biology was demonstrated in experimental models in which their genes were targeted in both cTECs and mTECs. On the one hand, the enriched expression and/or activation of these proteins in mTECs might determine their specific influence. On the other

hand, we hypothesized that the unique transcriptional and epigenetic states of mTECs (52) can facilitate the access of these TF to their targets. According to this conjecture, a given transcription factor drafts behind the molecular machinery involved in regulating pGE expression and exploit the induced changes in the chromatin to initiate a specific genetic program in mTECs. Still, the action of the newly identified transcription factor in mTEC homeostasis seems to be distinct from the prototypical roles of NF-κB in mTEC maturation or Aire and Fezf2 in TRA expression. Instead, these novel pathways appear to operate as a key rheostat to sustain the regular activity of the thymus medulla under physiological conditions, preventing the emergence of autoimmunity. Ultimately, understanding the mechanisms controlling the limits of the medullary microenvironment might lead to a better comprehension of the rules balancing immunity and tolerance induction. (Part of this section is adapted from Rodrigues *et al*, Trends Immunol. 2017)

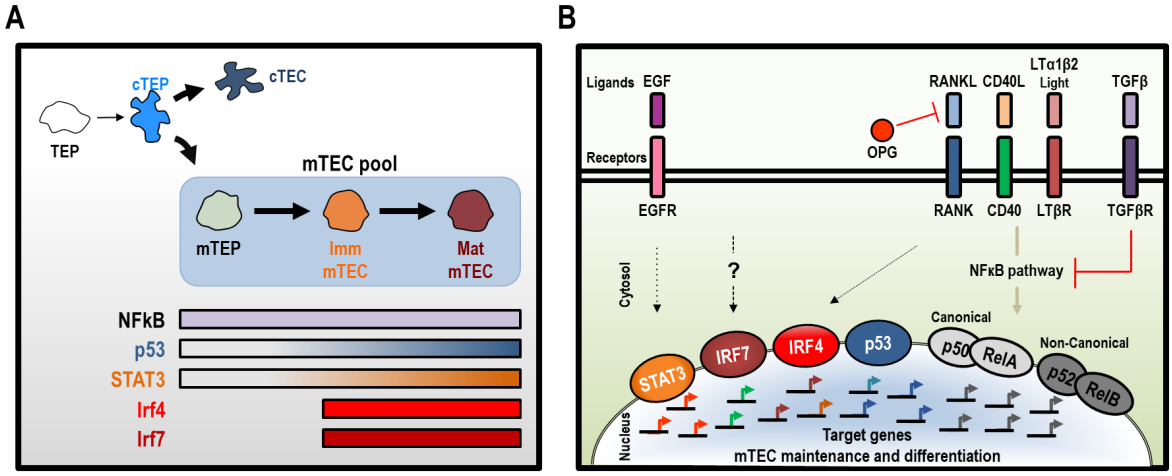

Figure 1 – Proposed model for the action of the recently identified regulators of mTEC homeostasis. (A) Thymic epithelial cell progenitors (TEPs) transverse through a "transitional TEC progenitor" stage that expresses phenotypic and molecular traits associated with cTECs precursors (cTEP) prior to the commitment into a cTEC or mTEC fate (78). The NFκB pathway regulates different stages of their differentiation, from mTEC progenitors (mTEPs) to immature (Imm) and mature (Mat) mTECs (79). While p53 (47) and STAT3 (48, 49) appear to control the maintenance of the broad mTEC compartment, IRF4 (45) and IRF7 (46) seem to regulate immature-mature mTEC transition. **(B)** Molecular interplay between the distinct signalling pathways and transcription factors governing the homeostasis and differentiation of mTECs. On the right side, it is represented the well-recognized role of members of the TNFRSF, RANK, CD40 and LTβR in mTECs, which upon interaction with their respective ligands, activate the canonical and non-canonical NFκB pathway. This pathway of mTEC differentiation is regulated at multiple levels. OPG acts as a decoy receptor for RANKL inhibiting RANK signalling (80). Additionally, signalling through TGFβR negatively regulates the NFκB pathway (81). On the left side, it is represented the role of p53-, IRF4-, IRF7- and STAT3-mediated signalling in coordinating mTEC differentiation and homeostasis. While p53 (47), IRF-4 (45) and IRF7 (46) appear to be activated downstream of TNFRSF signalling, STAT3 (48, 49) is suggested to be engaged by signalling through EGF receptor (EGFR). It remains unclear whether these pathways can be activated by other hitherto undefined signals (represented as "?"). Another uncertainty pertains to the overlapping or distinct nature of the gene expression program driven by the recently identified TFs in mTECs. Black lines with superscript coloured arrows represent purported target genes.

Bone marrow - The “missing link” that lies beneath the rejuvenation of the thymus upon androgen blockade

In the past two decades, sex steroid ablation (SSA) has been widely studied as an attractive therapeutic tool to either revert age-related thymic degeneration or to enhance immune recovery in bone marrow (BM) transplantation settings associated with cytoablative regimens (53). Nonetheless, despite its beneficial therapeutical effects, the pleiotropic impact of sex hormones in different cell types (54) has revealed a hurdle that hampers our understanding about the cellular and molecular regulators of SSA-mediated thymic regeneration. Previous studies revealed that modulation of thymic function by androgen-mediated signalling occurs as result of direct effects on the stromal microenvironment, in particular TECs (55, 56), rather than on thymocytes. In this regard, genome-wide transcriptomic analysis revealed that androgens negatively impact on the expression of numerous TEC-specific genes that are central in T cell development (e.g.: *Dll4* and *Ccl25*) (57). Hence, one can speculate that androgen withdrawal stimulates thymic regeneration by correcting the transcriptional signature of TECs, which eventually enhances their ability to support thymopoiesis. Yet, in addition to its intrathymic effects, several reports also described similar beneficial effects of SSA in the bone marrow (BM) (58, 59), particularly at reverting deficits in the hematopoietic compartment. Given the intricate relationship between these two key hematopoietic sites (BM and thymus), one can alternatively propose that thymic renewal upon androgen blockade might rely on upstream effects at the level of the BM, through the increased provision of thymic seeding progenitors.

Assessing the existence of a functional relationship between the response in the BM and thymus to androgen blockade represents a great challenge, mainly due to the lack of experimental models to uncouple the activity of these organs. Interleukin-7 (IL-7) is a fundamental cytokine in many facets of the immune system (60). In the thymus, IL-7 regulates several stages of T cell development and its mainly produced by TECs (12, 61–63). Also, IL-7 expression is detected in multiple cell types within the BM (64), where it plays a critical role in common lymphoid progenitor (CLP) maintenance and B lymphopoiesis (65). The deficiency in IL-7 results in severe combined immunodeficiency (SCID), a syndrome characterized by a markedly

inhibition of T and B lymphopoiesis in mice (66). Owing the multifaceted impact of IL-7 at distinct anatomical hematopoietic niches, we postulated that the specific disruption of this cytokine might offer an opportunity to examine the interplay between the BM and the thymus following SSA. In this thesis, using distinct loss-of-function genetic approaches to inactivate IL-7, we provide new evidence that positions the expansion of BM-derived precursors as the chief catalyst of thymic renewal induced by androgen blockade (**Chapter III**).

Past evidence considered IL-7 as a prime candidate involved in thymic rebound induced by androgen withdrawal. This notion originates from observations that aged IL-7 germline KO mice were unresponsive to androgen withdrawal (67). Conversely, our current data reveal that SSA is able to enhance the activity of young (but not aged) IL7KO thymus and demonstrate that the loss of SSA-driven thymic rebound in aged IL-7 KO mice correlated with a defective expansion of the hematopoietic stem cell compartment (HSC and CLPs). Moreover, the generation of a TEC-specific IL-7 knockout (Il7cKO) model allowed us to further conclude that: 1) thymic IL-7 is not required for thymic renewal during androgen blockade and 2) increase in thymopoiesis upon SSA is functionally linked to the BM compartment (**Figure 2)**. Nonetheless, it is currently unclear how androgen blockade influences the maintenance and expansion of the hematopoietic precursors. The discrepancy in SSA-driven thymopoiesis seen amongst young and aged IL7KO mice suggests the existence of a temporal window in which this regenerative process can be elicited independently of IL-7. Yet, how the hematopoietic niche responds to androgen withdrawal in the absence of IL-7 is intriguing given that, contrarily to CLPs (65), HSCs do not express IL-7 receptor and there is no evidence that directly place IL-7 as a regulator of their homeostasis (68). Hence, one possibility is that SSA induced compensatory microenvironmental signals that act on HSC and/or CLP, replacing the requirement of IL-7 in young mice. Alternatively, defects in the BM stromal niche and on its functional capacity to produce stimulatory signal(s) might accumulate with age in the absence of IL-7, which turns hematopoietic progenitors unresponsive to SSA. As previous data revealed that *Il7* transcript levels are increased in the BM of age mice following SSA (59), future studies exploiting the temporal and conditional deletion of IL-7 in different BM stromal cells would help us to better comprehend the physiological role of this cytokine during androgen withdrawal.

IL-7 belongs to a unique family of cytokines termed common cytokine receptor γ-chain (γ_c), which also includes IL-2, IL-4, IL-9, IL-15 and IL-21 (69). The γ_c family of cytokines were shown to have vital roles in the homeostasis of multiple cell lineages of the innate and adaptive immune system (70). Each cytokine has its own specific receptor, sharing the γ_c subunit is a unique feature among the different family members. Some years ago, while the project described in **Chapter III** was still at a premature stage, we decided to use Il2rgKO mice as a complementary approach to examine the contribution of IL-7 receptor-derived signals for the intrathymic effects of SSA. Remarkably, akin to aged IL7KO mice, we found that thymic renewal following androgen blockade was abrogated in young Il2rgKO mice (**Appendix, Figure 1A**). As a consequence, the growth of the mTEC microenvironment was blocked in Il2rgKO thymus during SSA (**Appendix, Figure 1B),** reinforcing the notion that androgen blockade impacts on the medullary epithelium through a non-cell autonomous mechanism that entails thymocyte-derived signals. Additionally, the lack of thymic rebound in castrated Il2rgKO mice directly correlated with a defective expansion of BM-derived hematopoietic compartment (**Appendix, Figure 1C and D)**. Hence, these findings propose that androgen withdrawal influences the BM-Thymus axis by stimulating the expansion of the BM hematopoietic compartment in a γ_c-dependent manner. Future studies are warranted to ascertain the putative identity of the γ_c cytokine(s) that drives the regenerative effects of SSA. Interestingly, our analysis revealed that the BM of young Il2rgKO mice holds an enlarged LSK compartment when compared to age-matched wild-type and/or IL7KO counterparts (**Chapter III, Figure 5B vs Appendix, Figure 1C**). This observation is intriguing, as an increase in HSC cellularity is detected during the ageing process as consequence of cumulative cell-intrinsic and -extrinsic alterations. Although we still lack important information about the possible influence of γ_c cytokines in the homeostasis of HSCs, our results demonstrate that absence of γ_c-derived signals perturbs the size of the hematopoietic stem cell niche. In this regard, we cannot rule out that young Il2rgKO mice are unresponsive to androgen blockade simply due to the existence of profound defects on HSCs caused by the lack of the γ_c subunit, which render them unable to react to any SSA-derived stimulatory signal. In this regard, recent observations uncovered the broad influence of androgen-signalling in the transcriptional profile of HSCs and BM stromal cells (59). Nonetheless, the complex interplay between these two cellular compartments makes difficult to

assess on whether the SSA-mediated expansion of HSCs happens due to initial intrinsic changes on these cells and/or is driven by the ameliorated functional capacity of the BM microenvironment to produce stimulatory signals for their rebound. The development of new mouse models bearing a specific and temporal controlled deletion of the γ_c subunit in HSCs would provide a unique framework to clarify these queries. Simultaneously, such studies would aid in identifying the target cues that drive the response of LSK/CLPs to androgen withdrawal.

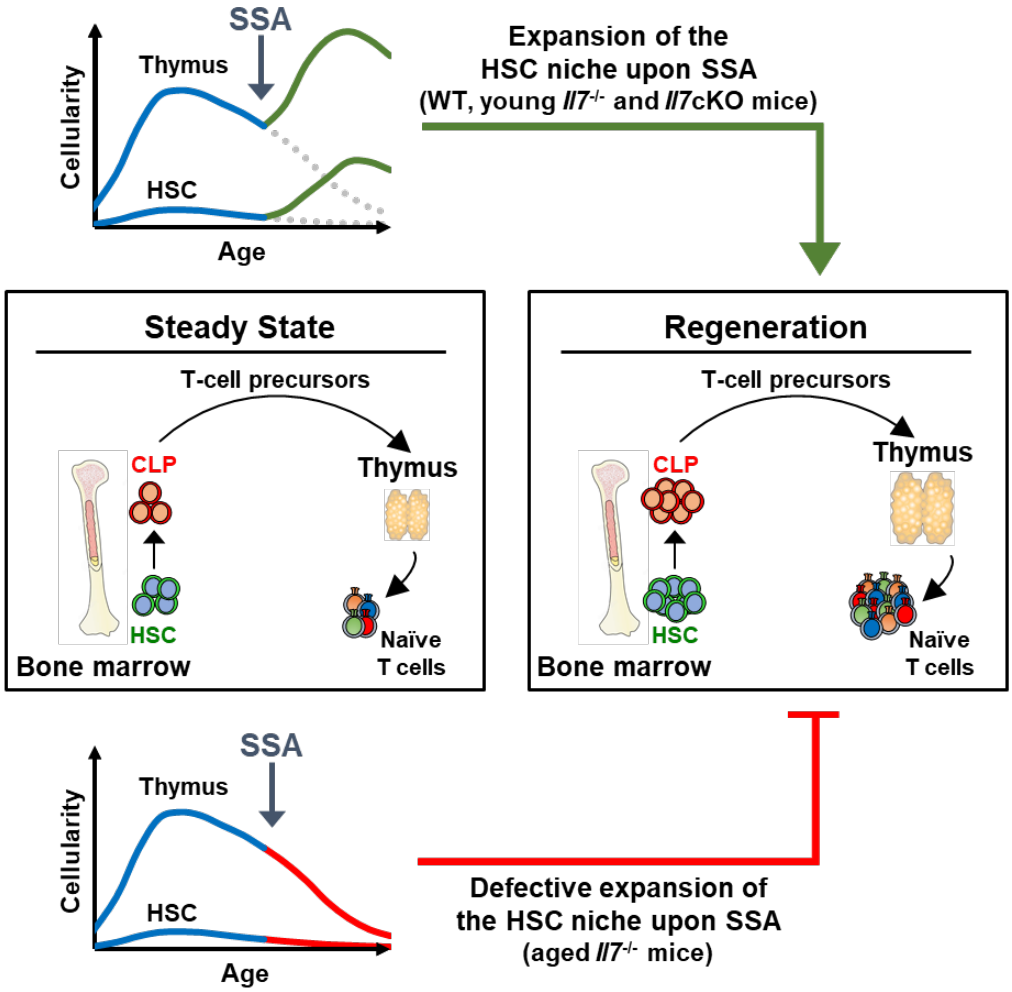

Figure 2 – Broad influence of sex steroid ablation (SSA) in the Bone marrow-Thymus axis. The production of a self-tolerant and diverse pool of naïve T cells depends on the continual recruitment of circulating T cell precursors by the thymus. These progenitors are originally derived from the bone marrow (BM) from a pool of primitive hematopoietic stem cells (HSCs) (Left panel). SSA has been shown to have a benefit impact in the regeneration of the hematopoietic and stromal niches of both primary lymphoid organs (BM and thymus). Some of these effects comprise an expansion in the number of HSC and common lymphoid progenitors (CLPs) in the BM and an enhanced thymic activity and T cell output (Right panel). Our findings reveal that the expansion of the HSC niche during SSA is the chief catalyst that drives thymic renewal (Top graph). Under circumstances where HSCs are unable to respond to SSA, such in aged interleukin-7 deficient mice, the rebound of the thymus is abrogated (Bottom graph).

Several other therapeutical strategies are known to revert the physiological consequences of thymic involution. For instance, beneficial effects on the thymic stromal compartment were observed after administration of FGF7 (also known as

keratinocyte growth factor), insulin-like growth factor 1 (IGF1) and Ghrelin to aged mice (71–73). However, as aged-related thymic degeneration seems to be a multifactorial process (4), rejuvenation of the involuted thymus to the levels found in young animals has been difficult to attain, particularly if using therapeutical approaches whose effects are mainly restricted to the thymus. During aging, the HSC niche undergoes several phenotypical and functional changes, including skewing towards the myeloid lineages, lower reconstitution potential and numerical accumulation of long-term HSCs (74). While cell-intrinsic mechanisms are known to contribute to the appearance of these defects, microenvironmental alterations of the BM stroma may also contribute to the functional deterioration of HSC with age (75, 76). Since thymic function relies on the continual supply of BM-derived progenitors (77), one can foresee that age-related alterations in the distinct BM niches might be a major impediment to achieve a sustained thymic regeneration. Therefore, the development of novel therapeutical strategies that promote the concurrent restoration of both the thymic microenvironment and the BM compartment (hematopoietic and stroma) stands as a more logical and efficient coordinated option towards the achievement of a long-term stable immune regeneration. Future studies should focus at identifying the molecular mediators that operate on the BM-thymus axis during aging.

Concluding remarks

Despite recent advances, our knowledge about the rules that govern TEC development and function is still incomplete. Furthermore, there is also little evidence about the molecular mediators involved in the damage and regeneration of the thymus. Hence, the characterization of the regulatory network underlying the maintenance of the thymic epithelium have received considerable attention in the last years, as perturbations on the TEC niches are closely associated with the development of autoimmune syndromes or immunodeficiency.

In this thesis, we provided new evidence that will expand our understanding on distinct aspects of TEC physiology. In **Chapter II**, we demonstrated that p53 is a critical regulator thymic function and immune tolerance, by mainly governing the homeostasis of the mTEC niche. Additionally, we found that p53 regulates a broad

transcriptional program in mTECs, including the expression of TRAs and genes associated with core processes of mTEC biology (e.g.: RANK). In **Chapter III**, we explored the temporal and spatial requirements for IL-7 in thymic regeneration induced by SSA. Using distinct and novel genetic approaches, which included the generation of Il7cKO mice, we established that 1) thymic IL-7 is dispensable for thymic renewal after SSA and 2) the increase in thymic activity upon castration is functionally linked to the BM compartment.

In conclusion, this thesis provides new insights on the cellular and molecular mechanisms that govern the homeostasis of the TEC microenvironments. This knowledge will have important repercussions to the development of therapeutic strategies for the clinical management of major conditions and diseases associated with the need to enhance and/or correct thymic function and reconstitution.

References

1. Abramson, J., and G. Anderson. 2016. Thymic Epithelial Cells. *Annu. Rev. Immunol.* 34: 85–118.

2. Takahama, Y., I. Ohigashi, S. Baik, and G. Anderson. 2017. Generation of diversity in thymic epithelial cells. *Nat. Rev. Immunol.* 17: 295–305.

3. Gray, D. H. D., N. Seach, T. Ueno, M. K. Milton, A. Liston, A. M. Lew, C. C. Goodnow, and R. L. Boyd. 2006. Developmental kinetics, turnover, and stimulatory capacity of thymic epithelial cells. *Blood* 108: 3777–85.

4. Taub, D. D., and D. L. Longo. 2005. Insights into thymic aging and regeneration. *Immunol. Rev.* 205: 72–93.

5. Linzer, D. I. H., and A. J. Levine. 1979. Characterization of a 54K Dalton cellular SV40 tumor antigen present in SV40-transformed cells and uninfected embryonal carcinoma cells. *Cell* 17: 43–52.

6. Lane, D. P., and L. V Crawford. 1979. T antigen is bound to a host protein in SV40-transformed cells. *Nature* 278: 261–263.

7. DeLeo, A. B., G. Jay, E. Appella, G. C. Dubois, L. W. Law, and L. J. Old. 1979. Detection of a transformation-related antigen in chemically induced sarcomas and other transformed cells of the mouse. *Proc. Natl. Acad. Sci. U. S. A.* 76: 2420–4.

8. Junttila, M. R., and G. I. Evan. 2009. p53 - a Jack of all trades but master of none. *Nat. Rev. Cancer* 9: 821–829.

9. Feng, Z., and A. J. Levine. 2010. The regulation of energy metabolism and the IGF-1/mTOR pathways by the p53 protein. *Trends Cell Biol.* 20: 427–434.

10. Munoz-Fontela, C., A. Mandinova, S. A. Aaronson, and S. W. Lee. 2016. Emerging roles of p53 and other tumour-suppressor genes in immune regulation. *Nat. Rev. Immunol.* 16: 741–750.

11. Vousden, K. H., and D. P. Lane. 2007. P53 in Health and Disease. *Nat. Rev. Mol. Cell Biol.* 8: 275–83.

12. Alves, N. L., O. Richard-Le Goff, N. D. Huntington, A. P. Sousa, V. S. G. Ribeiro, A. Bordack, F. L. Vives, L. Peduto, A. Chidgey, A. Cumano, R. Boyd, G. Eberl, and J. P. Di Santo. 2009. Characterization of the thymic IL-7 niche in vivo. *Proc. Natl. Acad. Sci. U. S. A.* 106: 1512–7.

13. Ribeiro, A. R., P. M. Rodrigues, C. Meireles, J. P. Di Santo, and N. L. Alves. 2013. Thymocyte selection regulates the homeostasis of IL-7-expressing thymic cortical epithelial cells in vivo. *J. Immunol.* 191: 1200–9.

14. Gudkov, A. V., and E. A. Komarova. 2003. The role of p53 in determining sensitivity to radiotherapy. *Nat. Rev. Cancer* 3: 117–129.

15. Jiang, D., M. J. Lenardo, and J. C. Zúñiga-Pflücker. 1996. p53 Prevents Maturation to the CD4+CD8+ Stage of Thymocyte Differentiation in the Absence of T Cell Receptor Rearrangment. *J. Exp. Med.* 183: 1923–1928.

16. Haks, M. C., P. Krimpenfort, J. H. N. Van den Brakel, and A. M. Kruisbeek. 1999. Pre-TCR signaling and inactivation of p53 induces crucial cell survival pathways in pre-T cells. *Immunity* 11: 91–101.

17. Guidos, C. J., C. J. Williams, I. Grandal, G. Knowles, M. T. F. Huang, and J. S. Danska. 1996. V(D)J recombination activates a p53-dependent DNA damage checkpoint in scid lymphocyte precursors. *Genes Dev.* 10: 2038–2054.

18. Weirich, G., P. Schneider, C. Fellbaum, H. Brauch, W. Nathrath, M. Scholz, H. Präuer, and H. Höfler. 1997. p53-Alterations in Thymic Epithelial Tumors. In *Epithelial Tumors of the Thymus: Pathology, Biology, Treatment* A. Marx, and H. K. Müller-Hermelink, eds. Springer US, Boston, MA. 35–40.

19. Petrini, I., P. S. Meltzer, I.-K. K. Kim, M. Lucchi, K.-S. S. Park, G. Fontanini, J. Gao, P. A. Zucali, F. Calabrese, A. Favaretto, F. Rea, J. Rodriguez-Canales, R. L. Walker, M. Pineda, Y. J. Zhu, C. Lau, K. J. Killian, S. Bilke, D. Voeller, S. Dakshanamurthy, Y. Wang, and G. Giaccone. 2014. A specific missense mutation in GTF2I occurs at high frequency in thymic epithelial tumors. *Nat. Genet.* 46: 844–849.

20. Vousden, K. H., and C. Prives. 2009. Blinded by the Light: The Growing Complexity of p53. *Cell* 137: 413–31.

21. Abramson, J., M. Giraud, C. Benoist, and D. Mathis. 2010. Aire's Partners in the Molecular Control of Immunological Tolerance. *Cell* 140: 123–135.

22. Bansal, K., H. Yoshida, C. Benoist, and D. Mathis. 2017. The transcriptional regulator Aire binds to and activates super-enhancers. *Nat. Immunol.* 18: 263–273.

23. Kawano, H., H. Nishijima, J. Morimoto, F. Hirota, R. Morita, Y. Mouri, Y. Nishioka, and M. Matsumoto. 2015. Aire Expression Is Inherent to Most Medullary Thymic Epithelial Cells during Their Differentiation Program. *J. Immunol.* 195: 5149–5158.

24. Giraud, M., N. Jmari, L. Du, F. Carallis, T. J. F. Nieland, F. M. Perez-Campo, O. Bensaude, D. E. Root, N. Hacohen, D. Mathis, and C. Benoist. 2014. An RNAi screen for Aire cofactors reveals a role for Hnrnpl in polymerase release and Aire-activated ectopic transcription. *Proc. Natl. Acad. Sci. U. S. A.* 111: 1491–1496.

25. Yang, A., M. Kaghad, Y. Wang, E. Gillett, M. D. Fleming, V. Dötsch, N. C. Andrews, D. Caput, and F. McKeon. 1998. P63, a P53 Homolog At 3Q27-29, Encodes Multiple Products With Transactivating, Death-Inducing, and Dominant-Negative Activities. *Mol. Cell* 2: 305–316.

26. Senoo, M., N. Seki, M. Ohira, S. Sugano, M. Watanabe, M. Tachibana, T. Tanaka, Y. Shinkai, and H. Kato. 1998. A Second p53-Related Protein, p73L, with High Homology to p73. *Biochem. Biophys. Res. Commun.* 248: 603–607.

27. Kaghad, M., H. Bonnet, A. Yang, L. Creancier, J.-C. Biscan, A. Valent, A. Minty, P. Chalon, J.-M. Lelias, X. Dumont, P. Ferrara, F. McKeon, and D. Caput. 1997. Monoallelically expressed gene related to p53 at 1p36, a region frequently deleted in neuroblastoma and other human cancers. *Cell* 90: 809–19.

28. Yang, A., M. Kaghad, D. Caput, and F. McKeon. 2002. On the shoulders of giants p63,p73 and the rise of p53. *Trends Genet.* 18: 90–95.

29. Senoo, M., F. Pinto, C. P. Crum, and F. McKeon. 2007. p63 Is essential for the proliferative potential of stem cells in stratified epithelia. *Cell* 129: 523–36.

30. Baik, S., M. Sekai, Y. Hamazaki, W. E. Jenkinson, and G. Anderson. 2016. Relb acts downstream of medullary thymic epithelial stem cells and is essential for the emergence of RANK+ medullary epithelial progenitors. *Eur. J. Immunol.* 46: 857–862.

31. Akiyama, N., N. Takizawa, M. Miyauchi, H. Yanai, R. Tateishi, M. Shinzawa, R. Yoshinaga, M. Kurihara, Y. Demizu, H. Yasuda, S. Yagi, G. Wu, M. Matsumoto, R. Sakamoto, N. Yoshida, J. M. Penninger, Y. Kobayashi, J. Inoue, and T. Akiyama. 2016. Identification of embryonic precursor cells that differentiate into thymic epithelial cells expressing autoimmune regulator. *J. Exp. Med.* 213: 1441–1458.

32. Mouri, Y., M. Yano, M. Shinzawa, Y. Shimo, F. Hirota, Y. Nishikawa, T. Nii, H. Kiyonari, T. Abe, H. Uehara, K. Izumi, K. Tamada, L. Chen, J. M. Penninger, J. Inoue, T. Akiyama, and M. Matsumoto. 2011. Lymphotoxin signal promotes thymic organogenesis by eliciting RANK expression in the embryonic thymic stroma. *J. Immunol.* 186: 5047–57.

33. Li, M., Y. He, W. Dubois, X. Wu, J. Shi, and J. Huang. 2012. Distinct Regulatory Mechanisms and Functions for p53-Activated and p53-Repressed DNA Damage Response Genes in Embryonic Stem Cells. *Mol. Cell* 46: 30–42.

34. Kenzelmann Broz, D., S. S. Mello, K. T. Bieging, D. Jiang, R. L. Dusek, C. A. Brady, A. Sidow, and L. D. Attardi. 2013. Global genomic profiling reveals an extensive p53-regulated autophagy program contributing to key p53 responses. *Genes Dev.* 27: 1016–1031.

35. Liu, Y., S. E. Elf, Y. Miyata, G. Sashida, Y. Liu, G. Huang, S. Di Giandomenico, J. M. Lee, A. Deblasio, S. Menendez, J. Antipin, B. Reva, A. Koff, and S. D. Nimer. 2009. p53 Regulates Hematopoietic Stem Cell Quiescence. *Cell Stem Cell* 4: 37–48.

36. Dai, C., and W. Gu. 2010. P53 post-translational modification: Deregulated in tumorigenesis. *Trends Mol. Med.* 16: 528–536.

37. Chao, C., Z. Wu, S. J. Mazur, H. Borges, M. Rossi, T. Lin, J. Y. J. Wang, C. W. Anderson, E. Appella, and Y. Xu. 2006. Acetylation of mouse p53 at lysine 317 negatively regulates p53 apoptotic activities after DNA damage. *Mol. Cell. Biol.* 26: 6859–6869.

38. Di Giovanni, S., C. D. Knights, M. Rao, A. Yakovlev, J. Beers, J. Catania, M. L. Avantaggiati, and A. I. Faden. 2006. The tumor suppressor protein p53 is required for neurite outgrowth and axon regeneration. *EMBO J.* 25: 4084–4096.

39. Kyewski, B., and L. Klein. 2006. A central role for central tolerance. *Annu. Rev. Immunol.* 24: 571–606.

40. Sansom, S. N., N. Shikama-Dorn, S. Zhanybekova, G. Nusspaumer, I. C. Macaulay, M. E. Deadman, A. Heger, C. P. Ponting, and G. A. Hollander. 2014. Population and single-cell genomics reveal the Aire dependency, relief from Polycomb silencing, and distribution of self-antigen expression in thymic epithelia. *Genome Res.* 24: 1918–1931.

41. Cloosen, S., J. Arnold, M. Thio, G. M. J. Bos, B. Kyewski, and W. T. V. Germeraad. 2007. Expression of tumor-associated differentiation antigens, MUC1 glycoforms and CEA, in human thymic epithelial cells: Implications for self-tolerance and tumor therapy. *Cancer Res.* 67: 3919–3926.

42. Derbinski, J., S. Pinto, S. Rosch, K. Hexel, and B. Kyewski. 2008. Promiscuous gene expression patterns in single medullary thymic epithelial cells argue for a stochastic mechanism. *Proc. Natl. Acad. Sci. U. S. A.* 105: 657–662.

43. Anderson, G., and Y. Takahama. 2012. Thymic epithelial cells: working class heroes for T cell development and repertoire selection. *Trends Immunol.* 33: 256–63.

44. Tamura, T., H. Yanai, D. Savitsky, and T. Taniguchi. 2008. The IRF Family Transcription Factors in Immunity and Oncogenesis. *Annu. Rev. Immunol.* 26: 535–584.

45. Haljasorg, U., J. Dooley, M. Laan, K. Kisand, R. Bichele, A. Liston, and P. Peterson. 2017. Irf4 Expression in Thymic Epithelium Is Critical for Thymic Regulatory T Cell Homeostasis. *J. Immunol.* 198: 1952–1960.

46. Otero, D. C., D. P. Baker, and M. David. 2013. IRF7-dependent IFN-beta production in response to RANKL promotes medullary thymic epithelial cell development. *J. Immunol.* 190: 3289–3298.

47. Rodrigues, P. M., A. R. Ribeiro, C. Perrod, J. J. M. Landry, L. Araújo, I. Pereira-Castro, V. Benes, A. Moreira, H. Xavier-Ferreira, C. Meireles, and N. L. Alves. 2017. Thymic epithelial cells require p53 to support their long-term function in thymopoiesis in mice. *Blood* 130: 478–488.

48. Satoh, R., K. Kakugawa, T. Yasuda, H. Yoshida, M. Sibilia, Y. Katsura, B. Levi, J. Abramson, Y. Koseki, H. Koseki, W. van Ewijk, G. A. Hollander, and H. Kawamoto. 2016. Requirement of Stat3 Signaling in the Postnatal Development of Thymic Medullary Epithelial Cells. *PLoS Genet.* 12: 1–20.

49. Lomada, D., M. Jain, M. Bolner, K. A. G. Reeh, R. Kang, M. C. Reddy, J. DiGiovanni, and E. R. Richie. 2016. Stat3 Signaling Promotes Survival And Maintenance Of Medullary Thymic Epithelial Cells. *PLOS Genet.* 12: e1005777.

50. Cosway, E. J., B. Lucas, K. D. James, S. M. Parnell, M. Carvalho-Gaspar, A. J. White, A. V. Tumanov, W. E. Jenkinson, and G. Anderson. 2017. Redefining thymus medulla specialization for central tolerance. *J. Exp. Med.* 1–13.

51. Cowan, J. E., S. M. Parnell, K. Nakamura, J. H. Caamano, P. J. L. Lane, E. J. Jenkinson, W. E. Jenkinson, and G. Anderson. 2013. The thymic medulla is required for Foxp3+ regulatory but not conventional CD4+ thymocyte development. *J. Exp. Med.* 210: 675–81.

52. Takaba, H., and H. Takayanagi. 2017. The Mechanisms of T Cell Selection in the Thymus. *Trends Immunol.* 38: 805–816.

53. Velardi, E., J. A. Dudakov, and M. R. M. van den Brink. 2015. Sex steroid ablation: an immunoregenerative strategy for immunocompromised patients. *Bone Marrow Transplant.* 50 Suppl 2: S77-81.

54. Tanriverdi, F., L. F. G. Silveira, G. S. MacColl, and P. M. G. Bouloux. 2003. The hypothalamic-pituitary-gonadal axis: Immune function and autoimmunity. *J. Endocrinol.* 176: 293–304.

55. Olsen, N. J., G. Olson, S. M. Viselli, X. Gu, and W. J. Kovacs. 2001. Androgen receptors in thymic epithelium modulate thymus size and thymocyte development. *Endocrinology* 142:

1278–83.

56. Lai, K.-P., J.-J. Lai, P. Chang, S. Altuwaijri, J.-W. Hsu, K.-H. Chuang, C.-R. Shyr, S. Yeh, and C. Chang. 2013. Targeting Thymic Epithelia AR Enhances T-Cell Reconstitution and Bone Marrow Transplant Grafting Efficacy. *Mol. Endocrinol.* 27: 25–37.

57. Dumont-Lagacé, M., C. St-Pierre, and C. Perreault. 2015. Sex hormones have pervasive effects on thymic epithelial cells. *Sci. Rep.* 5: 12895.

58. Dudakov, J. A., G. L. Goldberg, J. J. Reiseger, A. P. Chidgey, and R. L. Boyd. 2009. Withdrawal of sex steroids reverses age- and chemotherapy-related defects in bone marrow lymphopoiesis. *J. Immunol.* 182: 6247–6260.

59. Khong, D. M., J. A. Dudakov, M. V. Hammett, M. I. Jurblum, S. M. L. Khong, G. L. Goldberg, T. Ueno, L. Spyroglou, L. F. Young, M. R. M. van Den Brink, R. L. Boyd, and A. P. Chidgey. 2015. Enhanced hematopoietic stem cell function mediates immune regeneration following sex steroid blockade. *Stem Cell Reports* 4: 445–458.

60. von Freeden-Jeffry, U., P. Vieira, L. A. Lucian, T. McNeil, S. E. G. Burdach, and R. Murray. 1995. Lymphopenia in interleukin (IL)-7 gene-deleted mice identifies IL-7 as a nonredundant cytokine. *J. Exp. Med.* 181: 1519–26.

61. Ye, S. K., Y. Agata, H. C. Lee, H. Kurooka, T. Kitamura, A. Shimizu, T. Honjo, and K. Ikuta. 2001. The IL-7 receptor controls the accessibility of the TCRγ locus by Stat5 and histone acetylation. *Immunity* 15: 813–823.

62. Park, J.-H., S. Adoro, T. Guinter, B. Erman, A. S. Alag, M. Catalfamo, M. Y. Kimura, Y. Cui, P. J. Lucas, R. E. Gress, M. Kubo, L. Hennighausen, L. Feigenbaum, and A. Singer. 2010. Signaling by intrathymic cytokines, not T cell antigen receptors, specifies CD8 lineage choice and promotes the differentiation of cytotoxic-lineage T cells. *Nat. Immunol.* 11: 257–64.

63. Shitara, S., T. Hara, B. Liang, K. Wagatsuma, S. Zuklys, G. A. Holländer, H. Nakase, T. Chiba, S. Tani-ichi, K. Ikuta, G. A. Hollander, H. Nakase, T. Chiba, S. Tani-ichi, and K. Ikuta. 2013. IL-7 Produced by Thymic Epithelial Cells Plays a Major Role in the Development of Thymocytes and TCR + Intraepithelial Lymphocytes. *J. Immunol.* 190: 6173–9.

64. Cordeiro Gomes, A., T. Hara, V. Y. Lim, D. Herndler-Brandstetter, E. Nevius, T. Sugiyama, S. Tani-ichi, S. Schlenner, E. Richie, H. R. Rodewald, R. A. Flavell, T. Nagasawa, K. Ikuta, and J. P. Pereira. 2016. Hematopoietic Stem Cell Niches Produce Lineage-Instructive Signals to Control Multipotent Progenitor Differentiation. *Immunity* 45: 1219–1231.

65. Dias, S., H. Silva Jr., A. Cumano, and P. Vieira. 2005. Interleukin-7 is necessary to maintain the B cell potential in common lymphoid progenitors. *J. Exp. Med.* 201: 971–979.

66. Kovanen, P. E., and W. J. Leonard. 2004. Cytokines and immunodeficiency diseases: critical roles of the gamma(c)-dependent cytokines interleukins 2, 4, 7, 9, 15, and 21, and their signaling pathways. *Immunol. Rev.* 202: 67–83.

67. Goldberg, G. L., O. Alpdogan, S. J. Muriglan, M. V. Hammett, M. K. Milton, J. M. Eng, V. M. Hubbard, A. Kochman, L. M. Willis, A. S. Greenberg, K. H. Tjoe, J. S. Sutherland, A.

Chidgey, M. R. M. van den Brink, and R. L. Boyd. 2007. Enhanced immune reconstitution by sex steroid ablation following allogeneic hemopoietic stem cell transplantation. *J. Immunol.* 178: 7473–84.

68. Mazzucchelli, R., and S. K. Durum. 2007. Interleukin-7 receptor expression: intelligent design. *Nat. Rev. Immunol.* 7: 144–54.

69. Alves, N. L., F. A. Arosa, and R. A. W. van Lier. 2007. Common γ chain cytokines: Dissidence in the details. *Immunol. Lett.* 108: 113–120.

70. Rochman, Y., R. Spolski, and W. J. Leonard. 2009. New insights into the regulation of T cells by gamma(c) family cytokines. *Nat. Rev. Immunol.* 9: 480–90.

71. Chu, Y.-W., S. Schmitz, B. Choudhury, W. Telford, V. Kapoor, D. Howe, R. E. Gress, W. Dc, S. Garfield, D. Howe, and R. E. Gress. 2008. Exogenous insulin-like growth factor 1 enhances thymopoiesis predominantly through thymic epithelial cell expansion. *Blood* 112: 2836–2846.

72. Min, D., A. Panoskaltsis-Mortari, M. Kuro-o, G. A. Holländer, B. R. Blazar, and K. I. Weinberg. 2007. Sustained thymopoiesis and improvement in functional immunity induced by exogenous KGF administration in murine models of aging. *Blood* 109: 2529–2537.

73. Dixit, V. D., H. Yang, Y. Sun, A. T. Weeraratna, Y.-H. Youm, R. G. Smith, and D. D. Taub. 2007. Ghrelin promotes thymopoiesis during aging. *J. Clin. Invest.* 117: 2778–2790.

74. Geiger, H., M. Denkinger, and R. Schirmbeck. 2014. Hematopoietic stem cell aging. *Curr. Opin. Immunol.* 29: 86–92.

75. Wagner, W., P. Horn, S. Bork, and A. D. Ho. 2008. Aging of hematopoietic stem cells is regulated by the stem cell niche. *Exp. Gerontol.* 43: 974–980.

76. Waterstrat, A., and G. Van Zant. 2009. Effects of aging on hematopoietic stem and progenitor cells. *Curr. Opin. Immunol.* 21: 408–413.

77. Donskoy, E., and I. Goldschneider. 1992. Thymocytopoiesis is maintained by blood-borne precursors throughout postnatal life. A study in parabiotic mice. *J. Immunol.* 148: 1604–1612.

78. Alves, N. L., Y. Takahama, I. Ohigashi, A. R. Ribeiro, S. Baik, G. Anderson, and W. E. Jenkinson. 2014. Serial progression of cortical and medullary thymic epithelial microenvironments. *Eur. J. Immunol.* 44: 16–22.

79. Alves, N. L., and A. R. Ribeiro. 2016. Thymus medulla under construction: Time and space oddities. *Eur. J. Immunol.* 46: 829–833.

80. Akiyama, N., M. Shinzawa, M. Miyauchi, H. Yanai, R. Tateishi, Y. Shimo, D. Ohshima, K. Matsuo, I. Sasaki, K. Hoshino, G. Wu, S. Yagi, J. Inoue, T. Kaisho, and T. Akiyama. 2014. Limitation of immune tolerance-inducing thymic epithelial cell development by Spi-B-mediated negative feedback regulation. *J. Exp. Med.* 211: 2425–38.

81. Hauri-Hohl, M., S. Zuklys, G. A. Holländer, and S. F. Ziegler. 2014. A regulatory role for TGF-β signaling in the establishment and function of the thymic medulla. *Nat. Immunol.* 15: 554–61.

Chapter V

Appendix

Figure 1

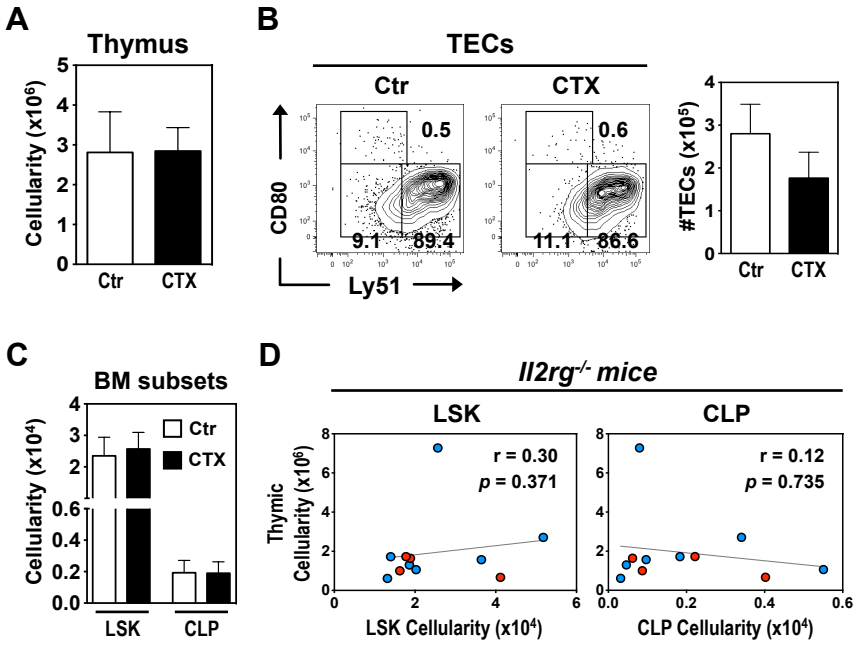

Figure 1 – The BM-Thymus axis is unresponsive to androgen withdrawal in the absence of γ_c-dependent signals. Young (4-week-old) *Il2rg*$^{-/-}$ mice were castrated and the thymus and bone marrow were analyzed 2 weeks post-surgery. Castrated mice (CTX) were compared to control sham-treated mice (Ctr) at the indicated time points. **(A)** Thymic cellularity. **(B)** The composition of the TEC microenvironment was analyzed by flow cytometry for Ly51/ CD80 expression on total TECs (defined as EpCAM^{+}CD45^{-}). Numbers indicate the percentage of gated cells. On the right, graphs represent the cellularity of the different TEC subsets. **(C)** Number of LSK (Lin^{-}CD127^{-}cKit^{+}Sca-1^{+}), CLP (Lin^{-}CD127^{+}cKit^{int}Sca-1^{int}) in control (Ctr) and castrated (CTX) mice. **(C)** Spearman correlation between the thymic cellularity and the number of LSK and CLPs in the BM of control (Ctr) and castrated (CTX) groups. Results are presented as mean ± SEM.

2017 130: 478-488
doi:10.1182/blood-2016-12-758961 originally published online May 30, 2017

Thymic epithelial cells require p53 to support their long-term function in thymopoiesis in mice

Pedro M. Rodrigues, Ana R. Ribeiro, Chiara Perrod, Jonathan J. M. Landry, Leonor Araújo, Isabel Pereira-Castro, Vladimir Benes, Alexandra Moreira, Helena Xavier-Ferreira, Catarina Meireles and Nuno L. Alves

Blood (print ISSN 0006-4971, online ISSN 1528-0020), is published weekly by the American Society of Hematology, 2021 L St, NW, Suite 900, Washington DC 20036.

Regular Article

blood

IMMUNOBIOLOGY AND IMMUNOTHERAPY

Thymic epithelial cells require p53 to support their long-term function in thymopoiesis in mice

Pedro M. Rodrigues,[1-3] Ana R. Ribeiro,[1-3] Chiara Perrod,[1,2] Jonathan J. M. Landry,[4] Leonor Araújo,[1,2] Isabel Pereira-Castro,[1,5] Vladimir Benes,[4] Alexandra Moreira,[1,5,6] Helena Xavier-Ferreira,[1,2] Catarina Meireles,[1,2] and Nuno L. Alves[1,2]

[1]Instituto de Investigação e Inovação em Saúde, Universidade do Porto, Portugal; [2]Thymus Development and Function Laboratory, Instituto de Biologia Molecular e Celular, Porto, Portugal; [3]Doctoral Program in Biomedical Sciences, Instituto de Ciências Biomédicas Abel Salazar, Universidade do Porto, Porto, Portugal; [4]Genomics Core Facility, European Molecular Biology Laboratory, Heidelberg, Germany; [5]Gene Regulation Laboratory, Instituto de Biologia Molecular e Celular, Porto, Portugal; and [6]Instituto de Ciências Biomédicas Abel Salazar, Universidade do Porto, Porto, Portugal

Key Points

- TEC-intrinsic ablation of p53 predominantly affects medullary TECs, altering their RANK-driven differentiation and transcriptome.
- Loss of p53 in TECs couples disrupted thymopoiesis to altered T-cell homeostasis and tolerance.

Thymic epithelial cells (TECs) provide crucial microenvironments for T-cell development and tolerance induction. As the regular function of the thymus declines with age, it is of fundamental and clinical relevance to decipher new determinants that control TEC homeostasis in vivo. Beyond its recognized tumor suppressive function, p53 controls several immunoregulatory pathways. To study the cell-autonomous role of p53 in thymic epithelium functioning, we developed and analyzed mice with conditional inactivation of *Trp53* in TECs (p53cKO). We report that loss of p53 primarily disrupts the integrity of medullary TEC (mTEC) niche, a defect that spreads to the adult cortical TEC compartment. Mechanistically, we found that p53 controls specific and broad programs of mTEC differentiation. Apart from restraining the expression and responsiveness of the receptor activator of NF-κB (RANK), which is central for mTEC differentiation, deficiency of p53 in TECs altered multiple functional modules of the mTEC transcriptome, including tissue-restricted antigen expression. As a result, p53cKO mice presented premature defects in mTEC-dependent regulatory T-cell differentiation and thymocyte maturation, which progressed to a failure in regular and regenerative thymopoiesis and peripheral T-cell homeostasis in the adulthood. Lastly, peripheral signs of altered immunological tolerance unfold in mutant mice and in immunodeficient mice that received p53cKO-derived thymocytes. Our findings position p53 as a novel molecular determinant of thymic epithelium function throughout life. (*Blood*. 2017;130(4):478-488)

Introduction

Within the thymus, thymic epithelial cells (TECs) orchestrate the development of functionally diverse and self-tolerant T cells.[1] Importantly, impaired TEC functions arise with aging, cytoablative regimens and infection, which compromise T-cell responses to pathogens, and vaccination in the elderly, and patients undergoing bone marrow transplantation (BMT) or chemotherapy. Equally, failures in TEC-mediated tolerance induction lead to autoimmunity.[2] Hence, the identification of novel regulators of TEC homeostasis is crucial to comprehend the foundations of immunity and to intervene medically in disorders linked to a dysfunctional thymus.

Cortical TECs (cTECs) and medullary TECs (mTECs) define 2 functionally distinct microenvironments, which differentiate from bipotent TEC progenitors.[1] Whereas cTECs drive T-cell lineage specification and positive selection, mTECs promote the maturation of positively selected thymocytes, regulatory T-cell differentiation, and elimination of autoreactive T cells.[1] Important to mTEC function is their ability to express tissue-restricted antigens (TRA),[2] which depends in part on autoimmune regulator (Aire) and Fezf2.[3,4] Past studies elucidated the role of members of tumor necrosis factor (TNF) receptor superfamily (TNFRSF) receptor activator of NF-κB (RANK), lymphotoxin β receptor (LtβR), and CD40 in the maturation of mTECs.[1] Still, the molecular determinants that control the function of these key inducers of mTECs remain unknown. Other uncertainties concern the signaling pathways that maintain the multilayered function of TECs in vivo.

The tumor suppressor protein p53 is a recognized regulator of cell-cycle arrest and apoptosis. Yet recent studies have revealed alternative roles for p53 in immunoregulation and autoimmunity.[5] In relation to the thymic epithelium, the observations that the p53 homolog p63 controls the turnover of TEC progenitors[6] imply a possible functional relationship within the p53 family. The analysis of the role of p53 in TEC physiology has been precluded because of its broad expression pattern and the complex phenotype of germline p53-null mice, which ultimately develop thymic lymphomas.[7] Despite such limitations, several studies link p53 to TEC homeostasis. Although germline deletion in wild-type p53-induced phosphatase 1, a p53-target gene, impairs the maturation of mTECs and thymic regeneration,[8] the

Submitted 28 December 2016; accepted 24 May 2017. Prepublished online as *Blood* First Edition paper, 30 May 2017; DOI 10.1182/blood-2016-12-758961.

The online version of this article contains a data supplement.

There is an Inside *Blood* Commentary on this article in this issue.

The publication costs of this article were defrayed in part by page charge payment. Therefore, and solely to indicate this fact, this article is hereby marked "advertisement" in accordance with 18 USC section 1734.

systemic administration of p53 inhibitors moderately improves TEC recovery and thymopoiesis following BMT.[9] Because genetically engineered mouse models and pharmacological studies often hide lineage-specific functions of broadly acting genes, the cell-autonomous relevance of p53 in the dynamic differentiation of TECs in vivo remains unexplored. Our findings underscore the requirement for p53 in TECs to support their role in T-cell development and selection.

Methods

All procedures are further detailed in the supplemental Methods section, available on the *Blood* Web site.

Mice

C57BL/6 $p53^{fl/fl}$, $Foxn1^{Cre}$, and Marilyn-$Rag2^{-/-}$ mice[10-12] were housed under specific pathogen-free conditions. Experiments were performed under the European guidelines for animal experimentation.

Flow cytometry

TECs and hematopoietic cells were isolated and stained as described.[12] Cells were analyzed on a fluorescence-activated cell sorter (FACS) Canto II and a LSR Fortessa and sorted on a FACSAria I (BD Biosciences) (purities were >96%). Data were analyzed on FlowJo software.

Histology

Thymic lobes were prepared for immunofluorescence analysis, as described.[12] Paraffin-embedded tissue sections from indicated organs were stained with hematoxylin and eosin (H&E). Analysis was done on a light microscope (Olympus CX31) and IN Cell Analyzer2000 (GE Healthcare). Images were processed using Fiji software.

Gene expression

Messenger RNA (mRNA) isolation and complementary DNA (cDNA) synthesis were done, as described.[12] Real-time polymerase chain reaction (RT-PCR) was performed using TaqMan Universal PCR Master Mix and probes for selected genes.

Fetal thymic organ culture (FTOC)

We established 2-deoxyguanosine (dGuo)-treated FTOC, as described[12] and cultured it in medium alone or with recombinant CD40L (5 μg/mL), agonist antibodies anti-RANK (1 μg/mL) (R&D Systems) or anti-LTβR (10 μg/mL; AC.H6), and Pifithrin-α (50 μg/mL; Sigma-Aldrich).

Luciferase assay

In silico analysis identified putative p53-binding sites in the promoter of *Tnfrsf11a*. p53-Deficient MEFs were transiently cotransfected with a reporter firefly luciferase plasmid containing genomic fragments of *Tnfrsf11a* or *Cdkn1a* promoters along with a p53-expressing vector. Renilla luciferase plasmid was cotransfected as an internal control (Dual-Luciferase Reporter Assay System, Promega).

RNA sequencing

Total RNA library preparation and high-throughput sequencing of sorted cTECs / mTECs samples from p53cKO and control littermates were performed at Gene Core facility (EMBL, Germany). The number of reads per gene was counted using HTSeq-count,[13] and data were analyzed with DESeq2 package.[14] Gene ontology (GO) enrichment analysis was done using a model-based gene set analysis.[15]

Regulatory T-cell suppression assay

Control and p53cKO-derived regulatory T cells were sorted as $CD25^{high}CD4^{+}$ T cells and cocultured with carboxyfluorescein diacetate succinimidyl ester–labeled T cells at various ratios in the presence of anti-CD3 mAb and irradiated splenocytes. The frequency of dividing cells was determined, as described.[16]

Statistical analysis

The 2-tailed Mann-Whitney test was used for statistical differences between groups, and a 2-way analysis of variance was used for multiple comparisons (GraphPad Prism).

Results

Inactivation of *Trp53* in TECs reduces the mTEC compartment

To investigate the function of p53 in the thymic epithelium, we conditionally deleted the p53 gene (*Trp53*) in TECs by crossing mice with loxP-flanked alleles of *Trp53* ($Trp53^{fl/fl}$)[10] with mice expressing Cre recombinase under the control of the *Foxn1* promoter ($Foxn1^{Cre}$), which directs the expression of Cre recombinase to virtually all TECs during embryonic and postnatal life.[11] $Foxn1^{Cre}$:$Trp53^{fl/fl}$ (p53cKO) mice were born without obvious abnormalities and did not develop spontaneous tumors in the thymus or skin, which also contains $Foxn1^{+}$ keratinocytes.[11] The Cre-mediated deletion of $Trp53^{fl}$ allele was detected in TECs but not in thymocytes from p53cKO mice nor in TECs from $Trp53^{fl/fl}$ littermate controls (Ctr) (Figure 1A and supplemental Figure 1A-B). Although not statistically different, *Trp53* levels were moderately increased in mTECs in comparison with cTECs from the control thymus (Figure 1B), indicating that p53 is expressed under physiological conditions. The same transcript was nearly absent in cTECs and mTECs from p53cKO mice (Figure 1B) but remained similarly expressed in thymocytes from Ctr and p53cKO mice (supplemental Figure 1C).

We started by comparing the thymic epithelium composition in control and p53cKO mice throughout life. Although with altered proportions in relation to controls, cTEC numbers were normal during fetal, postnatal, and prepuberty periods, becoming moderately diminished in 10-week-old p53cKO mice (Figure 1C-D). In contrast, though seemingly similar to control mice at E16.5, the frequency and numbers of mTECs were continually reduced in mutant mice from the postnatal period onward (Figure 1C-D). Concordantly, the global medullary compartment and the number of UEA^{+}mTECs were reduced in the adult p53cKO thymus, without affecting the compartmentalization into the cortex and medulla (supplemental Figure 1D). We assessed possible Cre-mediated cellular toxicity and found no major changes in thymic and cTEC/mTEC cellularities of $Foxn1^{Cre}$:$Trp53^{+/+}$ mice in comparison with $Trp53^{+/+}$ mice (supplemental Figure 1E). Age-matched $Trp53^{fl/fl}$ littermates were used as controls in subsequent experiments.

The impact of *Trp53* deletion in mTECs led us to examine their differentiation program. First, we subdivided mTECs into $CD80^{lo}$, which include immature cells and a minor subset of post-Aire terminally differentiated cells in the adult thymus, and mature $CD80^{hi}$, which contains Aire-expressing cells.[1,17] The development of $CD80^{hi}$ and $Aire^{+}$ mTECs was delayed in the embryonic p53cKO thymus but was normalized to the proportions of the control thymus during prepuberty (Figure 1E). Despite the restoration of complete mTEC differentiation, the number of $CD80^{hi}$ and $Aire^{+}$ mTECs was diminished in p53cKO thymus throughout life, whereas the $CD80^{lo}$ subset became affected only in adult mice (Figure 1F). Second, analysis of mTEC turnover revealed an increase in the rate of p53cKO mTECs in active cycling (S/G2/M) (supplemental Figure 1F). Moreover, we monitored the extent of DNA double-strand breaks[18] and apoptosis,

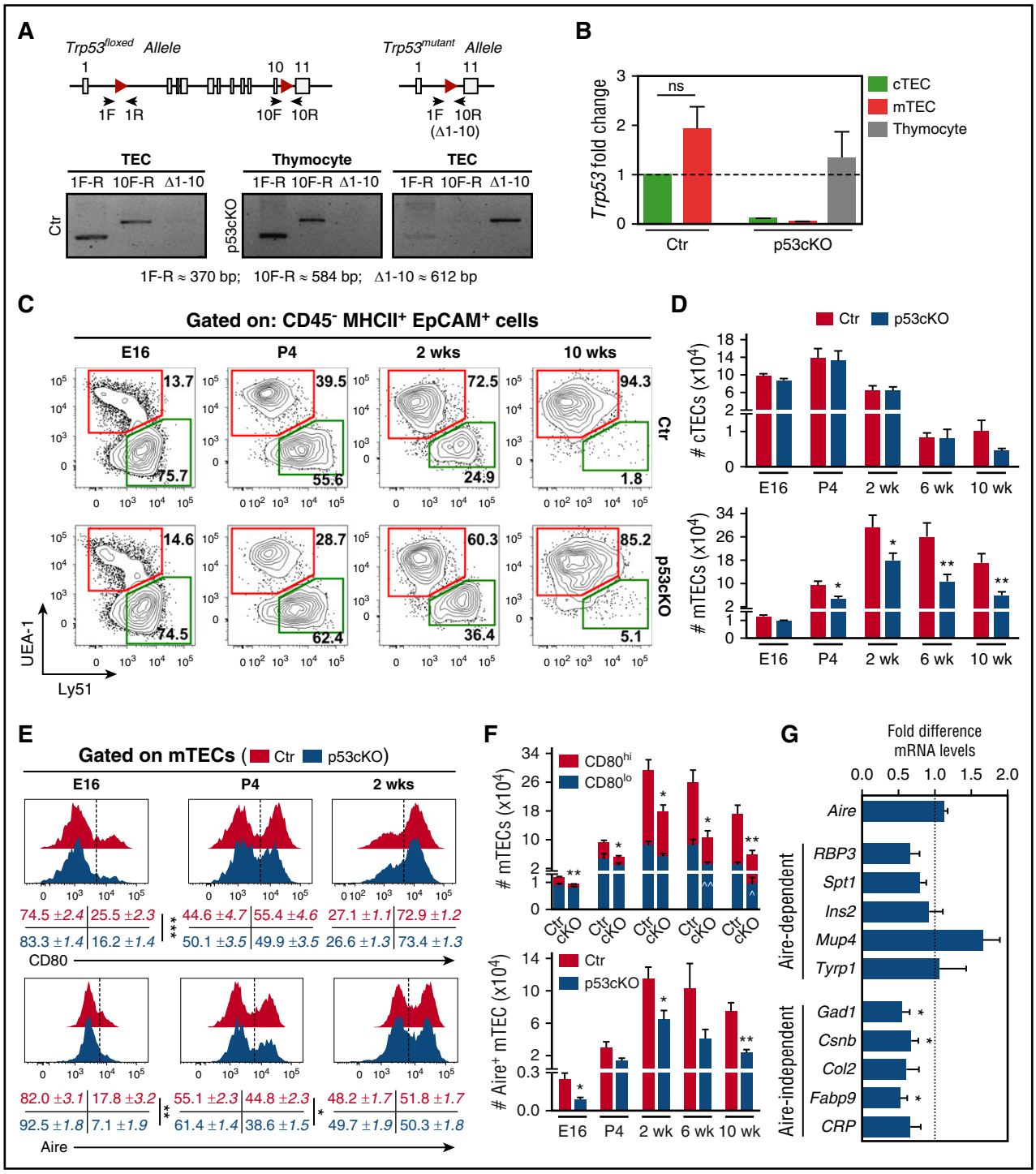

Figure 1. Ablation of *Trp53* in TECs diminishes the size of the mTEC niche. (A) Diagram of the genomic floxed and targeted *Trp53* alleles (top). *LoxP* sequences flank exons 2 through 10 (arrowheads). Examination of Foxn1:Cre-driven deletion of *Trp53* floxed allele by genomic PCR analysis (bottom) in FACS-sorted TECs (CD45$^-$EpCAM$^+$ MHCII$^+$) from Ctr mice and thymocytes (CD45$^+$) and TECs from p53cKO mice at 2 weeks of age, using the depicted primers (1F, 1R, 10F, and 10R). (B) qRT-PCR analysis of *Trp53* expression in FACS-sorted cTECs (UEA$^-$Ly51$^+$), mTECs (UEA$^+$Ly51$^-$), and thymocytes from 2-week-old Ctr and p53cKO mice. Products were detected by amplification of cDNA sequence-spanning exons 5 and 6. Values were normalized to *18s* ribosomal RNA. Values from Ctr cTECs were set as 1, and the fold change in *Trp53* was calculated in relation to the other subsets (mean ± standard error of the mean [SEM], representative of 4 independent experiments). (C-D) The composition of TECs was analyzed at the indicated time points. Flow cytometry analysis of cTECs and mTECs. Dot plots show representative Ly51/UEA staining in TECs (C). Average cellularity of cTECs (top) and mTECs (bottom) (D). Graphs represent data from 2 to 4 independent experiments per time point (n = 5 to 17 per group). (E) Expression of CD80 and Aire in mTECs of Ctr and p53cKO mice at the indicated time points. Numbers represent the average percentages (±SEM) of the gated mTEC subsets. (F) Average cellularity of the mTEC subsets depicted in panel E. Carats and asterisks (^ and *) compare immature and mature mTECs, respectively. The results in panels E and F are shown as mean ± SEM of 5 to 17 mice per group from 3 to 4 independent experiments. (G) Expression of Aire-dependent and Aire-independent TRAs measured by qRT-PCR in FACS-sorted mTECs from 2-week-old Ctr and p53cKO mice. Values were normalized to *18s* ribosomal RNA, and those in Ctr mTECs were set as 1. Graphs represent data from 3 independent experiments (mean ± SEM). ns, not significant; wk, week. */^$P < .05$; **/^^$P < .01$; ***$P < .001$.

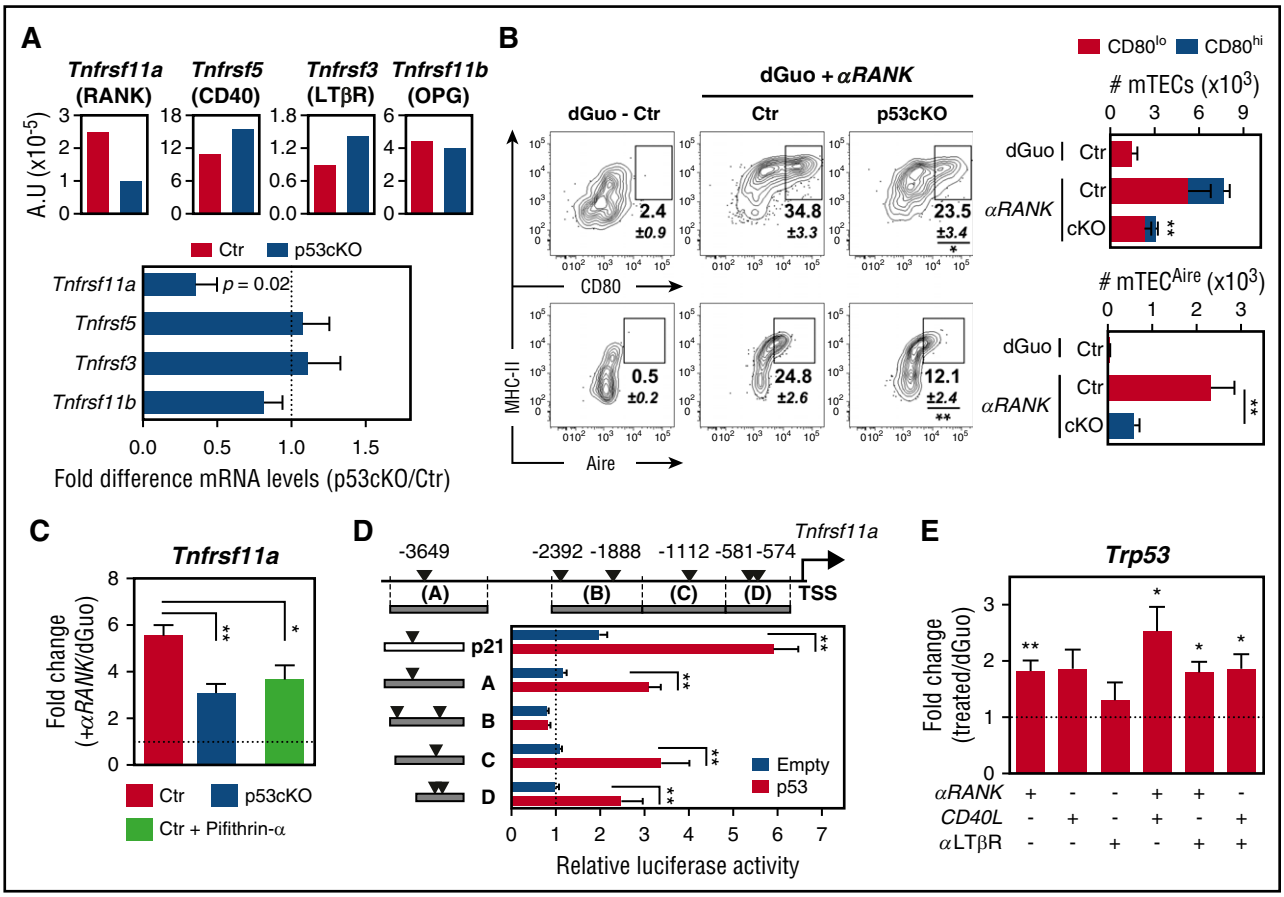

Figure 2. Ablation of *Trp53* in TECs limits the expression and responsiveness of RANK. (A) The expression of *Tnfrsf11a*, *Tnfrsf5*, *Tnfrsf3*, and *Tnfrsf11b* was assessed by qRT-PCR in FACS-sorted mTECs (UEA$^+$Ly51$^-$) from 2-week-old Ctr and p53cKO mice. Values were normalized to *18s* ribosomal RNA. Graphs represent data from 4 independent experiments (top). Fold difference in the relative mRNA levels between Ctr (dashed line) and p53cKO mTECs (bottom). (B) E15.5 dGuo-treated FTOCs from Ctr and p53cKO mice were cultured for 4 days with anti-RANK (αRANK). Expression of CD80 and Aire was analyzed in mTECs (UEA$^+$Ly51$^-$) by flow cytometry. Numbers indicate the mean percentage of gated cells. Graphs show the cellularity of mTEC subsets per thymic lobe. Number of asterisks compare mature mTECs from Ctr with p53cKO mice (top). Results are presented as mean ± SEM of 10 to 12 thymic lobes per group from 5 independent experiments. (C) The expression of *Tnfrsf11a* was analyzed by qRT-PCR in FACS-sorted TECs from Ctr and p53cKO E15.5 dGuo-treated FTOC stimulated over 24 hours with αRANK or αRANK plus Pifithrin-α. Values were normalized as in panel A, and those in TECs from nonstimulated dGuo-treated FTOC were set to 1. Graphs represent data from 3 to 6 independent experiments (mean ± SEM). (D) The region upstream of the *Tnfrsf11a* (RANK) TSS contains putative p53 response elements (REs) (triangles), identified on the basis of the p53 RE matrix logo (RRRC-A/T-A/T-GYYY motifs, in which R is a purine and Y is a pyrimidine) (MatInspector, rVista, or both, software tolls). DNA fragments (A-D) from the *Tnfrsf11a* (RANK) and *Cdkn1a* (p21) loci were cloned into the pGL3-Promoter reporter plasmid. p53 KO MEFs were transiently transfected with the indicated luciferase plasmids along with a p53 overexpressing construct (p53) or an empty construct (Empty). Luciferase reporter activity was normalized to the relative pGL3-promoter signal. Represented is the average of 3 independent experiments (±SEM). (E) The expression of *Trp53* was analyzed by qRT-PCR in FACS-sorted TECs from Ctr and p53cKO E15.5 dGuo-treated FTOC stimulated over 24 hours with anti-RANK, recombinant CD40L, and anti-LTβR at different combinations. Values were normalized as in panel A, and those in TECs from nonstimulated dGuo-treated FTOC were set to 1. Data are representative of 4 independent experiments (mean ± SEM). A.U., arbitrary units; MHC, major histocompatibility complex. *$P < .05$; **$P < .01$.

and found that the percentages of phosphorylated γ-H2AX and annexin V$^+$, respectively, were slightly increased in p53cKO mTECs, particularly within CD80^{lo} cells (supplemental Figure 1G-H). These findings suggest that increased apoptosis rather than defective proliferation might contribute to the reduced number of mTECs in p53cKO mice. Lastly, analysis of the expression of a panel of TRAs showed that Aire-independent genes were downregulated in p53cKO mTECs, whereas Aire-dependent genes presented a variable pattern in both mTEC subtypes (Figure 1G). Our data suggest that p53 is superfluous for cTEC/mTEC specification but instead controls mTEC homeostasis.

p53 regulates RANK expression in TECs

The similarity between the mTEC-phenotype of p53cKO mice and that of mice with defects in RANK, CD40,and LTβR[19] led us to evaluate whether p53 fine-tunes the expression of these TNFRSF members. Additionally, we analyzed the expression of osteoprotegerin (OPG), a decoy receptor of RANK ligand.[19] Although the levels of *Tnfrsf5* (CD40), *Tnfrsf3* (LTβR), and *Tnfrsf11b* (OPG) were normal, the expression of *Tnfrsf11a* (RANK) was reduced in p53cKO mTECs (Figure 2A). To examine the functional relationship between p53 and RANK, we used well-defined in vitro models of mTEC differentiation, in which E15.5 dGuo-FTOCs were depleted of hematopoietic cells and then stimulated through RANK.[12] Strikingly, the frequency and numbers of mature CD80$^+$ and Aire$^+$ mTECs in RANK-stimulated p53cKO dGuo-FTOCs were reduced in relation to controls (Figure 2B). Contrarily, CD40-mediated mTEC maturation and CD40 expression on p53cKO mTECs were unaffected (supplemental Figure 2A-B). Hence, loss of p53 appeared to specifically dampen in vitro mTEC differentiation induced by RANK. Given that RANK activation induces its own expression,[20] we evaluated whether p53 positively controls this self-amplification loop. Concordantly, RANK-mediated stimulation augmented the expression of *Tnfrsf11a*

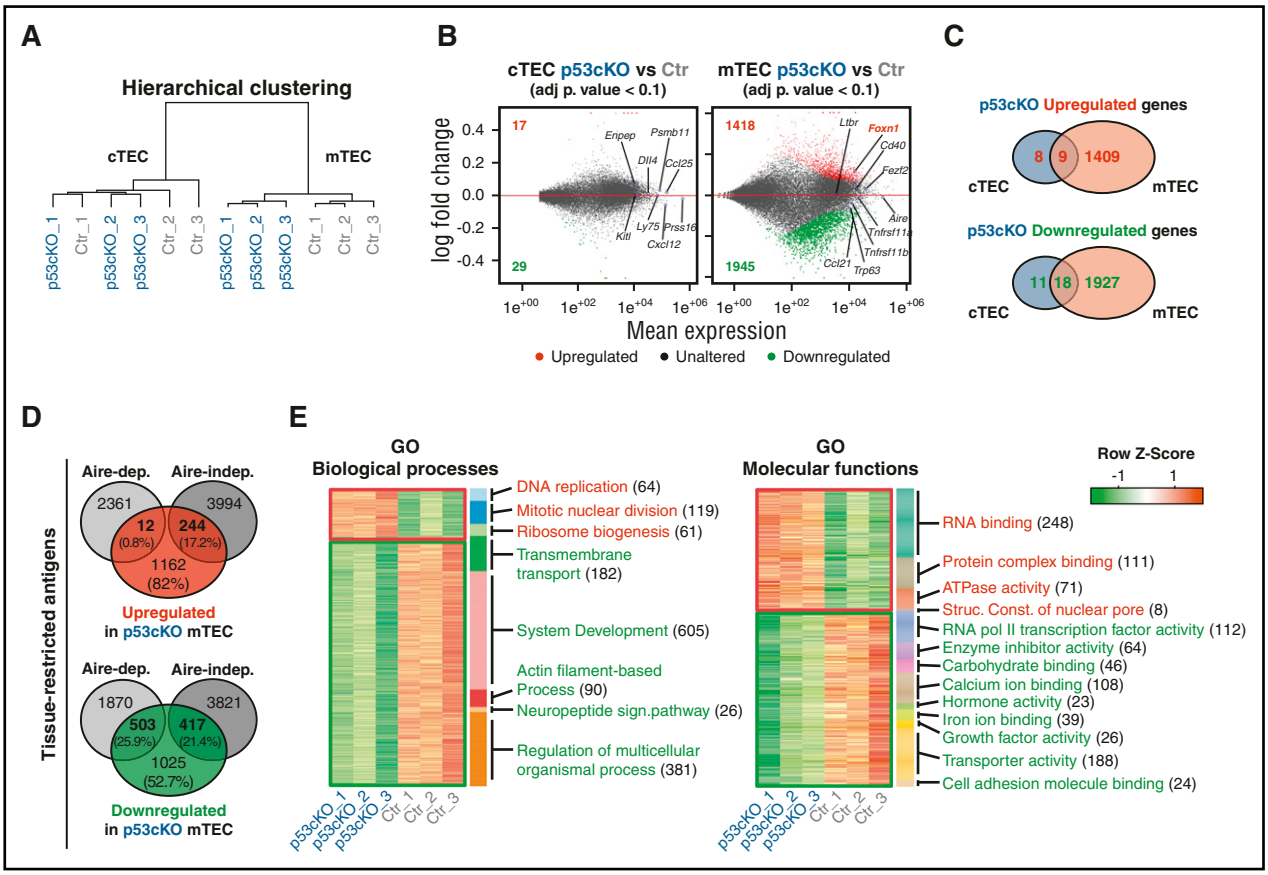

Figure 3. Impact of p53 in the transcriptome of cTECs and mTECs. RNA-Seq analysis of FACS-sorted cTECs and mTECs purified from 2-week-old Ctr and p53cKO mice, including 3 biological replicates per subset. (A) Hierarchical clustering of all samples by gene expression correlation distance for the top 1000 most diverse genes. (B) Comparison of the transcriptome of cTECs from p53cKO versus Ctr mice (left) and mTECs from p53cKO versus Ctr mice (right). Minus-average plots showed the log2-fold change (y-axis) versus the mean expression (x-axis) of total genes obtained by comparison. Genes with a log2-fold change that present an adjusted *P* value that is <0.1 were called differentially expressed (DE). Upregulated and downregulated DE genes in p53cKO samples are highlighted in red and green, respectively, together with their numbers. Unaltered genes are depicted in gray. (C) Venn diagrams represent the number of upregulated (top) or downregulated (bottom) DE genes in cTECs (blue) and mTECs (salmon) of p53cKO versus Ctr mice. (D) Venn diagrams show the number and proportion of upregulated (red) and downregulated (green) genes of p53cKO mTECs within Aire-dependent or Aire-independent TRA genes, as defined by Sansom et al.[25] (E) Heat map of enriched biological processes (left) and molecular functions (right) in upregulated (red) or downregulated (green) DE genes of p53cKO mTECs. Represented are activated (red) or inhibited (green) categories with a marginal posterior probability estimate that is >0.65. In parentheses are indicated the number of DE genes per GO category. Adj p, adjusted *P*; Aire-dep, Aire-dependent; Aire-indep, Aire-independent; ATP, adenosine triphosphate; Struc. Const., structural constituent.

in TECs from control dGuo-FTOC. Noticeably, this increase was attenuated in TECs from both RANK-activated p53cKO dGuo-FTOC and RANK-activated control dGuo-FTOC cotreated with the p53 inhibitor pifithrin-α (Figure 2C), indicating that p53 controls the expression of *Tnfrsf11a*. In silico analysis identified 6 putative p53 REs[21] within the 4kb region upstream of the transcription start site (TSS) of *Tnfrsf11a* (Figure 2D). We cloned 1kb genomic DNA fragments containing these potential p53 REs (named A-D) into a luciferase reporter plasmid and assessed their p53-mediated transactivation in p53-deficient MEFs, which were cotransfected with a p53-expressing vector. As a positive control, we used a *Cdkn1a* (p21)-derived fragment containing a bona fide p53 RE.[21] Notably, p53 increased luciferase expression driven by *Tnfrsf11a*-derived fragments A, C, and D, but not B (Figure 2D). These results imply that p53 has the potential to control the activity of *Tnfrsf11a* promoter. To study whether p53 was reciprocally induced under mTEC differentiating conditions, we activated control dGuo-FTOCs with RANK, CD40, and LTβR agonists. Contrary to LTβR stimulation, individual RANK- and CD40-engagement induced *Trp53* expression in TECs, an effect that was further augmented by combined activation (Figure 2E). These results indicate that both RANK and CD40 signaling induce p53, which in turn promotes RANK expression and RANK-driven mTEC differentiation.

p53 specifically regulates a broad network of the mTEC transcriptome

Given that p53 governs multiple transcriptional programs in distinct cells,[22-24] we examined its genome-wide influence in TECs. To do so, we performed RNA sequencing (RNA-Seq) analysis and compared the transcriptome of cTECs and mTECs isolated from 2-week-old control and p53cKO mice. We selected this age to permit the maturation of mTEC, the emergence of p53cKO phenotype, and the sufficient abundance of cTEC/mTEC subsets for analysis. The number of genes expressed in the control and p53cKO mTECs was higher than in their cTEC counterparts, resulting in the expected cTEC/mTEC segregation (Figure 3A and supplemental Figure 3A-B). *Trp53* levels were increased in control mTECs and markedly reduced in p53cKO-derived TEC subsets. The expression of cTEC- and mTEC-associated genes separated the 2 lineages independently of their genotype (supplemental Figure 3 C-D), validating the accuracy of sorted samples. Strikingly,

though randomly associated within cTEC subsets, the biological replicates of control and p53cKO mTECs defined 2 distinct clusters (Figure 3A). Accordingly, the number of differentially expressed genes between p53cKO and control mTECs was substantially larger than in cTECs (Figure 3B and supplemental Tables 1-2). The identification of 1418 upregulated genes and 1945 downregulated genes in p53cKO mTECs implies that p53 negatively and positively regulates gene expression in mTECs (Figure 3C). Concordant with previous observations, *Tnfrsf11a* expression was reduced in p53cKO mTECs analyzed by RNA-seq and quantitative RT-PCR (qRT-PCR) (supplemental Figure 3E). Yet, RANK was not identified among the list of differentially expressed genes most possibly due to the stringent statistical analysis of RNA-Seq, differences in gene normalization, and intrathymic sample variation.

Using a publicly available annotated list of TRA genes,[25] we next cross-examined their representation within differentially expressed genes of p53cKO mTECs. Notably, nearly half of the downregulated genes in p53cKO mTECs comprised purported TRAs, with a similar incidence of Aire-dependent and Aire-independent targets (Figure 3D). The proportion of TRAs within upregulated genes of p53cKO mTECs was lower, including mostly Aire-independent targets (Figure 3D). These data suggest that p53 regulates promiscuous gene expression in mTECs. Additionally, GO enrichment analysis in differentially expressed genes did not reveal any particular term in cTECs but was associated to diverse functional categories in p53cKO mTECs. Specifically, upregulated genes indicated an increase in DNA replication, mitosis, ribosome biogenesis, RNA and protein complex binding, ATPase activity, and constituents of nuclear pore. Conversely, downregulated genes suggested an attenuation in transmembrane transport; actin filament-based process; neuropeptide signaling pathway; carbohydrate and ion binding; and RNAPII transcription factor, enzyme inhibitor, hormone-factor, and growth-factor activity (Figure 3E and supplemental Tables 3-6). Concordant to the mTEC-restricted phenotype of p53cKO mice, these results suggest that p53 controls a multifaceted transcriptional program in mTECs.

Adult p53cKO mice display an impaired regular and regenerative thymopoiesis

We then analyzed how the described changes in TEC microenvironments affected the thymic activity of p53cKO mice. The frequency and abundance of major thymocyte subsets, including early thymic precursors (ETP), double-negative (DN) subsets, and double-positive (DP) and single-positive (SP) CD4 and CD8 cells, were comparable in control and mutant mice during fetal and prepuberty life (Figure 4A-C). Notably, a global deficit in thymopoiesis appeared in 10-week-old p53cKO mice (Figure 4A), without altering the global T-cell differentiation program. Namely, the progression through DN1-DN4 stages and the rate of positive selection, as measured by the frequency of $CD3^+CD69^+$ thymocytes, were largely similar between the control and p53cKO thymus (Figure 4B). However, we found a reduction in the proportion of DN1s and ETPs in the p53cKO thymus (Figure 4B). Correspondingly, the numbers of all major thymic subsets steadily declined in p53cKO mice, this trend being apparent in 6-week-old mice (Figure 4C). These perturbations extended to the peripheral T-cell compartment of adult p53cKO mice, with a reduction in splenic CD4 and CD8 T-cell counts (Figure 4D). The dysfunctional nature of the adult mutant thymus led us to further analyze their regenerative capacity following ionizing radiation. Although numerically different at baseline, mTECs were markedly depleted in both groups 5 days after sublethal total-body irradiation (supplemental Figure 4A). This reduction was attenuated in p53cKO mTECs supplemental Figure 4A), suggesting that ablation of p53 conferred a slight protection to radiation-induced apoptosis. Although the recovery of cTECs was similar in both groups, the restoration of mTEC cellularity, including $CD80^+$ and $Aire^+$ subsets, was markedly impaired in p53cKO mice (supplemental Figure 4A-C). Additionally, the recovery of thymopoiesis was also significantly compromised in p53cKO mice (Figure 4E), affecting de novo generation of all major thymic subsets (Figure 4F) and the reconstitution of the peripheral T cells (Figure 4G). Our findings indicate that adult p53cKO mice fail to maintain normal and regenerative thymopoiesis.

mTEC-dependent thymopoiesis is compromised in p53cKO mice

As the loss of mTECs preceded the deterioration of thymopoiesis during adulthood, we examined whether the stages of T-cell development that were functionally linked to mTECs[1] were prematurely affected in p53cKO thymus. To survey cortical and medullary clonal deletion, we assessed the frequency of DP and SP4 thymocytes that coexpressed PD-1 and Helios,[26] respectively, and found no major differences between control and p53cKO thymus (Figure 5A). Moreover, we crossed p53cKO mice with Marilyn-$Rag2^{-/-}$ TCR transgenic mice, in which thymocytes express $I\text{-}A^b$-restricted HY-specific TCR.[12] Thymocyte development in the p53cKO background reproduced that observed in controls, with a similar number of positively and negatively selected thymocytes in female and male mice, respectively (Figure 5B). In line with the absence of SP4 accumulation at steady state (Figure 4B), these results indicated that negative selection seemed intact in p53cKO mice. Strikingly, analysis of regulatory T-cell differentiation and postselection SP maturation showed a respective decrease in the proportions and numbers of $CD25^+Foxp3^+$ regulatory T cells and mature $CD24^{lo}CD62L^{hi}$ SP4 thymocytes in mutant thymus (Figure 5 C-D). These findings implicate a requirement for p53 in TECs to maintain continual mTEC-dependent thymopoiesis.

Signs of disturbed peripheral tolerance unfold in p53cKO mice

The alterations in mTECs led us to seek signs of peripheral autoimmune manifestations in mutant mice. We did not detect the presence of autoantibodies against multiple organs (stomach, testis, liver, salivary, and lacrimal glands) in the serum of aged p53cKO mice in comparison with controls (data not shown). Yet larger and more prevalent lymphocytic infiltrations were found in the salivary and lacrimal glands of aged p53cKO mice (Figure 6A-B, supplemental Figure 5A). Despite the reduction in the numbers of thymic regulatory T cells, their frequency in the spleen of adult p53cKO mice was normal (supplemental Figure 5B). However, as total peripheral CD4 T cell counts were reduced (Figure 4D), both conventional and regulatory T cells were diminished in mutant mice (supplemental Figure 5B). Moreover, p53cKO-derived peripheral regulatory T cells suppressed polyclonal T-cell activation in vitro (supplemental Figure 5C), showing a broad intact function and potentially explaining the mild autoimmune manifestations. These findings suggest that the perturbed mTEC niche of p53cKO mice might predispose to defects in tolerance. The development of autoimmunity coupled with defects in mTECs is normally contained in the C56BL/6 background but is potentiated by lymphopenia, as is observed in the case of Aire and XCL1 deficiencies.[27,28] To examine the functional link between scarce mTEC niches and disturbed T-cell tolerance in p53cKO mice, we adoptively transferred thymocytes derived from control and mutant adult thymus into $Rag2^{-/-}$ mice and monitored recipient mice for clinical signs of disease. Recipient mice that received p53cKO-derived thymocytes exhibited accelerated weight loss, developed diarrhea and presented

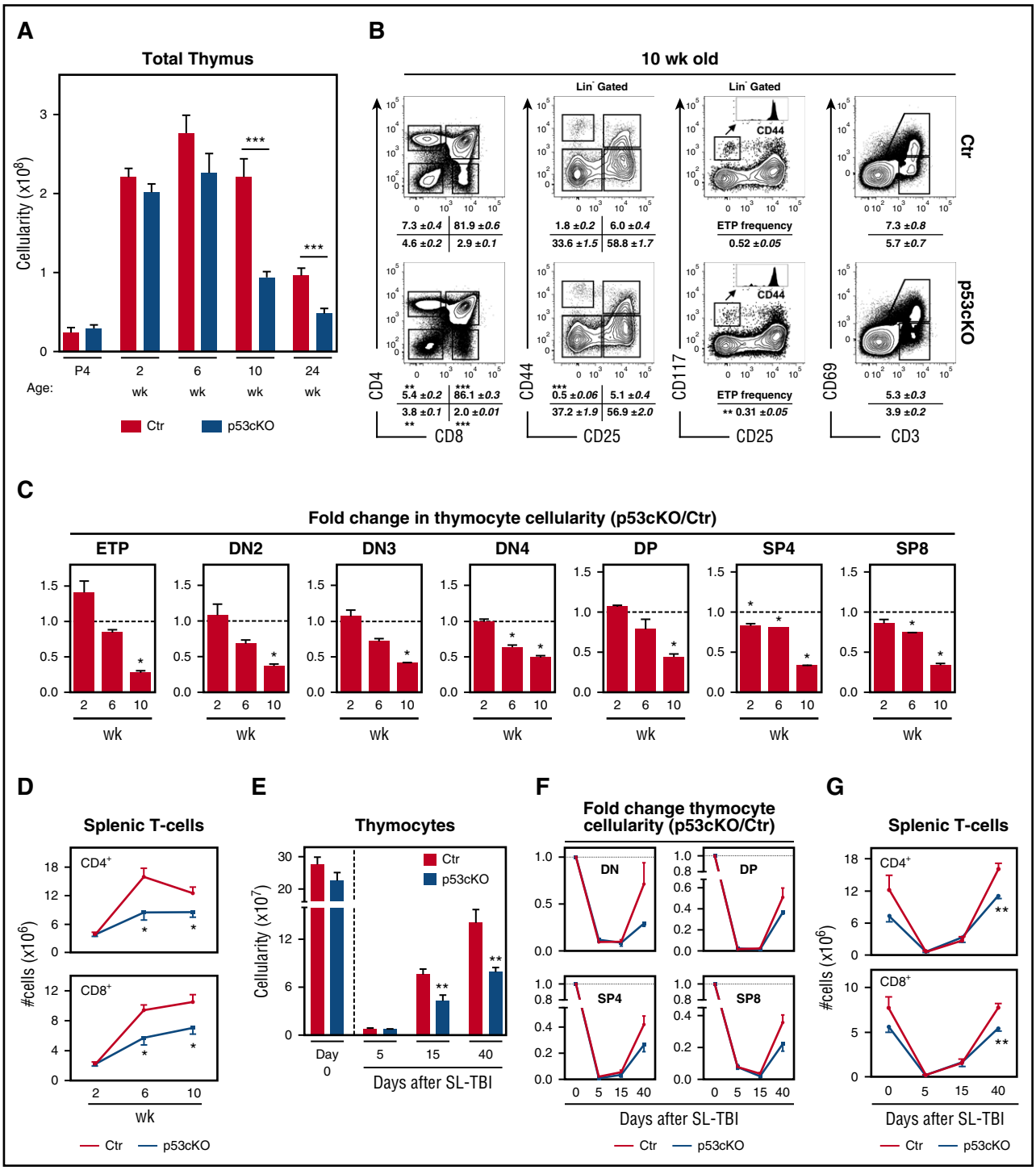

Figure 4. Altered thymopoiesis in p53cKO mice. (A) Thymic cellularity of Ctr and p53cKO mice at various ages. (B) Flow cytometry analysis of T-cell development in 10-week-old Ctr and p53cKO thymus: CD4/CD8 expression on total thymocytes (left); CD44/CD25 expression on DN thymocytes (gated on Lin^- cells) (middle left); CD177/CD25 expression on DN thymocytes (gated on Lin^- cells) (middle right). ETPs are defined as Lin^- $CD177^+CD44^+CD25^-$; CD69/CD3 expression on total thymocytes (right). Numbers indicate the frequencies of the different subsets (mean ± SEM). (C) Fold change in the number of the indicated thymocyte subsets. For each time point, the values of Ctr mice were set as 1 (dashed line) and compared in relation to p53cKO mice. Graphs represent data from 2 to 3 experiments per time point (n = 6 to 8 mice per group; mean ± SEM). (D) Absolute number of splenic $CD4^+$ and $CD8^+$ T cells in Ctr and p53cKO mice at different time points. (E) Thymocyte cellularity of sublethally irradiated 6-week-old Ctr and p53cKO mice at the indicated time points posttreatment. (F) Fold change in the cellularity of the thymocyte subsets following sublethal total-body irradiation (SL-TBI). For each time point, the values of nonirradiated Ctr or p53cKO mice were set as 1 (dotted line) and to the ones obtained for SL-TBI Ctr and p53cKO thymus, respectively, at each time point. (G) Numbers of splenic $CD4^+$ and $CD8^+$ T cells in Ctr and p53cKO mice after SL-TBI. SL-TBI, sublethal total-body irradiation. $^*P < .05$; $^{**}P < .01$; $^{***}P < .001$.

lymphocytic infiltration and tissue damage in the colon (Figure 6C). The presence of T cells in the spleen of both groups indicated an effective cell transfer (supplemental Figure 5D). Similar to the analysis at steady state, small lymphocyte infiltrates were also more frequent in the salivary glands of the same group (Figure 6D). Our results indicate that the p53 mutant thymus renders developing T cells more susceptible to

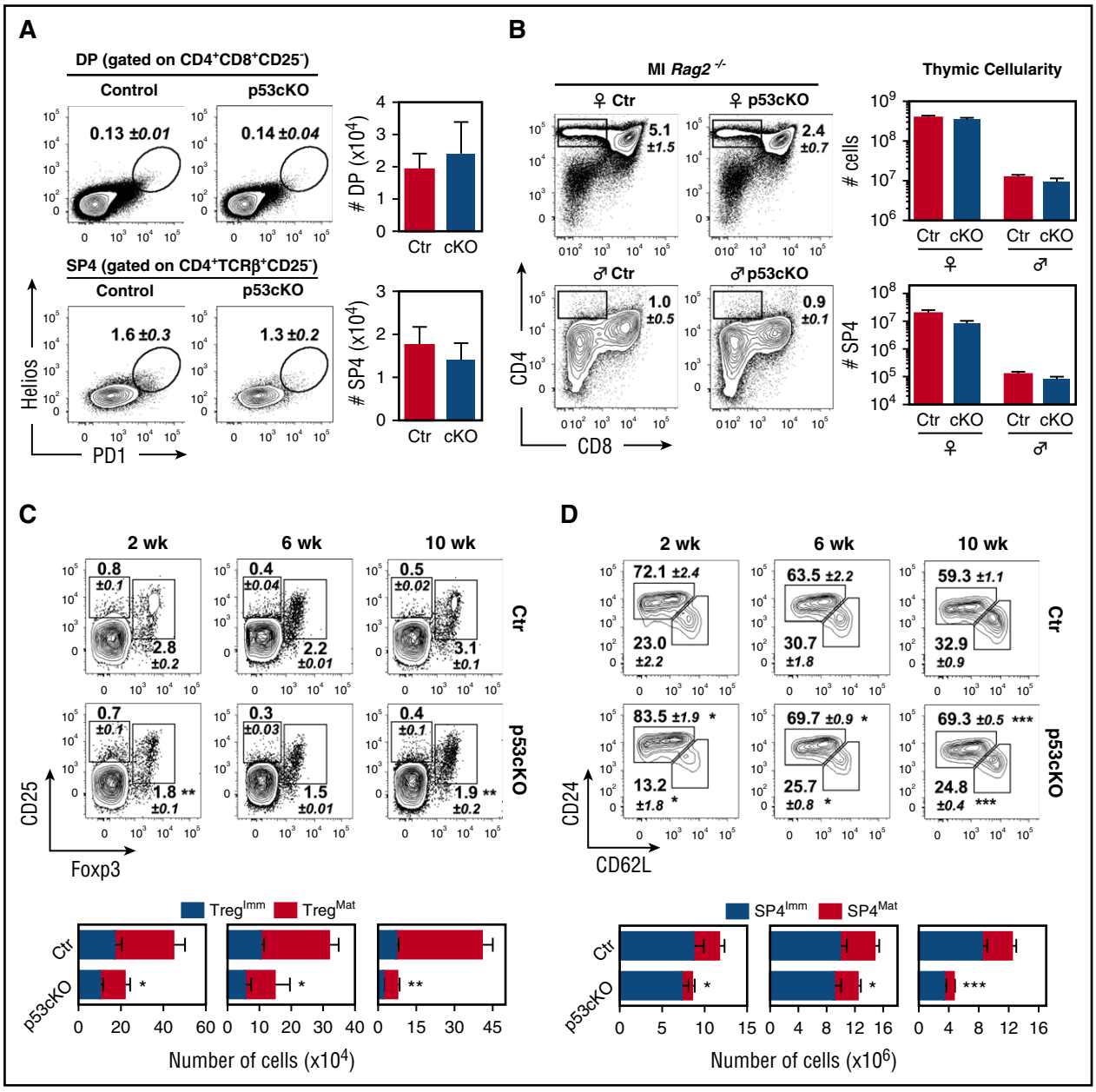

Figure 5. Loss of p53 in TECs reduces specific mTEC-mediated functions. (A) DP (TCRβ$^+$CD4$^+$CD8$^+$CD25$^-$) and SP4 (TCRβ$^+$CD4$^+$CD8$^-$CD25$^-$) thymocytes isolated from 8-week-old Control (Ctr) and p53cKO mice were analyzed for the expression of Helios and PD1. Numbers indicate the mean percentage of gated cells. Graphs show the total number of Helios$^+$PD1$^+$ thymocytes within the DP and SP4 stage and represent data from 2 independent experiments (n = 4 to 5 mice per group; mean ± SEM). (B) Flow cytometry analysis of thymic selection in 8-week-old female and male Ctr and p53cKO Marilyn-*Rag2*$^{-/-}$ thymus. Numbers indicate the frequencies of SP4 thymocytes (mean ± SEM). Thymic cellularity (top) and the number of SP4 thymocytes (bottom) are depicted on the graphs. Data represent the average of 3 independent experiments (n = 5 to 6 mice per group; mean ± SEM). (C-D) SP4 thymocytes (CD8$^-$CD4$^+$TCRβ$^+$) were analyzed for the expression of CD25 and Foxp3 (C) and CD24 and CD62L (D) at the indicated time points. Numbers indicate the average percentage of gated cells (±SEM). Graphs represent the number of immature (CD25$^+$Foxp3$^-$) and mature (CD25$^+$Foxp3$^+$) regulatory T cells (Tregs) (left) (C); the number of immature (CD24^{hi}CD62L^{low}) and mature (CD24^{low}CD62L^{hi}) SP4 thymocytes (right) (D). The asterisk compares mature Treg and mature SP4 cells between Ctr and p53cKO mice. In panels C-D, graphs represent data from 3 independent experiments (n = 4 to 13 mice per group). Results are presented as mean ± SEM. MI, Marilyn-*Rag2*$^{-/-}$ thymus. ♀, female; ♂, male; *P < .05; **P < .01; ***P < .001.

failure in establishing peripheral self-tolerance in aged and lymphopenia settings.

Discussion

Our study positions p53 as a prime determinant of mTEC integrity in vivo, mapping a functional link between p53 and RANK in mTECs. This was manifested by a reduced RANK-driven mTEC induction in the p53cKO thymus in vitro, an observation that curiously mirrored the delayed appearance of embryonic p53cKO mature mTECs in vivo. We found that mTECs express higher levels of p53 than do cTECs and that p53 was reciprocally induced following RANK and CD40 stimulation. These results are consistent with previous studies coupling p53 induction to the NFκB pathway,[29] which is in turn engaged by mTEC-inducing TNFRSF signaling.[19] Yet the reduction in mTECs of p53cKO mice was not as severe as that reported in RANK-deficient mice.[19] The

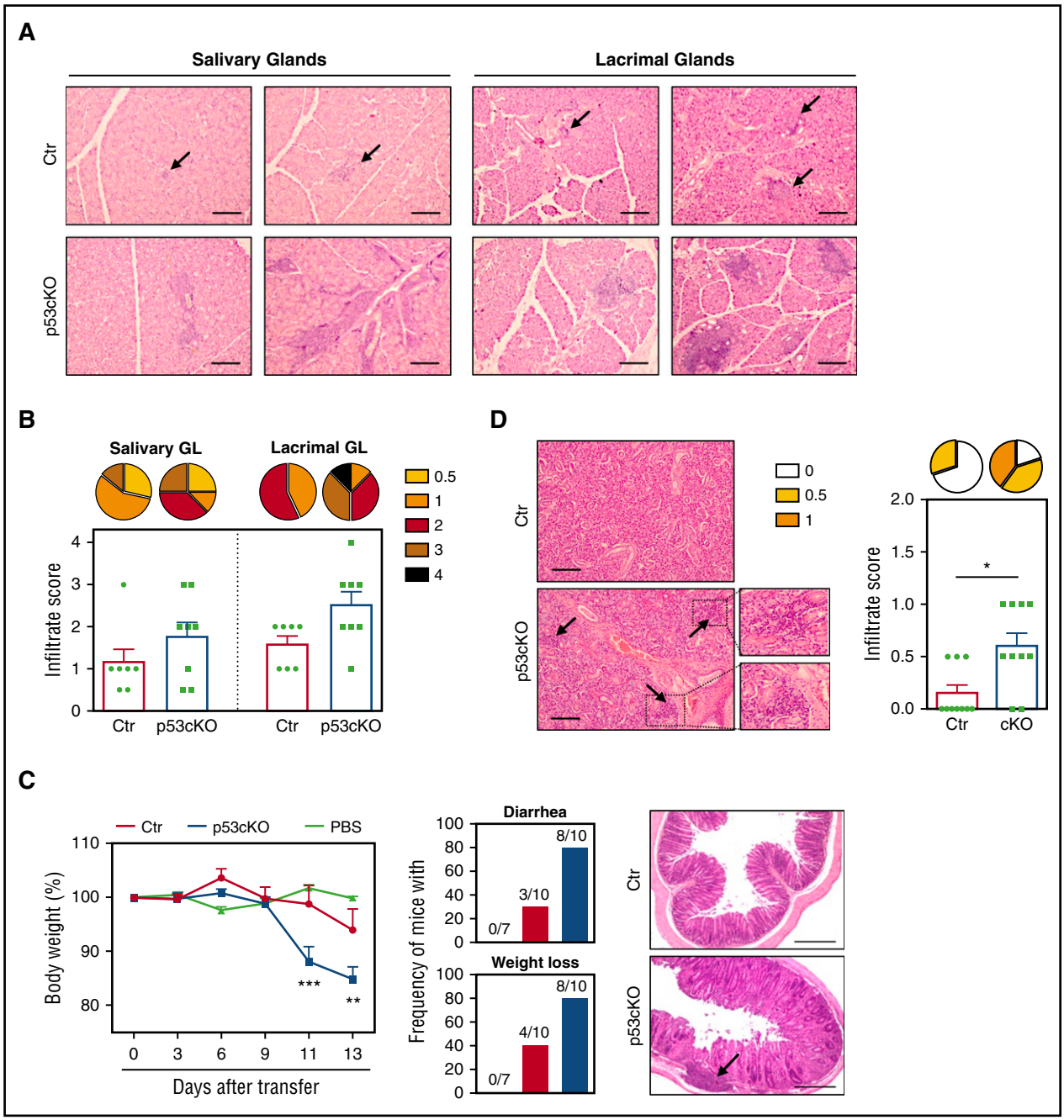

Figure 6. TEC-specific deletion of p53 affects the establishment of peripheral T-cell tolerance. (A) Representative analysis (H&E staining) of the salivary and lacrimal glands obtained from 6- to 7-month-old Ctr and p53cKO mice. (B) Histological scores of inflammatory infiltrates. Pie graphs show the frequency of inflammatory lesions according to their severity. (C) Thymocytes from 10-week-old Ctr (red line) and p53cKO (blue line) mice were intravenously transferred into *Rag2*$^{-/-}$ mice. As a control, *Rag2*$^{-/-}$ mice were treated with phosphate-buffered saline (green line). Change in the body weight of *Rag2*$^{-/-}$ recipients after thymocyte transfer (left). Incidence of diarrhea and weight loss, with the indicated number of recipient mice that develop symptoms (middle). Images show the histological analysis (H&E staining) of the colon of the *Rag2*$^{-/-}$ recipients 14 days after transfer (right). (D) Histological analysis and inflammatory score of the salivary glands. Pie graphs represent the frequency of inflammatory lesions according to their severity. Arrows in panels A, C, and D outline lymphocytic infiltrates. Results are presented as mean ± SEM. Scale bars, 100 μm. PBS, phosphate-buffered saline. *$P < .05$; **$P < .01$; ***$P < .001$.

differentiation of mTECs depends on the coordinated action of RANK, CD40, and LTβR signaling.[1] It is conceivable that compensatory signals via CD40 and LTβR contribute to the mTEC maturation program of p53cKO mice. Hence, p53 seems to fine-tune, rather than determine, RANK signaling in mTECs, cooperating in a functional feed-forward loop to sustain the medullary epithelial compartment.

Our results suggest that p53 functions as a molecular hub in mTECs, regulating a wide transcriptional program that extends beyond balancing RANK expression. Typically, p53 is maintained at low levels under steady-state conditions, being activated in response to various stress signals.[21] Nonetheless, p53 also has basal transcriptional functions in unstressed cells.[23] Apart from RANK and CD40, it is possible that additional extrinsic and intrinsic cues generated within the thymus trigger a p53-driven response in mTECs. Although the mechanisms that induce p53 in mTECs remain elusive, our observations argue that its activity is not dormant. Genome-wide

chromatin-binding approaches revealed extensive and distinct cell-specific p53-driven transcription programs,[22-24] indicating that p53-mediated gene expression is context dependent. We found that p53 controls a broad set of genes linked to core processes in mTEC biology, which are not related to other well-known mechanisms controlling mTEC maintenance. The increased apoptosis susceptibility of p53-deficient mTECs might be a corollary of these broad alterations, possibly explaining the reduced mTEC compartment of p53cKO mice. Yet the presumed asynchrony of apoptosis at a population level and the rapid clearance of dying cells may confound measurements of cell death in vivo. Moreover, it remains to be determined whether differentially expressed genes are directly regulated by p53 or indirectly influenced through the perturbation of downstream genes of the p53-induced pathway. Further studies should elucidate the individual contribution of these gene products or processes to the maintenance of mTEC homeostasis and their homo- and heterotypic cellular interactions within the thymus. It is also important to consider that the hyperactive transcriptional state of mTECs might facilitate the accessibility of p53 to its target genes. The large prevalence of TRAs among the differentially expressed genes of p53cKO mTECs suggests that p53 influences promiscuous gene expression. Still, the expression of Aire[25] and Fezf2[4] was normal in p53cKO mTECs. Because mTECs express clusters of TRAs at a single-cell level,[3,30] the reduction in TRAs might alternatively reflect an underrepresentation of certain mTEC subsets in mutant thymus.

The disruption in the mTEC niche appeared to spread to the cTEC compartment in the adult p53cKO mice, evolving to a global failure in regular and regenerative thymopoiesis. The deficit in thymic activity extended to a decrease in splenic T cells, reinforcing the notion that peripheral T-cell homeostasis in mice also depends on regular thymic output.[31] Thus, the sustainability of the mTEC niche seems to be a deterministic factor in regulating thymic function. How the changes in mTECs are reflected in the cortex is intriguing. The phenotype and transcriptional profile of cTECs, as well as the early T-cell development and positive selection, were apparently normal in p53cKO mice. Yet we cannot formally exclude that p53 directly regulates cTEC homeostasis later in life. Alternatively, changes in mTECs might perturb the corticomedullary junction and cortex, thereby limiting the number of BM-derived thymic progenitors and the magnitude of premedullary stages of T-cell differentiation. Accordingly, the numbers of ETPs, DN, and DP thymocytes were diminished in aged p53cKO mice, providing a possible explanation for thymic hypoplasia. These findings could implicate the existence of a complex functional and structural interplay between TEC and nonepithelial cell subsets (eg, endothelia and mesenchyme) in balancing thymopoiesis.

The contracted mTEC compartment of p53cKO mice was physiologically linked to abnormalities in mTEC-dependent regulatory T-cell differentiation and SP maturation, providing a possible molecular explanation for the signs of deregulated immunological tolerance in mutant mice. Albeit negative selection seemed normal at a polyclonal level, we cannot exclude the possibility that rare autoreactive thymocytes escape from the p53cKO thymus. In line with previous studies,[32] we reason that the underrepresentation of regulatory T cells and mature SP4 represents the footprint of a decrease in the availability of mTEC niches. Concordantly, mild signs of autoimmune manifestations unfolded in aged p53cKO mice and in immunodeficient mice receiving p53cKO-derived thymocytes. Although we did not provide a direct link between the disturbed tolerance and the deficiency in regulatory T- cell numbers or their specificities and the specificities of conventional T cells, our findings suggest that the insufficient mTEC niche of p53cKO mice predisposes to defects in immune tolerance under lymphopenia. Also, the signs of abnormal immunological tolerance in p53cKO mice were weaker in comparison with other mTEC-deficient conditions.[19] We reason that the remaining mTEC niche of mutant thymus, together with the genetic background and extrathymic compensatory mechanisms, allows the establishment of peripheral tolerance during the first weeks of age, a period that is sufficient to prevent the development of autoimmunity.[33] Future studies should identify the distinct contribution of altered thymic and peripheral T-cell subsets to the disturbed tolerance induction of mutant mice.

Beyond positioning p53 as a novel guardian of thymus function, our findings are also of clinical relevance and reinforce the notion of a modulatory role for p53 in immune homeostasis and autoimmunity.[5] Moreover, the use of p53 inhibitors, such as Pifithrin-β, has been approved in clinical trials to attenuate the side effects of chemotherapy.[9] Given the described adverse impact of disrupting p53 in TECs and in T cells,[5] the therapeutic use of p53 inhibitors must be implemented with care to safeguard the balance between immune reconstitution and tolerance induction.

Acknowledgments

The authors thank Thomas Boehm (Max Planck Institute of Immunology and Epigenetics) for Foxn1-Cre mice; Rui Appelberg (I3S) and Nuno Rodrigues dos Santos (I3S) for critical reading of the manuscript; Matthias Futschik and José Pedro Pinto (University of Algarve) for critical discussions; and Sofia Lamas, Rui Fernandes, Catarina Leitão, and the caretakers from the animal facility for technical assistance.

This study was supported by the European Research Council (ERC) under the European Union's Horizon 2020 research and innovation program (grant agreement No 637843-TEC_Pro) starting grant attributed to N.L.A., by FEDER (Fundo Europeu de Desenvolvimento Regional) funds through the Operational Competitiveness Programme–COMPETE, and by National Funds through Fundação para a Ciência e a Tecnologia (FCT) under the project FCOMP-01-0124-FEDER-021075 (PTDC/SAU-IMU/117057/2010), by NORTE-01-0145-FEDER-000012–Structured program on bioengineered therapies for infectious diseases and tissue regeneration, supported by Norte Portugal Regional Operational Programme (NORTE 2020), under the PORTUGAL 2020 Partnership Agreement, through the European Regional Development Fund (FEDER); by FEDER funds through the COMPETE 2020–Operational Programme for Competitiveness and Internationalisation (POCI), Portugal 2020, and by Portuguese funds through FCT/Ministério da Ciência, Tecnologia e Inovação in the framework of the project Institute for Research and Innovation in Health Sciences (POCI-01-0145-FEDER-007274). The Investigator Program and doctoral and postdoctoral fellowships from FCT support N.L.A., P.M.R., A.R.R., I.P.-C., and C.M.

Authorship

Contribution: N.L.A. conceived and performed the experiments, wrote the manuscript, and secured funding; P.M.R. conceived and performed the experiments and wrote the manuscript; A.R.R., C.P., L.A., J.J.M.L., V.B., I.P.-C., H.X.-F., and C.M. performed the experiments; and A.M. provided expertise and feedback.

Conflict-of-interest disclosure: The authors declare no competing financial interests.

ORCID profiles: N.L.A., 0000-0002-1567-8389.

Correspondence: Nuno L. Alves, Instituto de Investigação e Inovação em Saúde (I3S), Instituto de Biologia Molecular e Celular, Rua Alfredo Allen, 208, 4200-135 Porto, Portugal; e-mail: nalves@ibmc.up.pt.

References

1. Anderson G, Takahama Y. Thymic epithelial cells: working class heroes for T cell development and repertoire selection. *Trends Immunol*. 2012;33(6):256-263.
2. Kyewski B, Klein L. A central role for central tolerance. *Annu Rev Immunol*. 2006;24:571-606.
3. Meredith M, Zemmour D, Mathis D, Benoist C. Aire controls gene expression in the thymic epithelium with ordered stochasticity. *Nat Immunol*. 2015;16(9):942-949.
4. Takaba H, Morishita Y, Tomofuji Y, et al. Fezf2 orchestrates a thymic program of self-antigen expression for immune tolerance. *Cell*. 2015;163(4):975-987.
5. Muñoz-Fontela C, Mandinova A, Aaronson SA, Lee SW. Emerging roles of p53 and other tumour-suppressor genes in immune regulation. *Nat Rev Immunol*. 2016;16(12):741-750.
6. Senoo M, Pinto F, Crum CP, McKeon F. p63 is essential for the proliferative potential of stem cells in stratified epithelia. *Cell*. 2007;129(3):523-536.
7. Murray-Zmijewski F, Slee EA, Lu X. A complex barcode underlies the heterogeneous response of p53 to stress. *Nat Rev Mol Cell Biol*. 2008;9(9):702-712.
8. Sun L, Li H, Luo H, et al. Phosphatase Wip1 is essential for the maturation and homeostasis of medullary thymic epithelial cells in mice. *J Immunol*. 2013;191(6):3210-3220.
9. Kelly RM, Goren EM, Taylor PA, et al. Short-term inhibition of p53 combined with keratinocyte growth factor improves thymic epithelial cell recovery and enhances T-cell reconstitution after murine bone marrow transplantation. *Blood*. 2010;115(5):1088-1097.
10. Marino S, Vooijs M, van Der Gulden H, Jonkers J, Berns A. Induction of medulloblastomas in p53-null mutant mice by somatic inactivation of Rb in the external granular layer cells of the cerebellum. *Genes Dev*. 2000;14(8):994-1004.
11. Soza-Ried C, Bleul CC, Schorpp M, Boehm T. Maintenance of thymic epithelial phenotype requires extrinsic signals in mouse and zebrafish. *J Immunol*. 2008;181(8):5272-5277.
12. Ribeiro AR, Rodrigues PM, Meireles C, Di Santo JP, Alves NL. Thymocyte selection regulates the homeostasis of IL-7-expressing thymic cortical epithelial cells in vivo. *J Immunol*. 2013;191(3):1200-1209.
13. Anders S, Pyl PT, Huber W. HTSeq—a Python framework to work with high-throughput sequencing data. *Bioinformatics*. 2015;31(2):166-169.
14. Love MI, Huber W, Anders S. Moderated estimation of fold change and dispersion for RNA-seq data with DESeq2. *Genome Biol*. 2014;15(12):550.
15. Bauer S, Gagneur J, Robinson PN. GOing Bayesian: model-based gene set analysis of genome-scale data. *Nucleic Acids Res*. 2010;38(11):3523-3532.
16. Alves NL, Hooibrink B, Arosa FA, van Lier RA. IL-15 induces antigen-independent expansion and differentiation of human naive CD8+ T cells in vitro. *Blood*. 2003;102(7):2541-2546.
17. Gray DH, Seach N, Ueno T, et al. Developmental kinetics, turnover, and stimulatory capacity of thymic epithelial cells. *Blood*. 2006;108(12):3777-3785.
18. Abramson J, Giraud M, Benoist C, Mathis D. Aire's partners in the molecular control of immunological tolerance. *Cell*. 2010;140(1):123-135.
19. Irla M, Hollander G, Reith W. Control of central self-tolerance induction by autoreactive CD4+ thymocytes. *Trends Immunol*. 2010;31(2):71-79.
20. Mouri Y, Yano M, Shinzawa M, et al. Lymphotoxin signal promotes thymic organogenesis by eliciting RANK expression in the embryonic thymic stroma. *J Immunol*. 2011;186(9):5047-5057.
21. Vousden KH, Prives C. Blinded by the light: the growing complexity of p53. *Cell*. 2009;137(3):413-431.
22. Li M, He Y, Dubois W, Wu X, Shi J, Huang J. Distinct regulatory mechanisms and functions for p53-activated and p53-repressed DNA damage response genes in embryonic stem cells. *Mol Cell*. 2012;46(1):30-42.
23. Kenzelmann Broz D, Spano Mello S, Bieging KT, et al. Global genomic profiling reveals an extensive p53-regulated autophagy program contributing to key p53 responses. *Genes Dev*. 2013;27(9):1016-1031.
24. Liu Y, Elf SE, Miyata Y, et al. p53 regulates hematopoietic stem cell quiescence. *Cell Stem Cell*. 2009;4(1):37-48.
25. Sansom SN, Shikama-Dorn N, Zhanybekova S, et al. Population and single-cell genomics reveal the Aire dependency, relief from Polycomb silencing, and distribution of self-antigen expression in thymic epithelia. *Genome Res*. 2014;24(12):1918-1931.
26. Daley SR, Hu DY, Goodnow CC. Helios marks strongly autoreactive CD4+ T cells in two major waves of thymic deletion distinguished by induction of PD-1 or NF-κB. *J Exp Med*. 2013;210(2):269-285.
27. Anderson MS, Venanzi ES, Klein L, et al. Projection of an immunological self shadow within the thymus by the Aire protein. *Science*. 2002;298(5597):1395-1401.
28. Lei Y, Ripen AM, Ishimaru N, et al. Aire-dependent production of XCL1 mediates medullary accumulation of thymic dendritic cells and contributes to regulatory T cell development. *J Exp Med*. 2011;208(2):383-394.
29. Perkins ND. Integrating cell-signalling pathways with NF-kappaB and IKK function. *Nat Rev Mol Cell Biol*. 2007;8(1):49-62.
30. Brennecke P, Reyes A, Pinto S, et al. Single-cell transcriptome analysis reveals coordinated ectopic gene-expression patterns in medullary thymic epithelial cells. *Nat Immunol*. 2015;16(9):933-941.
31. Almeida AR, Borghans JA, Freitas AA. T cell homeostasis: thymus regeneration and peripheral T cell restoration in mice with a reduced fraction of competent precursors. *J Exp Med*. 2001;194(5):591-599.
32. Cowan JE, Parnell SM, Nakamura K, et al. The thymic medulla is required for Foxp3+ regulatory but not conventional CD4+ thymocyte development. *J Exp Med*. 2013;210(4):675-681.
33. Guerau-de-Arellano M, Martinic M, Benoist C, Mathis D. Neonatal tolerance revisited: a perinatal window for Aire control of autoimmunity. *J Exp Med*. 2009;206(6):1245-1252.

Trends in Immunology

CellPress REVIEWS

Forum

Setting Up the Perimeter of Tolerance: Insights into mTEC Physiology

Pedro M. Rodrigues,[1,2] Pärt Peterson,[3] and Nuno L. Alves[1,2,*]

Medullary thymic epithelial cells (-mTECs) play a central role in T cell tolerance. However, how the mTEC compartment is maintained remains elusive. We review recent discoveries on new transcription factors involved in mTEC homeostasis and discuss the possibility that their actions might be facilitated by the unique biology of mTECs.

The generation of multifunctional and self-tolerant $CD4^+$ and $CD8^+$ αβ T cells proceeds sequentially within dedicated microenvironments of the thymus formed by cortical TECs (cTECs) and mTECs [1]. Despite deriving from common bipotent progenitors, cTECs and mTECs specialize into functionally distinct cell types [2]. While cTECs drive T cell lineage commitment and positive selection, mTECs mediate the deletion of autoreactive thymocytes or promote their clonal deviation into regulatory T cells [1]. The central role of mTECs in tolerance induction depends on their unique capacity to express virtually all self-antigens, including tissue-restricted antigens (TRAs). This so-called promiscuous gene expression (pGE) potential is acquired during mTEC maturation in part through the action of two transcriptional regulators, Autoimmune regulator (Aire) and Fezf2, that coordinate the expression of a broad range of TRAs [3]. The development of mTECs commences during organogenesis and continues during adulthood. In recent years the identification of distinct subtypes of mTEC precursors, such as Claudin3,4^+stage-specific embryonic antigen $(SSEA)^+$, Claudin3,4^+, receptor activator of NF-κB $(RANK)^+$, and $podoplanin^+$ cells, has emphasized the dynamics of this process [4]. NF-κB signaling is critical to mTEC differentiation and is triggered by the engagement of members of the TNF receptor superfamily (TNFRSF) – RANK, CD40, and LTβR – by their ligands expressed in developing thymocytes [1]. Despite substantial advances in our understanding of the blueprint of mTEC differentiation, the molecular mechanisms that control the maintenance of the thymic medulla in postnatal life remain poorly defined. Interestingly, mature mTECs turnover every 1–2 weeks, indicating the need for their regular replacement by upstream precursors. Given that genetic or age-related defects in mTECs are linked to the development of autoimmunity, the study of how these cells influence thymic activity is of fundamental and medical importance. In this Forum we summarize recent studies that have uncovered the role of new classes of hitherto overlooked transcription factors (TFs) in the selective regulation of mTEC homeostasis.

Our laboratories independently generated experimental evidence using conditional loss-of-function mouse models that adds novel pieces to our understanding of thymus medulla homeostasis and function. Rodrigues *et al.* analyzed mice with a disrupted *Trp53* gene in TECs and showed that p53 is critical for mTEC maintenance and function [5]. TEC-intrinsic p53 deficiency causes a specific reduction in the size of the mTEC compartment, decreasing the expression of RANK in mTECs and conditioning their responsiveness to RANK stimulation. Beyond the functional link to RANK, we found that p53 regulates a broad transcriptional program in mTECs, including the expression of TRAs and genes associated with core processes of mTEC biology [5]. However, it is presently unclear how p53 maintains the mTEC niche. Given that p53 controls a basal transcriptional program in unstressed cells [6], the reduced mTEC compartment in p53 conditional knockout (KO) mice might result from broad failures in genes linked to essential mTEC biology. In a complementary study, Haljasorg *et al.* generated TEC-specific IFN regulatory factor 4 (IRF4) KO mice and found that disruption of *Irf4* leads to an increase in the frequency of mature mTECs and alters the expression of important chemokine and costimulatory molecules in these cells [7]. This observation raises the possibility that IRF4 controls a novel checkpoint in mTEC differentiation. Intriguingly, the absence of p53 and IRF4 provokes a common reduction in thymic regulatory T cell numbers, leading to peripheral autoimmune manifestations [5,7]. Future studies should dissect to what extent p53 and IRF4 control distinct and/or overlapping programs in mTEC biology. Interestingly, both reports suggest the involvement of TNFRSF signaling in the regulation of the expression of p53 and IRF4. While p53 is induced by RANK and CD40 stimulation [5], IRF4 expression is specifically controlled by RANK activation [7]. The RANK–IRF axis was previously implicated in mTEC differentiation with the observation that the activation of IRF7 downstream of RANK controls the production of IFN-β, which in turns promotes mTEC development [8]. Thus, p53-, IRF4-, and IRF7-driven pathways seem to branch downstream of TNFRSF-induced activation of the NF-κB signaling pathway and coordinate multiple aspects of mTEC homeostasis. However, it remains to be further investigated whether these pathways can be activated by alternative signals (Figure 1).

Besides agonist signals, the TNFRSF-mediated pathway is tempered by negative regulators that control the

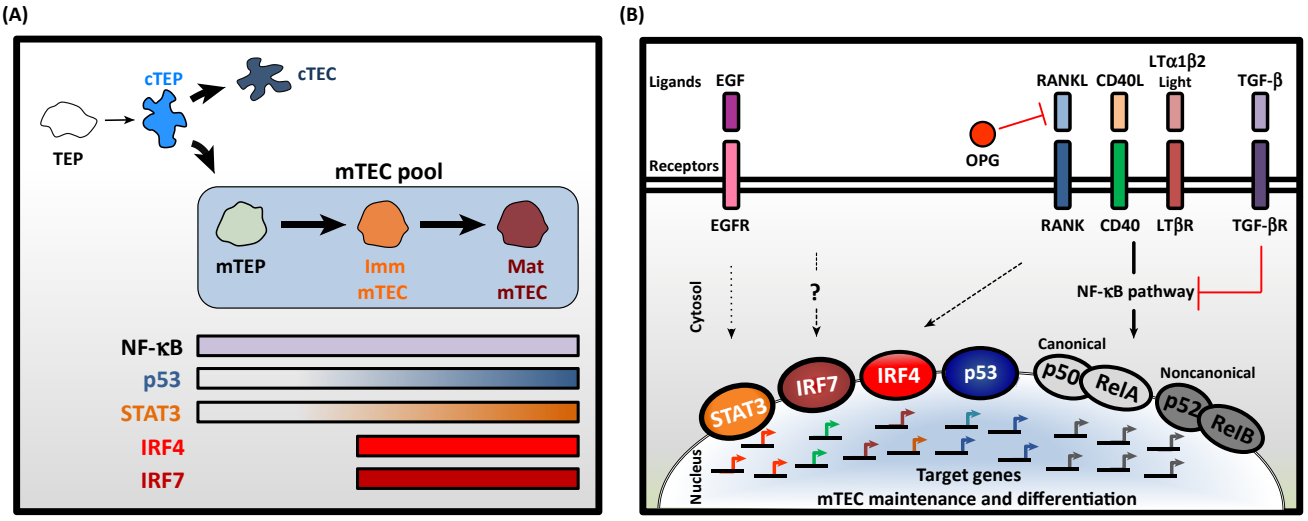

Figure 1. Proposed Model for the Action of the Recently Identified Regulators of Medullary Thymic Epithelial Cell (mTEC) Homeostasis. (A) TEC progenitors (TEPs) traverse through a 'transitional TEC progenitor' stage that expresses phenotypic and molecular traits associated with cortical TEC (cTEC) precursors (cTEPs) before the commitment to a cTEC or mTEC fate [2]. The NF-κB pathway regulates various stages of their differentiation, from mTEC progenitors (mTEPs) to immature (Imm) and mature (Mat) mTECs [4]. While p53 [5] and STAT3 [11,12] appear to control the maintenance of the broad mTEC compartment, IFN regulatory factor (IRF) 4 [7] and IRF7 [8] seem to regulate the immature–mature mTEC transition. (B) Molecular interplay between the distinct signaling pathways and transcription factors (TFs) governing the homeostasis and differentiation of mTECs. The right side represents the well-recognized role in mTECs of members of the TNF receptor superfamily (TNFRSF) – receptor activator of NF-κB (RANK), CD40, and LTβR – which on interaction with their respective ligands activate the canonical and noncanonical NF-κB pathway. This pathway of mTEC differentiation is regulated at multiple levels. Osteoprotegerin (OPG) acts as a decoy receptor for RANK ligand (RANKL), inhibiting RANK signaling [9]. Additionally, signaling through the TGF-β receptor (TGF-βR) negatively regulates the NF-κB pathway [10]. The left side represents the role of p53-, IRF4-, IRF7-, and STAT3-mediated signaling in the coordination of mTEC differentiation and homeostasis. While p53 [5], IRF-4 [7], and IRF7 [8] appear to be activated downstream of TNFRSF signaling, STAT3 [11,12] is suggested to be engaged by signaling through the epithelial growth factor receptor (EGFR). It remains unclear whether these pathways can be activated by other, as-yet-undefined signals (represented by '?'). Another uncertainty pertains to the overlapping or distinct nature of the gene expression program driven by the recently identified TFs in mTECs. Black lines with superscript colored arrows represent purported target genes.

bioavailability of TNFRSF ligands, the expression of the receptors, and the intensity of downstream signaling. Osteoprotegerin (OPG) is one of these regulators, operating as a soluble decoy receptor for RANK ligand. The expression of OPG in mTECs is controlled by the TF Spi-B, which is in turn activated by RANK [9]. Hauri-Hohl *et al.* identified TGF-β as an additional negative regulator of the mTEC compartment. Genetic ablation of TGF-β signaling in TECs expanded the mTEC niche and the functional capacity of the thymus medulla to maintain tolerance induction. Mechanistically, TGF-β signaling dampens the NF-κB pathway elicited by RANK and CD40 engagement [10]. These findings suggest that OPG and TGF-β are important liaisons in the negative feedback mechanism controlling TNFRSF signaling during mTEC differentiation.

Interestingly, two recent reports demonstrated that alternative signaling pathways also participate in the maintenance of the medullary microenvironment in the adult thymus. Satoh *et al.* and Lomada *et al.* have shown that conditional inactivation of *Stat3* in TECs prevents the expansion of thymic medullary areas during postnatal life [11,12]. Despite exhibiting a reduction in the mTEC compartment similar to that in p53 conditional KO mice, the number of thymic regulatory T cells is unaltered in mice with STAT3-deficient TECs, indicating that STAT3 and p53 regulate complementary programs in mTECs. STAT3 is activated by various cytokines and growth factors *in vivo*. Satoh *et al.* provide further evidence that STAT3 signaling in TECs is induced by the epithelial growth factor receptor (EGFR), although the intrathymic physiological source of its ligand remains unclear [11]. Cosway *et al.* have recently shown that targeted deletion of LTβR in TECs disturbs the architecture of mTECs without an overt effect on their functionality [13]. Unlike the profound defects caused by the lack of Relb signaling [14], conditional deficiency of LTβR does not affect thymic regulatory T cells and induces a milder phenotype

reminiscent of STAT3 deficiency. The new studies highlight that the establishment, maintenance, and architecture of the thymus medulla are determined by the integration of multiple signals, although it remains unclear whether proper mTEC structure is required for its functionality. Further studies should aim to unravel the genetic program driven by the recently identified TFs in mTECs and their possible relationship in maintaining a functional mTEC compartment (Figure 1).

Intriguingly, the specific role of these TFs in mTEC biology was demonstrated in experimental models in which their genes were targeted in both cTECs and mTECs. On the one hand, the enriched expression and/or activation of these proteins in mTECs might determine their specific influence. On the other hand, we hypothesized that the unique transcriptional and epigenetic states of mTECs [3] can facilitate the access of these TFs to their targets. According to this conjecture, a given TF drafts behind the molecular machinery involved in regulating pGE expression and exploits the induced changes in the chromatin to initiate a specific genetic program in mTECs. However, the action of the newly identified TFs in mTEC homeostasis seems to be distinct from the prototypical roles of NF-κB in mTEC maturation or Aire and Fezf2 in TRA expression. Instead, these novel pathways appear to operate as a key rheostat to sustain the regular activity of the thymus medulla under physiological conditions, preventing the emergence of autoimmunity. Ultimately, understanding the mechanisms controlling the limits of the medullary microenvironment might lead to a better comprehension of the rules balancing immunity and tolerance induction.

Acknowledgments

The European Research Council (ERC) under the EU's Horizon 2020 research and innovation program (grant agreement No 637843 – TEC_Pro) – starting grant attributed to N.L.A – supports the studies from the laboratory of N.L.A. The studies from the laboratory of P.P. are supported by Estonian Research Agency grant IUT2-2. The authors thank the members of their laboratories for their past and present contributions. They apologize for not referring to all primary literature owing to space limitations.

[1]Instituto de Investigação e Inovação em Saúde, Universidade do Porto, Porto, Portugal
[2]Thymus Development and Function Laboratory, Instituto de Biologia Molecular e Celular, Porto, Portugal
[3]Molecular Pathology, Institute of Biomedicine and Translational Medicine, University of Tartu, Tartu, Estonia

*Correspondence: nalves@ibmc.up.pt (N.L. Alves).
https://doi.org/10.1016/j.it.2017.11.001

References

1. Anderson, G. and Takahama, Y. (2012) Thymic epithelial cells: working class heroes for T cell development and repertoire selection. *Trends Immunol.* 33, 256–263
2. Alves, N.L. *et al.* (2014) Serial progression of cortical and medullary thymic epithelial microenvironments. *Eur. J. Immunol.* 44, 16–22
3. Takaba, H. and Takayanagi, H. (2017) The mechanisms of T cell selection in the thymus. *Trends Immunol.* 38, 805–816
4. Alves, N.L. and Ribeiro, A.R. (2016) Thymus medulla under construction: time and space oddities. *Eur. J. Immunol.* 46, 829–833
5. Rodrigues, P.M. *et al.* (2017) Thymic epithelial cells require p53 to support their long-term function in thymopoiesis in mice. *Blood* 130, 478–488
6. Munoz-Fontela, C. *et al.* (2016) Emerging roles of p53 and other tumour-suppressor genes in immune regulation. *Nat. Rev. Immunol.* 16, 741–750
7. Haljasorg, U. *et al.* (2017) Irf4 expression in thymic epithelium is critical for thymic regulatory T cell homeostasis. *J. Immunol.* 198, 1952–1960
8. Otero, D.C. *et al.* (2013) IRF7-dependent IFN-β production in response to RANKL promotes medullary thymic epithelial cell development. *J. Immunol.* 190, 3289–3298
9. Akiyama, N. *et al.* (2014) Limitation of immune tolerance-inducing thymic epithelial cell development by Spi-B-mediated negative feedback regulation. *J. Exp. Med.* 211, 2425–2438
10. Hauri-Hohl, M. *et al.* (2014) A regulatory role for TGF-β signaling in the establishment and function of the thymic medulla. *Nat. Immunol.* 15, 554–561
11. Satoh, R. *et al.* (2016) Requirement of Stat3 signaling in the postnatal development of thymic medullary epithelial cells. *PLoS Genet.* 12, e1005776
12. Lomada, D. *et al.* (2016) Stat3 signaling promotes survival and maintenance of medullary thymic epithelial cells. *PLoS Genet.* 12, e1005777
13. Cosway, E.J. *et al.* (2017) Redefining thymus medulla specialization for central tolerance. *J. Exp. Med.* 214, 3183–3195
14. Cowan, J.E. *et al.* (2013) The thymic medulla is required for Foxp3$^+$ regulatory but not conventional CD4$^+$ thymocyte development. *J. Exp. Med.* 210, 675–681